Terms and Conditions of Use of Digitised Theses from Trinity College Library Dublin

Copyright statement

All material supplied by Trinity College Library is protected by copyright (under the Copyright and Related Rights Act, 2000 as amended) and other relevant Intellectual Property Rights. By accessing and using a Digitised Thesis from Trinity College Library you acknowledge that all Intellectual Property Rights in any Works supplied are the sole and exclusive property of the copyright and/or other IPR holder. Specific copyright holders may not be explicitly identified. Use of materials from other sources within a thesis should not be construed as a claim over them.

A non-exclusive, non-transferable licence is hereby granted to those using or reproducing, in whole or in part, the material for valid purposes, providing the copyright owners are acknowledged using the normal conventions. Where specific permission to use material is required, this is identified and such permission must be sought from the copyright holder or agency cited.

Liability statement

By using a Digitised Thesis, I accept that Trinity College Dublin bears no legal responsibility for the accuracy, legality or comprehensiveness of materials contained within the thesis, and that Trinity College Dublin accepts no liability for indirect, consequential, or incidental, damages or losses arising from use of the thesis for whatever reason. Information located in a thesis may be subject to specific use constraints, details of which may not be explicitly described. It is the responsibility of potential and actual users to be aware of such constraints and to abide by them. By making use of material from a digitised thesis, you accept these copyright and disclaimer provisions. Where it is brought to the attention of Trinity College Library that there may be a breach of copyright or other restraint, it is the policy to withdraw or take down access to a thesis while the issue is being resolved.

Access Agreement

By using a Digitised Thesis from Trinity College Library you are bound by the following Terms & Conditions. Please read them carefully.

I have read and I understand the following statement: All material supplied via a Digitised Thesis from Trinity College Library is protected by copyright and other intellectual property rights, and duplication or sale of all or part of any of a thesis is not permitted, except that material may be duplicated by you for your research use or for educational purposes in electronic or print form providing the copyright owners are acknowledged using the normal conventions. You must obtain permission for any other use. Electronic or print copies may not be offered, whether for sale or otherwise to anyone. This copy has been supplied on the understanding that it is copyright material and that no quotation from the thesis may be published without proper acknowledgement.

The identification and functional characterisation of caspase substrates involved in inflammation

Alexander U. Lüthi

Thesis submitted to Trinity College Dublin
for the degree of Doctor of Philosophy

Thesis supervisor: Prof. Seamus J. Martin

Molecular Cell Biology Laboratory,
Department of Genetics,
University of Dublin,
Trinity College,
Dublin 2

DECLARATION

I certify that this thesis, submitted to Trinity College Dublin for the degree of Doctor of Philosophy, has not been submitted as an exercise for a degree at this or any other university. I certify that the work presented here is entirely my own, except where otherwise acknowledged. This thesis may be made available for consultation within the university library and may be copied or lent to other libraries upon request.

ACKNOWLEDGEMENTS

Firstly, I would like to thank my supervisor, Prof. Seamus Martin, for all the help and invaluable expertise he has provided throughout the course of my thesis.

I would also like to thank the people in the lab: Dr. Colin Adrain and Dr. Susan Logue who helped me with the proteomic screens, Dr. Sean Cullen, Clare Sheridan, Dr. Patrick Duriez, Inna Afonina and Dr Rebecca Taylor, who helped with the IL-33 project and contributed some of the data. I am also grateful to Dr. Ed Lavelle and Dr. Edel McNeela who performed the animal experiments, cell re-stimulation assays and also let me use their cytokine data.

Many thanks are due also to the other members of the lab, past and present, for all their help and support.

Finally, I am grateful to Science Foundation Ireland, who very generously funded this work.

TABLE OF CONTENTS

CHAPTER III:

CHAPTER IV:

CHAPTER V:

FIGURES

CHAPTER I

CHAPTER III

CHAPTER IV

CHAPTER V

TABLES

CHAPTER III

CHAPTER IV

APPENDICES

Table A.1 Constructs used in this study

SUMMARY

During inflammation the immune system responds to harmful stimuli, tries to control the stimuli and initiate a healing process for damaged tissue. After recognition of microbes by the innate immune system caspases are activated and are required to activate cytokines. Human caspases have been studied for over two decades with most work in the field focused on apoptotic caspases. As a result hundreds of apoptotic caspase substrates have been identified to date, but only 2 inflammatory caspase substrates have been confirmed. Identification of novel targets for the caspases activated during the inflammatory process could provide new insights into the molecular mechanism of host defense, identify important immuno-regulatory molecules and targets for anti-inflammatory drug development.

In order to discover new substrates cleaved by the inflammatory caspases, a proteomic approach was undertaken. Initially we adapted a cell-free extract model to specifically activate or inhibit the inflammatory caspases and then resolved control and inflammatory caspase activated proteomes on two-dimensional gels and subsequently identified protein spot alterations between the two gels by MALDI-TOF mass spectrometry analysis. Compared to apoptotic caspases, the activation of inflammatory caspases resulted in surprising few changes. A second proteomic approach was therefore taken whereby a small pool cDNA library was individually transcribed and translated and screened with recombinant caspase-1, -4 or -5 for proteolytic events. The identified novel inflammatory caspase substrates were then further verified in the THP-1 cell-free extract system.

A report suggesting that Interleukin-33 was a novel putative caspase-1 substrate with cytokine activities was published during the screening process (Schmitz *et al.*, 2005). Our aim was to confirm the processing of the cytokine by inflammatory caspases both with recombinant proteases and with the previously established cell-free extract model. To our surprise the cytokine was not processed by inflammatory caspases but instead was processed at a different cleavage site during programmed cell death by apoptotic caspases. We further investigated the

functional outcome of IL-33 cleavage by apoptotic caspases both and found ST2 receptor transactivation was strongly reduced *in vitro* and observed diminished cytokine responses *in vivo*. This suggests that Interleukin-33 may represent a novel alarmin, released from cells during necrosis as an active cytokine but is inactivated by caspases during apoptosis.

ABBREVIATIONS

Act D	Actinomycin D
AMC	7-amino-4-methylcoumarin
AIM2	Absent in melanoma 2
ALS	Amyotrophic lateral sclerosis
Alum	Aluminium salt
AMC	7-Amido-4-methylcoumarin
Apaf-1.	Apoptosis protease-activating factor-1
APC	Antigen presenting cell
ASC	Apoptosis-associated speck-like protein containing a C-terminal CARD
ATP	Adenosine triphosphate
BSA	Bovine serum albumin
CapG	Gelsolin like capping protein
CARD	Caspase activation and recruitment domain
CASPASE	Cysteinyl aspartate-specific protease
CEB	Cell extract buffer
Ced-3	Cell death defective-3
CFE	Cell-free extract
CFTR	Cystic fibrosis transmembrane conductance regulator
CHAPS	3-[(3-Cholamidopropyl)dimethylammonio]-1-propanesulfonate
CHX	Cyclohexamide
CPPD	Phosphate dehydrate
CTL	Cytotoxic T lymphocyte
Cyt c	Cytochrome c
dATP	Deoxyadenosine triphosphate
DAMP	Danger-associated molecular pattern
Dauno	Daunorubicin
DC	Dendritic cell
DD	Death domain
ddH_2O	Double distilled H_2O
DED	Death effector domain

DEVD	Aspartic acid-glutamic acid-valine-aspartic acid
DISC	Death Inducing Signalling Complex
DKK3	Dickkopf-3
DMEM	Dulbecco's modified eagle medium
DMSO	Dimethyl sulphoxide
DNA	Deoxyribonucleic acid
DTT	Dithiothreitol
EDTA	Ethylenediaminetetraacetic acid
ER	Endoplasmatic reticulum
FACS	Fluorescence-activated cell sorter
FADD	Fas-associated death domain-containing protein
FasL	Fas ligand
FCS	Fetal calf serum
FMK	Fluoreomethylketone
FTLD-U	Frontotemporal lobar degeneration with ubiquitin-positive inclusions
GDAP1L1	Ganglioside-induced differentiation-associated protein 1 like 1
GFP	Green fluorescent protein
GR-1	Granulocyte differentiation antigen 1
GST	Glutathione S-transferases
H&E	Hematoxylin and eosin
HEK	Human embryonic kidney
HEPES	N-(2-hydroxyethyl) piperazine-N'-(2-ethanesulphonic acid)
HMGB1	High mobility group box protein 1
hnRNPs	Heterogeneous ribonucleoprotein family
hp	Hydrophobic region
HSP	Heat shock protein
i.p.	Intra peritoneal
IAA	Iodoacetamide
IAPs	Inhibitors of apoptosis
ICE	Interleukin-1β-converting enzyme
iE-DAP	γ -D-glutamyl-meso-diaminopimelic acid
IEF	Isoelectric point focusing
IETD	Isoleucine-glutamic acid-threonine-aspartic acid
Ig	Immunoglobulin

IGIF	IFN-γ-inducing factor
IL	Interleukin
IL-1RAcP	IL-1 receptor accessory protein
Ipaf	ICE-protease-activating
IPG	immobilized pH gradient
IPTG	isopropylthio-beta-D-galactoside
ITT	*In vitro* transcription and translation
IVEC	*In vitro* expression cloning
JNK	c-Jun NH_2-terminal kinase
kDa	Kilo Dalton
LB	Luria -Bertani broth
LEHD	Leucine-glutamic acid-histidine-aspartic acid
LPS	Lipopolysaccharide
LRR	Leucine-rich repeats
L-SOX5	Transcription factor SOX-5, long isoform
MAGE-D1	Melanoma antigen family D1
MAL/TIRAP	MyD88-adaptor-like/TIR-associated protein
MALDI-TOF	Matrix-assisted laser desorption and ionisation time-of-flight
MAPK	Mitogen-activated protein kinases
MDP	MurNAc-L-Ala-D-isoGln
MEFs	Mouse embryonic fibroblasts
MHC	Major histocompatibility complex
MHD	MAGE homology domain
MOM	Mitochondrial outer membrane
MS	Mass spectrometry
MSU	Monosodium urate
MWCO	Molecular weight cut-off
MyD88,	Myeloid differentiation factor 88
M/Z	Mass:charge ratio
NF-κB,	Nuclear factor κB
NF-HEV	Nuclear factor from high endothelial venules
NK	Natural killer cell
NLRP	NLR family pyrin domain containing protein
NLR	Nucleotide-Binding Oligomerisation Domain NOD-like receptor

NLS	Nuclear localisation signal
NOD	Nucleotide-Binding Oligomerisation Domain
NP40	Nonidet P40
OA	Osteoarthritis
p75NTR	p75 neutrophin receptor
PAMP	Pathogen-associated molecular pattern
PCD	Programmed cell death
PAGE	Polyacrylamide gel electrophoresis
PARP	Poly(ADP-ribose) polymerase
PBS	Phosphate-buffered saline
PCR	Polymerase chain reaction
PGN	Peptidoglycan
PHAP I	Putative human leukocyte antigen-DR-associated protein I
PIPES	Piperazine-N-N'-bis(2-ethanesulphonic acid)
PMSF	Phenylmethylsulphonyl-fluoride
PRB	Protease reaction buffer
PRR	Pattern recognition receptor
PYD	Pyrine domain
RBC	RBC
RIG	Retinoic acid-inducible gene
RLH	RIG-I-like helicase
RNA	Ribonucleic acid
ROS.	Reactive oxygen species
RPL10	60S Ribosomal Protein L10
RRM	RNA-recognition motif
SDS	Sodium dodecyl sulphate
SEAP	Secreted alkaline phosphatase
sIL-1RII	Soluble IL-1 receptor type II
TAE	Tris acetate EDTA
TDP-43	TAR DNA-binding protein 43
TE	Tris EDTA
TFA	Trifluoroacetic acid
TGF	Transforming growth factor
Th1	T helper 1

Th2	T helper 2
TIR	Toll/IL-1 receptor
TMB	αTransmembrane domain
TNF	Tumour necrosis factor
TRAM	Toll-receptor-associated molecule
TRIF	TIR domain-containing adaptor inducing IFN-γ
TLR	Toll like receptor
VH	Volt-hour
WEHD	Tryptophan-glutamic acid-histidine-aspartic acid
YVAD	Tyrosine-valine-alanine-aspartic acid
z-VAD	Benzylocarbonyl-Val-Ala-Asp-(OMe)

PUBLICATIONS

Lüthi, AU, Cullen SP, McNeela EA, Duriez PJ, Afonina IS, Sheridan C, Brumatti G, Taylor RC, Kersse K, Vandenabeele P, Lavelle EC and Martin SJ (2009). "Suppression of interleukin-33 bioactivity through proteolysis by apoptotic caspases." *Immunity* **31**, 84-98.

Cullen SP, Afonina IS, Donadini R, Lüthi AU, Medema JP, Bird PI, Martin SJ. (2009). Nucleophosmin is cleaved and inactivated by the cytotoxic granule protease granzyme M during natural killer cell-mediated killing. *J Biol Chem.* **284**, 5137-47

Walsh JG, Cullen SP, Sheridan C, Lüthi AU, Gerner C, Martin SJ. (2008). Executioner caspase-3 and caspase-7 are functionally distinct proteases. *Proc Natl Acad Sci U S A.* **105**, 12815-9

Lüthi AU, Cullen SP, Martin SJ (2008). Two-dimensional gel-based analysis of the demolition phase of apoptosis. *Methods Enzymol.* **442**, 343-54

Cullen SP, Lüthi AU, Martin SJ (2008). Analysis of apoptosis in cell-free systems. *Methods* **44**, 273-9

Cullen SP, Adrain C, Lüthi AU, Duriez PJ, Martin SJ (2007) Human and murine granzyme B exhibit divergent substrate preferences. *J Cell Biol.* **176**, 435-44

Lüthi AU, Martin SJ. (2007). The CASBAH: a searchable database of caspase substrates. *Cell Death Differ.***14**, 641-50

CHAPTER 1

Introduction

1.1 THE CASPASE FAMILY

1.1.1 Identification of the caspases

In the late 1980s genetic screens in *Caenorhabditis elegans* identified 12 genes involved in nematode programmed cell death during development, one of which was cell death defective-3 (ced-3) (Ellis *et al.*, 1986; Yuan *et al.*, 1993). This was the founding member of a family of proteolytic enzymes, known as caspases (Cysteine Aspartate Proteases) (Alnemri *et al.*, 1996). Their pathways of activation leading to programmed cell death (PCD) are conserved from worms to mammals (Figure 1.1) (Lamkanfi *et al.*, 2002).

Human ICE (Interleukin-1β Converting Enzyme) was identified as the enzyme responsible for cleaving the cytokine IL-1β to its active form (Cerretti *et al.*, 1992; Thornberry *et al.*, 1992). The protease was subsequently found to be a human homologue of ced-3 (Miura *et al.*, 1993) and was later renamed as Caspase-1. Despite an amino acid homology of 23% and a similar active site to that of ced-3, caspase-1 is not part of the apoptotic machinery but rather involved in the inflammatory response mediated by the innate immune system (Kuida *et al.*, 1995; Li *et al.*, 1995). In subsequent years further members of the caspase family have been identified, currently totalling 15 members, of which 12 are found in man (reviewed in (Cohen, 1997)) and 10 in mouse (Figure 1.1).

1.1.2 Classification and structure of caspases

Homologues of the caspases have been identified across different vertebrates, in the worm *C. elegans* (Ced-3), in the fly *D. melanogaster* (Dronc, DrICE), in fish and in mammals. The caspase family can be divided according to their structure and hierarchy in the signalling cascade into initiator or executioner caspases. The N-termini of the initiator caspases contain either a caspase recruitment domain (CARD) or two death effector domains (DED). These domains are able to interact with upstream signalling platforms which in turn lead to the auto-proteolytic activation of the initiator caspases. These can now cleave and thereby activate the executioner caspases which do not contain any N-terminal CARD or DED domains.

Figure 1.1 The family of caspases
Overview of the 12 known mamalian caspases. Caspases-1, -4, -5 and -12 have been implicated in inflammation. Caspases-3, -6, -7, -8, -9, and -10 are involved in apoptotic processes. A polymorphism in the caspase-12 gene results in a truncated, inactive from in the majority of humans (depicted grayed out). Caspase-14 is only expressed in keratinocytes and was reported to play a role in keratinocyte differentiation. The colour key representing different caspase domains are shown at the bottom left hand side.

The caspase family can also be divided into two groups based on their functional role; caspases activated during an inflammatory response (inflammatory caspases, e.g. human caspase-1,-4 and -5 and murine caspase-1, -11 and -12) and caspases activated during PCD (apoptotic caspases, e.g. caspase-2, -3, -6, -7, -8, -9 and -10). Caspase-14 has been implicated in keratinocyte differentiation (Eckhart *et al.*, 2000) and does not match the criteria for either the apoptotic or the inflammatory sub-groups.

1.2 INFLAMMATION

Inflammation is the reaction of an organism to harmful stimuli, like pathogens, irritants or damaged cells. It is an attempt to rapidly assess, control and neutralise the stimuli as well as initiate the healing process for the damaged tissue. The inflammatory process is essential for wound healing and therefore for multicellular organisms.

1.2.1 The inflammatory pathway

The whole process of inflammation is controlled by many different components in a complex regulated network. Reduced to its core, the whole process can be broken down to a simple pathway consisting of inducers, sensors, mediator, effectors and finally the resolution (Figure 1.2). Inducers of inflammation are usually exogenous and can be microbes (bacterial or viral), irritants, allergens and toxic compounds. Recently research has also shifted to examine certain endogenous molecules, produced by damaged or stressed tissue which are also able to trigger an inflammatory response. The sensors for these different stimuli are generally on or within cells of the immune system (e.g. dentritic cells (DC), macrophages, lymphocytes and mast cells) and these sensors generally trigger an intracellular signalling cascade which leads to the production and release of autocrine and paracrine signalling molecules. The inflammatory mediators initially released range from vasoactive amines (e.g. histamine), vasoactive peptides (e.g. Angiotensin II), complement, lipid mediators (e.g. platelet-activating factors), cytokines (e.g. IL-1β, TNFα), chemokines (e.g. IL-8) and proteolytic enzymes (e.g. matrix metalloproteinases, cathepsins). They subsequently alter the functionality of specific cells in the immune system. Unfortunately, the exact mediator responses to specific inducers or triggers is not fully understood, as many of the messenger

molecules trigger the production of additional inflammatory mediators. The effectors in inflammation are comprised of all the cells affected by the mediators and they are found throughout the body. Together they identify and eradicate the pathogen, eliminate any infected or damaged cells by apoptosis / phagocytosis or isolate and / or expel an irritant. In a final step, the inflammatory response is actively terminated by new signalling molecules (e.g. TGFβ) (reviewed in Randow *et al.*, 1995). These down regulate the activity of any recruited inflammatory cells and prevent collateral damage to the surrounding healthy tissue. The recruited cells try to reinstate the condition of the affected tissue prior to the inflammatory insult. Macrophages partake in the removal of dead cells and debris while fibroblasts repair any tissue damage with collagen.

1.2.2 Chronic inflammation

The initial response of the body to a harmful stimuli described in 1.2.1 refers to acute inflammation. However, prolonged inflammation, known as chronic inflammation, leads to a simultaneous destruction and healing of the tissue at the site of inflammation. This can lead to further diseases, e.g. hay fever, rheumatoid arthritis and atherosclerosis. Inflammation is therefore a double-edged sword. It is a powerful tool to eradicate microbes efficiently but can also lead to severe tissue damage. For that reason inflammation is normally closely regulated by the body.

1.3 THE IMMUNE SYSTEM

Through evolution multi-cellular life forms, from sponges to vertebrates, developed a response to battle and resolve conditions of infection and tissue injury by pathogens or noxious stimuli. In vertebrate animals, additional, more specific immune-recognition systems developed over time. These systems can be broadly categorized into non-specific (innate) and specific (adaptive) immunity.

1.3.1 Innate Immunity

Innate immunity, first partially observed by Elie Metchnikoff in the late 18th century, consists of passive elements, e.g. physical barriers, blood proteins such as members of the complement family or defensins, antimicrobial peptides that inhibit or kill the pathogen directly. Specialised cell types of the immune system also

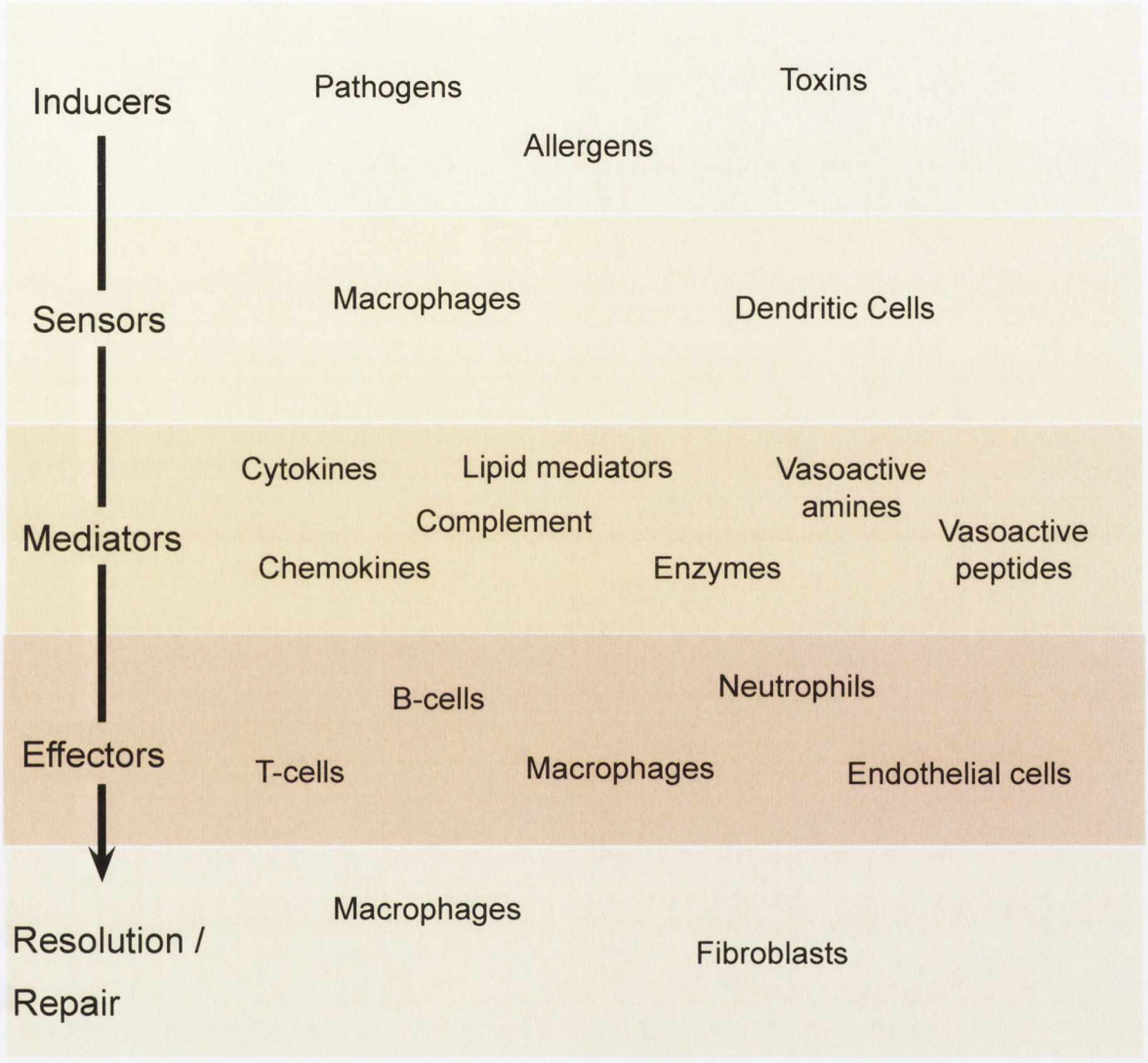

Figure 1.2 Inflammatory pathway
Schematic representation of the different steps of the inflammatory pathway (left) and examples of the associated molecules / cells in each phase (right).

provide an early and non-specific recognition of pathogens and act as a first line of defence. B1 cells, a subpopulation of B-cells, are activated independently of co-stimulatory signals and target specific microbes. Similarly, natural killer (NK) cells recognise and kill virally infected cells or tumour cells. Antigen presenting cells (APCs), such as macrophages or dendritic cells, recognise specific pathogen-associated molecular patterns (PAMPs) of bacteria, fungi or viruses with cell surface or intracellular pattern recognition receptors (PRR) (Figure 1.4). Upon detection, these receptors initiate signalling pathways, activating different transcription factors, e.g. nuclear factor κB (NF-κB), resulting in the strong up-regulation of pro-inflammatory cytokines (e.g. IL-1, IL-18 or TNF-α) and anti-microbial compounds (e.g. reactive oxygen species (ROS)). The secreted signalling molecules have different specific functions, like the attraction of other leukocytes to the site of infection and activation of the adaptive immune response. The innate immune response not only provides an early defense against microbes, but also plays an important role in the induction of a specific immune response. For a long time the main research focus centred on the adaptive immune response, as this was thought to play the key role in immunity. In the past few years it became clear that innate immunity has an important role as the first line of defense against pathogens as well as in the development of the correct adaptive immune response. Depending on the nature of the pathogen or cellular stress detected, essential cytokines are secreted by cells of the innate immune system which shape the adaptive immune response.

1.3.2 Adaptive Immunity

The evolutionarily developed adaptive immune system generates a random and highly diverse repertoire of antigen receptors on T- and B-cells and antibodies produced by activated B-cells. Upon encountering their specific antigen, lymphocytes become activated, secrete cytokines which enhance the functions of phagocytes and stimulate and direct the inflammatory response. B-cells simultaneously clonally expand exponentially, thereby potentiating their response. Antibodies bind to extracellular microbes, and as a result, activate the serum complement pathway to eliminate the antigen and also marking the pathogen for easier uptake by phagocytes. T-cells, on the other hand, detect peptides from either phagocytosed or intracellular particles of APCs presented on the major histocompatibility complex (MHC). Activated CD4+ helper T-lymphocytes

differentiate into different subpopulations depending on co-stimulatory signals received from the APC.

There are several T-cell subpopulations but immune reactions are typically dominated by three primary types:

- T helper 1 (Th1) cells arise from the co-stimulation of naïve CD4+ T-cells with IL-2 and IL-12. This subpopulation produce cytokines (e.g. IFNγ and TNFβ) that promote cell-mediated immunity directed against intracellular microbes by activating macrophages and cytotoxic T-lymphocytes. They in turn destroy the infected or malfunctioning cell by inducing apoptosis.
- If, on the other hand, the APC secretes IL-10 and/or IL-4 but not IL-12, T helper 2 (Th2) cell polarisation occurs. These cells are primarily induced in response to extracellular microbes, allergens and toxins. Th2 cells produce cytokines (e.g. IL-4 and IL-13) that promote the production of antibodies (e.g. IgG1, IgE and IgA) that neutralize extracellular microbes and toxins.
- T helper 17 (Th17) cells produce interleukin-17 which in turn, stimulates stromal cells to produce IL-6 and IL-8. These in turn attract neutrophils and further promote inflammation.

During the immune response, a fraction of the clonally expanded leukocytes survive and form a long-lasting immunological memory. This is a major advantage for the multi-cellular organism and provides a significant adaptive fitness to vertebrate animals for any future encounters with the same microbe.

1.3.3 Pattern recognition receptors (PRRs)

Pattern recognition receptors are a class of innate immune response proteins. They sense pathogen-associated molecular patterns (PAMPs) and stress signals termed danger-associated molecular patterns (DAMPs). The R proteins in plants are structurally and functionally similar proteins and give plants a crude defense system against plant pathogens. The exact mechanism by which the different receptors detect PAMPs has only been resolved for a few molecules. Additionally new molecules are still being added to the group of PRRs. Upon sensing of their specific ligand, PPRs activate downstream singling cascades resulting in the activation of transcription factors and in some instances the inflammatory caspase

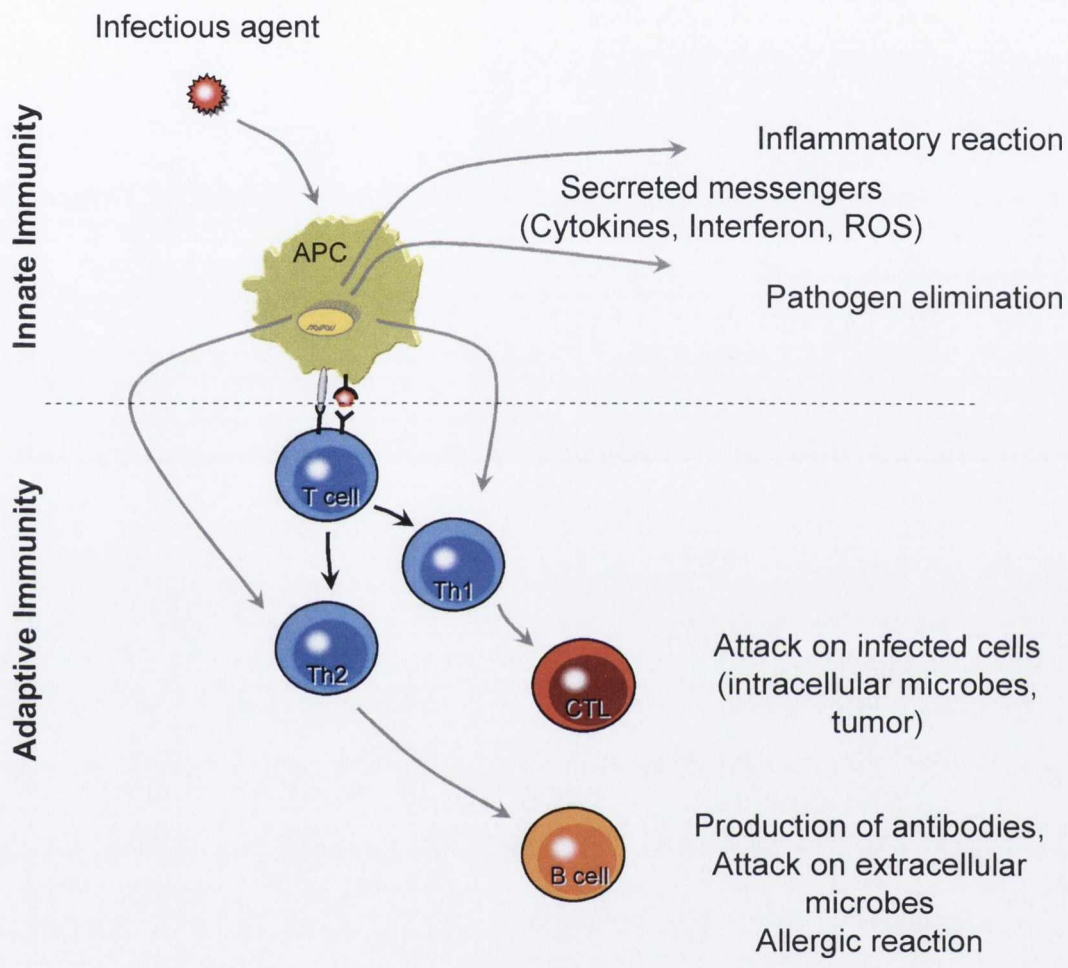

Figure 1.3 Overview Innate / Adaptive Immunity

Immunity in vertebrates can be divided into nonspecific 'Innate Immunity' (top) and specific, aquired 'Adaptive Immunity' (bottom).

Antigen-presenting cells (APC) are activated through recognition of pathogen or danger associated molecular patterns (PAMPs / DAMPs). This leads to the production and secretion of inflammatory mediators, the expression of antigen presenting complexes and co-stimulatory molecules. This leads to the activation of naive T-cells, which in conjunction with the secreted cytokines of the APC, differentiate into Th1 or Th2 cells. The now active T-cells then further stimulate either the cytotoxic T lymphocytes (CTLs) or B-cells and coordinate the immune response.

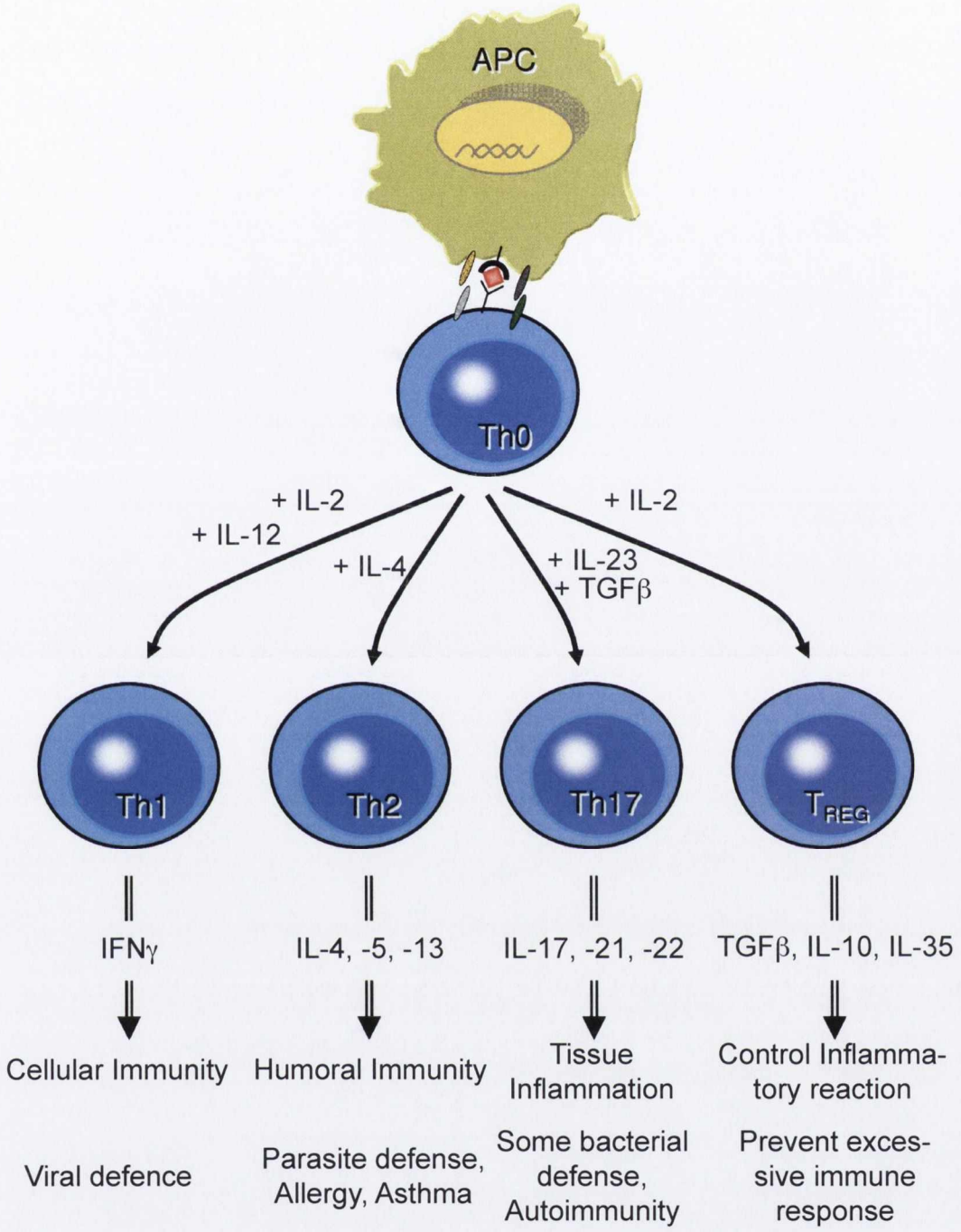

Figure 1.4 T-helper cell differentiation from naive CD4$^+$ T cells
Naive CD4+ T-cells are activated by antigen-presenting cells (APCs) in the presence of co-stimulatory ligands. The cytokine enviroment released by the APC determines the cell lineage commitment and subsequent cytokine expression profiles. IL-12 and IL-2 differentiate the cell to the Th1 cell lineage which upregulate and secrete IFNγ and TNF thereby activating the cellular immunity with CTLs and NK cells. By contrast IL-4 determines a Th2 cell lineage differentiation, producing IL-4, -5 and -13 taking part in the humoral immunity, activating B-cells. IL-6 differentiates the naive CD4+ T-cells to the Th17 cell lineage, upregulating IL-17 thereby attracting neutrophils. T_{REG} cells maintan tolerance and limit chronic inflammation by negatively stimulating or even reducing the numbor of effector T-cells.

activation complex termed the inflammasome (Figure 1.5). Overall the different PRRs can be divided into different groups according to their structure:

(I) Toll-like receptors (TLRs)

Initially identified in *Drosophila* for its role in development (Anderson *et al.,* 1985), Toll was later discovered to be essential for the detection of fungal proteins (Lemaitre *et al.*, 1996). A murine homologue, today known as TLR4, was subsequently cloned and identified as the lipopolysaccharide (LPS) receptor required for an effective immunological response to Gram-negative bacteria (Poltorak *et al.*, 1998). There are 10 functional human TLRs (reviewed in Takeda *et al.*, 2005), recognising a wide range of pathogen-associated molecular patterns (PAMPs) (Janeway *et al.*, 1998) originating from protozoa (Campos *et al.*, 2001), fungi (Meier *et al.*, 2003), bacteria (Takeuchi *et al.*, 1999) and viruses (Heil *et al.*, 2004).

The TLRs are type I transmembrane receptors that share extracellular leucine-rich repeats (LRR) by which they recognize distinct ligands (reviewed in Bell *et al.*, 2003) and an intracellular Toll/IL-1 receptor (TIR) domain (Medzhitov *et al.*, 1997). The formation of TLR homodimers or heterodimers has been demonstrated (Xu *et al.*, 2000; Park *et al.*, 2009) and this dimerisation is believed to activate downstream signalling through the adaptor proteins myeloid differentiation factor 88 (MyD88), MyD88-adaptor-like/TIR-associated protein (MAL/TIRAP), TIR domain-containing adaptor inducing IFN-β (TRIF) and Toll-receptor-associated molecule (TRAM).These adaptors, in turn, activate downstream protein kinases which trigger the activation of transcription factors (e.g. NF-κB, AP-1, IRF3 or 7) mitogen-activated protein kinases (MAPK) family including p38 and c-Jun N-terminal kinase (JNK). In the case of the TLR4 receptor, recognition of LPS from Gram-negative bacteria results in receptor dimerisation and downstream signalling through the adaptors MAL and MyD88 leading to the formation of a ubiquitination complex containing TNF receptor associated factor 6 (TRAF6). This activates the TRAF6-regulated inhibitor of NF-κB kinase activator 2 complex which in turn phosphorylates IkB kinase (IKK)–β, resulting in the IKK complex activation releasing NF-κB for translocation to the nucleus (Figure 1.5). This quite complex

signalling pathway possibly also leads to a potent signal amplification requiring only a few TLR4 receptors.

(II) Nucleotide-Binding Oligomerisation Domain (NOD)-like receptors (NLRs)

The NLR family, also know as CATERPILLER or NOD-LLR family, can be subdivided into further subfamilies: the NODs and the 'NLR family pyrin domain containing proteins' (NLRPs).

NODs are cytoplasmic proteins consisting of a leucine rich repeats (LRR), a NOD and at least one CARD domain (Bertin *et al.*, 1999; Ogura *et al.*, 2001). They both recognize different breakdown products of peptidoglycan (PGN): γ-D-glutamyl-meso-diaminopimelic acid (iE-DAP) is the minimal structure detected by NOD1, whereas NOD2 recognises Muramyl dipeptide (MDP) (Girardin *et al.*, 2003). Upon ligand detection they both activate signalling cascades, activate MAP kinases and the IKK complex resulting in the activation of NF-κB transcription.

14 NLRPs, formerly known as 'NACHT leucine rich repeat and pyrin domain containing proteins' (NALPs), have been identified in the human to date (Martinon *et al.*, 2007) but most are still lacking functional characterisation. Structurally they contain an N-terminal pyrine domain (PYD), a central NACHT-associated domain (NAD) and C-terminal LRRs, which appear to act as a regulatory domain and may be involved in the recognition of microbial pathogens. NALPs appear to recognize PAMPs and possibly DAMPs and oligomerise at the NAD to form a caspase-1 activation platform.

Mutations in most of the NLR family members studied are associated with inflammatory diseases. Mutations in NOD2 are associated with Crohn's Disease, a chronic mucosal inflammation possibly caused by bacteria from the lumen (Ogura *et al.*, 2001) and Blau Syndrome, attributed to mutations in the NOD and clinically characterized by arthritis and dermatitis (Miceli-Richard *et al.*, 2001). Mutations in NLRP1 have been associated with vitiligo-associated autoimmune disease (Jin *et al.*, 2007) although the exact mechanisms are still unclear. Autosomal dominant mutations in *NLRP3* have been linked to autoinflammatory diseases including

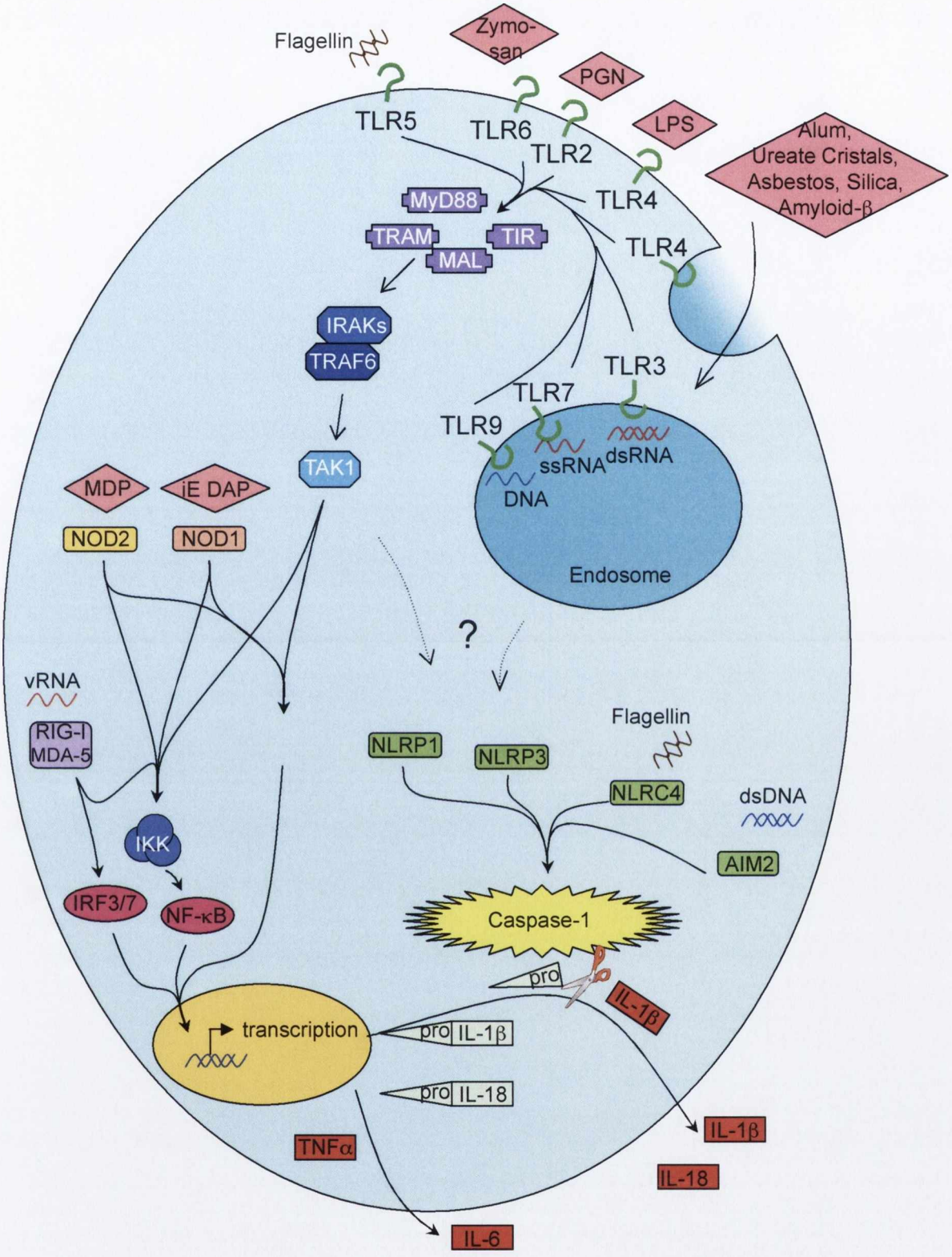

Figure 1.5 Caspase activation pathways during inflammation

The pathogen or danger associated molecular patterns (PAMPs/ DAMPs) are recognised by intracellular or transmembrane receptors on the cell surface or in phagosomes/endosomes. All receptors trigger signaling cascades, activating transcription factors like NF-κB which upregulates pro-inflammatory cytokines e.g. IL-1β. A parallel yet unknown pathway leads to inflammasome assembly and caspase-1 activation. Active caspase-1 subsequently processes proIL-1β to its mature form which is secreted. The cytokines now exert their systemic proinflammatory action.

familial cold autoinflammatory syndrome, Muckle-Wells syndrome and neonatal-onset multi-systemic inflammatory disease (reviewed in Ting *et al.*, 2006). Symptoms include fever, skin rash and arthropathy, possibly all linked to a hyper-activation of the NLRP3 inflammasome (Agostini *et al.*, 2004) described in section 1.5.1. NLRP3 was also shown to react to monosodium urate (MSU) crystals (Martinon *et al.*, 2006) deposited in joints of gout patients, resulting in the autoinflammatory disease.

(III) Retinoic acid-inducible gene (RIG)-I-like helicases (RLHs)

Members of the latest group of RLHs are cytoplasmic helicases that recognize viral RNA. These RNA helicases recruit other proteins via twin N-terminal CARD domains and thereby activate protein complexes resulting in antiviral IRF3, 7 and NF-κB activation.

1.3.4 Caspase activation pathways in inflammation

After the sensing of pathogens by the PRRs and subsequent activation of corresponding singling pathways, the APC produces and secretes the molecules as described above. Some of the pro-inflammatory cytokines require proteolytic maturation in order to become fully active (Figure 1.4). This adds an additional regulatory step in the inflammatory response to finely control a potentially devastating response. Caspase-1 was the protease identified to activate IL-1β and IL-18. Besides caspase-1, the other inflammatory family members, caspase-4, -5 and -12, more than likely also take part in the innate immune response against microbes. When any of these protease genes (or caspase-11 as the closest related homologue for caspase-4 and -5) are knocked out in mice, the animals show clear defects in the immune response to bacterial infection. Vital signalling pathways seem to be interrupted and the bacterial infection is not cleared compared to wild type animals (Kui *et al.,* 1995; Li *et al.,* 1995; Wang *et al.*, 1998). The exact molecular pathway that leads to the activation of caspase-1 has so far not been found and is still subject of intensive research.

1.4 APOPTOSIS

Apoptosis is a highly controlled mode of cell death and is used to eliminate specific cells from a multicellular organism without harming the cells in the surrounding tissue. This is an ongoing process and plays a crucial role throughout life in different situations.

First and foremost, apoptosis is required for the control of cell numbers. Cell homeostasis is important in organs with a high turnover rate such as intestinal surface epithelia (Hall *et al.*, 1994), skin or lymphocytes (Nagata, 1997). Additionally, remodelling of organs during embryonic development is precisely controlled by apoptosis. As an example, during the digit formation of a developing foetus, apoptosis eliminates the excess tissue between the digits (Yokouchi *et al.*, 1996). Additionally, cells encountering irreparable damage to their genome or exposed to intolerable stress, upregulate specific proteins like p53, Noxa or Puma which subsequently trigger cell death by apoptosis (Youle *et al.*, 2008). This way the cell can be removed without any damage to its surrounding area and avoiding activation of cells of the immune system.

Apoptosis is also a mechanism used to destroy infected cells and thus prevent the further multiplication and spread of the microorganism (Meinl *et al.*, 1998). Cells of the immune system constantly screen for abnormal cells and can trigger apoptosis externally. With co-evolution, many viruses developed strategies to inhibit apoptosis and therefore prolong the survival of the infected cell to proliferate longer.

Apoptosis is also essential in the development and regulation of the immune system. Developing lymphocytes with either inactive receptors or receptors recognising self-antigens are externally triggered to die by apoptosis. This process eliminates the vast amount of newly formed but defective lymphocytes in the thymus (Nagata, 1997).

The morphology resulting from this controlled dismantling of the cell from within is typical of apoptosis. Cytoplasmic shrinkage, cell membrane blebbing, chromatin condensation and finally packaging of the disassembled cellular organelles into membrane-enclosed vesicles called “apoptotic bodies” was originally identified as a new form of cell death (Kerr *et al.*, 1972; Wyllie *et al.*, 1980). Phagocytes

endocytose the membrane-enclosed debris, making sure none of the cells contents, which may cause an inflammatory response if released into the extracellular space, are released into the extracellular space.

Necrosis, another form of cell death, differs from apoptosis. This form of uncontrolled cell death is usually the result of cell membrane rupture, which leads to a disastrous loss of cellular contents into the extracellular space. Necrosis can often be observed in physical tissue wounds or damaged cells caused by aggressively multiplying bacteria or viral budding. This form of cell death is therefore often a first sign of danger to the organism and often activates a strong innate immune response.

Recently, a further mode of cell death has been coined as pyroptosis. This phenotype is induced by over expression of Apoptosis-associated speck-like protein containing a C-terminal CARD (ASC) which results in a strong activation of caspase-1 and does not depend on the other apoptotic caspases (Fernandes-Alnemri *et al.*, 2007). Overall the phenotype of this cell death does not appear to be closely regulated and is therefore more necrosis-like. The recently described AIM2 inflammasome has also been reported to induce a loss of viability, most likely also induced by pyroptosis like cell death (Fernandes-Alnemri *et al.*, 2009).

Autophagy has previously been associated with a caspase independent cell death, but rather relies on genes of the ATG family (reviewed in (Tsujimoto *et al.*, 2005)). It is characterised by the appearance of autophagosomes, large vacuoles which usually appear after nutritional starvation. Today however, it is regarded as a vital cellular function to recycle amino acids, generally keep the cell alive under stressful conditions and to take part in the regulation of the innate and adaptive immune response (Deretic and Levine, 2009).

By contrast, apoptosis is the controlled removal of superfluous cells from the body. As apoptotic cells maintain plasma membrane integrity and are fast and efficiently removed by phagocytes without generating an immune response, this mode of physiological cell death is typically immunogically 'silent'. Further, it has been shown that macrophages endocytosing apoptotic bodies actively suppress the release of pro-inflammatory mediators.

1.4.1 Caspase activation pathways in apoptosis

If a cell is destined to die by apoptosis, the caspases orchestrating this process can be activated by different triggers. This redundancy may also provide a fail-safe in case one of the pathways is inhibited or disrupted. Mitochondrial cytochrome *c* release is directly involved in one pathway and feedback mechanisms from the other pathways. The mitochondrial integrity therefore plays a central role and loss thereof is regarded as a point of no return for the cell undergoing apoptosis.

To induce apoptosis in a cell, three major pathways have been identified to trigger the activation of the caspases, namely the intrinsic, extrinsic and granzyme mediated pathways (Figure 1.6).

The intrinsic pathway is generally triggered by stress, e.g. excessive DNA damage, oxidative stress, heat shock or protein mis-folding (Youle and Strasser, 2008). By a yet not fully understood process, these pro-apoptotic signals can lead to an increase in BH3-only protein levels, post-translational modifications like dephosphorylation or caspase cleavage and translocation from the cytoplasm to the nucleus. The activated BH-3 only proteins can now overcome the repression of the pro-survival Bcl-2 family members and trigger the oligomerisation and pore-formation of Bax and Bak in the mitochondrial outermembrane (reviewed in Chipuk *et al.*, 2008). This leads to the release of mitochondrial intermembrane space proteins like cytochrome *c* into the cytoplasm. This in turn drives the assembly of the apoptosome, a multi protein complex. Apaf-1, the scaffold protein of the caspase-activating complex, undergoes a conformational change upon cytochrome *c* and dATP binding and recruits and activates caspase-9. The initiator caspase subsequently cleaves and activates the executioner caspases.

The extrinsic pathway is induced by another cell engaging and activating the death receptor complex. Upon binding of extra-cellular ligands such as TNF, FasL or TRAIL to TNFR1 , Fas or DR4 or DR5 respectively, the receptor trim rises and recruits caspase-8 through the adaptor proteins FADD (Fas-associated death domain) and Tumour necrosis factor receptor type 1-associated DEATH domain protein (TRADD), thereby activating caspase-8 followed by the executioner caspases (Nagata, 1997).

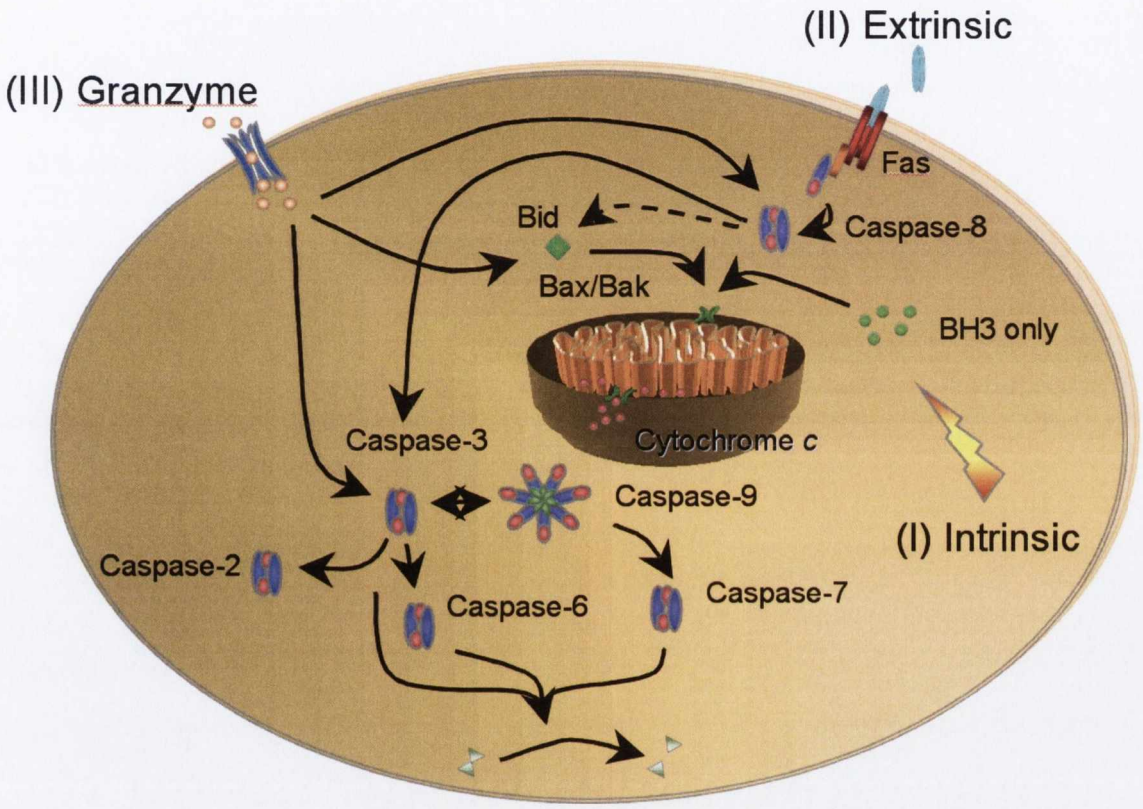

Figure 1.6 Caspase activation pathways during apoptosis
Caspases can be activated via three different pathways. (I) Endogenous signals can trigger the intrinsic pathway via the BH3 only proteins, (II) ligands bind the death receptor and trigger the formation of the DISC, or (III) Granzymes delivered by CTLs diectly activate caspases. All pathways ultimately lead to the activation of the apoptotic caspase cascade and the proteolysis of specific substrates.

In the Granzyme pathway, cytotoxic lymphocytes (CTLs) and natural killer cells (NKs) deliver granzymes through a perforin permeabilized plasma membrane to the cell cytosol, where they cleave and activate caspase-3 and -8, and in humans, bid (reviewed in Cullen and Martin, 2008).

Besides these by now well characterised pathways, other receptors such as p75 neurotrophin receptor (Yoon et al., 1998) have been shown to induce apoptosis. Though, the exact molecular mechanisms leading to caspase activation have not yet been fully characterised.

1.5 CASPASES

Caspases are proteases produced as mainly inactive zymogens and are activated by undergoing proteolytic processing and dimerisation. This processing can be initiated by three mechanisms. Firstly, the same family type of caspase can be forced into a cluster usually on a scaffold protein. The close proximity then leads to autoproteolysis and activation of the caspases (Nicholson, 1999). Secondly, a caspase can be cleaved and activated by a different member of the caspase family, resulting in a proteolytic activation cascade (Slee *et al.*, 1999). Thirdly, a caspase can be processed and activated by other proteases, e.g. granzymes. Initiator caspases are generally activated by the first mechanism, where as executioner caspases by the second. Granzymes can process and activate both initiator and executioner caspases (Martin *et al.*, 1996).

The cleavage of the pro-enzyme occurs at a characteristic caspase cleavage site located between the large and the small subunit. Most of the family members have a spacer between the subunits which is cut away at an additional cleavage site. Through hydrophobic interactions, the large and small subunit form a catalytically active heterodimer which then further dimereses with an identical heterodimer, forming a heterotetramer. This represents the fully active protease containing two active sites located on opposite faces of the molecular complex (Figure 1.7) (reviewed in Cohen, 1997).

Dimerisation of initiator caspases (caspase-1, -8, -9) by different platforms like the Apoptosome, the DISC or the Inflammasome brings the caspase precursors to close proximity and initiates their autoprocessing (Salvesen *et al.*, 1999) (Figure 1.7). The executioner caspases (caspase-3, -6, -7) are able to form dimers as pro-enzymes but become only active when processed by other caspases or granzymes.

1.5.1 Caspase activation platforms

(I) The Apoptosome

The best characterized caspase activation platform is the Apoptosome (Zou *et al.*, 1997; Adrain *et al.*, 2001). Different pro-apoptotic stimuli induce the release of cytochrome *c* from the mitochondria, which subsequently bind the WD40 region of apoptosis protease-activating factor-1 (Apaf-1). This in turn leads to a structural change of the scaffolding protein and reveals sites for dATP binding.
After the nucleotide binding, Apaf-1 becomes active and oligomerises to a form a heptameter through the central NOD domain. The N-terminal CARD domains then bind the CARD domains of caspase-9 and the protease activates by autoprocessing (Figure 1.8 A) (Adrain and Martin, 2001).

(II) The DISC

The DISC (Death Inducing Signalling Complex) is another apoptotic caspase activation platform (Nagata, 1999). Death receptors, e.g. Fas, oligomerise upon ligand binding and recruit FADD via a death domain (DD) (Chinnaiyan *et al.*, 1995). This is then followed by caspase-8 or -10 binding FADD through a death effector domain (DED) interaction, forming the DISC (Kischkel *et al.*, 1995) (Figure 1.8 B). The initiator caspase-8 then is activated through autolytic processing and activates the executioner caspase-3 (Fernandes-Alnemri *et al.*, 1996).

(III) The Inflammasome(s)

The inflammasome is a multiprotein caspase-1 activation platform similar to the apoptosome. To date 4 different inflammasomes have been described and well characterised, and further ones will more than likely be added to this list (Martinon *et al.*, 2007). Currently the exact molecular mechanisms leading to the formation of

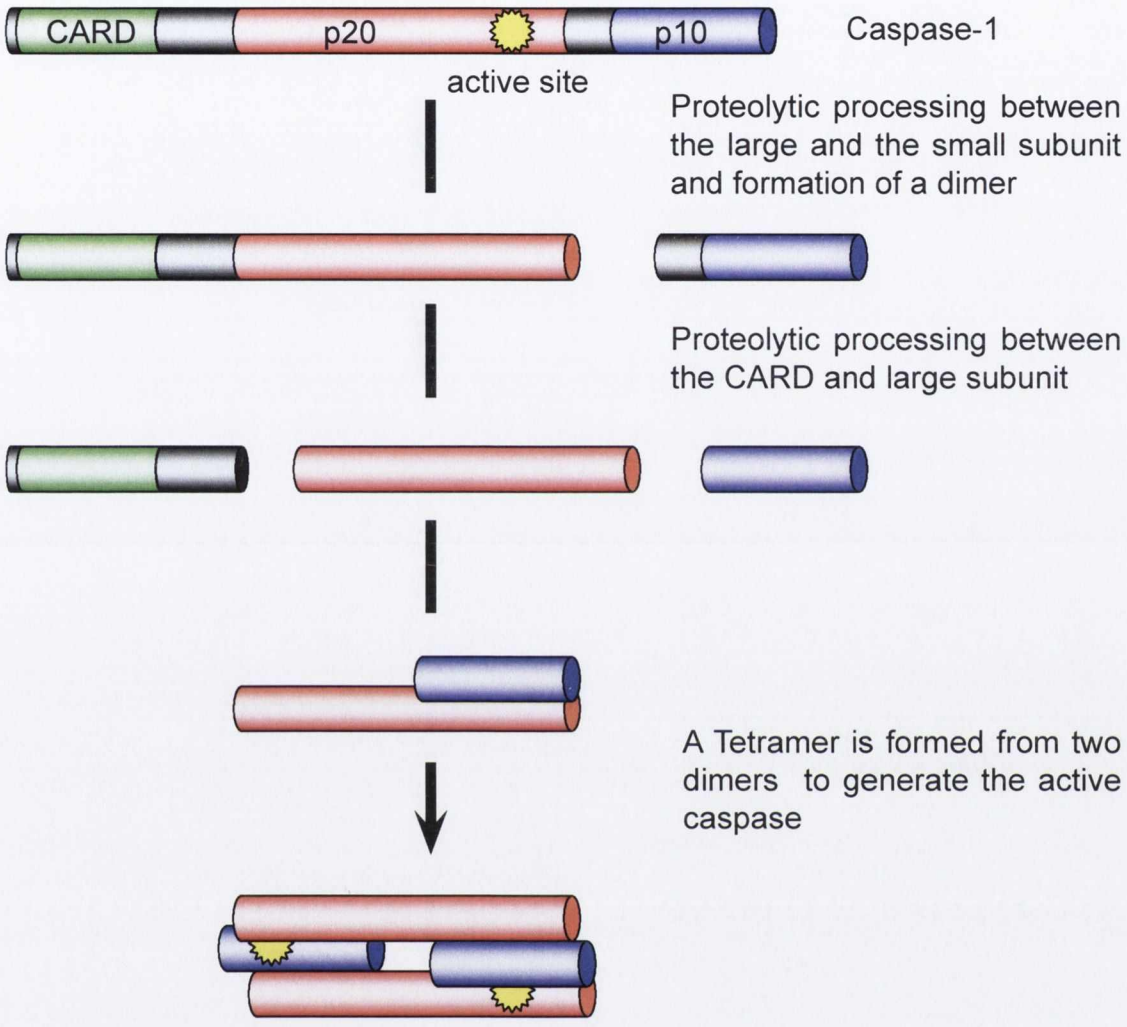

Figure 1.7 Caspase activation
Schematic of caspase activation is shown with caspase-1 used as an example. The inactive zymogen is processed into its p20 and p10 subunits. Caspases are generally only proteolytically active once the tetramer is formed.

the inflammasomes and subsequent caspase-1 activation are still unknown. The adaptor protein ASC has been shown to be associated with all but the NLRC4 inflammasome (Mariathasan *et al.*, 2004) by acting as an adaptor protein between the PYR domain of the NLRPs and the CARD domain of Caspase-1 by its own PYR and CARD domain. ASC was reported to be essential for the activation of caspase-1 *in vivo* after cell stimulation with different pro-inflammatory stimuli like LPS, *Salmonella typhimurium* (Mariathasan *et al.,* 2004) or influenza virus (Ichinohe *et al.*, 2009).

NLRP1 (NALP1) Inflammasome

In 2002 Jürg Tschopp's group suggested that NLRP1 formed a complex which they named the inflammasome (Figure 1.9) (Martinon *et al.*, 2002). In a THP-1 cell-free system a 700 kDa molecular weight complex was described, containing NALP1, ASC and caspase-1 (Figure 1.8 C) leading to caspase-1 processing and activation and subsequent IL-1β maturation. Initially, caspase-5 was shown to interact at the C-terminus of NALP-1 through another CARD binding motif, but the requirement or function of caspase-5 in the caspase-1 activation platform is currently not known. Recently, an *in vitro* reconstitution assay found ASC not to be required for caspase-1 activation but to merely enhance the NLRP1 inflammasome activity (Faustin *et al.*, 2007)

NLRP3 (NALP3) Inflammasome

The NLRP3 inflammasome is the best characterised caspase-1 platform to date (Figure 1.8 D). The assembly can be triggered in macrophages upon stimulation with PAMPs, such as LPS, peptidoglycan or bacterial nucleic acids (Figure 1.5). A secondary stimuli like ATP or the bacterial toxin nigericin can massively enhance the caspase-1 activity by activating the purigenic P2X7 receptor and the hemichannel pannexin-1. This large pore opening causes a rapid potassium efflux, changing the intracellular ion concentration. Although this system is used in many publications to enhance the caspase-1 activity, its physiological relevance *in vivo* has still to be proven. Other described pathways of NLRP3 inflammasome activation are triggered by crystals of monosodium urate (MSU), calcium phosphate dehydrate (CPPD) or aluminium salt (Alum), asbestos, silica and amyloid-β. It is thought that phagocytosis of these substances causes lysosomal swelling and damage, leading to the release of possibly additional proteins like

cathepsin B. In all described cases the exact molecular mechanisms are still unknown and it is therefore not known what exact pathways lead to the oligomerisation of NLRP3 and the subsequent caspase-1 activation through the adaptor protein ASC (Agostini *et al.*, 2004).

NLRC4 Inflammasome

NLRC4 (also known as ICE-protease-activating (Ipaf)), another member of the NLR family, has also been shown to activate caspase-1 when overexpressed (Poyet *et al.*, 2001). The domain structure of NLRC4 is similar to the one of apaf-1, the core of the apoptosome assembly involved in activating caspase-9 (Figure 1.8A). NLRC4 consists of an N-terminal CARD, a central NOD and multiple leucine-rich repeats at the C-terminus. The LRR domain is thought to act as a pathogen sensor setting off its oligomerisation and subsequently the binding of caspase-1 through a CARD-CARD interaction. Multiple caspase-1 molecules are brought in close proximity and process themselves. The NLRC4 inflammasome assembles upon detection of cytoplasmic flagellin (Mariathasan *et al.*, 2004). This indicates that NLRC4 does play a crucial role in caspase-1 activation upon intracellular parasite infection.

AIM2 Inflammasome

Recently several groups identified absent in melanoma 2 (AIM2) as a receptor for cytoplasmic DNA (Burckstummer *et al.*, 2009; Fernandes-Alnemri *et al.*, 2009; Hornung *et al.*, 2009). AIM2 senses double-stranded DNA through the C-terminal oligonucleotide/oligosaccharide-binding domain and recruits ASC with its N-terminal pyridin domain which in turn forms a CARD-CARD interaction with caspase-1 and activates the protease. The AIM2 inflammasomes assemble into a few but large oligomers which can be seen in cells as specs by immunofluorescence detection methods. This phenotype is similar to the 'pyroptosome' reported by ectopically expressing ASC in THP-1 (Fernandes-Alnemri *et al.*, 2007) but which has still to be confirmed under more physiological conditions.

1.5.2 Caspases activated during inflammation

Caspase-1

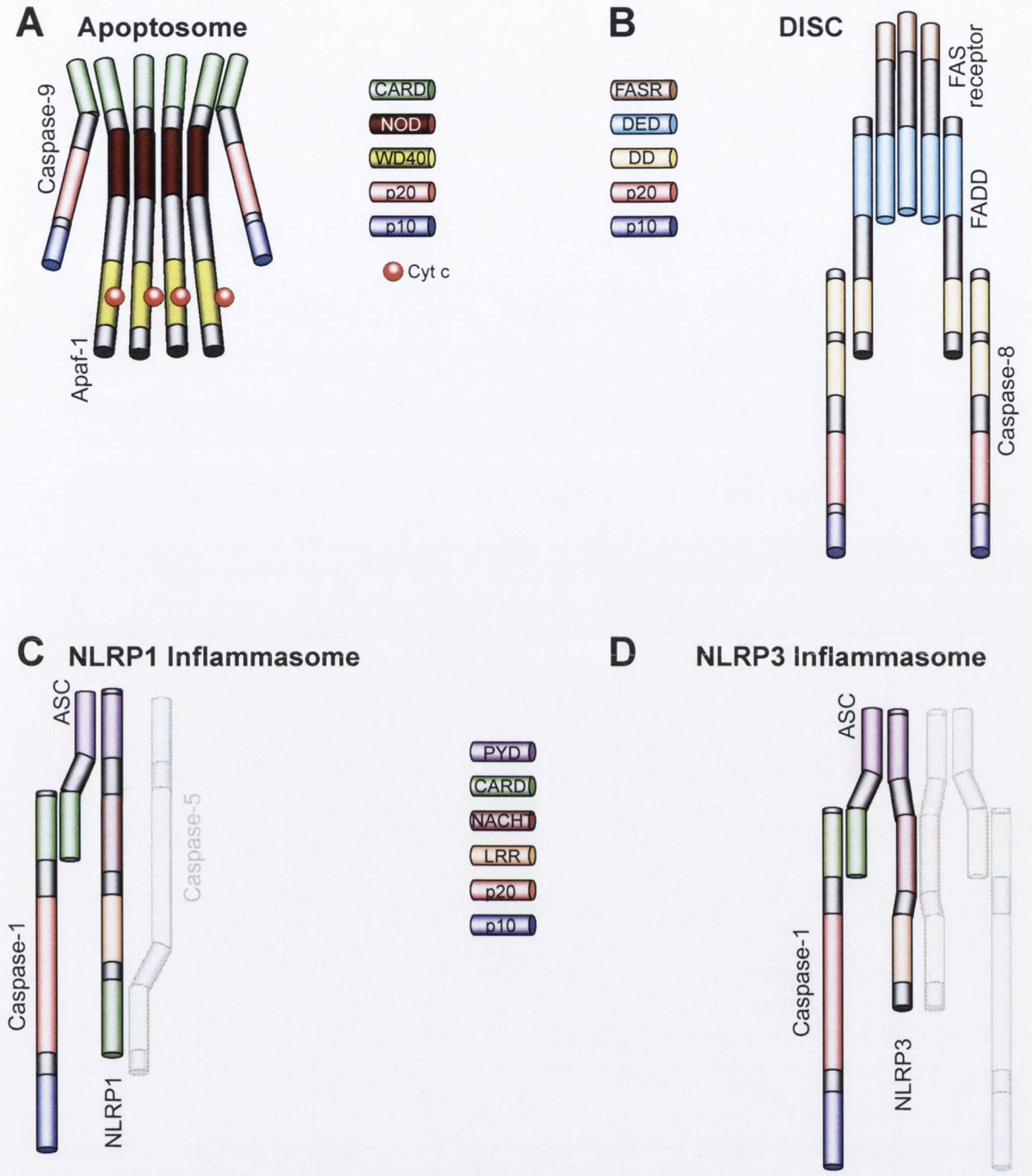

Figure 1.8 Caspase activation platforms

Simplified schematics of caspase activation through molecular platforms. (A) Cytochrome *c* released from the mitochondria binds the WD40 region of Apaf-1. dATP binding induces the oligomerisation of the heptamere (for simplicity only a tetramer is shown) which in turn activates caspase-9. (B) Fas ligand binding to the Fas receptor leads to its trimerisation. Intracellularly FADD is recruited by a Death Effector Domain (DED) interaction and binds caspase-8 through its Death effector domain (DED). Caspase-8 in turn autoprocesses by induced close proximity. (C) ASC binds NLRP1 through its N-terminal pyrin domain (PYD) and recruits caspase-1 on its C-terminal CARD domain. Caspase-5 is possibly also associated with the complex (greyed out) (D) The NLRP3 inflammasome binds and activates caspase-1 via ASC identical to NLRP1. Inflammasomes possibly oligomerise on their NACHT domain (shown grayed out).

Caspase-1 was identified initially as the protease responsible for cleaving the 35 kDa precursor pro-IL-1β to its mature and biologically active 17 kDa form (Thornberry *et al.,* 1992). At first caspase-1 was thought to be implicated in apoptotic events and even recent publications suggest an involvement in PCD. The homology to the *C. elegans* ced-3 (Yuan *et al.,* 1993) and other human caspase members involved in PCD as well as the overexpression of murine caspase-1 in rat-1 fibroblasts (Miura, Zhu *et al.,* 1993), human caspase-1 overexpression in HeLa cells (Hawkins *et al.*, 1996) or human embryonic kidney cells (Feng *et al.*, 2004) leading to apoptosis, supported the role of caspase-1 in a programmed cell death pathway. Other observations implicated caspase-1 in cleavage of Bid in a mouse model of amyotrophic lateral sclerosis (ALS) (Guegan *et al.*, 2002) which would result in activation of apoptotic caspases and PCD. However mice deficient in caspase-1 (Kuida *et al.,* 1995; Li *et al.,* 1995) developed normally and suggested that there was no involvement of caspase-1 in PCD as they had no obvious cell death phenotype compared to caspase-9 or caspase-3 and -7 double knock outs (Kuida *et al.*, 1996; Hakem *et al.*, 1998). Survival of cells to lethal doses of LPS and LPS treatment of monocytes from caspase deficient mice clearly established a function of caspase-1 in inflammation as IL-1β and IL-18 processing and export was completely abolished and levels of IL-1α were reduced (Kuida *et al.,* 1995; Li *et al.,* 1995).

While caspase-1 does not play a major role in apoptosis but undoubtedly does so in inflammation, the determination of its crystal structure shows clearly that it belongs to the caspase family (Walker *et al.*, 1994; Wilson *et al.*, 1994). The mature caspase forms a tetramer with the two small subunits surrounded by the two large subunits. (Figure 1.7). Each small / large subunit dimer forms an active site with four loops, which determines the substrate specificity of caspase-1.

Caspase -4 and -5

Caspase-4 and -5 map genetically next to caspase-1 on the human chromosome at location 11q22 and also show a high sequence homology to this protease; 55% and 50% respectively (Faucheu *et al.*, 1995). Murine caspase-11, the closest orthologue of human caspase-4 and -5, is required for the activation of murine caspase-1 (Wang et al., 1998). Based on this observation and their chromosomal

location, caspase-4 and -5 are placed in the inflammatory caspase family. Both caspase-4 and -5 mRNA are up-regulated upon LPS challenge (Lin *et al.,* 2000) strengthening their possible role in inflammation and caspase-1 activation. As mentioned earlier, caspase-5 is associated with the NALP1 inflammasome and is possibly involved in caspase-1 activation (Martinon, Burns *et al.,* 2002) but further investigation is required to confirm the involvement of both caspases in inflammation

Caspase -12

Caspase-12 has been reported to be involved in the activation of apoptosis through the endoplasmatic reticulum (ER) stress response which is due to the accumulation of misfolded proteins (Nakagawa *et al.*, 2000; Rao *et al.*, 2002). However, cells from caspase-12 deficient mice show the same sensitivity to different apoptotic stimuli as their wild type counter part, forming today's belief that this protease is not involved in apoptosis (Saleh *et al.*, 2006). In humans, the caspase-12 gene clusters phylogenetically together with caspase-1, -4, and -5 on chromosome 11q22, suggesting it rather belongs to the inflammatory caspase family (Saleh *et al.*, 2004). Recent studies bolster this observation by suggesting that this caspase acts as a negative regulator of pro-inflammatory cytokine production (Saleh *et al.*, 2006). Most humans carry a single-nucleotide polymorphism leading to premature termination of translation resulting in a catalytically in-active caspase-12 (Fischer *et al.*, 2002; Saitoh *et al.*, 2004). Only about 18% or 2% of humans of African descent have one or two fully coding alleles respectively. No substrates for caspase-12 have yet been published, and it remains unclear how this protease may act as a restraining influence on inflammatory cytokine production. The molecular mechanisms involved in the activation of caspase-12 also require further investigation.

1.5.3 Caspases activated during apoptosis

Caspase-2

Mice lacking caspase-2 show an essentially normal phenotype and stress induced apoptosis of casp2-null lymphocytes behave identically to wild type cells. In analogy to the 'apoptosome' or the DISC, the PIDDosome – comprised of PIDD and RAIDD molecules – was proposed as a caspase-2 activation platform (Read *et al.*, 2002; Tinel *et al.*, 2004; Park *et al.*, 2007). But to date caspase-2 has not

been firmly placed in apoptosis. No trigger to activate an apoptotic caspase-2 pathway has been conclusively shown, the caspase substrate specificity differs greatly from other apoptotic caspases and only a handful of substrates have been identified so far. Caspase-2 has been found to be involved in DNA damage detection, however its activation did not result in apoptosis (Shi *et al.*, 2009). Additionally a recent report has instead suggested an involvement of caspase-2 in cell-cycle transitions (Ho *et al.*, 2009).

Caspase-3 and -7

These are the major executioner caspases responsible for the vast majority of substrates cleaved during apoptosis (Walsh *et al.*, 2008). Mice of the 129 background deficient in caspase-3 showed an enlarged brain, due to excess cells failing to undergo apoptosis during development resulting with death *in utero* or within weeks of birth in most animals (Kuida *et al.,* 1996). Alternately, mice of this background lacking caspase-7 displayed a mild phenotype, most likely because caspase-3 could compensate for some of the loss of this protease. Surprisingly, in the C57BL6 background, both deficiencies show an almost normal phenotype (Leonard *et al.*, 2002) where as the double knock outs are embryonically lethal (Lakhani et al., 2006). Due to the fact that both caspases have an almost identical preference for the synthetic poly-peptide DEVD (Thornberry *et al.*, 1997) it was presumed that they cleaved identical substrates and were essentially redundant for the processing of substrates during apoptosis. This assumption is in opposition to the observations in the gene knock-out models and has been shown to be incorrect in cell-free extract of individually depleted caspases (Slee *et al.*, 2001). A recent screen with equimolar levels of either caspase against previously characterised apoptotic caspase substrates came to the same conclusion: the findings show that e.g. XIAP or gelsolin were more efficiently processed by caspase-3, whereas caspase-7 cleaves co-chaperone p23 at a higher rate compared to caspase-3 (Walsh *et al.,* 2008; Inoue *et al.*, 2009). Overall, caspase-3 appears to be the more abundant protease in most tissues.

Caspase-6

Caspase-6 belongs to the group of effector caspases, but most of its substrates are also cleaved by caspase-3 or -7 (Slee *et al.,* 2001). Lamin A/C and SATB1 are so far the only exclusive caspase-6 substrates, but a cell lacking caspase-6 will

still undergo apoptosis, albeit without complete nuclear condensation due to the lack of Lamin A/C processing (Ruchaud *et al.*, 2002). Recently, caspase-6 was also shown to be required for axonal degeneration, a process required during neuronal development (Nikolaev *et al.*, 2009)

Caspase-8 and -10

Caspase-8 and the close homologue caspase-10 are the initiator caspases of the extrinsic pathway as described in section 1.5.1. Besides its role in apoptosis, caspase-8 has also been linked to the differentiation (Kang *et al.*, 2004) and proliferation of immune cells (Chun *et al.*, 2002). This finding is also reflected in reports of impaired proliferation of T-, B- and NK cells in patients with an inactivating mutation in *Casp-8*. A different complex - containing caspase-8, FADD, FLIP and RIP1 - was shown to activate caspase-8 and cleave RIP1, resulting in the inhibition of NF-κB, characteristic of the differentiation of monocytes into macrophages (Rebe *et al.*, 2007). This protease has been further implicated in the regulation of cell migration and adhesion (Helfer *et al.*, 2006). Although caspase-10 and caspase-8 share an identical domain structure and are both activated at the DISC, the functions of caspase-8 can not be replaced by caspase-10 in a cellular model (Sprick *et al.*, 2002) and further investigation is required into the exact role of caspase-10.

Caspase-9

Like caspase-8, caspase-9 is an initiator caspase and activates caspase-3 and -7 upon assembly of the apoptosome. The phenotype of mice deficient of caspase-9 is similar but more severe than the one of Casp-3-null mice: superfluous cells in the brain. Upon stimulation of caspase-9 deficient cells with death stimuli, cytochrome *c* release was still observed while caspase-3 processing was strongly reduced (Kuida *et al.*, 1998; Hakem *et al.*, 1998). Addition of Apaf-1 stimuli to cell-free extracts of the caspase-9 deficient mice did not form an active apoptosome.

1.6 DOWNSTREAM OF CASPASE ACTIVATION – CASPASE SUBSTRATES

1.6.1 Caspase substrate specificity

Interactions between amino acids of the caspase substrate and of both the large and the small caspase subunit and an accessibility of the substrate cleavage site to the active site of the protease are crucial for efficient proteolysis by the caspase (Shi *et al.*, 2003). The processing site on a substrate protein is generally characterised by a tetrapepdide with an absolute requirement for an Asp residue at the P1 position (Thornberry *et al.,* 1997) and an uncharged and small residue in P1' (e.g. Gly, Ala, Thr Ser or Asn). The caspase family itself is defined by its highly conserved active site QACXG (where X is R, Q or G). Within this pentapeptide the cysteine residue breaks the peptide bond of the substrate after the P1 asparagine by nucleophilic attack. Further, the composition of other amino acids in the substrate cleavage site determines the specificity of the protease.

As previously mentioned, caspases can be sub-grouped according to their function and this is also reflected in their substrate specificity (Talanian *et al.*, 1997; Thornberry *et al.,* 1997). The inflammatory caspases 1, 4 and 5 prefer a peptide sequence of WEHD. Apoptotic caspases 2, 3, 7 cleave DEXD whereas caspase 6, 8 and 9 most efficiently cleave I/L/VEXD (where X is either V or H). Importantly, caspase-3 also cleaves the latter peptides with almost similar efficiencies (McStay *et al.*, 2008). Not surprisingly, the DXXD motif is often found in proteins cleaved during apoptosis, consistent with the role of caspase-3 and -7 as executioner caspases of PCD.

1.6.2 Inflammatory caspase substrates

To date the only *in vivo* confirmed caspase-1 substrates are IL-1β (Thornberry, Bull *et al.,* 1992; Yamin *et al.*, 1996), IL-18 (also called IFN-γ-inducing factor, IGIF) (Ghayur *et al.*, 1997; Gu *et al.*, 1997) and caspase-1 itself. *In vitro* caspase substrate screens with recombinant caspase-1 show processing of actin (Kayalar *et al.*, 1996), parkin (Kahns *et al.*, 2003), HSP90 and a handful of proteins involved in the glycolysis pathway (Shao *et al.*, 2007) by caspase-1. These are most likely *in vitro* artefacts due to the use of high doses of recombinant caspase-1 or the

overexpression assays in non- relevant cell lines and have so far not been confirmed with endogenous proteins.

Caspase-7 has been recently identified to be processed by caspase-1 *in vitro*, and bone marrow derived macrophages deficient of caspase-1 did not process endogenous caspase-7 upon a strong microbial stimuli or infection with Salmonella (Lamkanfi *et al.*, 2008). Additionally, lymphocytes from caspase-7 deficient mice were reported to be more resistant against LPS induced cell death (Lamkanfi *et al.*, 2009). Further investigation would be required to show that caspase-7 is indeed a *bona fide* caspase-1 substrate or if the observation is an *in vitro* artefact produced by unnaturally high concentrations of microbial stimuli.

In recent times, IL-33 was also shown to be cleaved by recombinant caspase-1 in vitro (Schmitz *et al.*, 2005). The ligand of the so far orphan ST2 receptor has been identified by an *in silico* search for structural homologues of the β trefoil of IL-18. IL-33, initially cloned from high endothelial cells and hence called nuclear factor from high endothelial venules (NF-HEV) (Baekkevold *et al.*, 2003), was found to bind and activate the ST2 receptor (Schmitz *et al.*, 2005) in conjunction with the IL-1R accessory protein (IL-1RAcP) (Ali *et al.*, 2007). Like IL-1β and IL-18, IL-33 contains a C-terminal β-trefoil fold (Figure 1.9). Based on the structural homology to IL-18, Schmitz *et al* assumed a proteolytic activation just prior to the β-trefoil fold activates this novel cytokine.

So far no substrates for human caspase-4, -5 and mouse caspase-12 have been published and verified.

1.6.3 Consequences of inflammatory caspase substrate cleavage

After synthesis, proIL-1β and proIL-18 are mainly cytosolic until they are processed and activated by caspase-1. A reservoir of inert signalling molecules can thereby be rapidly activated and released. Once cleaved, the cytokines are secreted, although the exact mechanism, possibly even active transport and membrane crossing, is not resolved. Active IL-1β cytokine is a systemic, hormone-like mediator with effects on various cells throughout the body, amplifying inflammation in general. IL-18 acts on Th1 cells, non-polarized T cells, NK cells

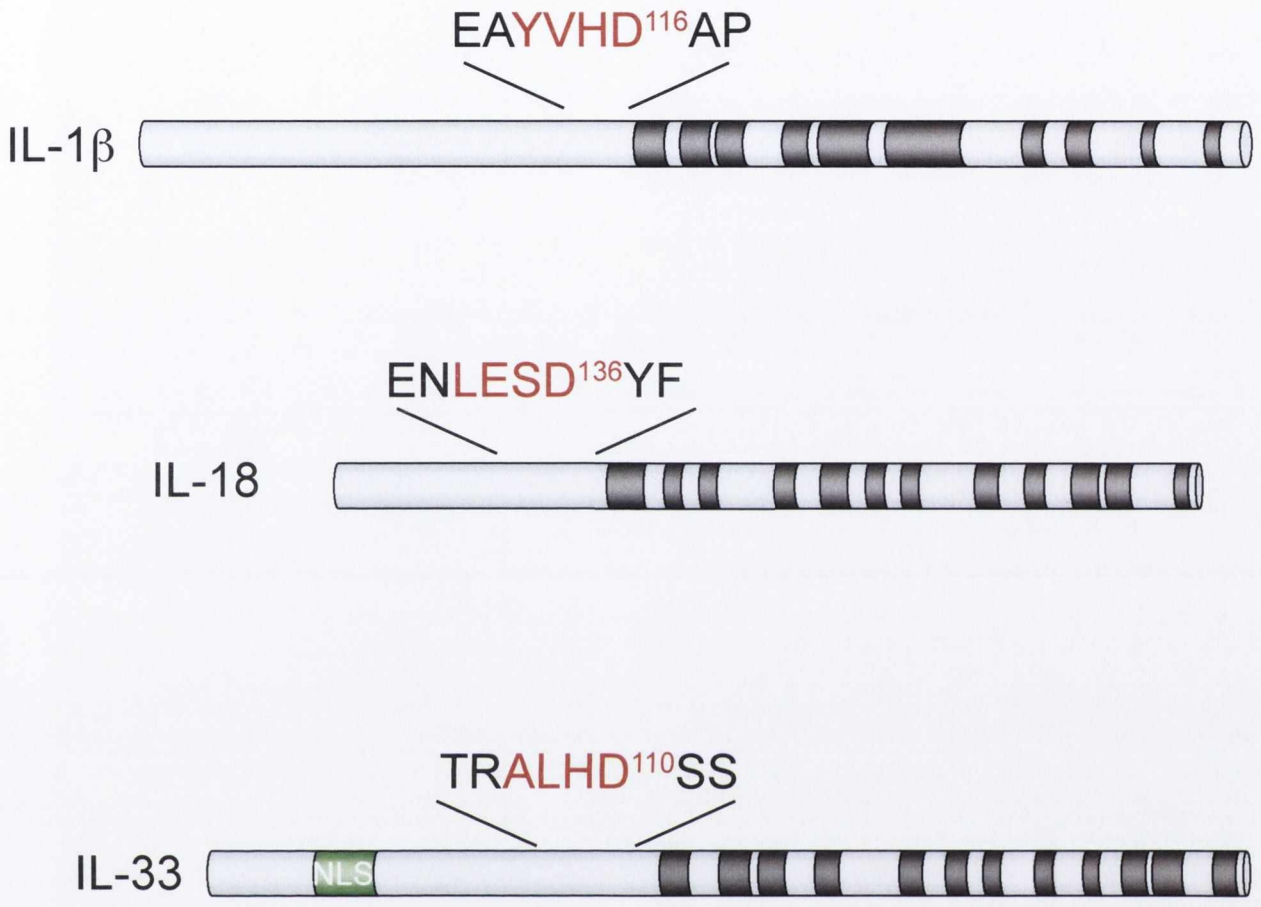

Figure 1.9 Cytokines cleaved by caspases
Schematic representation of the domain structure of IL-1β, IL-18 and IL-33. β sheets of the β-trefoil structure are in dark grey, nucleotide localisation signals in green. Confirmed (IL-1β and IL-18) and putative (IL-33) caspase-1 cleavage sites are indicated above each structure.

and B cells to produce IFN-γ when co-stimulated with IL-12 (Ghayur *et al.,* 1997; Gu *et al.,* 1997; Yoshimoto *et al.*, 1998). Both cytokines bind to their respective IL-1 and IL-18 receptors in the target cells (Sims *et al.,* 1988). These receptors belong to the immuno globulin (Ig) receptor superfamily and activate downstream signalling pathways to induce the NF-κB and the stress related mitogen-activated protein kinases (MAPKs) pathways, thereby enhancing the inflammatory signal even further. Additionally, other cytokines like IL-6 or IL-8 are induced as a result of this. IL-1β also has a systemic effect on the central nervous system by inducing an increase in body temperature (Reviewed in (Dinarello, 2000)).

In contrast to the other IL-1 family members IL-1β and IL-18 which generally induce a cellular immunity against extracellular pathogens, Interleukin-33 triggers a strong Th2 associated response, with the production of IL-4, -5, -13, IgA and IgE (Schmitz, Owyang *et al.,* 2005; Lüthi *et al.*, 2009).

1.6.4 Apoptotic caspase substrates

Over 700 proteins have been identified in various screens *in vitro* (Lüthi *et al.*, 2007) and of those numerous caspases substrates were confirmed *in vivo* and are used by investigators as a readout for apoptotic caspase activity today (Taylor *et al.*, 2008).

1.6.5 Consequences of apoptotic caspase substrate cleavage

Although almost countless substrates have been identified during apoptosis, the exact consequences of the proteolytic event have only been identified for a few of the substrates. This could indicate that the majority of the identified substrates are merely caught up in the final phase of apoptosis and are processed as 'innocent bystanders' (Taylor *et al.,* 2008). The apoptotic caspase substrates can be divided into three broad categories according to the identified function:

In the first group, proteolysis of the substrate leads to an amplification of the caspase cascade. Caspase-3 for example is able to proteolytically activate other caspases, even upstream of itself and the cleavage of bid by either caspase-3 or -8 activates the mitochondrial pathway through bax and bak (Luo *et al.*, 1998).

Caspase substrates in the second category either gain a new function or strongly enhance their usual activity after proteolytic processing. PAK-2 becomes constitutively active after cleavage of the regulatory N-terminal domain from its catalytic C-terminal domain thereby contributing to the cytoskeletal changes seen during apoptosis (Rudel *et al.*, 1997). Removal of the C-terminal auto-inhibitory domain of ROCK1 by apoptotic caspases thereby activates the kinase which enhances the actin-myosin motility which leads to membrane blebbing is an other example.

The third group contains caspase substrates where cleavage leads to an irreversible loss of function. For example, catenins and lamins are part of this group. Degradation of beta and gamma catenin leads to disruption of cell-cell contacts and subsequent cell detachment (Bannerman *et al.*, 1998), processing of lamin A/C results in the disruption of the nuclear lamina followed by nuclear fragmentation (Rao *et al.*, 1996).

The vast majority of these proteins are processed by the possibly more abundant caspase-3 (Walsh *et al.*, 2008) which is also able to proteolytically activate other caspases and hence positively feed back and amplify the caspase cascade.

1.7 AIMS OF THIS STUDY

The aim of this work was to identify novel caspase substrates which may be important immuno-regulatory molecules and should provide new insights into the mechanism of host defense and the pathogenesis of autoimmune diseases. The processes involved in inflammation, especially in innate immunity, are still not fully understood and are essential to treat inflammatory disorders. A novel substrate for inflammatory caspases are putative targets for future anti-inflammatory drugs.

1.7.1 Chapter III and IV

Human caspases have been identified and their function described for over two decades. Most of the work in the field has been focused on apoptotic caspases. As a result over 700 apoptotic caspase substrates have been identified to date (Lüthi and Martin, 2007), but only 2 inflammatory caspase substrates have been confirmed. In order to find new substrates cleaved by the inflammatory caspases,

a proteomic approach is described in chapter III. A cell-free extract model was adapted where we could specifically activate or inhibit the inflammatory caspases and the activated extracts were then resolved on two-dimensional gels and compared to control extracts resolved in an identical way. Protein spot alterations were identified by MALDI-TOF mass spectrometry analysis. As only very few changes were found using this method a second proteomic approach was adopted in chapter IV. A small pool cDNA library was individually transcribed and translated and screened for caspase-1, -4 or -5 substrates. Novel caspase substrates were then verified in the THP-1 cell-free extract system.

1.7.1 Chapter V

During the screening process, Interleukin-33, a novel putative caspase-1 substrate with cytokine activities was reported (Schmitz *et al.*, 2005). Our aim was to confirm the processing of the cytokine by inflammatory caspases with the methods set up in chapter III. To our surprise the cytokine was not processed by inflammatory caspases but was processed at a different cleavage site during apoptosis. We further investigated the functional outcome of IL-33 cleavage by apoptotic caspases which are described in chapter V.

CHAPTER 2

Materials and Methods

2.1 Reagents

Chemicals and general reagents

All reagents unless otherwise stated were obtained from Sigma-Aldrich.

Antibodies

Antibodies used were from the following companies:

Primary antibodies:

α–Caspase-1 CARD	sc-611 Santa Cruz
α-Caspase-1 p10	sc-515 Santa Cruz
α-Caspase-1 p20	Imgenex
α-Caspase-2	BD Translabs
α-Caspase-3	Cell Signaling
α-Caspase-4	MBL
α-Caspase-5	MBL
α-Caspase-6	Upstate
α-Caspase-7	BD Translabs
α Caspase-7 cleaved	Pharmingen
α-Caspase-8	Apotech
α-Caspase-9	Oncogene
α-Rho GDI2	Pharmingen
α-Gelsolin	BD Translabs
α-XIAP	BD Translabs
α-Bid	Cell signalling
α-IL-1β	RnD Systems
α-IL-33	Alexis
α-IL-33 pep1: ^{58}CYFRRETTKRPSLKT^{72}	Sigma Genosys
α-IL-33 pep2: ^{157}CDKVLSYYESQH^{168}	Sigma Genosys
α-CapG	Chemicon
α-co-chaperone p23	Affinity Bioreagents
α-Actin	ICN Bomedicals
α-GR-1-FITC	ImmunoTools
α -GST	Sigma
α -ST2	RnD Systems

Secondary Peroxidase-conjugated antibodies:

Rabbit α-Chicken IgY, Goat α-Rabbit IgG, Goat α-mouse IgG (Jackson Immuno research labs).

2.2 DNA RELATED PROTOCOLS

2.2.1 Preparation of competent bacteria

Two different E.coli strains, DH5α and BL21 (DE3) (Invitrogen) were made competent by the calcium chloride method. A single colony from a freshly streaked bacterial plate was grown overnight in Luria-Bertani broth (LB: 10 g/L Bacto-tryptone (BD), 5 g/L Bacto-yeast extract (BD), 10 g/L NaCl, pH 7.0). 2 ml of this culture were then inoculated in 100 ml LB and grown at 25°C to an OD_{600} of 0.4 to 0.6. The culture was chilled on ice for 10 minutes and pelleted at 800g for 10 minutes at 4°C. The supernatant was completely removed and the pellet was gently resuspended in 10 ml of ice cold, sterile 0.1 M $CaCl_2$. After a 5 minute incubation on ice the bacteria were pelleted again at 800g for 10 minutes at 4°C. The supernatant was removed and the pellet was resuspended in 4 ml of fresh ice cold sterile 0.1 M $CaCl_2$. 3.5% DMSO (140 µl) were added and gently mixed by swirling. After a 15 minute incubation on ice another 3.5% DMSO (140 µl) were added and the bacteria were aliquoted and snap frozen in liquid nitrogen and stored at -70°C.

2.2.2 Transformation of Competent Bacteria

50 µl of competent bacteria were typically used for the transformation of about 1 µg of plasmidic DNA. After 30 minutes on ice, time required for the plasmid to coat the bacteria, the cells were heat-shocked at 42°C for 40 seconds and allowed to recover on ice for

2 minutes. 450 µl of LB were added and the bacteria were incubated at 37°C at 220 rpm for one hour to allow the expression of the antibiotic resistance gene. 2.5 µl to 100 µl of each transformation in a total volume of 200 µl of LB were then plated on LB Agar plates containing 100 µg/ml Ampicillin.

2.2.3 Crude Plasmid DNA Preparation

DNA plasmids were prepared following the alkaline lysis protocol. 1 ml of a 3 ml overnight starter culture was pelleted at top speed in a microcentrifuge for 1 minute and the supernatant was removed completely. The pellet was resuspended in 100 µl of P1 buffer (50 mM Tris-HCL, pH 8, 10 mM EDTA) by vortexing. 200 µl of P2 buffer (0.2 M NaOH, 1% SDS) was added and the tube inverted 6 times to lyse the bacteria before adding 200 µl P3 buffer (3 M KAc, pH 5.5) to precipitate the bacterial genomic DNA. The tube was inverted 6 times, chilled on ice for 5 minutes and the precipitate was pelleted at top speed for 15 minutes. The supernatant which contains the plasmid DNA was transferred to a new Eppendorf tube and 0.7 volume of isopropanol was added to precipitate the DNA. The tube was mixed by inversion every 5 minutes for 20 minutes at room temperature before pelleting the plasmidic DNA at top speed for 10 minutes. The supernatant was removed completely and the pellet was washed in 1 ml of ice cold 70% Ethanol. After another centrifugation, the supernatant was removed completely and the DNA pellet was allowed to air dry for 10 minutes before resuspending it in 10 µl of RNAse/DNAse free H_2O, followed 5 minutes later by 10 µl of TE (10 mM Tris-HCL pH 8, 1 mM EDTA). 1 µl to 3 µl of each miniprep was checked on a 0.6% Agarose gel and the DNA was stored at 4°C.

2.2.4 Agarose gel electrophoresis

DNA yield was typically assessed by electrophoresis through agarose gels alongside a ladder of marker DNA fragments of known sizes. Agarose suspensions of 0.6 % to 1.2 % agarose were prepared in TAE (40 mM Tris-HCl, pH 8, 1 mM EDTA), melted by microwaving, and solidified in gel casting rigs. DNA was diluted in loading buffer and electrophoresed through the gel at 5-10V /cm. Gels were incubated an ethidium bromide solution for 20 minutes and visualised and documented in a Biorad Gel Doc 2000 system under UV light.

2.2.5 DNA quantitation

DNA was accurately quantitated by spectrophotometry. Double-stranded DNA was diluted 1:200 in nuclease free H_2O and triplicate readings of $OD_{260/280}$ measured in a quartz cuvette using a Bio-Rad spectrophotometer.

2.2.6 Genecleaning procedure

Genecleaning was used to generate ultra-pure DNA for cloning. The gel band or solution containing the amplified PCR product was excised and melted in 3 volumes of 6 M NaI at 50°C for 5 to 10 minutes. 5 µl of silica / µg of nucleic acid were typically added to capture the DNA under constant rotation for 10 minutes at room temperature. The DNA bound on the silica was spun down at 20,000 g for five seconds and washed three times with 750 µl of wash buffer (10 mM Tris-HCL, pH 7.5, 50 mM NaCl, 2.5 mM EDTA, 50% ethanol). The silica pellet was air-dried for 2 minutes and resuspended in ddH_2O, pelleted again at 20,000 g for 5 seconds and the supernatant containing the purified DNA was kept.

2.2.7 Restriction digest

DNA was digested using restriction endonucleases, following the manufacturers instructions (NEB UK) at 37°C for 16 hours. Digestion controls were included where no or only a single enzyme was added. Digestion products were run on agarose gels, gel extracted and purified by genecleaning as previously described.

2.2.8 DNA ligation reactions

The DNA mix consisting of 200 ng of digested and genecleaned vector alone or with a 2 fold greater molar amount of digested and genecleaned PCR product was incubated at 45°C for 5 minutes to melt re-annealed DNA stretches. 0.1 Weiss unit T4 DNA ligase (NEB) was added and the reaction was incubated for 16 hours at 16°C. 5µl of the control ligation (vector only) and the ligation with the PCR product were transformed into competent DH5α. Single colonies were picked and grown overnight in 3 ml LB culture containing the selective antibiotic. The following day, DNA minipreps were made as described previously. The DNA was submitted to migration on a 0.6% agarose gel and compared to the vector alone. Upshifted DNA containing an insert were digested with the restriction enzymes used for the subcloning to verify the release of the insert. The DNA of positive clones was isolated and sent for sequencing (MWG Biotech).

2.2.9 PCR

PCR reactions were carried out to amplify genes for cloning. PCR reaction volumes were typically 50 µl for gene amplification and 25 µl for control reactions.

The DNA polymerase used for amplification was Taq (Qiagen), at 2.5 units per reaction. Other reaction constituents were:

100 - 500 ng of Qiagen-purified template DNA
Taq buffer from a 10 x stock supplied by the manufacturer
200 μM each of dATP, dTTP, dCTP, dGTP
100 - 200 nM forward and reverse oligonucleotide primers, typically incorporating restriction sites for cloning purposes

Reactions were then put through a PCR programme involving:

- initial denaturing:		3 minutes 94 °C
- 30-35 cycles of:	*denaturation*	1 minute 94 °C
	annealing	1 minute 55 - 60 °C
	elongation	1 minute/ kB 72 °C
- final elongation:		10 minutes 72 °C

Primer sequences used for cloning caspase-1.p30 into pET.15b (BamHI, XhoI site):

Caspase-1.p30.Forward	5'-AAA CTC GAG AAC CCA GCT ATG CCC -3'
Caspase-1.p30.Reverse	5'-TTT GGA TCC TTA ATG TTC TGG GGA G-3'

2.3 PROTEIN RELATED PROTOCOLS

2.3.1 Induction of fusion proteins in bacteria

His-tagged proteins were expressed from the pET15b, pET23b and pET45b vectors, which encode an N-terminal His^6 tag and contain a T7-driven promoter sequence. Plasmids encoding the tagged protein were transformed into *E. coli* BL21 DE3 pLysS bacteria that contain an inducible T7 polymerase gene.

GST-tagged proteins were expressed from the pGEX4TK2 vector, which encodes an N-terminal GST tag. Plasmids encoding the tagged protein were transformed into DH5α bacteria.

Transformed bacteria were inoculated to 3 ml cultures in LB with antibiotic. After overnight growth in a 37 °C shaker incubator, cultures were diluted to between 50 ml and 5 L in LB with antibiotic, to give an OD_{600} of 0.1. Cultures were then incubated in a 37°C shaker incubator until bacteria reached an OD_{600} of 0.4 - 0.6. isopropylthio-β-D-galactoside (IPTG) (Melford) was then added to a final concentration of 200 μM -1mM. Cultures were incubated at 18 - 37 °C in a shaker incubator, typically for 1 to 3 hours. After induction, cells were pelleted at 5000 g for 10 minutes and frozen at -70°C.

2.3.2 Purification of fusion proteins expressed in bacteria

(I) His^6-tagged proteins

Pellets of bacteria induced to express His^6-tagged protein were thawed and resuspended in TM lysis buffer (50 mM Tris-HCl, pH 8.5, 10 mM β-mercaptoethanol, 1 mM PMSF, 2 μg/ ml aprotonin, 10 μg/ ml leupeptin) at 2 % of the original culture volume. Resuspended bacteria were lysed by sonication using 6 x 30 second 4 to 7 W pulses on ice in a Branson 150 sonifier. Insoluble material was removed by centrifugation at 15,000 g for 15 minutes. Supernatant was then incubated with 2.5 - 50 μl/ ml Ni-NTA agarose (Qiagen) on a rotating platform at 4 °C for 4 to 18 hours.

The Ni-NTA agarose was pelleted at 1000 g for 1 minute and washed twice in imidazole wash buffer (20 mM Tris-HCL, pH 8.5, 100 mM KCl, 10 mM 2-Mercaptoethanol, 10% glycerol, 20 mM imidazole). To elute the recombinant protein from the Ni-NTA agarose, the beads were incubated in imidazole elution buffer (Protease reaction buffer (PRB: 50 mM HEPES pH 7.4, 75 mM NaCl, 0.2% CHAPS, 2 mM DTT) containing 100 mM imidazole, 1 mM Phenylmethylsulphonyl-fluoride (PMSF), 2 μg/ml aporotinin, 10 μg/ml leupeptin) under constant rotation at 4°C. After 30 minutes the Ni-NTA agarose beads were pelleted at 1000 g for 1 minute and the supernatant containing the His-tagged protein was kept. The elution was repeated another 2-5 times until no further protein was liberated.

(II) GST-tagged proteins

Bacteria induced to express GST-tagged proteins were brought up in NETN buffer (20 mM Tris-HCl, pH 8, 100 mM NaCl, 1 mM EDTA, 0.5 % NP40) at 2 % of the original culture volume and the cells were lysed by sonication as described above. GST-tagged protein was then captured from cell supernatants on 10 - 20 µl/ ml glutathione sepharose resin (Amersham) under rotation at 4 °C for 4 to 18 hours. The resin with captured protein was washed in 3 x 1 ml of PBS and 1 ml of PRB. The protein was then eluted by incubation in 0.5X volumes of PRB or PBS containing 10 to 20 mM glutathione, under rotation at room temperature. The elution was repeated another 2-5 times until no further protein was liberated.

2.3.3 *In vitro* protein synthesis in rabbit reticulocyte lysates

Radio-labelled recombinant proteins were synthesised using a coupled *in vitro* transcription and translation system based on rabbit reticulocyte lysates depleted of amino acids (TNT, Promega). Proteins were labelled with ^{35}S methionine (10 mCi/ ml, Amersham or ISIS).

Individual reactions were set up on a 25 µl scale:

12.5 µl rabbit reticulocyte lysate
1 µl TNT reaction buffer
1 µl amino acid mix (without methionine)
0.5 to 1 µl ^{35}S methionine
1 µg Qiagen-pure template plasmid DNA
1 µl RNAsin
1 µl T7 polymerase
dd$H_2$0 to 25 µl

For the small pool cDNA library screen a commercially available master mix containing all enzymes and buffer constituents was used:

200 to 400 ng Qiagen-pure small pool cDNA
20 µl SP6 TNT Quick Mastermix rabbit reticulocyte lysate (Promega)
2 µl ^{35}S methionine
dd$H_2$0 to 25 µl

Reactions were incubated at 30 °C for 2 hours.

2.3.4 Purification and endotoxin removal of bacterial produced protein

Eluted IL-33 was extensively dialysed 2 to 3 times against PBS in 5kDa MWCO Slidealyzer (Promega) for 4 to 12 hours each time. Subsequently, at least three rounds of agarose-immobilized polymyxin-B (Sigma) depletion were performed according to the manufacturer's protocol.

2.3.5 *In vitro* protein cleavage with recombinant proteases

The bacterial expressed or *in vitro* transcribed and translated proteins were incubated with the indicated amount of recombinant protease in PRB at 37°C for 2 to 4 hours. 2 mM DTT was added to reactions containing caspase-7 as this dramatically increased the activity of the protease. It remains unclear whether this is a similar effect observed with caspase-2 where possible disulfide bridges between the large and small subunit are broken by the addition of the strong reducing agent.

2.3.6 *In vitro* protein pull-down assay

1 μg GST-IL-33 was immobilised on 30 μl Glutathione Sepharose 4B (Amersham Biosciences, UK) by rotation at 4°C for 30 minutes, followed by addition of 1 μg of recombinant ST2.Fc (Alexis, UK) and further incubation for 4 h in 1 ml of reaction buffer (50 mM Tris, pH 7.6, 120 mM NaCl, 0.1% CHAPS).

2.4 PROTEIN ANALYSIS

2.4.1 SDS Polyacrylamide Gel Electrophoresis

Proteins were separated using standard SDS-PAGE conditions. Protein samples were denatured by resuspension in SDS loading buffer (2% SDS, 50 mM Tris-HCL, pH 6.8, 10% glycerol, 2.5% β-mercaptoethanol) and heated at 94°C for 7 minutes. The samples were loaded on 8% to 15% polyacrylamide gels and the gels were resolved at 55 V (stacking gel) / 75 V (resolving gel) on Protean III apparatus (BioRad) and at 60 V / 90 V on Criterion apparatus (BioRad).

2.4.2 Coomassie Blue staining

After electrophoresis, the acrylamide gels were stained overnight in a solution of Coomassie Blue (45% Methanol, 10% acetic acid, 0.25% Coomassie Brilliant Blue) followed by destaining in destain solution (45% methanol, 10% acetic acid) and stored in ddH_2O or dried down at 50°C in a GelAir Dryer (BioRad).

2.4.3 Immunoblotting

Proteins separated by SDS PAGE were transferred for 12 to 16 hours at 35 mA onto 0.2 µm nitrocellulose membranes (Schleider and Schull) in transfer buffer (48 mM Tris-HCL, pH 8.3, 39 mM Glycine, 0.037% SDS, 20% Methanol). Membranes were then blocked for 30 minutes in TBST (10 mM Tris-HCL, pH 8.0, 150 mM NaCL, 0.05% Tween-20) with 5% (w/v) non-fat dried milk (Marvel) and then probed with the primary antibody diluted at 1:500 to 1:5000 for two hours in blocking buffer. The membranes were then washed for three times for 10 minutes in TBST and re-incubated with the appropriate horse-radish peroxidase coupled secondary antibody at 1:1000 in TBST with 5% (w/v) non-fat dried milk for one hour. The membranes were washed again for 3 times for 10 minutes in TBST and the signal was detected with enhanced chemiluminescence Supersignal West Dura / Pico (Pierce) by exposing the blots to sensible film (HyperfilmMP, Amersham)

2.4.4 Detection of ^{35}S-methionine labelled proteins

^{35}S-methionine labelled proteins were resolved by SDS-PAGE. The gels were incubated for 2 hours or overnight in fixing solution (45% methanol, 10% acedic acid) and then incubated for 25 minutes in Amplify reagent (Amersham). The gels were dried down at 80°C under vacuum on a 3MM Whatman paper (Whatman) and exposed to autoradiographic film (HyperfilmMP, Amersham) for 12 to 72 hours at -70°C.

2.4.5 2-Dimensional SDS-PAGE

First Dimension Isoelectric Focusing

The protein samples were brought up to 400 µl of 2D solubilisation buffer (8 M urea, 4% CHAPS, 0.1 M DTT, 0.05% SDS, 0.5% ampholytes pI 3-10 (BioRad), 0.03% bromophenol blue) and actively rehydrated at 50 V into 17 cm IPG strips (BioRad) at 20°C for 14 to 16 hours in a BioRad Protein Iso Electrical Focusing (IEF) Cell system. The following day isoelectric point focusing was done as follows:

- Linear voltage ramp to 500 V over one hour;
- 500 V for five hours;
- Linear voltage ramp to 3500 V over five hours;
- 3500 V for 11 hours.

Second Dimension Electrophoresis

The IPG strips were incubated in reducing buffer (6 M urea, 375 mM Tris-HCL, pH 8.8, 2% SDS, 20% glycerol, 2% DTT) for 5 minutes and then in alkylating buffer (6 M urea, 375 mM Tris-HCL, pH 8.8, 2% SDS, 20% glycerol, 2.5% Iodoacetamide (IAA)) for 5 minutes. The strips were then placed on top of a 12% SDS-PAGE gel in easy-melt agarose (BioRad) and proteins were separated at 37.5 mA per gel in the BioRad Protein II xi electrophoresis cell for about 4 hours.

2.4.6 Mass-Spectrometry Compatible Silver Staining Protocol

The gels were fixed for at least 30 minutes in 50% Methanol / 10% acetic acid, washed for 10 minutes in 50% methanol and then three times for 10 minutes in ddH_2O. After a one minute sensitation (0.02% $Na_2S_2O_3$) and two brief rinses in ddH_2O, the gels were incubated in a chilled silver nitrate stain solution (0.1% $AgNO_3$) for 20 minutes. After two brief rinses in ddH_2O, the gels were developed in 0.04% Formalin / 2% Na_2CO_3. About 3 changes of the solution were required to obtain the development which was stopped by changing the developer for a solution of 5% acetic acid. The gels were stored in 1% acetic acid at 4°C.

2.4.7 Trypsin Digestion for MALDI-TOF mass spectrometry

The spots of interest were manually excised from the gel and destained in 15 mM $K_3Fe(CH)_6$, 50 mM $Na_2S_2O_3$ for 5 minutes in an orbital shaker at 800 rpm. After 5 washes (50% methanol, 10% acetic acid) and setting the pH in 50 mM NH_4HCO_3

the gel spots were dehydrated in 500 µl CH_3CN and dried for 5 minutes in a speed-vac (ThermoSavant). The dried gel-piece was rehydrated in 3 µl digestion buffer (12.5 mM NH_4HCO_3, 0,05% n-octyl β-D-glucopyranoside) with 150 ng trypsin for 5 minutes, then another 10 µl digestion buffer was added and the protein was digested in the gel at 37°C for 14 to 16 hours.

2.4.8 MALDI-TOF mass spectrometry

0.5 µl of the supernatant of the digest was spotted on a Teflon-coated 96-well MALDI target plate (Applied Biosystems) followed by 0.5 µl of the matrix solution (10 mg/ml α-cyano-4-hydroxy-cinnamic acid, 60% acetonitrile, 0.1% TFA). The samples were allowed to crystallise before being analysed on a Voyager DE-Pro mass spectrometer (Applied Biosystems) in positive reflector mode. Peptide fingerprint data of 600 to 1200 laser shots were collected per sample, deisotoped and internally mass calibrated against known trypsin peptides. The MASCOT (http://www.matrixscience.com) and MS-Fit (http://prospector.ucsf.edu/ucsfhtml4.0/msfit.htm) databases were searched with the peptide mass data against theoretical trypsin digested proteins of the NCBI or SwissProt protein data base.

2.4.9 Fluorimetric analysis of enzymatic activity

The proteolytic activity of each caspase was measured by the rate of hydrolysis of fluorogenic peptide substrates. These included the tetrapeptides WEHD, YVAD, DEVD and IETD conjugated to 7-Amido-4-methylcoumarin (AMC) (Bachem). The assay was done in a 50 to 100 µl reaction volume with 50 µM fluorogenic substrate in PRB and the recombinant caspase. The increase of released AMC was measured and recorded in a SpectraFluor Plus (Tecan) at an excitation wavelength of 360 nm and detection wavelength of 465 nm.

2.4.10 NF-κB reporter assay

10 µl of cell supernatant of control or treated HEK293.ST2L.NFkB-SEAP cells were incubated with 90 µl Quanti-Blue (InvioGen) and 100 µl ddH_2O for 2 to 8 hours at 37^0C. The absorption was measured and recorded in a SpectraFluor Plus (Tecan) at a wavelength of 590 nm. The detected values were then graphed as fold increase against untreated cell supernatant.

2.4.11 Active site titration of caspases

To determine the activity of each batch of expressed caspase, the proteases were active site titrated against zVAD-fmk. The recombinant caspase-1, -3 and -7 were incubated in a 20 μl volume with a range of concentrations (0, 6.25, 12.5, 25, 50, and 100 nM) of zVAD-fmk for 30 min at 4°C. Residual caspase activity of each reaction was then individually determined by monitoring the hydrolysis of WEHD-AMC or DEVD-AFC as described above. The hydrolosys rate of each reaction was graphed against the correspondingly used concentration of zVAD-fmk. The point at which a calculated regression line intersects the x-axis (where the protease was completely inhibited) represented a 2 fold molar activity of the caspase (as there are two active sites in each molecule).

2.4.12 Enzyme-linked immunosorbent assay

Cells were lysed in buffer containing 150 nM NaCl, 50 nM Tris (pH 8), 1% NP-40, and 0.1% SDS. Cytokines in cell lysates or medium were detected by ELISA with paired antibodies for IL-4, IL-5, IL-6 (BD PharMingen, UK), IL-33, and IL-1β (R&D Systems, UK) according to the manufacturer's recommendation.

2.5 CELL CULTURE BASED METHODS

2.5.1 Cell culture

Origin of the cell lines:

THP-1	Prof. Steven Whitehead and ACC
JURKAT	Prof .Doug Green
HEK293T	Prof. Inder Verma
HEK293.ST2L.NfkB-SEAP	Opsona
HeLa	Prof. Doug Green

The human monocytic cell line THP-1 cultured in RPMI medium (Gibco) supplemented with 10% FCS (Sigma) and 2 mM L-glutamine (Gibco).

Human embryonic kidney (HEK) 293T and HEK293 cells were grown in DMEM medium (Gibco) supplemented with 10% bovine calf serum (Sigma) and 2 mM L-glutamine (Gibco). The HeLa and Jurkat T lymphocyte cell lines were cultured in RPMI (Gibco) supplemented with 5% bovine calf serum (Sigma) and 2 mM L-glutamine (Gibco).

Cells were passaged every 2-4 days. Adherent cells were trypsinised with Trypsin-EDTA (0.25% trypsin, 1 mM EDTA, in Hank's balanced salt solution) (Gibco) at 37 °C. The trypsin was inactivated by addition of fresh medium with bovine calf serum. The cells were pelleted at 250g for 5 minutes, resuspended in culture medium and transferred to new plates or flasks.

2.5.2 Preparation of Cell-Free Extract

$2x10^8$ to $1x10^9$ THP-1 cells were incubated with 1 µg/ml of LPS from *E.coli* or S. typhimorium for 5 hours at 37 °C with 5 % CO_2. The cells were then spun down at 400 g for 10 minutes and the pellet was washed twice with PBS (137 mM NaCl, 2.7 mM KCl, 4.3 mM Na2HPO4, 1.4 mM KH2PO4) and resuspended and transferred in 1ml Buffer A (20 mM Hepes-KOH, pH 7.5, 10 mM KCl, 1.5 mM MgCl2, 1 mM EDTA, 1 mM EGTA, 1 mM dithiotheritol (DTT), 100 µM phenylmethylsuphonyl fluoride (PMSF), 10 µg/ml leupeptin, 2 µg/ml aprotinin) to a 2 ml Dounce-type homogenizer. The cells were pelleted at 800g for 10 minutes and the supernatant was removed. To one volume of cell pellet, 3 volumes of Buffer A were added to resuspend the pellet. After a 15 minute swelling in the hypotonic buffer on ice the cells were disrupted with a B-type pestle with 15 to 30 strokes, taking samples after every 5 strokes and examining a small aliquot under a light microscope. The crude lysate was then cleared with two sequential centrifugations of 15,000g for 10 minutes at 4 °C. The supernatant was aliquoted and stored at -70°C until used. For in vitro activation of caspases involved in inflammation, THP-1 cell-free extracts were diluted to 80% in CEB and incubated at 37°C for 2 hours. To provoke apoptosome-dependent caspase activation, bovine heart cytochrome c and dATP were added to reactions to final concentrations of 50 µg/ml and 1 mM, respectively.

2.5.3 Transient transfection

(I) Calcium phosphate precipitation method

HEK293T cells were seeded at a density of 2 x 10^5 cells/well in 6-well tissue culture plates 24h prior to transfection. Precipitates were prepared by mixing the appropriate amount of Qiagen-pure filter-sterilized DNA made up to 125 µl with sterile 0.5X TE (5 mM Tris-Cl, pH 8.0, 0.5 mM EDTA) with 25 µl sterile $CaCl_2$. The DNA/$CaCl_2$ mixture was added drop-wise 125 µl 2X HBS (280 mM NaCl, 10 mM KCl, 1.5 mM Na_2HPO_4, 12 mM dextrose, 50 mM HEPES, pH 7.05). Following a 20 min incubation period the complexes were added to the cells. DNA complexes were typically allowed to remain on cells for 6h before replacing with fresh medium. The cells were then incubated for 24 to 72 hours to allow protein expression.

(II) Genejuice method

HeLa cells were plated at 10^5 cells/well in 6-well tissue culture plates 24h prior to transfection. 1 µl GeneJuice transfection reagent (Novagen) was diluted in 100 µl RPMI, incubated for 5 minutes and then added drop-wise to the Quiagen-pure filter-sterilised DNA. After 20 min incubation, the mixture was added to the cells. The cells were then incubated for 24 to 48 hours to allow protein expression.

2.5.4 Induction of apoptosis

Adherent cells were typically plated at 10^5 cells/ well in 6-well plates, or 1 - 2 x 10^6 cells/ plate in 10 cm plates, on the day before treatment. Apoptosis was induced by incubation with the indicated concentrations of daunorubucin (Dauno), tumour necrosis factor (TNF), cyclohexamide (CHX) or cisplatin for 8 to 12 hours. The percentage of apoptotic cells was assessed by morphological features (cell shrinkage, chromatin condensation, blebbing, detachement).

2.5.5 Cell lysate preparation

To make cell lysates for SDS-PAGE analysis, cells were pelleted at 800 g, washed in PBS pH 7.2, and brought up at 2 x 10^7 cells/ ml in SDS-PAGE loading buffer. Lysates were then denatured for 7 minutes at 93 ^{0}C and analysed by SDS-PAGE.

2.5.6 Light microscopy

Cytospins were analysed at 40 - 100 x magnification under an Olympus BX51 and documented with an attached FluoView Cam.

2.6 *IN VIVO* EXPERIMENTS

2.6.2 Animals

C57BL/6 and BalbC mice were obtained from Harlan U.K under the licence of EC Lavelle. Animal experiments and maintenance were approved and regulated by the Trinity College ethics committee and the Irish Department of Health.

2.6.2 Preparation of peripheral blood samples

Approximately 150 to 300 µl blood was collected from the tail vein and immediately anticoagulated with 100 µM EDTA.

(I) Cytospins

Of 50 µl anti-coagulated blood the red blood cells were lysed with 1 ml of RBC buffer (150 mM NH_4Cl, 10 mM $NaHCO_3$, 100 µM EDTA, pH8). After 3 to 5 minutes the remaining leukocytes were spun down at 500g for 5 minutes. The cells were resuspended in 150 µl PBS and transferred to a glass slide in a Cytospin 4 (ThermoShandon) at 300 rpm for 3 minutes.

(II) FACS analysis

50 µl anticoagulated blood was fixed and lysed in FACS lysis buffer (BD, UK) for 5 minutes, pelleted at 500g for 5 minutes and resuspended in 200 µl PBS. The samples were enumerated with a hemostatometer and scored for lymphocytes (medium to high forward scatter, low side scatter), monocytes (medium to high forward scatter, low to medium side scatter) and neutrophils (low to medium forward scatter, high side scatter) on a FACScalibur (BD, UK).

2.7 STATISTICS

Data are presented in this study by mean ± S.E.M where available. Statistical analyses were made with unpaired Student's t test where *: $p<0.05$ and ** $p<0.01$

CHAPTER 3

Identification of caspase-1 substrates by two-dimensional SDS-PAGE

3.1 INTRODUCTION

Caspases are a family of proteases involved in critical cellular processes; from orchestrating the cellular destruction during apoptosis to playing an essential part in the innate immune system. In this initial first line of defence inflammatory caspases participate in signalling cascades involved in recognition and removal of harmful pathogens or the detection of tissue injury. While our knowledge of what our immune system senses has greatly expanded in the past decade, relatively little is known about the exact signalling pathways initiated within the cell following interaction with a pathogen.

The identification of caspase substrates during apoptosis has greatly enhanced our understanding of the specific steps involved in a cell undergoing programmed cell death. To date, over 700 substrates for the apoptosis-associated caspases have been described (Lüthi and Martin, 2007) (for an up to date list see www.casbah.ie). Strikingly, only 2 inflammatory caspase substrates, IL-1β and IL-18, have been confirmed. Both of these caspase-1 substrates are integral to the inflammatory response requiring caspase-1 processing to become mature, functional cytokines. Therefore, discovery of additional caspase-1 substrates would be predicted to identify further important inflammatory mediators or regulators.

3.2. SUMMARY

The aim of the first part of this study was to identify novel inflammatory caspase substrates in order to gain further insight into the process of inflammation. Our initial approach is outlined in Figure 3.1. The first stage of the analysis involved developing a system to generate a large proteome pool in which we could specifically activate inflammatory caspases. Since the discovery of caspases, cell-free systems of cytosolic cellular extracts have proven to be a valuable tool for monitoring the degradation of the proteome during caspase-activation *in vitro*. The cell-free system has been used extensively in our lab to screen in different species (man, mouse, fly and worm) for novel protease substrates involved in apoptosis.
The cell-free extract system was adapted for the use of THP-1 cells, a well established monocytic cell line used as a tissue culture model for research in

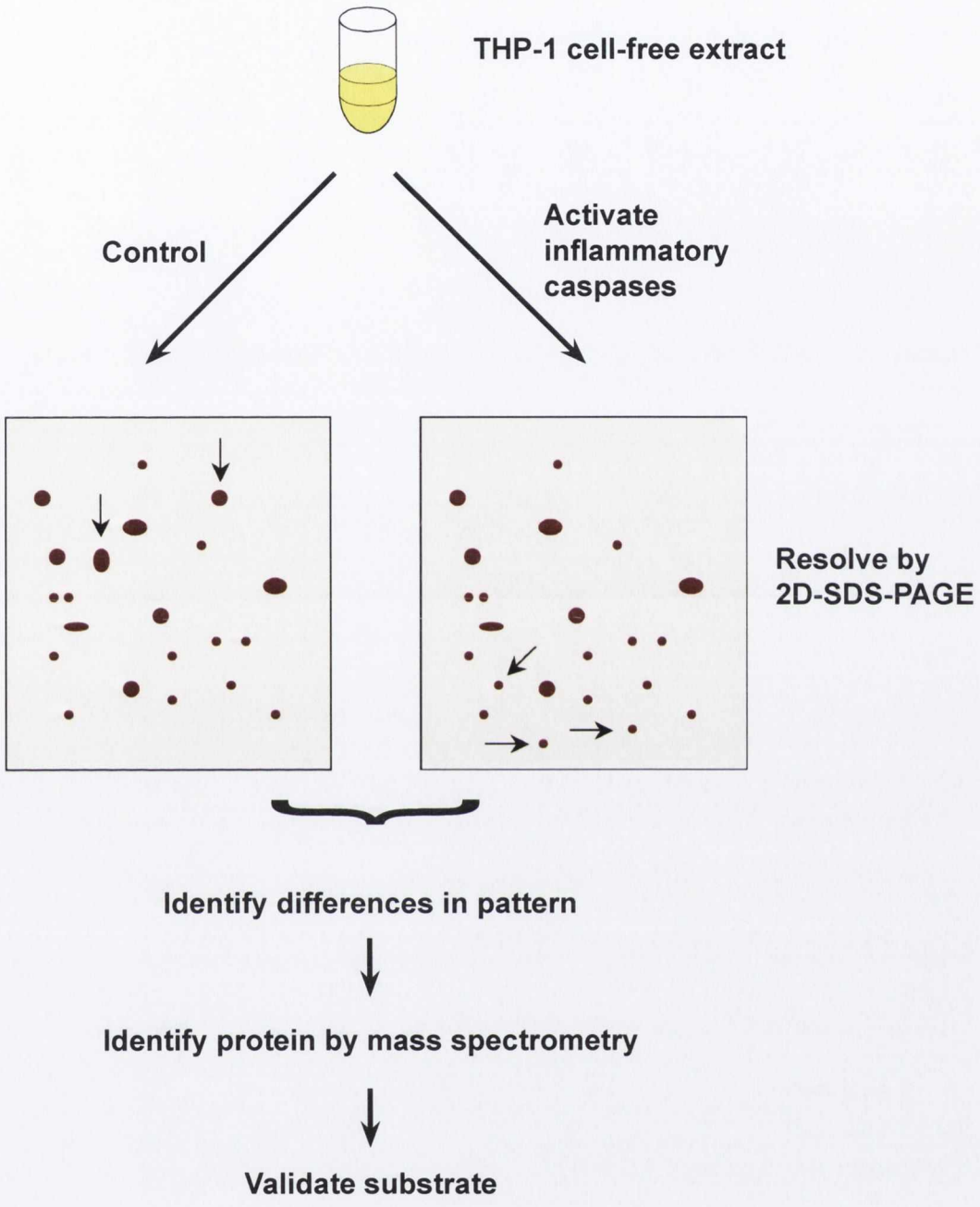

Figure 3.1

Identification of inflammatory caspase substrates using 2D SDS-PAGE and mass spectrometry

Endogenous inflammatory caspases are activated in a proteome and separated according to their isoelectric point and molecular weight on large-format gels. The resolved protein was stained with silver nitrate and the changes in the protein profiles of inflammatory caspase activated versus control gels was visualy compared. Altered protein spots were excised from gels and in-gel trypsin digested. The resulting peptide fingerprint measured by mass spectrometry was compared to an *in silico* digested database of proteins.

inflammation. We manipulated this monocyte cell-free system to specifically activate caspases-1, -4 and -5 and avoided activation of the caspases involved in apoptosis.

Larger amounts of control and inflammatory caspase activated cell-free extracts were separated into discrete protein spots according to their isoelectric point and molecular weight on 2D SDS-PAGE gels. The proteins were stained with silver nitrate and to our surprise only very few, but highly reproducible, alterations to the proteome could be detected. Repeating the experiment where caspases involved in apoptosis were activated, a great number of reproducible changes were detected. The altered proteins identified were excised from the gels, digested with trypsin and identified by MALDI-TOF mass spectrometry. Besides IL-1β and a proteolytic fragment of caspase-1, the only protein showing a mobility shift on the gels where inflammatory caspases were activated was Gelsolin like capping protein (CapG).

Further analysis in the THP-1 cell-free extract indicated that neither *in vitro* transcribed and translated nor endogenous CapG was processed by any caspase associated with inflammation.

3.3. RESULTS

3.3.1 Establishing a controllable caspase-1 activation assay

Our first approach to identify novel caspase-1 substrates was to use an endogenous system where we could control the activity of inflammatory caspases. Cell-free systems have previously been used to identify caspase substrates cleaved under apoptotic conditions (Lazebnik *et al.*, 1994; Martin *et al.*, 1995) and identify components and processes of the cell-death machinery (Liu *et al.*, 1996; Slee *et al.,* 1999). To obtain the large amount of soluble proteins required for 2D analysis we adapted a previously used cell-free based protocol for THP-1 cells, a monocytic cell line established from a patient with acute monocytic leukaemia (Tsuchiya *et al.*, 1980). THP-1 cells are a monocytic cell line known to express caspase-1 and secrete active IL-1β upon LPS treatment. A similar cell-free system was previously used to discover the caspase-1 activation platform and identify the components of the NALP1 inflammasome (Martinon *et al.,* 2002).

THP-1 cells were activated by incubation with LPS from *E. coli*, thereby inducing the expression of pro-IL-1β and any other proteins potentially involved in inflammatory caspase activation or signalling. Additionally, this enabled us to use the processing of endogenous IL-1β as a readout for caspase-1 activity. Subsequent steps were performed on ice to prevent spontaneous formation of the inflammasome, activation of the inflammatory caspases and processing of any putative substrates. Activated THP-1 cells were pelleted and as much buffer as possible was removed, as high salt concentrations inhibit the formation of the inflammasome (Petrilli *et al.*, 2007) and can interfere with subsequent isoelectric focusing of the proteins during the 2D SDS-PAGE gel analysis. The cells were incubated in a hypotonic buffer, containing only 10 mM KCL to favour inflammasome assembly and inflammatory caspase activation. The swollen cells were ruptured by homogenisation leaving nuclei and mitochondria still intact. The homogenate was cleared of debris and unbroken cells by centrifugation, and the cytosolic component (cell-free extract) was used for further experiments.

Incubation of the THP-1 cell-free extract at 37°C triggers the spontaneous activation of caspase-1 which was processed to an intermediate p35 form

representing the N-terminal CARD domain and the large subunit, and the p10 form representing the small subunit (Figure 3.2A upper panel). After only 15 minutes incubation, full-length caspase-1 was processed to the p35 form and the p10 subunit becoming visible at 30 minutes. After two hours incubation, pro-caspase-1 completely disappeared. The rate of caspase-1 activity was directly proportional to the total protein concentration of the cell-free extract (Data not shown). 80% of THP-1 cell-free extract in buffer A was used in this example, which resulted in a total protein concentration of 10 μg/μl. This showed a gradual processing pattern of caspase-1 over the investigated time points. Using IL-1β as a readout for caspase-1 activity, the processing of the pro-IL1β p35 subunit to the active p17 form was apparent after 15 minutes of incubation. The pro-IL-1β protein was completely processed by activated caspase-1 after 90 minutes incubation (Figure 3.2 A lower panel).

We could not detect endogenous levels of IL-18, another known caspase substrate in the THP-1 cell-free extract by immunobloting, as the protein concentration was not sufficient for the sensitivity of our antibody (data not shown).

Having thus identified a system where we can induce and monitor caspase-1 activity, we also needed to establish a control system where no caspase-1 substrate processing occurred. The control cells were also LPS treated in the same way, allowing for any other proteome modifying reactions during the incubation. To block caspase-1 activity we utilised a caspase inhibitor to prevent caspase-1 mediated processing of substrates. By this method, alterations in protein spots on two-dimensional SDS-PAGE gels in the absence of caspase inhibitors should be solely attributed to the caspase-1 activity.

Known caspase inhibitors were titrated into the above system to establish whether the activity of spontaneously activated caspase-1 could be inhibited. We used synthetic aldehyde peptides which bind the protease active site and act as reversible inhibitors. Three peptide inhibitors were tested at three different concentrations (0.5 μM, 5 μM and 50 μM). N-acetyl-Tyr-Val-Ala-Asp aldehyde (YVAD-CHO) is a close representative of the caspase-1 cleavage site in IL-1β and

is an inhibitor widely used for caspase-1 inhibition (Thornberry *et al.,* 1997). The aldehyde inhibitor greatly reduced the processing of pro-IL-1β when added to the cell-free extract at 0.5 μM and abolished processing of the caspase-1 substrate completely at 5 μM and higher (Figure 3.2B). DEVD-CHO was used as a control. It has been shown to be selective for caspase-3 and should inhibit caspase-1 activity much less efficiently (Thornberry *et al.,* 1997). Indeed, over 10-fold higher concentrations of DEVD-CHO was required to achieve the same amount of inhibition of caspase-1 activity (Figure 3.2B). zVAD-fmk acts as a broad spectrum caspase inhibitor, but as with DEVD-CHO, a 10-fold higher concentration was required to achieve the same inhibitory effect as YVAD-CHO on caspase-1 activity.

Having established optimal inhibitory conditions, 5 μM of YVAD-CHO was added to THP-1 cell-free extract and the processing of caspase-1 and IL-1β were analyzed by Western Blot over a 2 h period. While incubation of the THP-1 cell-free extract at 37°C resulted in robust caspase-1 activation and IL-1β processing after 60 minutes, the incubation of the THP-1 cell-free extract in the presence of YVAD-CHO resulted in complete inhibition of caspase-1 activity, shown by its inability to cleave IL-1β even after 2 hours incubation (Figure 3.2C). This provided us with a system where we could specifically activate or inhibit caspase-1 and test its activity by monitoring IL-1β processing.

3.3.2 Independent activation of inflammation-associated and apoptosis-associated caspases in the THP-1 cell-free extract system

Cell-free systems have mainly been used for the study of apoptosis-related caspase activation and identification of substrates cleaved by caspases during apoptosis. It was therefore important to verify that caspases associated with apoptosis were not active under conditions where inflammatory caspases were activated. To ensure that the THP-1 cell-free system was selective for inflammatory caspase substrates, we undertook a variety of control experiments to examine the behaviour of a repertoire of caspases and some of their substrates in this system.

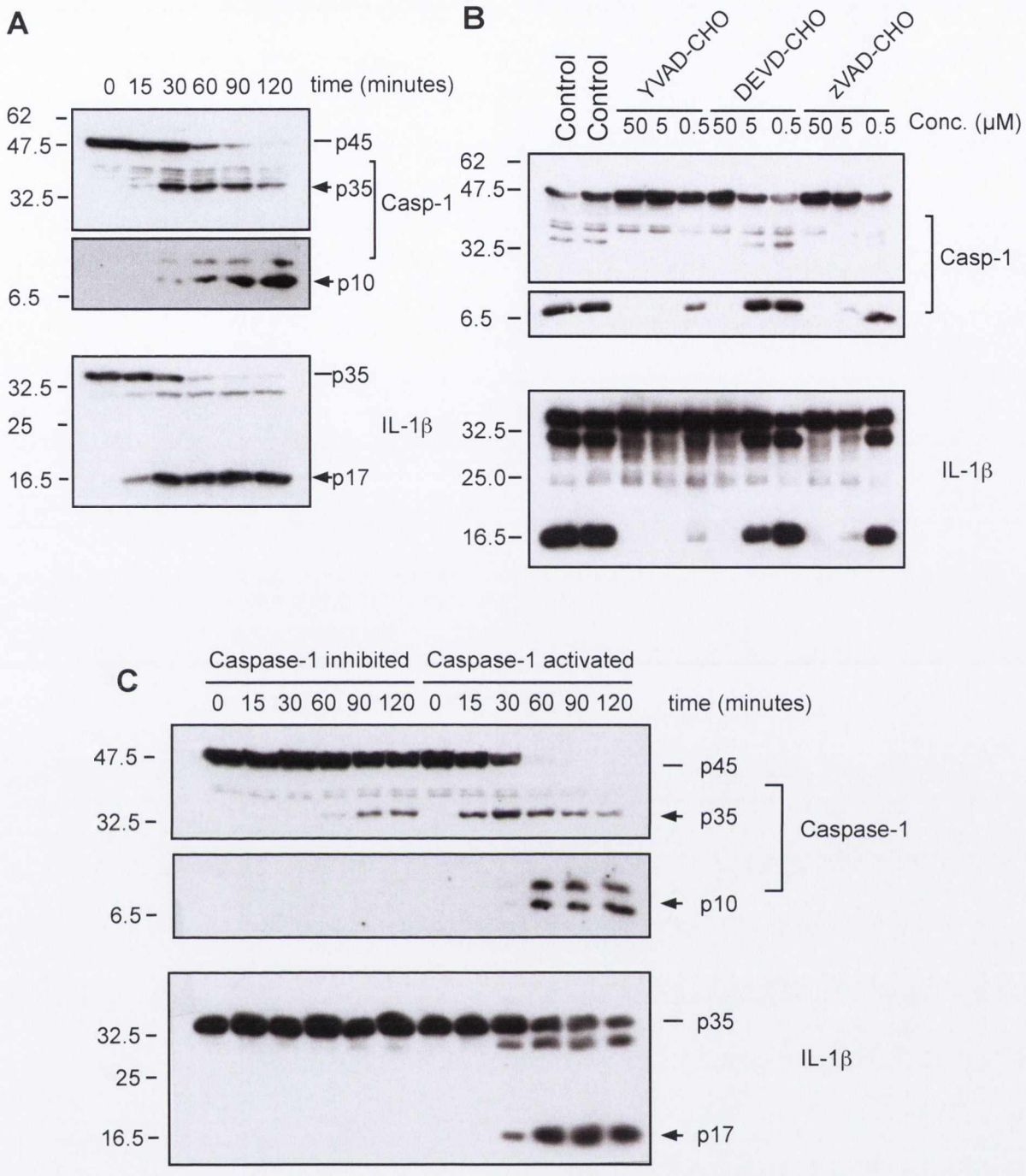

Figure 3.2

Caspase-1 activation / inhibition in a THP-1 cell-free extract time course

(A) LPS-treated THP-1 cell-free extract was incubated at 37°C for the time indicated. Protein samples were resolved by SDS-PAGE and pro-Caspase-1 (p45), its processed form (p10) and the processing of IL-1β were detected by Western Blot.

(B) Various caspase inhibitors were titrated in THP-1 cell free extract. The reactions were incubated at 37°C for 2 hours before resolving the protein samples on SDS PAGE gels and analysing caspase-1 and IL-1β processing by Western Blot.

(C) THP-1 cell free extract was incubated with 5 μM YVAD-CHO (Caspase-1 inhibited) or buffer (caspase-1 activated) at 37°C for the time indicated. Protein samples were resolved on 12% SDS PAGE and Caspase-1 and IL-1β processing were detected by Western Blot. Molecular weight markers in kDa are shown on the left of each blot. The bars on the right side indicate the pro forms, the arrows indicate the active / mature forms of the proteins.

Firstly, the THP-1 cell-free extract was incubated under conditions conducive for activation of inflammatory caspases. Processing of caspase-1 was confirmed by appearance of the p10 fragment within 30 minutes and activation determined by monitoring the processing pr pro-IL-1β from 32kDa to the 17 kDa mature IL-1β (Figure 3.3 and 3.4, lanes 5 to 9). Caspase-4 and -5 also underwent processing under these conditions (Figure 3.3, lanes 5 to 9). However, as substrates for these caspases have not been identified, their activity could not be verified. Significantly, neither apoptotic caspases (caspase-3, -7) nor their known substrates were processed during inflammatory conditions. Only caspase-8 was partially processed and p43/p41 fragments were detectable by Western blot but pro-caspase-8 did not seem to disappear significantly. This finding was surprising, but caspase-8 did not seem to be active as two specific caspase-8 substrates, caspase-3 (Fernandes-Alnemri *et al.,* 1996) and Bid (Luo *et al.,* 1998) were not cleaved under these conditions (Figure 3.3 and Figure 3.4).

Thus, incubating THP-1 cell-free extract by itself activated only inflammatory caspases and none of the apoptosis-associated caspases (caspase-2, -3, -6, -7 and -9) as indicated by the lack of processing of known substrates cleaved by apoptotic caspases (Figure 3.4).

Secondly, the cell-free extract was incubated in the presence of the inflammatory caspase inhibitor YVAD-CHO. The addition of this inhibitor completely blocked the processing of caspases-4 and -5 (Figure 3.3 lanes 1-4) and reduced processing of pro-caspase-1 to the intermediary 35 kDa form with only a trace amount of fully processed caspase-1 detectable by Western blot. Most importantly, no processing of IL-1β was detectable under these conditions (Figure 3.4) clearly indicating the suppression of caspase-1 proteolytic activity by YVAD-CHO.

As an additional control to verify that caspases involved in apoptosis could be activated in this system, THP-1 cell-free extract was incubated in the presence of cytochrome c and dATP, known activators for the apoptosome (Slee *et al.*, 1999). In this situation processing of pro-caspases-2, -3, -6, -7, -8, and -9 was evident as early as 30 minutes after addition of Cytochrome c and dATP (Figure 3.3 lanes 10-14). Apoptotic caspase activity was monitored by examining known substrates e.g.

XIAP, gelsolin, bid, co-chaperone p23 and PAK2 (Figure 3.4). The inflammatory caspases-1, -4 and -5 were processed under these conditions also but to a lesser extent than under inflammatory conditions. Similarly, IL-1β was converted by caspase-1 in a less efficient way, indicated by a delayed disappearance and appearance of the pro and processed form respectively (Figure 3.4).

These results demonstrate that the THP-1 cell-free system is a suitable assay to screen for caspase-1 substrates. Under conditions where caspase-1 and possibly caspase-4 and -5 were active, no other 'non-inflammatory' caspase was activated and no substrate other than IL-1β was cleaved, especially none of the substrates cleaved under apoptotic conditions, indicating independent control of caspase activation.

3.3.3 Two-dimensional SDS-PAGE analysis of THP-1 cell-free extracts

(i) Inflammatory caspase activated conditions

Having established conditions for controlled caspase-1 activation we scaled up the experiment to analyse the processing of caspase-1 substrates by resolving control or activated proteomes on two-dimensional SDS-PAGE.

500 µg of THP-1 cell-free extract was incubated with or without YVAD-CHO at 10 µM for two hours at 37 °C. A 10 µg reaction sample was separated by SDS-PAGE and immunoblotted for caspase-1, IL-1β and co chaperone p23 to confirm specific inflammatory caspase activity in the activated sample and complete absence thereof in the control (Data not shown). 400 µg of each sample were solubilised with 2D loading buffer and actively rehydrated into pI 3-6 or pI 5-8 immobilized pH gradient (IPG) strips. The absorbed samples in the strips were isoelectrically focused, allowing the proteins to migrate to the section of the strip matching their own pI. After separation in the first dimension, the proteins were then further resolved in the second dimension by placing the focused strip onto a large-format 12% SDS-PAGE gel where separation occurred according to molecular weight. The gels were stained with silver-nitrate, developed and the protein spot patterns of control and caspase-1 activated gels were compared (Figure 3.5).

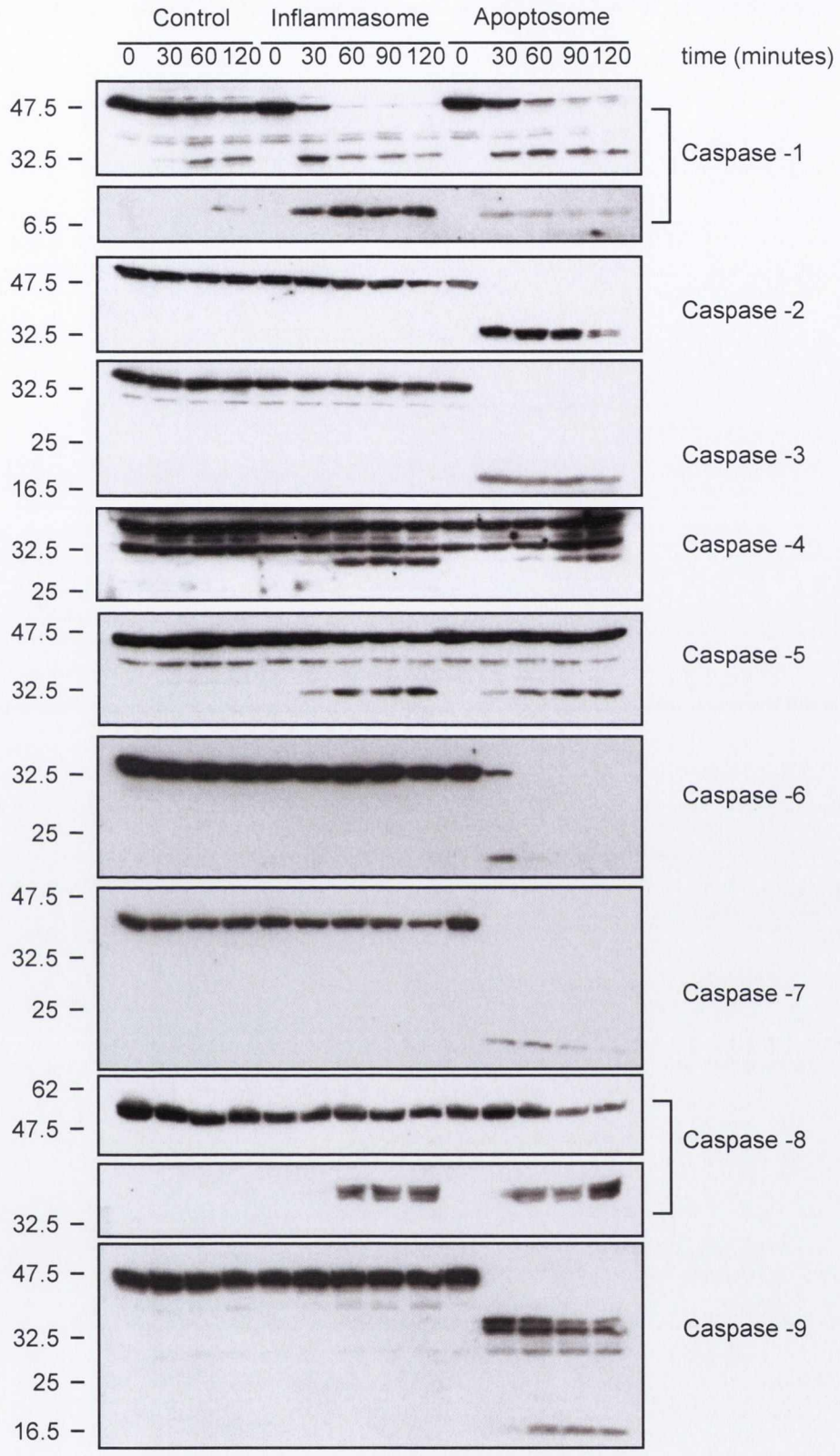

Figure 3.3

Processing of endogenous caspases in a THP-1 cell-free extract time course under inflammatory and apoptotic conditions

THP-1 cell-free extract was incubated under various conditions at 37°C for the indicated times. Control: 10 µM YVAD-CHO; Inflammasome: buffer A; Apoptosome: 50 µg/µl Cytochrome c, 1 mM dATP. The processing of the caspases was monitored by Western blot. Molecular weight markers in kDa are shown on the left of the figure.

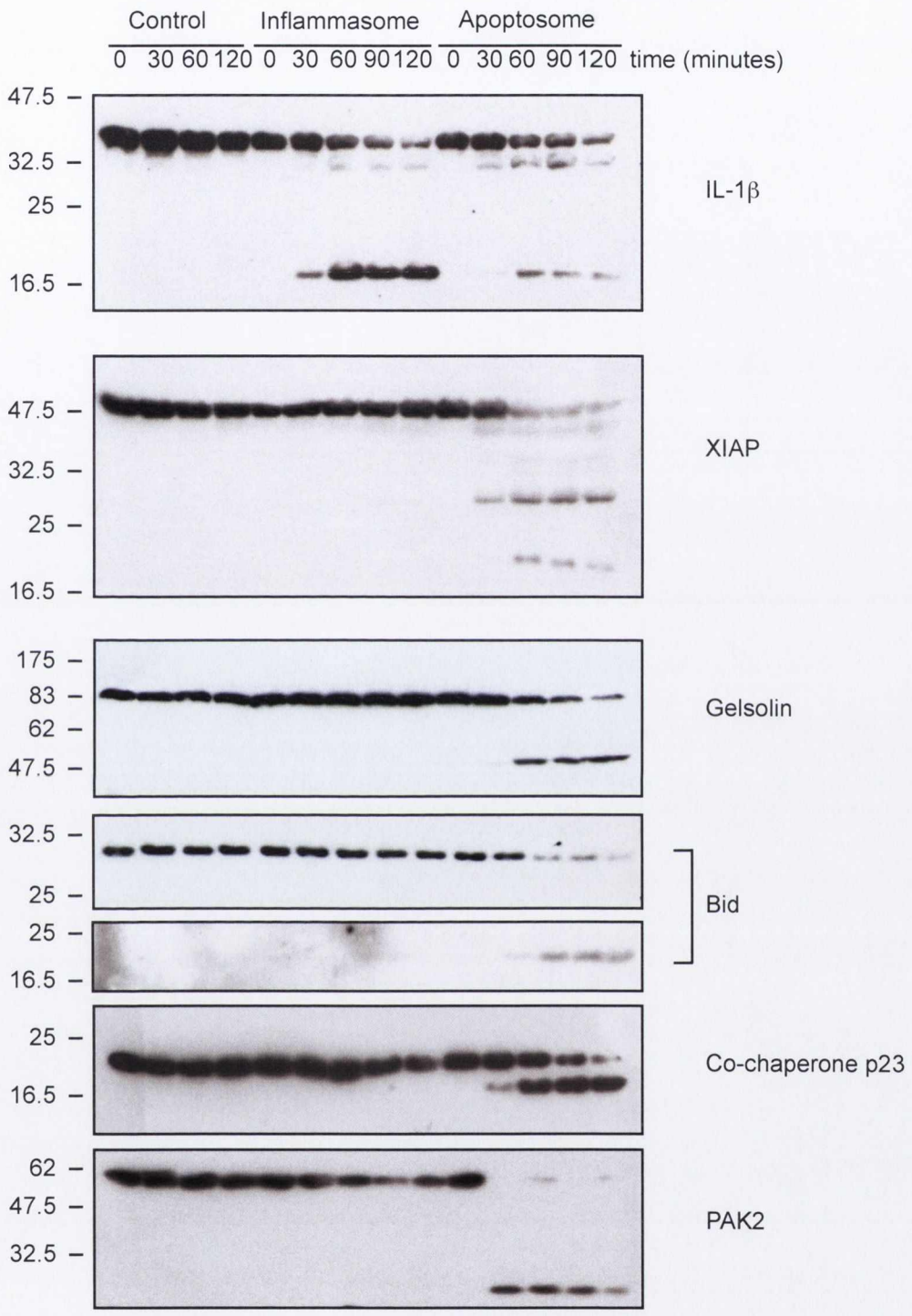

Figure 3.4

Processing of endogenous caspase substrates in a THP-1 cell free extract time-course under inflammatory and apoptotic conditions

THP-1 cell free extract was incubated under various conditions at 37°C for the indicated times. Control: 10 μM YVAD-CHO; Inflammasome: buffer A; Apoptosome: 50 μg/μl Cytochrome c, 1 mM dATP. The processing of the caspase substrates was monitored by Western blot. Molecular weight markers in kDa are shown on the left of the figure.

Strikingly, the comparison revealed far fewer changes than expected. Of about 3000 protein spots analysed on the gels over the pI 3-6 and pI 5-8 range, only 1 disappearing and 2 appearing spots were reproducibly detected over several independently repeated experiments. A number of protein spots were found to be altered on a single set of gels among all the replicates but these were barely detectable by silver nitrate staining and identification by mass spectrometry was unachievable as too little protein was present for a confident identification by MALDI-TOF.

(ii) Apoptotic caspase activated conditions

To compare 'apoptotic' versus 'inflammatory' caspase-dependent alterations to the proteome, we repeated the analysis by adding cytochrome c and dATP to trigger the activation of caspases involved in apoptosis and screened for apoptotic caspase substrates (Figure 3.6). Under conditions where apoptosis associated caspases were activated, a total of 76 protein spots were altered between the control and the apoptotic caspase activated gels. 8 protein spots showed a reduction or disappearance on the control gel and 68 appeared upon apoptotic caspase activation (Figure 3.6 and 3.7). The newly appearing protein spots were most likely protein fragments of higher molecular weight proteins as a result of caspase-dependent proteolysis.

Additionally, this experiment allowed us to compare the apoptotic proteome of THP-1 cells versus other more commonly used proteomes, such as the T-lymphocytic cell line Jurkat. Interestingly, THP-1 cell-free extracts showed similar changes to those of Jurkat cell-free extract upon activation of caspases involved in apoptosis (Walsh *et al.*, 2008).

3.3.4 Identification of protein spots by MALDI-TOF mass spectrometry

To identify the protein spots altered by inflammatory caspases, we used mass spectrometry. A selection of spots altered by caspases activated during apoptosis was analysed in parallel (Figure 3.8). The gel pieces harbouring the spots of interest were excised, de-stained, dehydrated, rehydrated with trypsin solution and the protein was then in-gel digested overnight. The mixture of tryptic fragments

was analyzed by MALDI-TOF mass spectrometry (Figure 3.9) and the resulting peptide fingerprint of the protein spot was searched against *in silico* trypsin-digested fragments of the *Homo sapiens* NCBI protein database, using MS-Fit (http://prospector.ucsf.edu/cgi-bin/msform.cgi?form=msfitstandard) and MASCOT (http://www.matrixscience.com/cgi/search_form.pl?&SEARCH=PMF) software.

The identified spots from the pI 3-6 gels (three sets) and pI 5-8 gels (ten sets) from inflammatory caspase activated proteomes and spots from four sets of pI 5-8 gels of apoptotic caspase activated proteomes were compiled in Table 3.1.

The caspase-1 substrates identified by mass spectrometry were gelsolin like capping protein (CapG), caspase-1 and IL-1β. IL-1β was identified twice, the pro-form disappearing from the control gel and the mature form appearing on the caspase-1 activated gel. CapG is a member of the gelsolin / villin family involved in the control of actin-based motility in non-muscle cells. This protein has not been described as a caspase substrate, whereas IL-1β and a proteolytic fragment of caspase-1 clearly demonstrate that this model is suitable to identify inflammatory caspase substrates. The majority of proteins cleaved by caspases activated during apoptosis have been described as apoptotic caspase targets in the literature.

3.3.5 Failure of CapG to be processed in a THP-1 cell-free extract time course

To confirm that CapG is a substrate for an inflammatory caspase, we examined the processing of *in vitro* transcribed / translated and ^{35}S-methionine labelled CapG in a THP-1 cell-free extract time course by fluorography. Surprisingly, we could not detect any processing of CapG, either with caspases activated during inflammation or apoptosis. Extended exposures did not reveal any possible cleavage fragments either (Figure 3.10A). As the *in vitro* transcribed / translated protein could have been in a misfolded state, possibly obstructing the substrate cleavage site, we also examined the processing of endogenous CapG protein by Western blot in a THP-1 cell-free time-course. Like the *in vitro* produced protein, the endogenous protein showed neither processing by caspases activated during inflammation nor during apoptosis (Figure 3.10B).

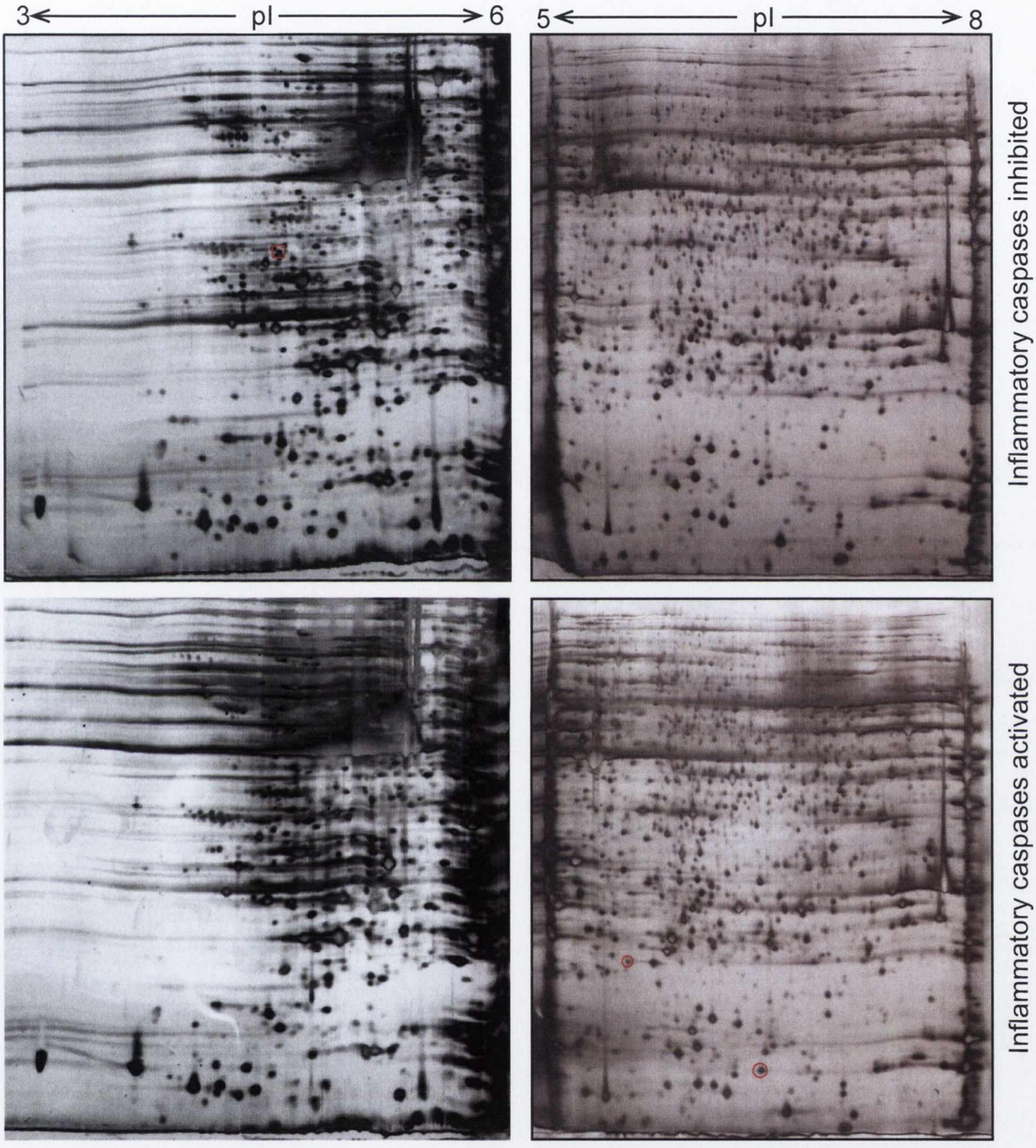

Figure 3.5

Two dimensional gel analysis of THP-1 cell-free extract with inhibited / active inflammatory caspases

400 µg of THP-1 cell-free extract was incubated with 10 µM YVAD-CHO (top) or without (bottom) for 2 hours at 37°C. The protein samples were focused either on a pI 3-6 (left) or pI 5-8 (right) IPG strip, resolved on a 12% SDS PAGE gel and silver stained.

The only spot disappearing from the control gel is marked with a square. The two spots appearing on the inflammatory caspases activated gel are marked with circles.

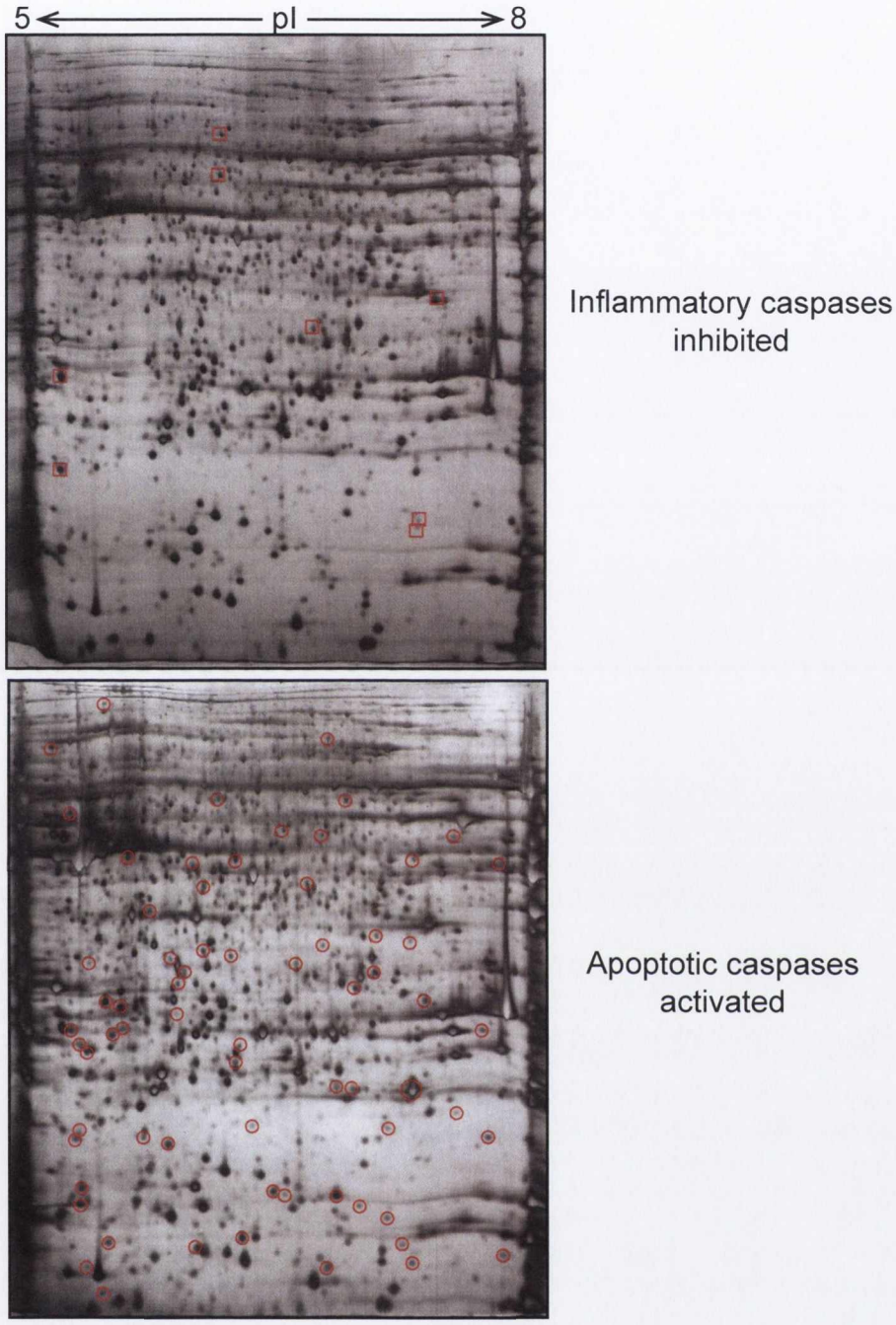

Figure 3.6

Two dimensional gel analysis of THP-1 cell-free extract with inhibited / active apoptotic caspases

350 µg of THP-1 cell-free extract was incubated with 10 µM YVAD-CHO (top) or 50 µg/µl Cytochrome c, 1 mM dATP (bottom) for 2 hours at 37°C. The protein samples were focused on a pI 5-8 IPG strip, resolved on a 12% SDS PAGE gel and silver stained. Spots disappearing from the control gel are marked with a square while the ones on the gel with activated apoptotic caspases are shown with a circle

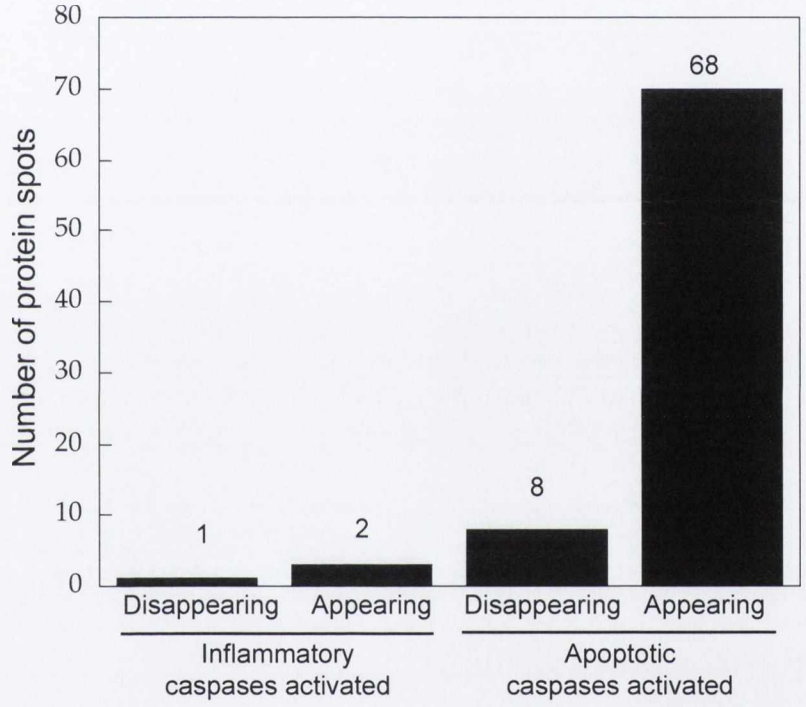

Figure 3.7

Graphical overview of spots disappearing / appearing under Inflammasome / Apoptosome conditions in THP-1 cell-free extracts by 2D gel analysis

The total amount of protein spots disappearing / appearing on pI 3-6 and pI 5-8 gels of Inflammasome and Apoptosome conditions are summarized.

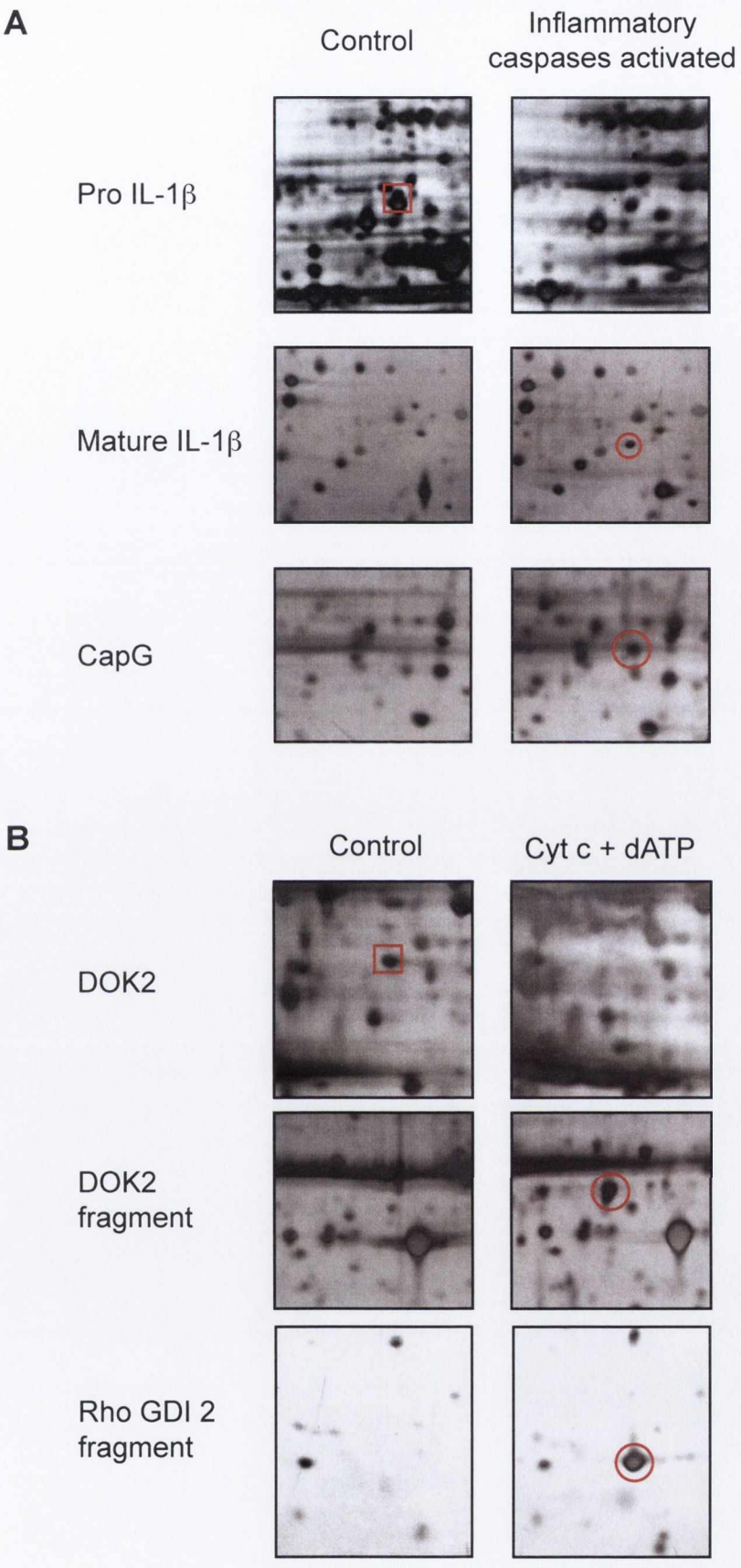

Figure 3.8

Identification of disappearing and appearing protein spots

Samples of proteins showing alteration on 2-D gels after activation of inflammatory caspases (A) or caspases involved in apoptosis (B). Protein identifications were obtained by MALDI-TOF mass spectrometry.

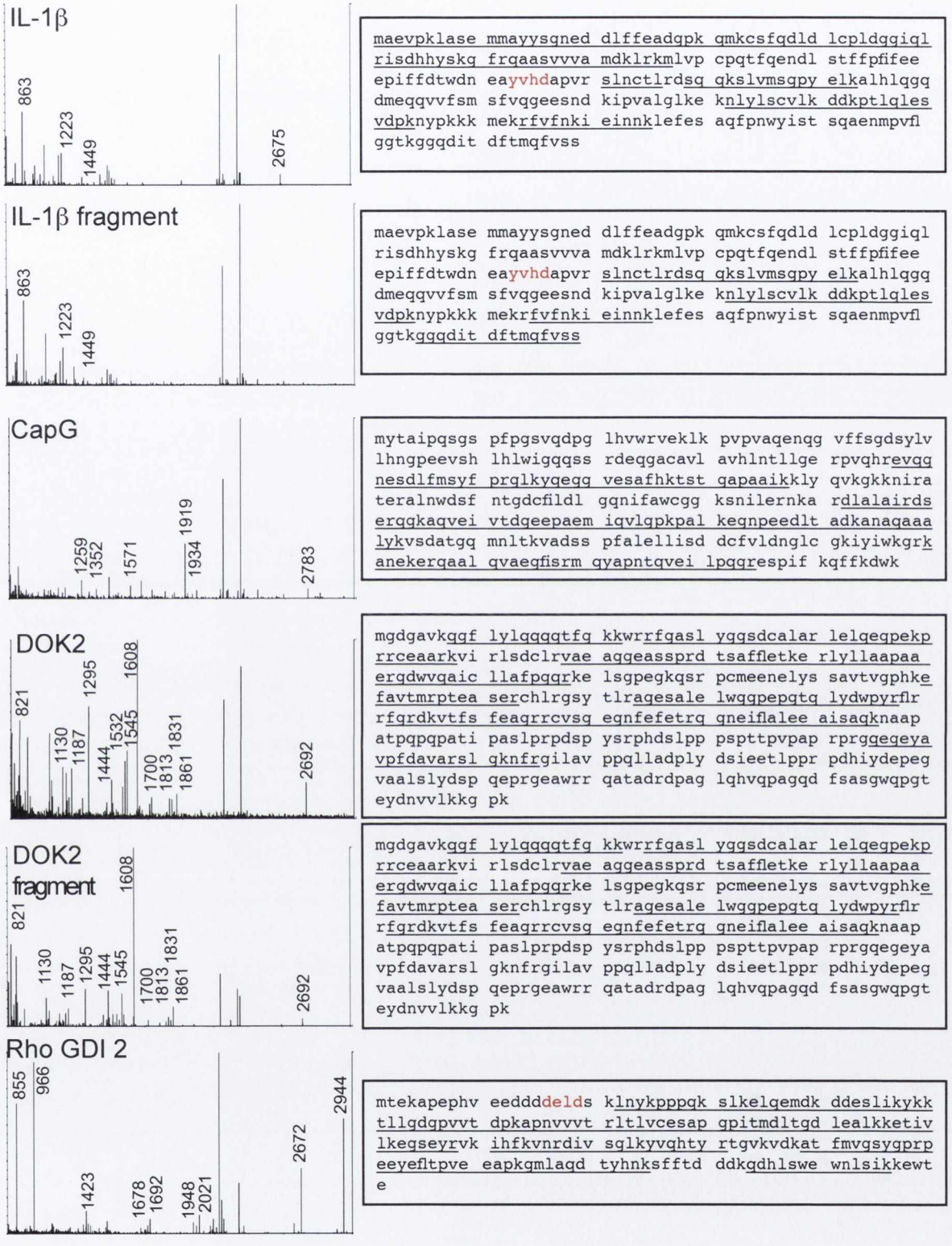

Figure 3.9

Peptide spectra of caspase substrates

Peptide spectra obtained from MALDI-TOF mass spectromeric analysis of protein spots shown in Figure 3.7. The Y-axis shows the percentage intensity of each peptide peak. The X-axis shows the m/z value of the peptides. Labels indicate the most abundant specific peaks of each protein. Peptide coverage is indicated by underlined sequence. Known caspase cleavage sites are highlighted in red.

Identified as	UniProt ID	Peptides matched	Coverage of protein
Disappearing on control gels vs inflammatory caspases activated gels			
Pro IL-1β	P01584	6	22 %
Appearing on inflammatory caspases activated gels			
Caspase-1	P29466	16	36 %
CapG	P40121	9	29 %
Mature IL-1β	P01584	8	26 %
Disappearing from control gels vs apoptotic caspases activated gels			
Bid	P55957	14	66 %
Calponin 2	Q99439	15	38 %
Heterogeneous nuclear ribonucleoprotein K	P61978	31	55 %
DOK2	O60496	26	5 %
PAK2	Q13177	13	30 %
Proteasome ß3, chain HsC10-II	P28070	7	32 %
RAN binding protein 1	P43487	14	46 %
RhoA	P61586	5	32 %
Appearing on apoptotic caspases activated gels			
Actin	P60709	25	67 %
CapG	P40121	5	18 %
DOK2	O60496	22	52 %
EF hand domain containing protein	Q5JYW8	24	64 %
Gelsolin	P06396	21	19 %
Glia Maturation Factor Gamma	O60234	13	60 %
Hematopoietic cellspecific Lyn substrate 1	P14317	13	23 %
Hsp27	P04792	9	53 %
Regulator of G-protein 10	O43665	16	61 %
IL-1ß	P01584	8	36 %
Nascent polypeptide associated complex alpha	Q13765	10	41 %
Heterogeneous nuclear ribonucleoprotein Q	O60506	22	40 %
L-Plastin	P13796	9	19 %
Poly(rC) binding protein 1	Q15365	8	30 %
Rho GDP disassociation inhibitor GDI alpha	P52565	12	39 %
Rho GDI2	P50395	18	74 %

Table 3.1

List of identified appearing / disappearing protein spots of inflammatory or apoptotic caspase activated THP-1 cell-free extracts

Appearing and disappearing protein spots from pI 3-6 and pI 5-8 gels were tryptically digested and analysed by MALDI-TOF mass spectrometry. The proteins were identified by database searches against *in silico* trypsin digested proteins. The protein name, accession number, number of peptides identified and coverage of these peptides over the full length protein are shown.

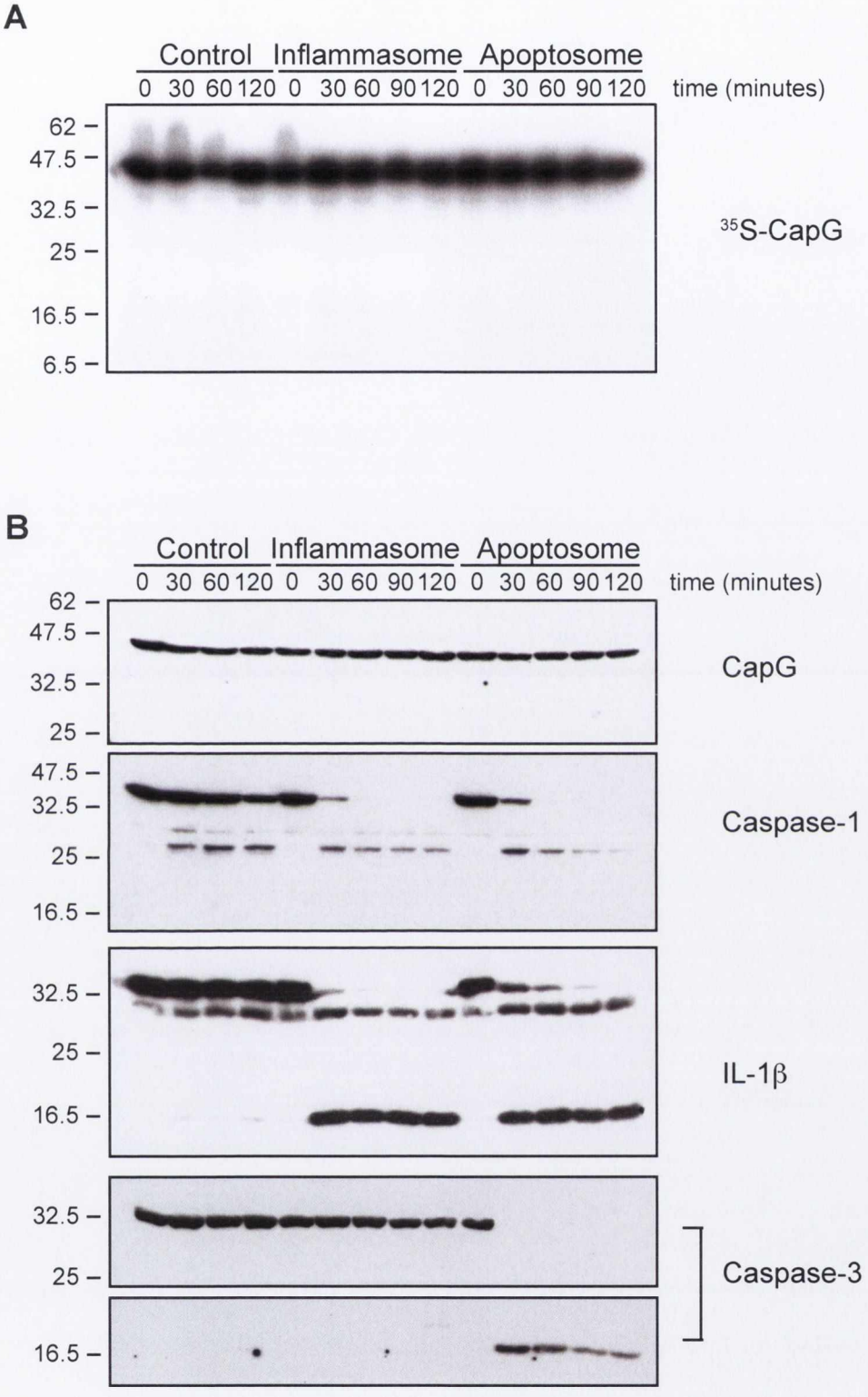

Figure 3.10

CapG fails to be processed in a THP-1 cell-free extract time course

The processing of ^{35}S labelled (A) or endogenous (B) CapG in a THP-1 time course was monitored as described in Figure 3.5. Caspase-1, IL-1β and caspase-3 are included as controls. Molecular weight markers in kDa are shown on the left of the figure.

This indicates that the CapG protein spot appearance identified by MALDI-TOF mass spectrometry is not a substrate for the inflammatory caspases. Although reproducible, the protein spot on the gel is possibly a gel running artefact or the protein was modified, for example by phosphorylation or another protein modifying event, leading to a shift in mobility in the first or second dimension of the gel.

3.4 DISCUSSION

3.4.1 Summary

In order to identify novel inflammatory caspase substrates using a proteomic approach we first adapted and tested a THP-1 cell-free system in which we could specifically activate the inflammatory associated caspases. Caspases associated with apoptosis were not processed to their active form and showed no activity under these conditions but could be activated separately by addition of cytochrome c and dATP as an additional control. By resolving either control or caspase activated proteomes on 2D SDS-PAGE and visualising the protein by silver nitrate staining surprisingly few alterations were detected upon inflammatory caspase activation. Proteomes with caspases activated during apoptosis on the other hand showed a similar amount of protein spot disappearances / appearances as we have detected in cell-free systems of human and other species. The identified spot alterations during inflammatory caspase activation and a selection of spots showing differences compared to caspase activation during apoptosis were excised from the gel and tryptic in-gel digested. The proteins were identified by mass spectrometry of the peptides and subsequent database searches against *in silico* digested protein.

Besides the already known substrates IL-1β and caspase-1, the only other spot alteration was identified as CapG. Subsequent analysis of either *in vitro* transcribed / translated or endogenous CapG in a THP-1 cell-free extract time-course could not confirm any proteolytic activity by any caspase, indicating that this is not a substrate cleaved by inflammatory caspases.

3.4.2 The THP-1 Cell-free system

Cell-free extracts have been extremely valuable in the past to analyse apoptosis by identifying novel protease substrates in a variety of different species (Lazebnik *et al.,* 1994; Newmeyer *et al.*, 1994; Martin *et al.,* 1995). It was especially useful in the initial identification of caspase substrates during apoptosis, the assembly of the apoptosome (Liu *et al.,* 1996), the ordering of the caspase cascade (Slee *et al.,* 1999; Murphy *et al.*, 2003; Inoue *et al.,* 2009) or for a comparison of caspase

substrates during apoptosis between different species (Adrain *et al.*, 2004; Taylor *et al.*, 2007; Creagh *et al.*, 2009).

A cell-free extract of the THP-1 cell line was used in both initial discoveries of the protease caspase-1 (Kostura *et al.*, 1989) and 13 years later in the characterisation of the caspase-1 activation platform, the inflammasome (Martinon *et al.,* 2002). The process that leads to the auto-activation of caspase-1 in the THP-1 cell-free extract though is still not yet resolved. Caspase-11 is required for the activation of caspase-1 and the subsequent maturation of IL-1β in mice (Wang et al., 1998), therefore one could assume the human orthologues caspase-4 and -5 play a similar role in the formation of the inflammasome. The pre-treatment of the cells with LPS induces many genes, some of which are probably required in the subsequent formation and activation of the inflammasome. During the swelling of the cells in hypotonic buffer and subsequent rupture of the cell membrane by homogenisation other organelles most likely shatter as well, releasing their contents. The rupture of lysosomes or phagosomes has been previously suspected of facilitating the passage of microbial molecules such as MDP (Marina-Garcia *et al.*, 2008), non degradable particulate matter like fibrillar amyloid-β (Halle *et al.*, 2008), silica or aluminium hydroxide (Hornung *et al.*, 2008) or ureic acid into the cytosol. Some of this endocytosed matter or possibly an endogenous protein then triggers the inflammasome in a yet unidentified way.

Firstly, we set up a THP-1 cell free extract system where we could control spontaneous caspase-1, -4 and -5 activation. A similar method has been described in the literature and was used for identifying the components of the NLRP1 inflammasome, the first identified caspase-1 activating complex (Martinon *et al.,* 2002).

The other inflammatory caspases-4 and -5 were also processed under conditions where caspase-1 was active (Figure 3.3). The exact mechanism still remains to be solved. Caspase-5 has been associated with the NLRP1 inflammasome (Martinon *et al.,* 2002), but this has so far not been independently confirmed. Unfortunately, we had no means of assessing their specific activity, as no substrates for these proteases are known. Commercially available antibodies for caspases-4 and -5

detect the full-length and the intermediary p30 form of the proteases (Figure 3.3, lanes 6-9 and 11-14). Interestingly this processing was completely inhibitable by YVAD-CHO, whereas caspase-1 processing was not. This could indicate that like IL-1β, caspase-4 or -5 processing is downstream of caspase-1 but further experiments would have to be done to confirm the exact pathway of inflammatory caspase activation.

The processing of caspase-8 was surprising but although the protease was processed it was not active as some of its substrates, caspase-3 (Fernandes-Alnemri *et al.,* 1996) and Bid (Luo *et al.,* 1998), were not processed under these conditions. However, an inflammatory caspase might inactivate caspase-8 by cleaving it at a non-classical site. More likely, the protease could be inhibited by inhibitors of apoptosis (IAPs) which are also NF-κB responsive genes (Wang *et al.*, 1998) and therefore upregulated in LPS pre-treated of the THP-1 cells. Caspase-8 conditional knockout mice, where the first two exons were deleted, showed defects in monocyte differentiation into macrophages by Macrophage Colony-Stimulating Factor (Kang *et al.,* 2004). This indicates a possible involvement of caspase-8 in haematopoietic development but the exact molecular role remains obscure.

3.4.3 Two-dimensional SDS PAGE analysis of caspase inhibited and caspase activated THP-1 cell free extract

THP-1 cell free extract where inflammatory caspases were either inhibited or activated were resolved by two-dimensional SDS-PAGE. With this method we could resolve approximately 3000 individual protein spots over two overlapping pI ranges from pI 4 to pI 8 on 12% and 8% SDS-PAGE gels. Although we could survey a vast range of proteins, this represented possibly less than 10% of the total THP-1 cell proteome. Multiple factors contribute to this bias in protein detection.

Proteomic analysis by two-dimensional SDS PAGE have been used for many years and while this method is well established and optimised there are certain known drawbacks to this approach. The abundance of an individual protein can be

below the sensitivity of silver staining and would go undetected in the initial comparison of the differently treated cell free extract separated on the gels. Additionally proteins with an isoelectric point below 3 or above 8 cannot be resolved properly. Another factor to reduce the amount of protein resolved is the molecular weight of the protein. Large proteins above 60 kDa do not enter the IPG strip efficiently and small proteins below 15 kDa are not resolved effectively by SDS-PAGE. Proteins with a signalling function are usually small in size and could therefore go undetected by this analysis. 8% SDS-PAGE can resolve proteins to about 10 kDa but going any lower proved impossible due to the fragility of such gels. Salt carry-over from the THP-1 cell free extract preparation also has an inhibitory effect on isoelectric focusing of the proteins in the first dimension. Different approaches like protein precipitation and resolubilisation in salt free loading buffer or washing cell-free extract through 5 kDa molecular weight cut off spin filters was attempted but only the active rehydration of the IPG strip improved the focusing result. Despite some of these technical difficulties and bias, we found 2-D SDS-PAGE is still a useful tool to analyse a snapshot view of the resolvable proteome.

3.4.4 Restricted substrate specificity of inflammatory caspases

Very limited changes were detectable when comparing the cell-free extracts containing activated inflammatory caspases against the proteome where inflammatory caspases were inhibited. Only four spot alterations were reproducibly detectable upon inflammatory caspase activation and were identified by mass spectrometry. To ensure and verify that the results obtained were not due to some technical issues, we used the THP-1 cell free extract under conditions where apoptotic caspases were activated. The determination of substrates for apoptotic caspases and Granzyme B in Jurkat cell free extract by two-dimensional analysis has already been successful in our group (Adrain *et al.,* 2004; Adrain *et al.*, 2005; Walsh *et al.,* 2008). Indeed, the number of changes detectable by comparing control versus apoptotic caspase activated THP-1 proteomes by two-dimensional SDS PAGE to Jurkat proteomes was very similar (Adrain *et al.,* 2004). This confirmed that proteolytic changes in the THP-1 cell-free extract induced by caspases can be detected by two-dimensional SDS-PAGE and silver staining.

This comparison of the substrate specificity of both caspase groups in Figure 3.7 clearly shows that the inflammatory caspases have a very strict and restricted substrate specificity compared to the apoptotic caspases. This result also implicates that inflammatory caspases cleave only very specific target substrates and not random bystander proteins as is possibly observed with apoptotic caspases.

3.4.5 Inflammatory caspases do not act as apoptotic caspases

Additionally the result in Figure 3.5 and 3.6 strongly suggest that caspase-1 and possibly caspase-4 and -5 are not involved in programmed cell death as none of the hundreds of proteolytic events inflicted by the apoptotic caspases took place when only the inflammatory caspases were activated. All publications demonstrating caspase-1 involvement in apoptotic events have used overexpressed caspase-1 or high levels of caspase-1 inhibitors (Miura *et al.,* 1993; Hawkins *et al.,* 1996; Guegan *et al.,* 2002; Feng, Li *et al.,* 2004), whereas our experiment used endogenous levels of this protease. Involvement of any inflammatory caspases in apoptosis is therefore very unlikely in the THP-1 cell line. In addition, the caspase-1 knockout phenotype supports our observation where in comparison to the caspase-9 or caspase-3 and -7 knockouts no developmental defect was observed (Li *et al.,* 1995; Kuida *et al.,* 1995).

3.4.6 Identification of protein spots by mass spectrometry

Of the identified spot alterations on a set of 2-D SDS-PAGE gels, we could identify over 40% by tryptic digestion and mass spectrometry analysis with subsequent database searches. This number could be increased by repeated analysis of the same protein spot on replicate gels. Protein identification by mass spectrometry is dependant on multiple factors. First, sufficient abundance of the protein is critical. Although we are able to detect proteins in the higher picogram range by silver nitrate staining, approximately 10 to 50 ng of protein is required for confident identification by mass spectrometry. Smaller proteins are generally harder to identify as they generate fewer tryptic fragments for database searches. Some proteins also have too many or too few cleavage sites for trypsin resulting in peptides below 800 Dalton or over 3500 Dalton which lie outside the ideal

sensitivity window of the mass spectrometer. This yields incomplete peptide coverage of the protein. Additionally, a positive identification can only be made if the protein is present in the database searched and without any sequencing errors.

3.4.7 Identified inflammatory caspase substrates

Two of the three protein spot alterations identified were IL-1β, both the pro form disappearing and the mature form appearing. IL-1β is the classical substrate used to verify caspase-1 activity (Thornberry *et al.*, 1992; Martinon *et al.*, 2002). The disappearance of the pro-form and the clear appearance of the processed IL-1β on the two-dimensional SDS-PAGE gels validated the experimental setup used for this proteomic screen. The fourth altered spot was identified as CapG, a protein of the gelsolin family involved in actin regulation. CapG binds actin at the barbed end and blocks monomer exchange thereby inhibiting actin filament growth (Southwick *et al.*, 1986). Mice deficient of CapG show a decline in cell ruffling, a 50% decrease in phagocytosis and a 50% reduction in actin-based vesicle motility (Witke *et al.*, 2001). Interestingly these mice are also more susceptible to *Listeria* infections compared to the wild type animals but no difference was observed for *Salmonella* (Parikh *et al.*, 2003). This indicates a possible function for CapG in the detection or the response to different intracellular pathogens.

However, the appearance of a spot by two-dimensional gel analysis was not corroborated by Western blot analysis. As shown in Figure 3.10, the processing of CapG was not detectable by Western blot either under conditions where inflammatory caspases or apoptotic caspases were active. The spot appearance on the inflammatory caspase activated gel reproduced consistently on six replication gels and could therefore only be explained as either a gel running artefact or a post-translational modification of the protein. This would result in the gel-shift of the protein in the first and / or the second dimension. Additionally the peptides identified by MALDI-TOF mass spectrometry covered a large region of the full-length protein from AA97 to AA335 and a putative caspase-1, -4 or -5 cleavage site was not found in the protein sequence prior or after the peptide coverage. Taken together this indicates a possible false-positive identification.

Overall the two-dimensional SDS-PAGE proteome analysis clearly showed very few changes when inflammatory caspases were activated compared to the activation of caspases involved in apoptosis. This further supports the idea that inflammatory caspases, although very efficient in processing their substrates, are very specific in their substrate preference and are not capable of inducing apoptosis.

Having established a system where we could confirm putative inflammatory caspase substrates but having failed so far to identify any novel caspase targets, we changed the method of screening to overcome some of the limitations of the 2D SDS-PAGE / mass spectrometry approach. This next screen is described in the following chapter.

CHAPTER 4

SMALL POOL cDNA LIBRARY SCREEN FOR CASPASE-1, -4 AND -5 SUBSTRATES

4.1 INTRODUCTION

As outlined in the previous chapter our first approach towards identifying novel inflammatory caspase substrates by comparison of control versus activated THP-1 cell-free extract using two-dimensional gel electrophoresis resulted in the processing of very few proteins. Only 3 out of roughly 3000 spots analyzed showed a change of mobility on 2D gels. Clearly, two possibilities may account for this outcome. Firstly the three changes identified are representative of the inflammatory substrates, indicating that caspase-1 is an extremely specific protease and cleaves very few substrates. Secondly, there may be technical limitations in the analysis of THP-1 cell-free extract by two-dimensional SDS-PAGE and subsequent identification by MALDI-TOF mass spectrometry as discussed in the previous chapter. Additionally not all proteins are expressed in THP-1 cells at all times and especially at the same abundance.

To circumvent some of the drawbacks associated with 2-D SDS-PAGE and protein identification by MALDI/TOF mass spectrometry we explored an alternative approach by using a small pool cDNA library *in vitro* transcription and translation technique. The use of this method would permit the access to a much larger part of the proteome. Additionally this small pool cDNA library has already been successfully used to screen for caspase-8 substrates (Byun *et al.*, 2001).

4.2. SUMMARY

This part of the broadened inflammatory caspase substrate screen can be divided into three parts. First, we expressed, purified and titrated the inflammatory caspases. For the screening process, each cDNA pool was individually *in vitro* transcribed and translated to produce ^{35}S-methionine labelled proteins. This was carried out by using a rabbit reticulocyte lysate where transcription and translation are combined in a single reaction. The resulting protein pools were then screened for inflammatory caspase substrates by adding each recombinant caspase at approximately physiological concentrations to replicate protein pools. The proteolysis pattern was analysed by SDS-PAGE and positive pools identified (Figure 4.1). In a third step, we decoded the pool down to the single cDNA and

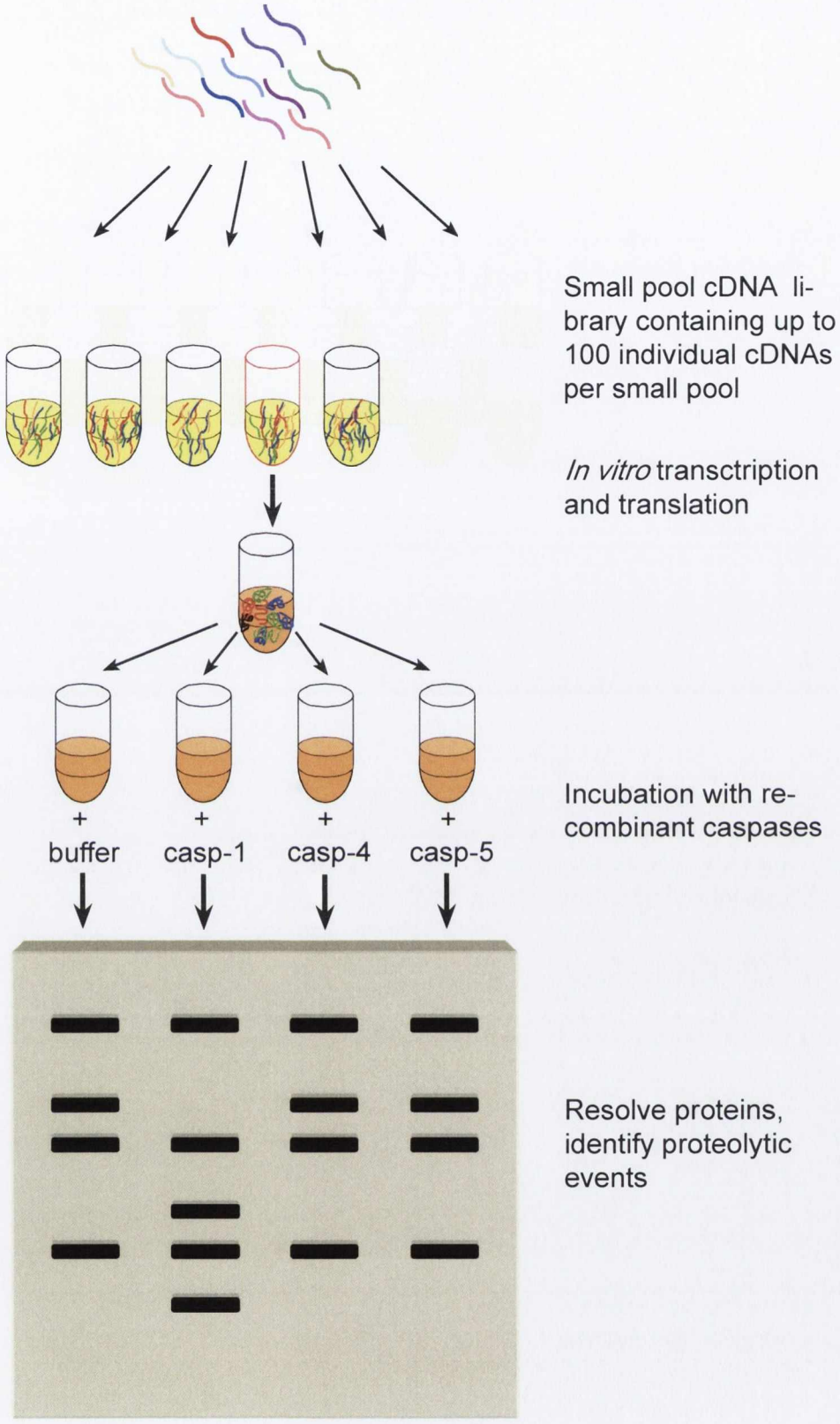

Figure 4.1

Identification of inflammatory caspase substrates using a small pool cDNA library

Schematic representation of the small pool cDNA library screen for proteins cleaved by caspase-1, -4 or -5. Each small pool is individualy *in vitro* transcribed and translated. The resulting proteins are split into four reactions and incubated with either buffer or a recombinant caspase. Each digest is resolved by SDS-PAGE and proteins undergoing proteolysis were identified in a second step.

identified the protein by DNA sequencing. Finally, any *in vitro* identified substrates would be verified in the THP-1 cell-free system described in the previous chapter.

To increase the probability of identifying substrates involved in inflammation we decided to screen the small pool cDNA library for substrates of not just caspase-1, but also inflammatory caspases-4 and -5 and thereby possibly also acquire a better understanding of their involvement in the inflammatory process.

Twenty of the 240 pools screened were found to harbour a possible inflammatory caspase substrate. Of these 20 pools 10 were decoded to a single protein and identified. None of the identified putative inflammatory caspase substrates have previously been associated with any aspect of inflammation.

We then verified the processing of the identified *in vitro* expressed substrates in the THP-1 cell-free extract assay, where specifically only inflammatory endogenous caspases were activated.

We tried to validate the identified substrates and characterise any possible effect of the proteolytic event in a tissue culture based model by either knocking down the gene of interest by siRNA or overexpressing it by viral transduction or electroporation. However, due to large variation in the different readouts, possibly caused by the nucleic acid delivery method, we were unable to confirm the involvement of any of the identified substrates in inflammatory processes. However, work is ongoing in the Martin laboratory to pursue the possible role of these substrates in caspase-dependent inflammatory events.

4.3. RESULTS

4.3.1 Subcloning of human Caspase-1 in pET15b

To screen hundreds of *in vitro* transcribed / translated cDNA pools and then decode any positive pools required a large amount of active and purified caspase-1, -4 and -5. Initially, endogenous caspase-1 was isolated from cytosolic extracts of THP-1 cells by high-performance liquid chromatography and affinity chromatography to identify and characterize the novel protease (Cerretti *et al.,* 1992; Thornberry *et al.,* 1992).

The simplest and most cost effective way to obtain large amounts of active protease is by expressing recombinant proteins in bacteria. This is a commonly used method which, depending on the construct used, usually works quite efficiently. Caspase-3 and -7 haven been previously expressed as full-length polyhistidine-tagged proteins (Stennicke *et al.*, 1997; Walsh *et al.,* 2008). While other caspases, such as caspase-6 or -8 have been expressed without their pro-domains, as this region of the protein can lead to aggregation and therefore insolubility (Srinivasula *et al.*, 1996; Stennicke and Salvesen, 1997). Different caspase-1, -4 and -5 constructs have been successfully used to express and purify inflammatory caspases with this method (Alnemri *et al.*, 1995; Malinowski, *et al.,* 1995; Ramage *et al.*, 1995).

To express recombinant caspase-1 in a bacterial expression system, a CARD deletion mutant of human caspase-1 was amplified by PCR and subcloned into the pET15b vector to generate an N terminally His tagged protease (Figure 4.2A). A full length caspase-1 construct was also generated but this produced mainly insoluble protein within the bacteria and was not used for the screen (Data not shown).

GST tagged Caspase-4 and -5 p30 constructs (i.e. lacking the N-terminal CARD domain) in pGEX-4T-1 vector to be used in this screen were previously described (Lin, *et al.,* 2000) and kindly provided by Prof. Alan Porter (University of Singapore).

4.3.2 Expression and purification of recombinant caspase-1, -4 and -5 from bacteria

The pET15b.Caspase-1.p30 construct was transformed into *E. coli* BL21 De3 pLysS bacteria, which contain an IPTG-inducible T7 polymerase. IPTG was added to a culture in logarithmic growth phase to induce recombinant caspase-1 expression. Optimization of the conditions of protein induction (temperature, duration of the induction and IPTG concentration) were performed to obtain the highest soluble yields of active caspase. Samples of the bacterial lysates after the induction confirmed the appearance of a band at the expected size of 35 kDa (Figure 4.2B). His-tagged caspase-1 captured on Ni-NTA beads appeared to be autoprocessed to the p20 and p10 subunits as most of the captured protein was detected at approximate molecular weight of 26, 12 and 6 kDa by Coomassie staining (Figure 4.2B).

To generate soluble, unbound proteases, the HIS_6-caspase-1 was eluted with imidazole, competing for the Ni-NTA agarose. Multiple rounds of elutions in protease reaction buffer (PRB) were sequentially performed. Each eluate fraction and the remaining beads were checked for WEHD-AMC cleavage activity by fluorimetry until no caspase-1 activity remained on the Ni-NTA agarose beads (Data not shown). As the imidazole could potentially inhibit subsequent protease reactions, its concentration was lowered by combining the most active eluates, diluting these with protease reaction buffer and concentrating them back down to the original volume in a 5 kDa molecular weight cut off spin filter. This was repeated at least three times to reduce the imidazole concentrations to the nanomolar range. The protein content of the final eluate was aliquoted and frozen.

A similar process was performed for both caspase-4 and -5. GST-tagged caspase-4 and -5 in the bacterial lysates were captured on glutathione immobilised to sepharose beads and eluted with glutathione to compete for the binding of GST. The most active elutions were pooled, washed, aliquoted and frozen until used as described for recombinant caspase-1 above.

Samples of each recombinant caspase were resolved by SDS-PAGE and either stained with Coomassie blue or transferred onto nitrocellulose membrane and immunoblotted with antibodies against the protease itself or the purification tag used (Figure 4.1C). The 35 kDa His-Caspase-1 construct clearly auto-processed to its p20 and p10 active form as indicated by the cross-reactive bands running at 26 kDa and 6 kDa respectively. The eluted GST-caspase-4 was mainly in unprocessed form, whereas about half of GST-caspase-5 was processed to its p10 / p20 form. There was a considerable amount of residual GST in the elutions of both caspase-4 and caspase-5 preparations, most likely cleaved off the protease during the capture / elution / purification process (Figure 4.2C).

4.3.3 Testing the activity of recombinant caspase-1, -4 and -5

Next, we established the activity of each recombinant caspase against the synthetic peptide substrates WEHD-AMC, YVAD-AMC, DEVD-AMC and IETD-AMC (Figure 4.3). In agreement with previously published reports, WEHD-AMC was the most efficiently hydrolysed by recombinant caspase-1 compared to all other peptide substrates tested here (Thornberry *et al.,* 1997; Talanian *et al.,* 1997). We chose dilutions of recombinant caspase-4 and -5 that matched the WEHD-AMC ase activity of caspase-1 (Figure 4.2A). To our surprise the peptide substrate IETD-AMC, representing an optimal caspase-8 substrate, was processed by recombinant caspase-1 almost as efficiently as YVAD-AMC, the proteotypic caspase-1 substrate representing the $YVHD^{118}$ cleavage site in IL-1β. This ability of caspase-1 to hydrolyze IETD to this extent has not been reported previously. As expected, no significant processing of DEVD-AMC, an established caspase-3 substrate, was observed by caspase-1, further proving the specificity of this protease. The WEHD-AMC peptide was also the preferred substrate of caspase-4 and -5. YVAD-AMC and IETD-AMC were even more efficiently cleaved by caspase-5 compared to caspase-1 at these concentrations, whereas caspase-4 displayed a similar activity against this peptide substrate as caspase-1.

These results demonstrated that the bacterial recombinant caspases-1/ -4 /-5 generated were active and were specific towards peptide substrates with a high preference for the WEHD motif. The results also indicated that each protease has

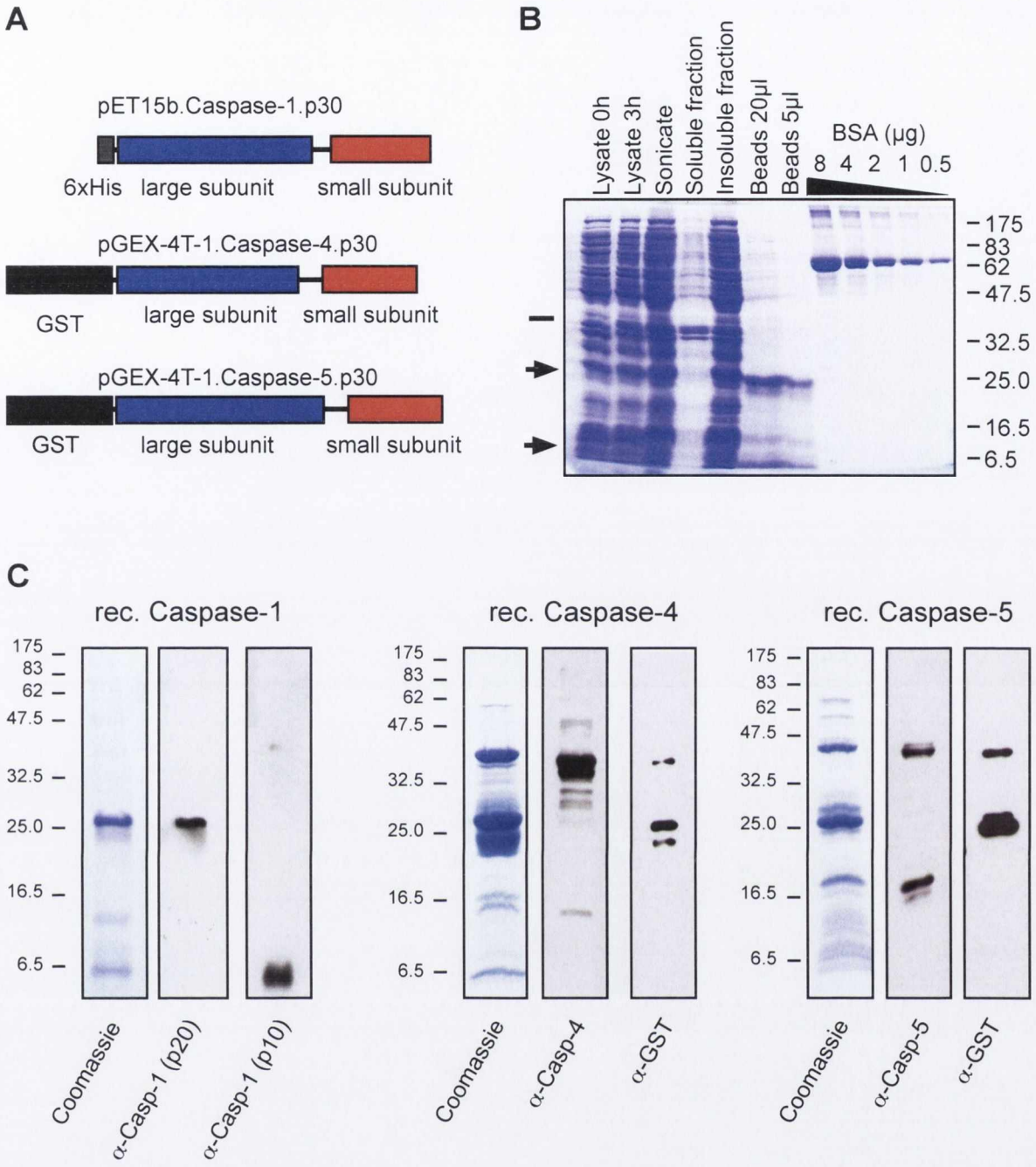

Figure 4.2

Expression and purification of recombinant caspase-1, -4 and -5

(A) Schematic representation of the N-terminal His or GST tagged truncated constructs used for protein expression of the caspases in *E.coli.*

(B)pET.15b.Casp-1.p30 plasmid was transformed into *E.coli* bacteria. Expression of caspase-1 was induced by the addition of 600 µM IPTG, followed by 3 hours of incubation at 37°C. Cells were lysed by sonication and soluble supernatant incubated with Ni-Agarose beads. Samples before and after the protein induction (0.5 ml of the culure), total, soluble and insoluble fractions after lysis (10 µl) and beads (20 µl, 5 µl) were run on a 12% SDS-PAGE gel along a BSA standard. Protein bands were visualised with coomassie blue. The line indicates the induced caspase-1 p30 and the arrows indicate the autoproteolytic p20 and p10 forms.

(C) Eluted, purified and washed caspase-1, -4 and -5 were resolved by 12% SDS-PAGE and either coomassie stained or immunoblotted with the antibody specified.

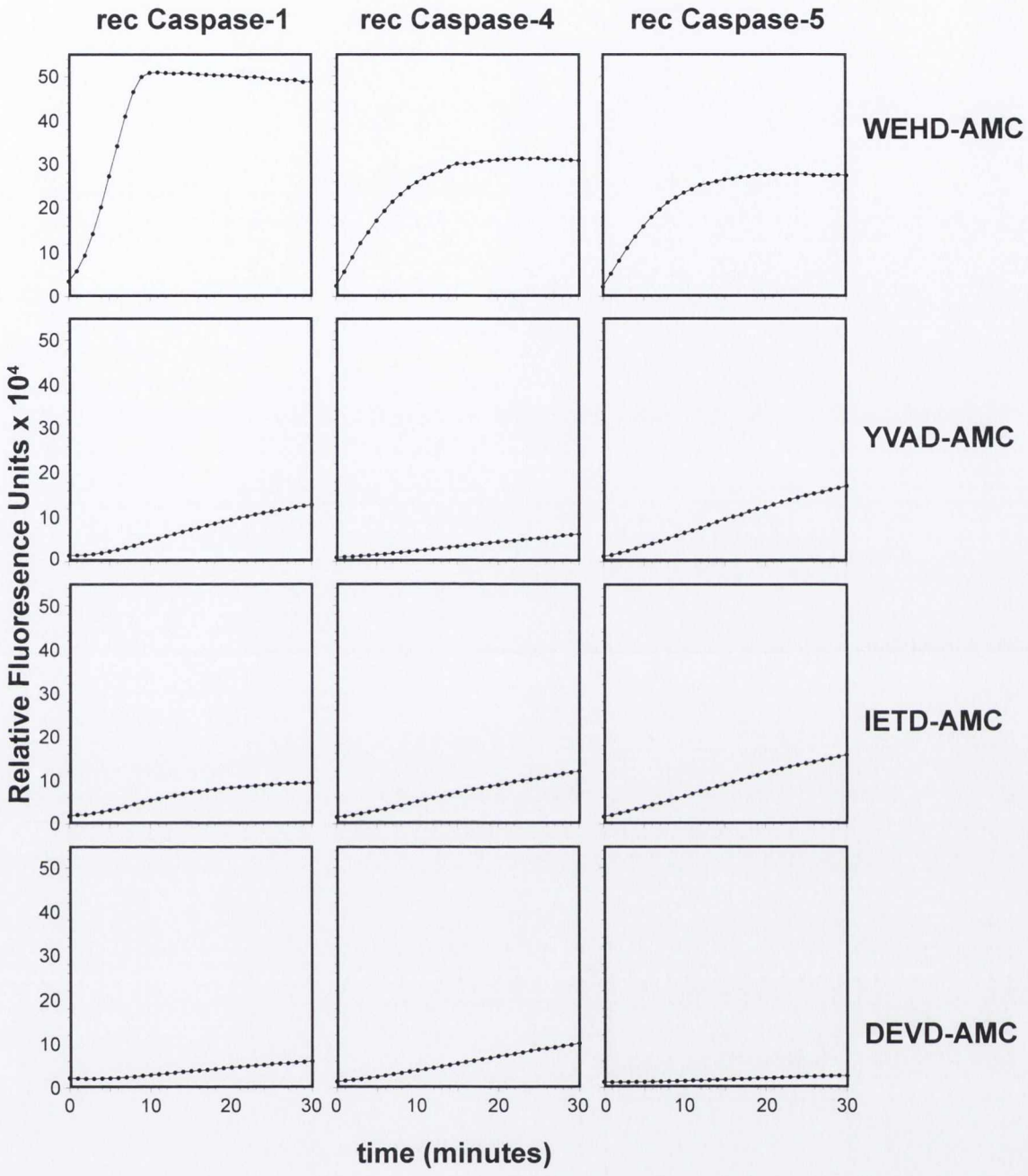

Figure 4.3

Characterisation of recombinant human caspase-1, -4 and-5

WEHD-, YVAD-, DEVD- and IETD-ase activity of recombinant caspase-1, -4 and -5 were tested in a 100 µl assay with 50 µM of flurogenic substrate. The increase of the relative fluorogenicity was detected and recorded over time.

a slightly different selectivity profile, hence we could expect to see a different substrate preference for each caspase.

4.3.4 Testing the activity of recombinant caspase-1 against ^{35}S-methionine labelled and endogenous proteins

It was important to use a physiologically relevant amount of recombinant caspase in order to avoid false positive results that could be produced by using an excessive amount of active recombinant caspase. This was achieved by titrating the recombinant caspase against a known substrate *in vitro*. To date the only independently confirmed substrates for caspase-1 are IL-1β, IL-18. To choose an optimal but non-saturating concentration for caspase-1, we titrated the recombinant protease against *in vitro* transcribed and translated IL-1β, caspase-1 and caspase-3 (Figure 4.4A upper panels). Additionally we added the same amount of recombinant caspase-1 to a THP-1 cell-free extract and immunoblotted for endogenous IL-1β (Figure 4.4A lower panel). Both *in vitro* transcribed and translated and endogenous IL-1β were processed by recombinant caspase-1, even at dilutions as low as 1/500 of the stock preparation. Using ^{35}S-methionine labelled caspase-3 as a negative control, caspase-1 dilutions of 1/100 cleaved only a minimal amount of ^{35}S-caspase-3, while at a dilution of 1/250 and below processing of the nonspecific caspase-1 substrate was undetectable.

The previous two-dimensional gel analysis with endogenous proteases and substrates clearly showed that only very few alterations were detectable when caspases involved in inflammation were activated. We therefore decided to use a rather high concentration of the protease and choose a dilution of 1/80 of recombinant caspase-1 to ensure detection of even poorly cleaved substrates. Any false positives would be eliminated after the screen by detecting processing of the putative caspase substrates by endogenous caspases in the already established THP-1 cell-free system.

4.3.5 Titration of recombinant caspase-4 and -5 against caspase-1 by WEHD-AMC proteolytic activity of the proteases

As there are no confirmed caspase-4 and -5 substrates we decided to use dilutions of the enzymes with equal *in vitro* cleavage activities of WEHD-AMC compared to caspase-1, as this substrate has been shown to be the preferred peptide for all three caspases (Figure 4.3). Recombinant caspase-4 and -5 were titrated against the chosen dilution of recombinant caspase-1 and dilutions of 1/30 and 1/25 of the stock preparations respectively gave similar rates of WEHD-AMC hydrolysis to a 1/80 dilution of recombinant caspase-1 (Figure 4.4B). These dilutions were therefore used in the small pool screen.

4.3.6 Screening small pool library for caspase-1, -4 and -5 substrates

The ProteoLink human adult brain cDNA library (Promega) consists of 960 individual cDNA pools. Each of these pools contains 50 to 100 unique cDNAs, theoretically representing over 50,000 expressed 'genes'. Expression of caspase-1 has been shown in astrocytes, microglia cells and also in neurons. The protease is fully functional and has been linked to neurodegenerative processes such as in Alzheimer's disease (Halle *et al.*, 2008). Due to the limited amount of soluble cDNA available we expanded the cDNA by transforming each pool separately and growing the bacteria to a near lawn density on agar plates. All bacteria from the plates were collected by scraping and the plasmid DNA was isolated. The screen was then performed as outlined in Figure 4.1. Each cDNA pool was individually transcribed / translated in the presence of ^{35}S-methionine, split into four and then individually treated with either buffer alone or each recombinant caspase. Each incubated sample was then resolved on a 12% SDS-PAGE gel and the ^{35}S-methionine labelled proteins were detected by fluorography (Figure 4.5). Pools positive for a caspase substrate were identified by comparing the banding pattern of buffer-incubated reactions versus caspase-treated samples. Protein bands of caspase-treated samples that shifted to a lower molecular weight, compared to the buffer incubated control band, indicated proteolysis.

A total of 240 pools were screened of which 20 were positive for proteolytic cleavage by a recombinant caspase. Interestingly, when the identified proteolytic

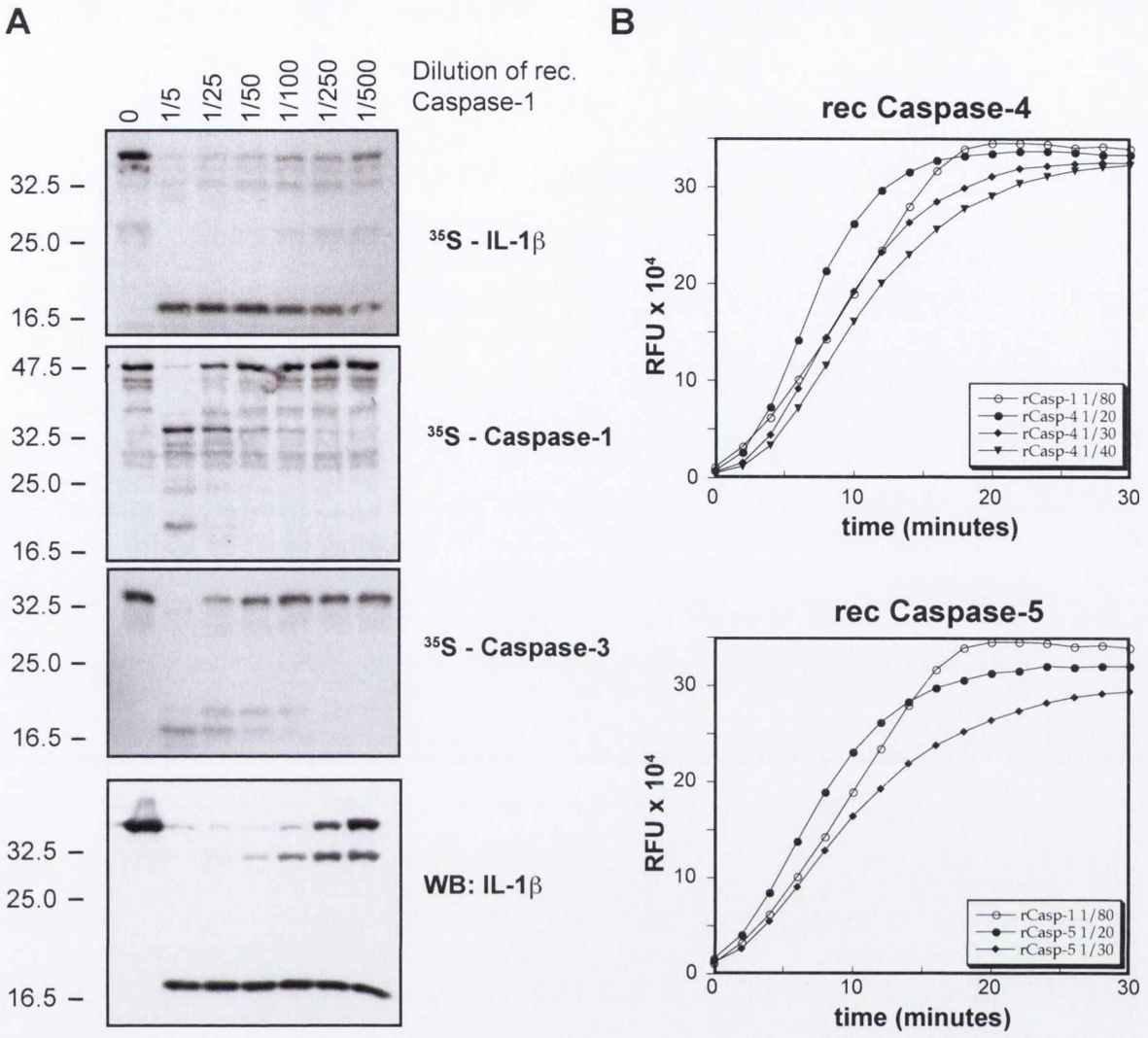

Figure 4.4

Titration of recombinant caspase-1, -4 and-5

(A) A dilution series of recombinant caspase-1 was incubated at 37 ^{0}C with ^{35}S-methionine labelled proteins for 2 hours (top) or with THP-1 cell free extract (bottom). Protein samples were resolved by 12% SDS PAGE and proteins were detected by autoradiography (top) or Western blot for IL-1β (bottom). Molecular weight markers in kDa are shown on the left.

(B) Calibration of recombinant human caspase-4 and-5 against recombinant caspase-1. Recombinant caspase-4 (Top panel) and -5 (Bottom panel) were titrated against a 1/80 dilution of recombinant caspase-1 The WEHD-ase activity of each protease dilution was assayed in a 100 µl reaction with 50 µM of flurogenic substrate. Fluorescence was measured and graphed over time. A 1/30 dilution of recombinant caspase-4 and a 1/25 dilution of recombinant caspase-5 were chosen for further experiments. RFU: Relative Fluorescent Units.

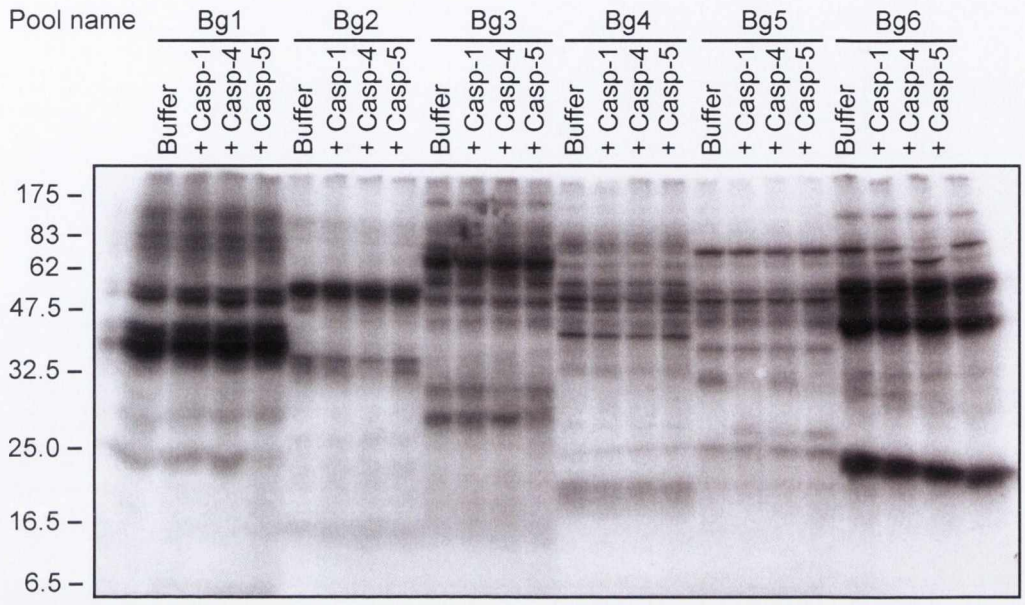

Figure 4.5

Example of the inflammatory caspase substrate small pool screen

An autoradiograph of six transcribed and translated ^{35}S-methionine labelled pools incubated with either buffer or a recombinant caspase. Molecular weight markers in kDa are indicated on the left. Pool Bg5 contains a caspase-1 and -5 substrate (cleaved from 30 kDa to 25 kDa), pool Bg6 contains a caspase-4 substrate (cleaved form 80 kDa to 60 kDa).

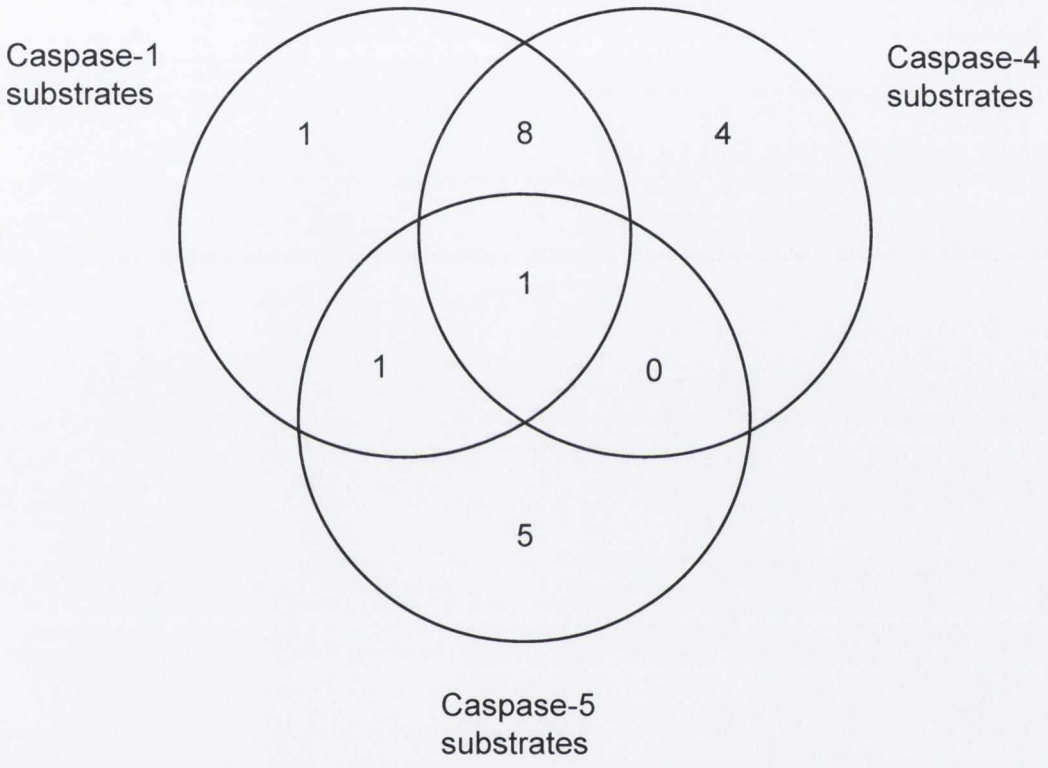

Figure 4.6
Identified caspase-1, -4 and -5 poteolytic events of the screened 240 pools
Proteins undergoing a proteolytic event in the screened pools are grouped according to the recombinant caspase they are processed by.

events were graphed according to the caspase responsible, most substrates were processed either by both caspase-4 and caspase-1 or solely by caspase-5 (Figure 4.6). These data suggest that caspase-1 and -4 share overlapping protease specificities and could possibly perform redundant actions, whereas caspase -5 is expected to have unique substrates.

4.3.7 Decoding of positive pools to a single positive clone

Having identified positive pools, we then needed to isolate the putative substrate within the small pool. An initial attempt to resolve the *in vitro* transcribed and translated pool by SDS-PAGE and identify the single protein by mass spectrometry was not achievable. This failure was due to the low abundance of the protein of interest versus the high concentration of proteins contained in the rabbit reticulate lysate used in the *in vitro* transcription and translation (ITT). We next attempted to isolate the single positive cDNA clone harbouring the gene of interest and subsequently identify it by DNA sequencing. The decoding strategy is shown in a schematic diagram (Figure 4.7A).

To identify a single clone out of the potential 50 to 100 cDNAs in the pool, we transformed the pools containing the positive cDNA in *E.coli* DH5α and grew up 100 individual clones of this transformation in small liquid cultures. A sub-pooling approach was taken to reduce the amount of cDNA extractions and ITTs required. We split the liquid culture in two and froze the pelleted bacteria of one half for possible cDNA extraction at a later stage. The remaining half of 10 single liquid cultures was combined into a new subpool. Of all 10 new subpools the cDNA was extracted, *in vitro* transcribed and translated and analyzed to determine which one contained a band running at the correct molecular weight compared to the band of interest in the positive pool. As an example, results from the decoding stages of the positive pool Eh6 are shown (Figure 4.7B). If a subpool contained a band at the similar molecular weight as in the initial pool, the individually frozen bacterial pellets of this positive subpool were processed identically as above to identify the single clone coding for the protein of interest. Before identifying the cDNA by DNA sequencing, proteolytic cleavage of the protein by the appropriate inflammatory caspase was confirmed. If none of the subpools contained a band at the desired

molecular weight, a further 100 clones were picked, subpooled and analyzed. The decoding of a pool was abandoned if after screening 500 individual clones no match was found.

By using the small pool cDNA library we screened approximately 4000 detectable proteins as substrates of inflammatory caspases. Out of a total of 20 positive pools, 11 were successfully decoded to a single clone and identified by sequencing. Two of the clones turned out to be identical proteins originating from different pools. Of the 10 identified sequences, 6 clones contained the full length coding sequence of the protein (Table 4.1). We focused our next studies on the full-length clones only, because truncations were more likely to represent cleavage artefacts due to improper folding and exposure of internal, artificial cleavage sites.

4.3.8 The identity of the novel full-length inflammatory caspase substrates

Amongst the full-length proteins identified in the inflammatory caspase screen, none have been previously implicated in the regulation or signalling of inflammation. A summary of the known functions of each substrate identified is presented below.

Dickkopf-3 (DKK3)

DKK3 is a member of the Dickkopf family and may be involved in the negative regulation of the Wnt signalling pathway. This pathway is important for cell differentiation and development. A downregulation of DKK3 was observed in many cancer cell lines and may therefore act as a tumour suppressor gene (Hsieh *et al.*, 2004). Recently it was found that the secreted protein can induce differentiation of human monocytes to a dendritic like cell type (Watanabe *et al.*, 2009).

Ganglioside-induced differentiation-associated protein 1 like 1 (GDAP1L1).

Very little is known about GDAP1L1 but more studies have been done on its 72% homologous GDAP1 family member which is mainly expressed in tissue of the CNS. They both contain two putative GST domains which are probably not active. A C-terminal tail-anchor domain localises GDAP1 into the mitochondrial outer

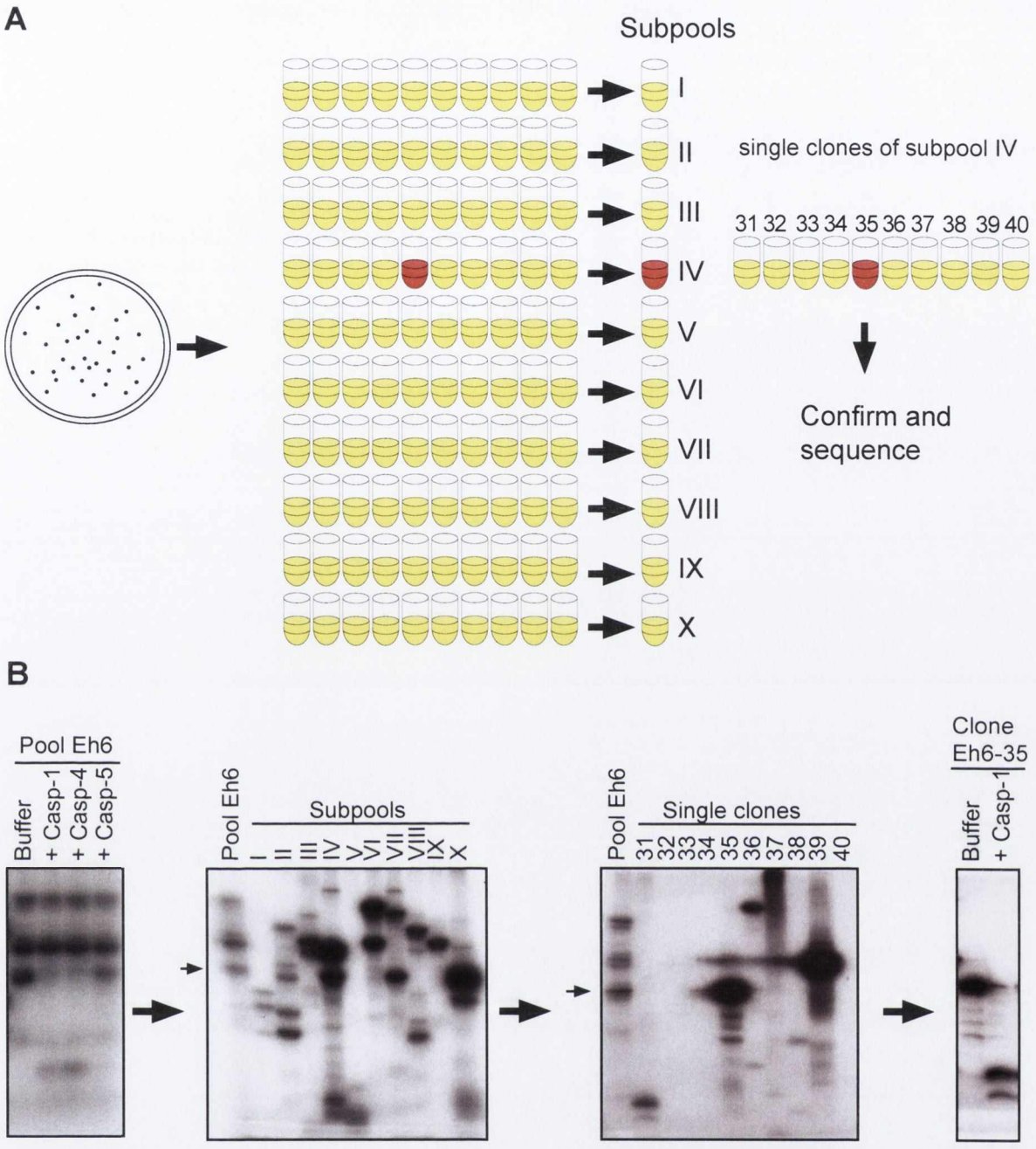

Figure 4.7

Decoding of the positive pools

Schematics of the decoding strategy for positive pools (A) and the decoding of pool EH6 as an example (B). The positive pool of cDNA was transformed in DH5α and 100 individual clones were grown in starter cultures. Half the volume of the starter culture was pelleted and frozen for later decoding. The remaining culture of 10 clones was subpooled. cDNAs of the 10 subpools (I to X) were then extracted, transcribed and translated and the ^{35}S methionine labelled proteins were analysed by SDS-PAGE. Autoradiography identifies the subpool containing the band migrating at the same molecular weight as the proteolyticaly disappearing band. The single clones (31 to 40) of the positive subpool were then tested the same way as the subpools and the positive clone was verified by cleavage by the recombinant caspase and sequenced for identity.

membrane and is thought to mediate mitochondrial fision (Wagner *et al.*, 2009). Mutations in GDAP1 are associated with Charcot Marie Tooth type 4A disease, a slow and progressive weakness and atrophy of muscles and distal sensory deficits (Baxter *et al.*, 2002).

Melanoma antigen family D1 (MAGE-D1, NRAGE, Dlxin-1)

MAGE-D1 contains two MAGE domains and is ubiquitously expressed in embryonic and adult somatic tissues (Barker *et al.*, 2002). Initial studies showed that MAGE-D1 is possibly involved in transcription (Masuda *et al.*, 2001), interaction with XIAP (Jordan *et al.*, 2001) and binding to the p75 neutrophin receptor (p75NTR) to mediate nerve growth factor dependant apoptosis in neurons (Salehi *et al.*, 2000). Sympathetic neurons of mice lacking MAGE-D1 show a massive reduction in brain derived neutropic factor induced JNK signalling through p75NTR and a reduction in apoptosis in these cells as well as developmental apoptosis in motor neurons (Bertrand *et al.*, 2008).

60S Ribosomal Protein L10 (RPL10)

RPL10 is a highly conserved protein throughout evolution and co-purifies with the 40S ribosomal subunit. The yeast homologue Qsr1p is required for the joining of the 40S and 60S subunits to form the active 80S ribosome.

Transcription factor SOX-5, long isoform (L-SOX5)

Sox5 forms an enhancer complex with Sox6 for the transcription of cartilage matrix genes by Sox9 or other transcription factors (Lefebvre *et al.*, 1998). Sox5 / Sox6 deficient mice showed a defect in the chondrocyte differentiation pathway leading to defects in formation of cartilage matrix (Smits *et al.*, 2001).

TAR DNA-binding protein 43 (TDP-43)

TDP-43 was cloned through its ability to bind the HIV LTR and acts by repressing the promoter activity of HIV LTR (Ou *et al.*, 1995). Subsequently it has been shown to function as an activator for exon skipping in the cystic fibrosis transmembrane conductance regulator (CFTR) gene (Buratti *et al.*, 2001) and was identified in aggregates in the CNS. These poly-phosphorylated and ubiquitinated aggregates of TDP-43 are used today to identify and classify neurodegenerative

diseases. Recently TDP-43 has been identified as a caspase substrate cleaved during apoptosis although the consequences remain to be determined (Van Damme *et al.*, 2005).

4.3.9 Titration of recombinant caspases against the identified substrates

In the next stage of our screen we analysed the processing of the full-length substrates by the recombinant caspases in more detail. All of these cDNA clones were individually translated and were re-tested for proteolysis by all of the inflammatory caspases. The original concentration for the screen and a two step dilution was used to verify the robustness of the proteolysis (Figure 4.8). Caspase-1 only processed MAGE-D1 efficiently at the highest caspase-1 concentration, whereas caspase-4 cleaved all at concentrations tested. Caspase-5 showed activity against MAGE-D1, RPL10 and L-SOX5.

As a control, the same amount of recombinant proteases were also incubated with *in vitro* transcribed and translated products of the proteases themselves and control proteins IL-1β and caspase-9 (Figure 4.9). All proteases were clearly active against themselves. Besides IL-1β, caspase-1 also processed caspase-4 but not caspase-5. On the other hand, caspase-4 was also able to process a small amount of caspase-9 albeit not to the active p20 / p10 subunits.

4.3.10 Proteolytic cleavage of identified substrates in a THP-1 cell-free extract time course

Having identified several potential novel inflammatory caspase substrates, the next step was to confirm their proteolysis with an endogenous amount of inflammatory caspases using the THP-1 cell-free system described in chapter 3. The identified ^{35}S-methionine labelled full-length inflammatory caspase substrates were incubated in a THP-1 cell-free extract under conditions where either the endogenous caspases involved in inflammation, or apoptosis, were separately activated as described in chapter 3 (Figure 4.10).

Name	Accession number	Full lenght	known function
Activating signal co-subunit 2 (ASCC2)	Q9H1I8	No	Part of the TRIP4 complex, which enhances NF-κB, AP1 and SRF transcription
Dickkopf-3 (DKK-3)	Q9UBP4	Yes	Secreted protein with potentialy inhibits Wnt signaling pathway
Ganglioside induced differentiationassociated protein 1 like 1 (GDAP1L1)	Q96MZ0	Yes	Unknown
Glutamate dehydrogenase 1 (GLUD1)	P00367	No	Catalyses the oxidative deamination of glutamate
Melanoma-associated antigen D1 (MAGE-D1)	Q9Y5V3	Yes	Antagonises association between TrkA and p75NTR thereby inducing apoptosis.
Nuclear pore complex interacting protein (NPIP)	Q9UND3	No	Unknown, localised to the nuclear pore complex
60S Ribosomal Protein L10 (RPL10)	P27635	Yes	Part of the 40S ribosomal complex
BR serine/threonine protein kinase 2 (SAD-A)	Q81WQ3	No	Unknown, similarity to other serine/ threonine kinases involved in polarisation and axon growth of neurons
Transcription factor SOX-5 (L-Sox5)	P35711	Yes	Transcriptional enhancer involved in cartilage formation
TAR DNA binding protein (TDP-43)	Q13148	Yes	DNA and RNA binding protein regulating splicing and exon-skipping in the CFTR gene.

Table 4.1

List of identified full-length clones from the small pool library screen

Identified full-length clones cleaved by an inflammatory caspase. Indicated are the name and abbreviation of the protein, its accession number, if the isolated clone-covers the total coding sequence of the protein and any published function of the protein.

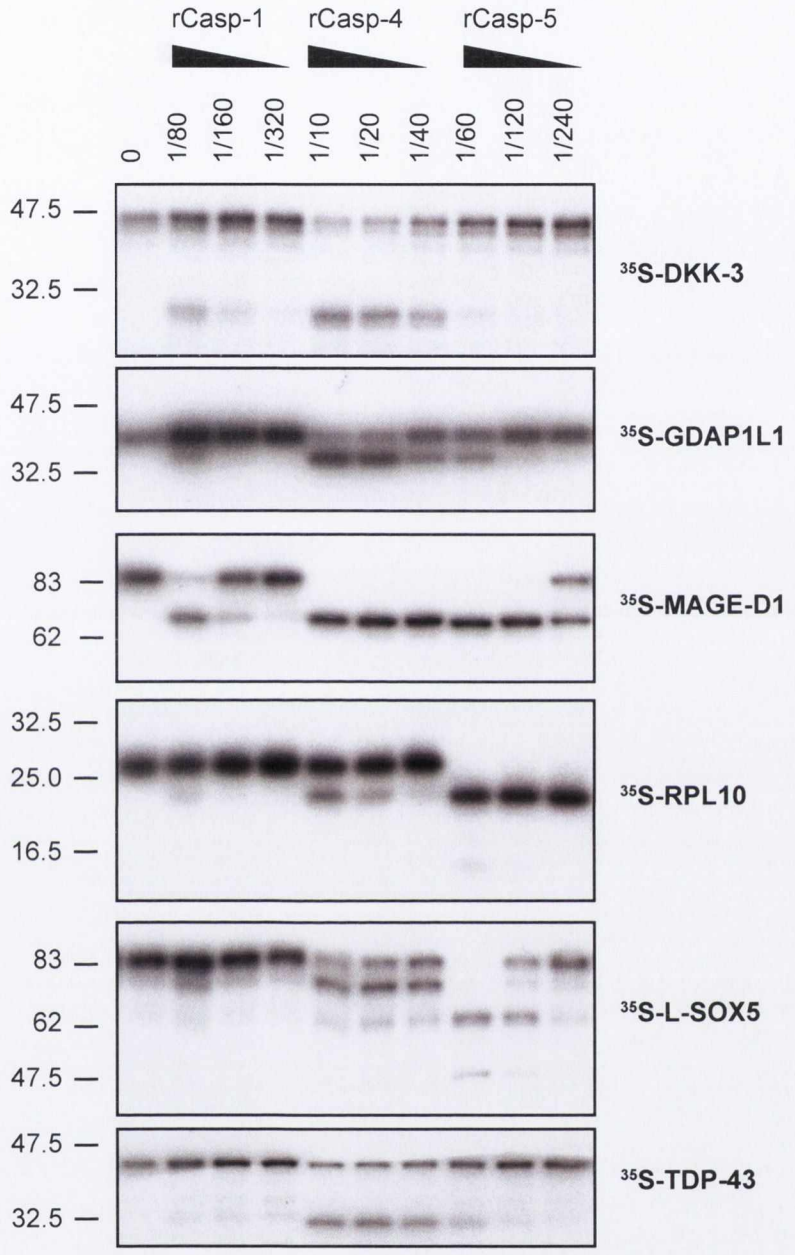

Figure 4.8

^{35}S-methionine labelled substrate cleavage by recombinant caspases -1, -4 and -5

In vitro transcribed / translated ^{35}S-methionine labelled identified caspase-1, -4 or -5 substrates were incubated with different concentrations of recombinant caspase-1, -4 and -5. The time-point samples were resolved on 12% SDS-PAGE and the proteolysis of the ^{35}S-methionine labelled proteins was visualised by autoradiography. Molecular markers in kDa are shown on the left.

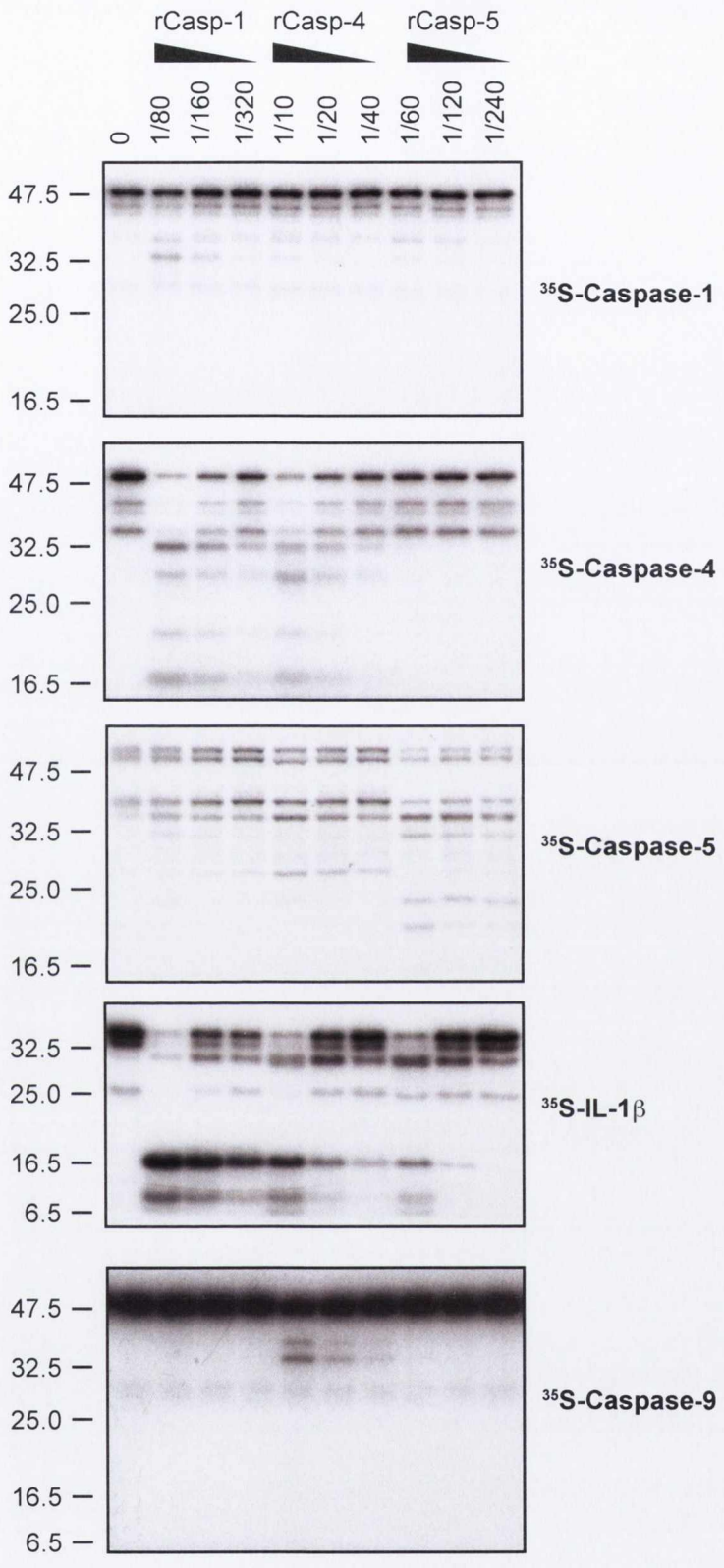

Figure 4.9

^{35}S-methionine labelled substrate cleavage by recombinant caspases -1, -4 and -5

In vitro transcribed / translated ^{35}S-methionine labelled caspases-1, -4, -5, the caspase-1 substrate IL-1β and caspase-9 as a control were incubated with different concentrations of recombinant caspase-1, -4 and -5. The samples were resolved on 12% SDS-PAGE and the proteolysis of the ^{35}S-methionine labelled proteins was visualised by autoradiography. Molecular markers in kDa are shown on the left.

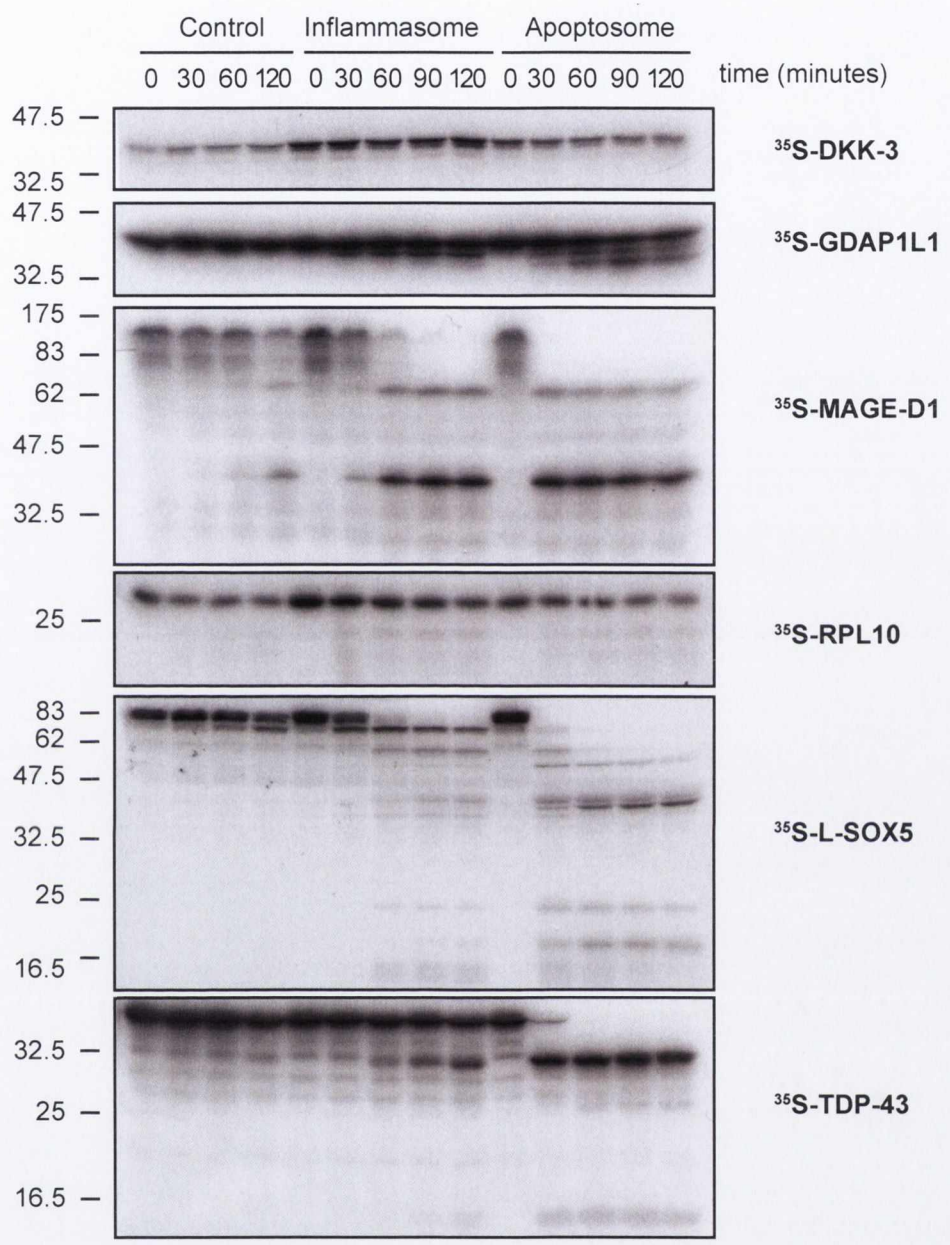

Figure 4.10

^{35}S-methionine labelled substrate cleavage of identified caspase-1, -4 and -5 substrates in a THP-1 cell-free extract time course

In vitro transcribed / translated ^{35}S-methionine labelled identified caspase-1, -4 or -5 substrates were incubated with THP-1 cell-free extract over a time course under different conditions: Control: 10 µM YVAD-CHO; Inflammasome: Buffer A; Apoptosome: 50 µg/µl Cytochrome c, 1 mM dATP.

The time point samples were resolved on 12% SDS-PAGE and the proteolysis of the ^{35}S-methionine labelled proteins was visualised by autoradiography. Molecular markers in kDa are shown on the left.

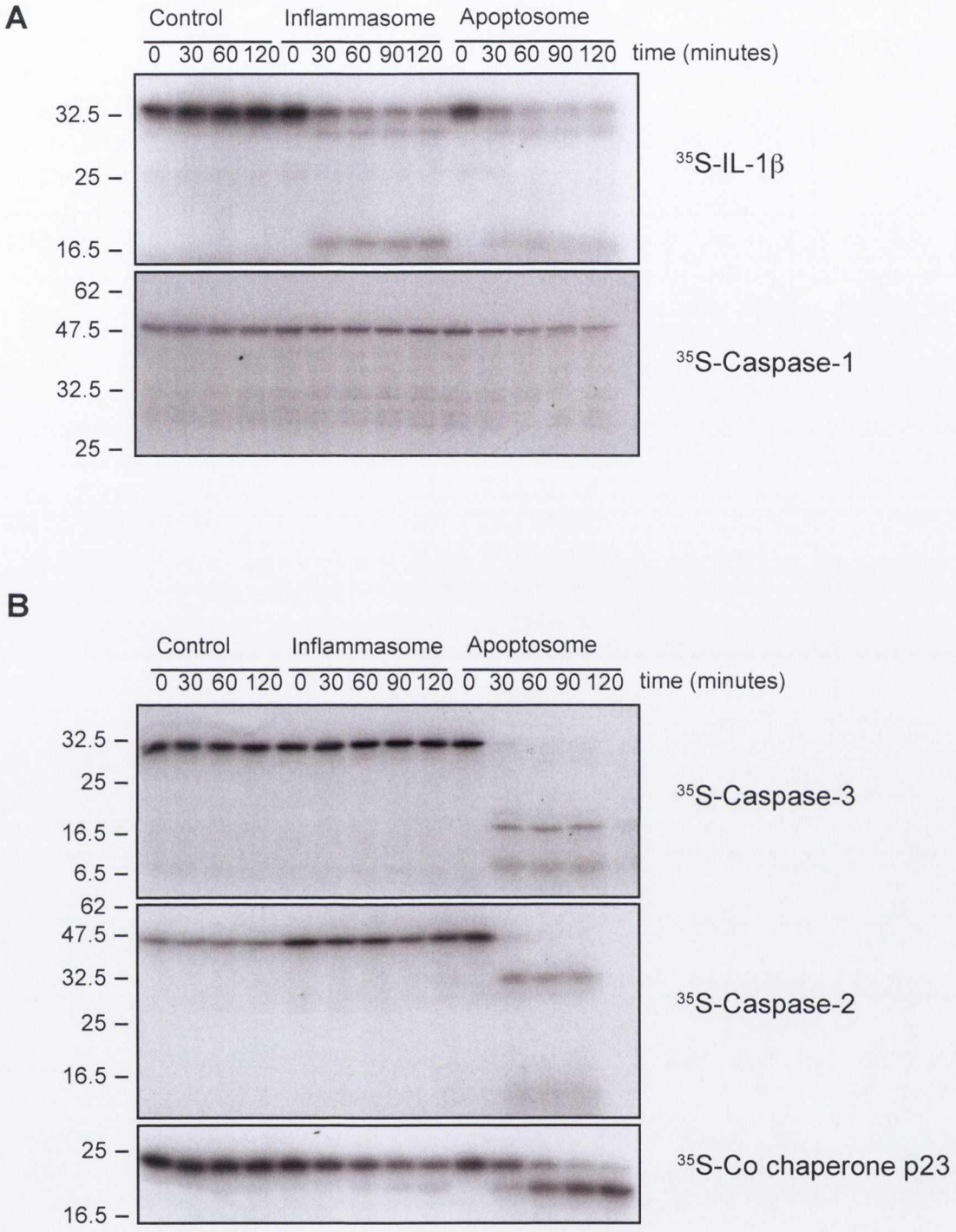

Figure 4.11

^{35}S labelled substrate cleavage of known caspase substrates in a THP-1 CFE time-course

In vitro transcribed / translated ^{35}S-methionine labelled known inflammatory (A) and apoptotic (B) caspase substrates were incubated with THP-1 cell free extract over a time-course under different conditions: Control: 10 µM YVAD-CHO; Inflammasome: Buffer A; Apoptosome: 50 µg/µl Cytochrome c, 1 mM dATP.

The time-point samples were resolved on 12% SDS-PAGE and the proteolysis of the ^{35}S-methionine labelled proteins was visualised by autoradiography. Molecular weight markers in kDa are shown on the left.

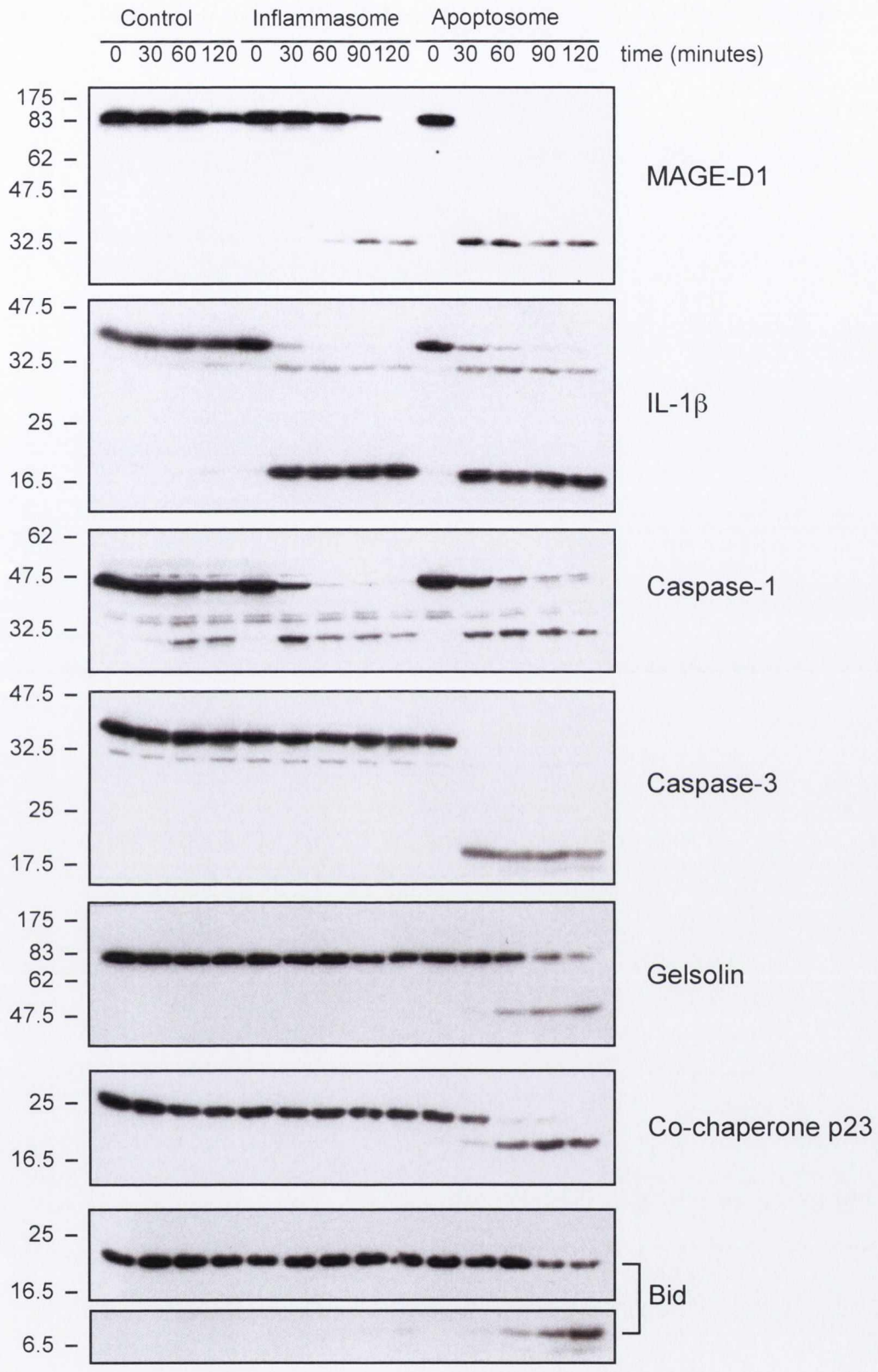

Figure 4.12

Endogenous processing of MAGE-D1 in THP-1 cell-free time course

THP-1 cell free extract was incubated under various conditions at 37°C for the indicated times. Control: 10 µM YVAD-CHO; Inflammasome: buffer A; Apoptosome: 50 µg/µl Cytochrome c, 1 mM dATP. The processing of the caspases and caspase substrates was monitored by Western Blot. Molecular weight markers in kDa are shown on the left.

GDAP1L1

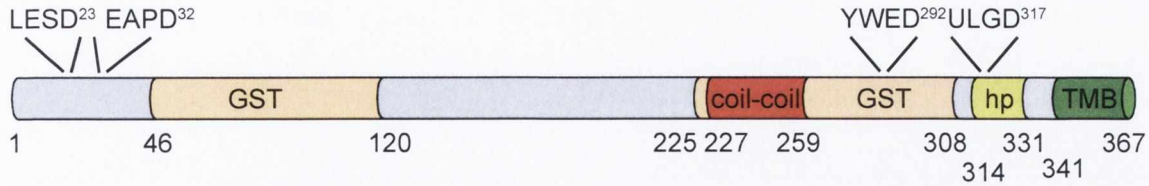

MAGE-D1

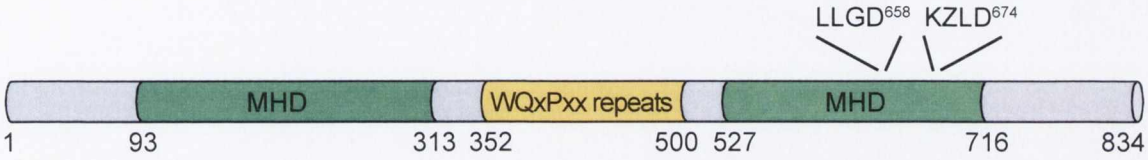

L-SOX5

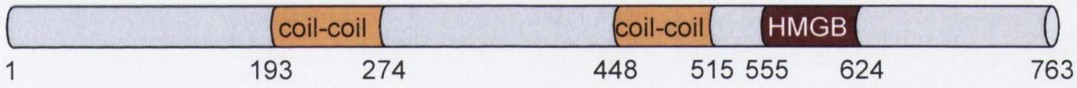

TDP-43

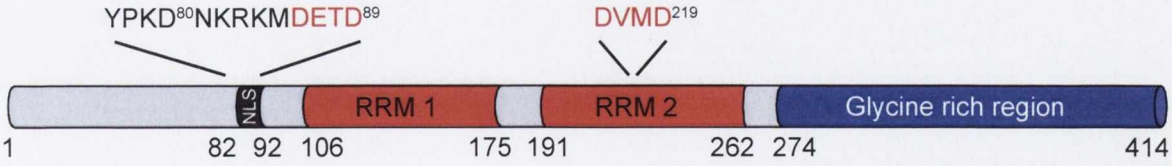

Figure 4.13

Stick-diagrams of the identified proteins

Schematic representation of the identified inflammatory caspase substrates. Known domains are highlighted in color and putative caspase cleavage sites are indicated above the diagram. The known TDP-43 caspase cleavage sites are highlighted in red.

GST, Glutathione S-transferase domain; hp, hydrophobic region; TMB, transmembrane domain; MHD, MAGE homology domain; HMGB, High Mobility Group Box; NLS, nuclear localisation signal; RRM, RNA recognition motiv

As shown in Figure 4.10, GDAP1L1, MAGE-D1, L-SOX5 and TDP-43, were processed under inflammatory and apoptotic caspase activation conditions in a manner similar to the cleavage of the positive control substrate, IL-1β (Figure 4.11) By contrast, DKK3 and RPL10 were not efficiently cleaved by either group of caspases. Thus, from the original group of candidate substrates identified in this screen, only GDAP1L1, MAGE-D1, L-SOX5 and TDP-43 were validated as inflammatory caspase targets.

4.3.11 MAGE-D1 represents a substrate for inflammatory and apoptotic caspases

Since MAGE-D1 was described to be involved in NGF receptor signalling, a pathway capable of inducing cell death and also associated with inflammatory macrophage survival (Salehi *et al.,* 2000) we decided to focus on this protein.

Endogenous MAGE-D1 processing was verified in the THP-1 cell-free extract time course under the different endogenous caspase activation conditions by Western blot (Figure 4.12). The processing pattern was similar to the *in vitro* synthesized MAGE-D1 (Figure 4.10). Caspase-3, Gelsolin, Co chaperone p23 and Bid, all proteins processed during apoptosis were not cleaved under conditions where inflammatory caspases were activated, confirming that apoptotic caspases were not active. Significantly, under the same conditions both MAGE-D1 and IL-1β were processed in a time dependant manner, demonstrating that endogenous MAGE-D1 was indeed processed when endogenous inflammatory caspases were active. Additionally, the cleavage of both proteins was completely inhibitable by the peptide inhibitor YVAD-CHO, further indicating the involvement of an inflammatory caspase in the processing of MAGE-D1. These results suggest that MAGE-D1 represents a genuine, novel inflammatory caspase substrate.

4.4 Discussion

4.4.1 Summary

In this part of the study, we used an alternative proteomic approach to identify novel inflammatory caspase substrates to overcome some of the drawbacks encountered with 2D SDS-PAGE in the previous chapter. By using an *in vitro* expression cloning approach of a small pool cDNA library we were able to express and monitor single proteins while still screening a substantial amount of the total proteome. We started by purifying recombinant caspases from a bacterial expression system. In a step to reduce the number of false positive candidates, we determined the near physiological concentration of the recombinant proteases against known substrates. The screen of 240 small pools identified a total of 20 potential inflammatory caspase substrates of which 10 where subsequently decoded down to a single clone. None of the identified potential inflammatory caspase substrates have been implicated in an inflammatory process before and their involvement in such a context requires further investigation.

For the next steps we focused on full-length clones and determined whether these proteins are substrates of endogenous inflammatory caspases. We used the THP-1 cell-free system described in the previous chapter and confirmed that *in vitro* synthesized GDAP1L1, MAGE-D1, L-SOX5 and TDP-43 were processed under conditions where endogenous inflammatory caspases were activated. We could also show that the endogenous MAGE-D1 protein is cleaved by inflammatory caspases.

4.4.2 Small pool cDNA library screen

The two-dimensional SDS-PAGE proteome analysis clearly showed the high specificity of the inflammatory caspases as only very few spot alterations were detectable compared to proteomes where apoptotic caspases were activated. A possible hampering fact was the slightly biased and not complete representation of the THP-1 proteome by two-dimensional SDS-PAGE. To screen a wider source of proteins another approach was taken.

A small pool cDNA library consists of a cDNA library which was subdivided into pools containing a certain number of individual cDNAs. These cDNA pools could then be individually tested for the desired activity. Containing only a limited number of cDNA clones, a positive pool could be decoded and the single cDNA clone be identified by DNA sequencing. This method of *in vitro* expression cloning has been previously used. Initially pools of cDNA transcribed *in vitro* into RNA were injected in oocytes of *Xenopus laevis* and they were screened for receptor protein expression. Positive pools were progressively subdivided and reassayed until a single clone was identified (Masu *et al.*, 1987). Other groups have adapted this technique and refined it by reducing the pool size to 100 cDNAs and using HeLa or mouse cDNA libraries as a source. Small pool libraries can be used for different functional screens like protease and kinase substrates (Lustig *et al.*, 1997), activity screens (Haushalter *et al.*, 1999) or interaction screens (Pridgeon *et al.*, 2003). The apoptosis inducing Bcl-2 protein Bid was identified by such a similar screen (Wang *et al.*, 1996).

The Proteolink *in vitro* expression cloning system we used in this screen was a commercially available small pool cDNA library from human adult brain. While using this as a source for an inflammatory caspase screen may be less ideal than an activated macrophage cDNA library, caspase-1 and IL-1β have been shown to be expressed and implicated in an inflammatory response in the brain (Halle *et al.*, 2008; and reviewed in Oprica *et al.*, 2003).

This method of screening was also found to have some limitations. None of the known caspase-1 substrates were isolated by this screen, which could have served as a positive control for this method. As the mRNA of both pro-IL-1β and pro-IL-18 is only massively unregulated upon an encounter with a PAMP, the cDNA of both genes was probably not present in the cDNA library which was prepared from normal tissue. Ideally, primed macrophages could have been utilised as an mRNA source, but the production of a qualitative and extremely comprehensive small pool cDNA library as part of this project would have taken too long and would have been too labour intensive.

This proteomic screen approach depends on a system whereby cDNA is *in vitro* transcribed and translated into proteins. The specifically prepared rabbit reticulcyte lysate used for this purpose also has its limitations in producing proteins of identical structure found *in vivo*. Proteins lack any post-transcriptional modifications and could also end up mis-folded. The *in vitro* transcribed and translated caspase-1 serves as a good example, as it is clearly less efficiently cleaved by recombinant (Figure 4.4A) or endogenous (Figure 4.11A) caspase-1. IL-1β on the other hand is cleaved very efficiently in the same experiments, similar to the endogenous protein (Figure 4.4A and 4.12).

Additionally, in each transcribed and translated cDNA pool an average of 16 bands (9 to 25) were detectable after *in vitro* expression and labelling, although each pool of the library contained between 50 to 100 cDNA clones. This observation is very similar to another screen published (Pridgeon *et al.,* 2003). It is possible that some fragments were cloned in the wrong direction resulting in the non transcription of the gene. Further more, some of the genes could have been too small to be resolved by 12% SDS-PAGE or too big to be efficiently *in vitro* transcribed and translated. The identified inflammatory caspase substrates indicate this, as most of the identified full-length clones encoded proteins smaller than 60 kDa. Translating the individual single clones of a pool showed, not surprisingly, that not all cDNAs gave rise to a detectable ^{35}S labelled protein (Figure 4.7B), although a single DNA band was detectable by agarose gel electrophoresis and ethidium bromide staining for each clone (Data not shown). Proteins with a single methionine in the coding sequence would result in a poorly labelled substrate making it difficult to detect, especially with a strongly labelled protein migrating at a similar molecular weight. Some plasmids or proteins might have outcompeted or inhibited others during the *in vitro* transcription / translation or have autodegraded into small fragments when incubated at 37°C for two hours. The plasmids of the small pool cDNA library most likely also contained non coding sequences or mutations leading to an early stop codon and abortion of the protein translation.

A further drawback of the small pool cDNA screening techniques is that almost half of all identified clones (4 out of 10) only contained a partial open reading frame encoding only the C-terminal part of the protein. This is in line with other

reports using this screening method (Cryns *et al.*, 1997; Rao *et al.*, 1999). These truncations are probably due to the way the library was generated. By using oligo(dT) primers for the cDNA synthesis from poly(A)-containing mRNA, a premature termination of the reverse translation would result in the C-terminal fragments observed.

This inflammatory caspase substrate screen was performed with Rosie Söllner who screened 240 separate pools in parallel. The substrates identified by her also indicated no clear cut connection to inflammation and are described in her MSc. thesis.
Detecting an average of 16 different protein bands in an *in vitro* transcribed and translated small pool (Figure 4.5), together we assayed almost 8000 proteins, which represent almost three times as many proteins detectable and identifiable by 2D SDS-PAGE / mass spectrometry

4.4.3 Substrate specificity of recombinant caspases

When assaying different recombinant caspase-1 dilutions for cleavage of fluorogenic substrates, WEHD-AMC was most efficiently processed followed by YVAD-AMC. Similar results have previously been published by other groups (Thornberry *et al.,* 1997; Talanian *et al.,* 1997). The relatively high efficiency of IETD-AMC processing, a preferred substrate of caspase-8 or -10, was shown here for the first time. A peptide substrate screen does indicate a possibility for caspase-1 to cleave after IETD, although not nearly as efficient as after YVAD (Thornberry *et al.,* 1997) as seen in Figure 4.3. DEVD-AMC, an amino acid sequence present in many apoptotic caspase substrates, was in turn only proteolysed with large, unphysiological amounts of recombinant caspase-1. These results clearly show that the recombinant protein was highly active against known caspase-1 substrates and only cleaved apoptotic caspase substrates when used at high recombinant protein levels.

While we established the non saturating amount of recombinant caspase to be used for the screen, *in vitro* transcribed and translated IL-1β was cleaved at a higher efficiency than caspase-1. This could indicate that IL-1β is either the better

caspase-1 substrate than the protease itself or that some *in vitro* translated proteins were possibly less efficiently cleaved by the recombinant proteases than *in vivo* (Figure 4.4A). The negative control protein caspase-3 was very faintly processed to the intermediary p22 at a recombinant caspase-1 dilution of 1/100. This experiment clearly shows that saturating amounts of recombinant protease cannot be used to prove a protein to be a substrate of this recombinant protease. Additional control experiments to verify the proteolysis with endogenous protein level are always required. Ideally the processing should be examined *in vivo*, induced by a natural stimulus to activate the corresponding protease.

4.4.4 Grouping of inflammatory caspases according to their substrate specificity

Of the transcribed / translated cDNA pools tested we detected a proteolytic change in 20 pools when these were incubated with an inflammatory recombinant caspase compared to buffer alone. By grouping the proteolytic events according to the protease involved, two groups became apparent: proteins cleaved by recombinant caspase-4 and / or caspase-1 and proteins cleaved by caspase-5 only. This indicates that the substrate specificity of caspase-1 and -4 are quite similar, whereas caspase-5 mainly cleaved substrates which are not cleaved by caspase-1 and -4. According to the substrate specificity of this screen, the inflammatory caspases can be further subdivided into two distinct groups by their substrate recognition sequence.

4.4.5 Identified substrates of the inflammatory caspase small pool cDNA library screen

Of the 20 positive cDNA pools we decoded 10 to the single clone stage and confirmed processing of the resulting protein by the inflammatory caspases. None of the identified proteins have been previously implicated in inflammatory responses.

A drawback of cDNA libraries is the possibility of partial clones. Fragments of RNA can be reverse transcribed and cloned in the expression vectors resulting in either N- or C-terminally deleted mutants. These shorter proteins usually do not fold

properly and/or expose parts of their structure which are usually buried inside the globular molecule to the exterior and hence accessible to proteases. This can lead to false positive identifications. The expression vectors containing clones ASCC2, GLUD1, NPIP and SAD-A covered only a partial sequence of the identified protein and were therefore not further investigated. RPL10 and DKK3 were not cleaved under conditions where inflammatory caspases were active and are therefore not pursued further. However, they possibly could still be processed by inflammatory caspases in other cell types, e.g. astrocytes. The possible involvement of the four remaining identified inflammatory caspase substrates in inflammatory process are described below:

Almost no information exists about ganglioside-induced differentiation-associated protein 1 like 1 (GDAP1L1), but it shares a 73% amino acid homology to the better characterised ganglioside-induced differentiation-associated protein 1 (GDAP1). Although structurally related to the glutathione S-transferases (GST), no GST activity has been found (Shield *et al.*, 2006). Mutations in this gene lead to Charcot Marie Tooth type 4 disease, characterized by slow, progressive weakness and atrophy of muscles and distal sensory deficiencies indicating a possible function in the CNS (Marco *et al.*, 2004). Recently GDAP1 has been located at the mitochondrial outer membrane (MOM) and overexpression of GDAP1 induces fragmentation of mitochondria, suggesting that GDAP1 plays a role in the fission mechanism of mitochondrial dynamics (Niemann *et al.*, 2005 Shield *et al.*, 2006; Wagner *et al.*, 2009). This may not be the case for GDAP1L1, as it lacks the last 8 amino acids of the transmembrane domain. This protein was not efficiently cleaved by both inflammatory and apoptotic caspases. A second cleavage site was recognised by the apoptotic caspases (Figure 4.10). Currently, based upon the literature available it is difficult to link GDAP1L1 to inflammatory processes.

Melanoma-associated antigen D1 (MAGE-D1), also named NRAGE or Dlxin-1 belongs to a family of over 25 members, containing a MAGE homology domain of unknown function. The C-terminal portion of MAGE-D1 has been shown to interact with the cytosolic portion of the nerve growth factor p75 (p75NTR) (Salehi *et al.*, 2000) and XIAP (Barker and Salehi, 2002). p75NTR is a member of the tumour necrosis factor receptor superfamily and acts as a co-receptor for neutrophins with

TrkA (reviewed in Kaplan *et al.*, 2000) although not through direct extracellular interactions (Wehrman *et al.*, 2007). Upon nerve growth factor binding, TrkA mediates neuronal differentiation and survival. Ectopically expressed MAGE-D1 antagonises the p75NTR – TrkA interaction and induces cell cycle arrest and apoptosis, possibly through activation of JNK and the intrinsic cell death pathway (Salehi *et al.*, 2002). Putative caspase cleavage sites were identified in both MAGE homology domains (Figure 4.13) Proteolytic cleavage of MAGE-D1 by inflammatory caspases could lead to binding of the p75NTR by the C-terminal cleavage product and induce apoptosis under nerve growth factor deprivation (Salehi *et al.,* 2000). For cells lacking growth stimulants, mounting an inflammatory response would not be beneficial, as the required resources would most likely be unavailable. The whole organism therefore benefits more if the infected cells are killed and removed by programmed cell death instead of a poor immune response further weakening the organism. MAGE-D1 was also shown to bind Dlx5 (Masuda *et al.,* 2001), a transcriptional factor required for osteoblast differentiation and complete formation of bone (Acampora *et al.*, 1999). Dlx5 itself appears to be a transcriptional repressor of osteocalcin (Acampora *et al.,* 1999), a protein involved in bone formation.

Transcription factor Sox5 (L-SOX5) belongs to the SoxD group of the Sry-related high mobility group box gene family, of which most act as transcription factors playing a role in differentiation and cell fate. Knockout data from mice implicates the protein in cartilage formation (Smits *et al.,* 2001; Dy *et al.*, 2008). L-Sox5 does not appear to have a typical transactivation domain, but contains two characteristic leucine-zipper coiled-coil domains allowing the protein to homo- or heterodimerize with other SoxD proteins. L-Sox5 can, for example, interact with SOX6 or SOX9 and can thereby activate Col2a1, a protein involved in chondrocyte differentiation (Lefebvre *et al.,* 1998). Both SoxD group family members are therefore redundant transcriptional co-activators required for development and an involvement in inflammation or apoptosis is not apparent. Our *in vitro* data show that the protein is cleaved at multiple sites by inflammatory and apoptotic caspases (Figure 4.10) indicating rather a disabling of any function of L-SOX5 activity rather than its activation.

TAR DNA binding protein 43 (TDP-43) was initially identified by its binding and repressor capability to DNA containing the TAR element of the human immunodeficiency virus (Ou *et al.,* 1995). The 414 amino acid long protein is widely expressed in tissues, including heart, lung, liver, spleen, kidney, muscle and brain (Buratti *et al.,* 2001). The overall structure of TDP-43 shows strong homology to the heterogeneous ribonucleoprotein family (hnRNPs), involved in pre-mRNA processing. TDP-43 contains two N-terminal nuclear localisation signals (NLS), followed by two RNA-recognition motifs (RRM) and a glycine rich domain at the C-term. This C-terminal glycine rich region is known to bind hnRNP protein family members (Buratti *et al.*, 2005; Zhang *et al.*, 2009) and can regulate exon skipping on the Cystic Fibrosis Transmembrane Conductance Regulator (CFTR) gene (Buratti *et al.,* 2001; Zhang *et al.,* 2009). This results in a non-functional protein, reduced sodium chloride export of the cell and as a result dysfunction of several organs producing the symptoms associated with cystic fibrosis.

A phosphorylated and poly-ubiquitinated 25 kDa C-terminal fragment of TDP-43 has been identified as the major component in detergent-resistant fractions of amyotrophic lateral sclerosis (ALS) and frontotemporal lobar degeneration with ubiquitin-positive inclusions (FTLD-U) patient brain samples (Arai *et al.*, 2006; Neumann *et al.*, 2006). As with other neurodegenerative diseases, the hyper phosphorylation, poly ubiquitination and deposition of aggregates in inclusion bodies of TDP-43 is found in many patients suffering from both ALS and FTLD-U and is used as a histopathological diagnostic tool. Although it is unclear whether the aggregation of TDP-43 is a primary event or a by-product of the disease process, a few mutations mainly in the C-terminal glycine rich region of the gene have been identified in patients suffering from either neurodegenerative disease.
TDP-43 has been independently identified in large scale proteomic screens as a caspase substrate cleaved during apoptosis at $DETD^{89}$ (Van Damme *et al.,* 2005; Thiede *et al.*, 2005) and has been later confirmed with another possible site at $DVMD^{219}$ (Zhang *et al.*, 2007). A careful comparison of the TDP-43 processing patterns between caspases associated with inflammation or apoptosis (Figure 4.10) and analysis of the protein sequence could reveal an additional inflammatory caspase processing site at $YPKD^{80}$ (Figure 4.13).

A recent publication using different truncations of TDP-43 found that TDP-43$^{76-414}$ lost its exon skipping capability on the CFTR gene. Additionally it strongly inhibited the activity of full-length TDP-43 (Zhang *et al.,* 2009). The finding is surprising, as the truncation contained all of the functional domains and showed a nuclear expression pattern. This inadvertent truncation does not reflect any published caspase cleavage site but is most similar to a putative fragment possibly caused by an inflammatory caspase at YPKD^{80}. Further experiments would have to be carried out to confirm the inflammatory caspase cleavage site by site-directed-mutagenesis. Furthermore, it should be examined if the resulting fragment indeed has a dominant negative effect on TDP-43 regulated exon-skipping on the CFTR gene. More than likely the CFTR gene is not its only target and any additionally identified genes affected by the TDP-43 exon-skipping machinery are potentially regulators of the inflammatory response.

4.4.6 Involvement of inflammatory caspase substrates in cartilage and bone formation

Interestingly, functions of both L-SOX5 and MAGE-D1 were previously associated with cartilage or bone formation. Caspase-1 itself has been shown to be involved in bone homeostasis in the mouse (Clements *et al.*, 2003) and rabbit (D'Lima *et al.*, 2006) models for Osteoarthritis (OA). However, in the original caspase-1 knockout studies, no defect in bone homeostasis was reported and the animals developed normally (Li *et al.,* 1995). OA, also known as degenerative arthritis, is the most common joint disorder characterised by loss of cartilage in one or more joints leading to pain, disability, and a reduction in quality of life. This disease is usually coupled with a chronic inflammation of the joint at a later stage of the disease, possibly explaining the involvement of the inflammatory caspase and cytokine network. Although the role of the cytokine IL-1β in the pathophysiology of rheumatic diseases is well established, processing of L-SOX5 or MAGE-D1 by the inflammatory caspases could also be involved in the effects seen by Clements *et al* and would require further investigation.

4.4.7 Setting up of assays to functionally characterise the identified substrates under inflammatory stimuli

In order to gain some understanding of the physiological role of the identified caspase substrates during inflammation further cell culture based model systems were tested. By knocking down a specific gene of interest, or by over expressing the full-length or the individual cleavage fragments in a cell and subsequently monitoring different readouts, clues can be obtained as to what the physiological function of the gene of interest might be in the inflammatory context. We deliberately chose to continue to work with the THP-1 cell line and not supplement the epithelial cell line HEK293 with components of the inflammatory machinery, as this can lead to overexpression artefacts. After setting up a transfection system, we planned to detect the processing of the endogenous substrates by the caspases triggered with an inflammatory stimuli. Additionally, we assessed subsequent alterations in cytokine production, cell migration, rate of phagocytosis, change of morphology, inhibition / enhancement of cell death stimuli and gene expression profiling. To deliver the different cDNA and siRNAs constructs to the suspension cells by traditional methods of transfection by either lipids or standard electroporation proved unsuccessful as either the transfection efficiency was too low or the background cell death was too high (Data not shown). With the help of Dr Susan Logue a lentiviral gene delivery approach increased the transfection efficiency to over 40% but upon stimulation of the cells with or without LPS a huge variability of cytokine release was recorded between different assays. This is most likely due to detection of viral products by the THP-1 cell and an uncontrollable antiviral response. Using the electroporation method by Amaxa, we achieved similar transfection levels as with the retroviral system, although the inter-assay variability remained high. Studies are currently ongoing within the Martin Laboratory to resolve these issues and develop a system suitable for the investigation of the role of substrates identified in inflammation.

Overall, the in vitro expression cloning assay enabled us to investigate a greater part of the human proteome and we were able to identify 10 novel inflammatory caspase substrates of which the four full-length clones GDAP1L1, MAGE-D1, L-

SOX5 and TDP-43 were specifically processed by endogenous levels of inflammatory caspases.

In the course of setting up a cell culture assay to explore the effects of the identified inflammatory caspase substrates, it was reported that a novel cytokine, IL-33, was cleaved and activated by caspase-1 (Schmitz *et al.,* 2005). Having invested so much effort searching for novel caspse-1 substrates, we decided to test whether IL-33 was indeed a substrate for inflammatory caspases. As the next chapter discusses, it transpired that IL-33 was not a specific substrate for the inflammatory caspases, rather, this interleukin was preferentially cleaved by caspases-3 and -7. Furthermore, rather than activating IL-33, caspase-dependant proteolysis inactivated this cytokine. These analyses are described in the next chapter.

CHAPTER V

Characterisation of the novel caspase substrate IL-33

5.1 INTRODUCTION

During the course of our inflammatory caspase substrate screen a novel cytokine, IL-33, was identified and was reportedly a substrate for caspase-1 (Schmitz *et al.,* 2005). In this study the authors used an *in silico* approach to identify ligands for the orphan ST2 receptor by using the IL-1/FGF β-trefoil structure of IL-18. The canine sequence of DVS-27 and its human orthologue were identified as HEV-NF and after confirmation of ST2 receptor activation and cytokine-like activities the protein was renamed Interleukin-33 / IL-1F11 (Schmitz *et al.,* 2005).

The IL-1R family member ST2 has been previously shown to activate NF-κB as well as MAP kinases and to induce maturation of Th2 cells. Due to its structural homology to IL-1β and IL-18, it has been proposed that IL-33 requires proteolytic processing by caspase-1 to produce the mature form of this cytokine (Schmitz *et al.,* 2005). However, the authors of this study utilized non-physiological amounts of recombinant caspase-1 to cleave IL-33 *in vitro*. It was therefore not clear whether IL-33 is processed *at* physiological concentrations of caspase-1 or indeed by any other members of the caspase family. Additionally, whereas IL-1β and IL-18 promote a pro-inflammatory and Th1 directed response, IL-33 has been shown to induce the production of Th2-associated cytokines and increased levels of serum immunoglobulins associated with humoral immunity. Furthermore the initial study did not identify the proposed caspase cleavage site or test whether this cytokine requires proteolytic processing for activation. Having established the tools to answer some of these questions in the previous chapters, we hoped to verify whether IL-33 was indeed a bona fide inflammatory caspase substrate and to determine any functional characteristics of the proteolytic event.

5.2 SUMMARY

In our first approach to verify IL-33 as an inflammatory caspase substrate we incubated *in vitro* transcribed and translated IL-33 with recombinant caspase-1, -4 and -5. To our surprise, we could not reproduce the findings of Schmitz *et al*, IL-33 was a poor substrate for caspase-1 compared to IL-1β. However, when using the apoptotic caspases-3 and -7, IL-33 was readily processed. This result was confirmed using the THP-1 cell-free system where IL-33 was not cleaved when the

inflammatory caspases were activated, but was robustly processed upon activation of the apoptotic associated caspases. From these results we also noted a discrepancy in the proteolytic fragment sizes and the molecular weight of the proposed active form of IL-33. This indicated that the cleavage site described originally at $ALHD^{110}$ to be unfounded and that the utilised 'active' IL-33 was non-existent in this form *in vivo*. All experiments published to date have utilised the artificial truncation and it remains unclear whether the full-length or caspase cleaved form of IL-33 exhibits cytokine activity.

To resolve these questions we mapped the site of cleavage by apoptotic caspases to $DGVD^{178/175}$ in human and mouse respectively. We further showed that either endogenous or ectopically expressed IL-33 but not a caspase cleavage site mutant was processed in cells by endogenous caspases upon different pro-apoptotic stimuli.

We next examined the consequences of the proteolytic processing of IL-33 by caspases during apoptosis. Using an NF-κB reporter assay in cells overexpressing the ST2 receptor, we demonstrated that the full-length IL-33 activated the ST2 receptor, whereas the caspase-7 cleaved cytokine or its individual cleavage products did not. As IL-33 was described as a secreted protein we determined the half-life of the full-length versus the processed form of the protein with various serum proteases and found that caspase cleaved IL-33 was degraded much faster by α-chymotrypsin and proteinase K *in vitro*.

Finally, we determined the activity of full-length and caspase cleaved IL-33 *in vivo*. Schmitz *et al* and successive publications showed that intra peritoneal (i.p.) delivery of truncated IL-33 induced various changes to the mucosal tissues possibly through induction of Th2 associated cytokines. We could reproduce the reported observations, however we detected a dramatic attenuation of the IL-33 induced effects when mice were treated with the caspase cleaved cytokine.

5.3. RESULTS

5.3.1 Processing of IL-33 by recombinant caspases

To verify whether IL-33 was cleaved by caspases associated with inflammation, we first incubated *in vitro* transcribed and translated human and mouse IL-33 with a range of concentrations of the inflammatory recombinant caspases-1, -4 and -5 (Figure 5.1A). In this experiment we active-site titrated the proteases zVAD-fmk to determine the precise concentration of the recombinant protease (Data not shown). For the highest concentration we used a similar amount of recombinant caspase-1 as previously used in the small pool cDNA library screen and an equimolar amount of caspases-4 and -5. As expected, the recombinant caspase-1 fully processed IL-1β at 20 nM and the cleavage fragment was still visible with an 8 fold lower concentration. However, while caspase-1 readily cleaved IL-1β, human and murine IL-33 were not processed to any significant degree under the same conditions (Figure 5.1A). Caspases-4 and -5 also failed to process IL-33 at the concentrations tested, although they did exhibit activity against the synthetic peptide substrate WEHD-AMC albeit at a lower rate than caspase-1 (Figure 5.1B). This result suggests that IL-33 is not processed *in vitro* by caspase-1 at the concentrations that are more than sufficient to cleave IL-1β. The other caspases (caspase-4 and -5) activated during inflammation were also incapable of processing either IL-33 or IL-1β over the concentration range tested.

We next widened our approach and included caspases that participate in apoptosis rather than inflammation to investigate whether IL-33 could be cleaved under these conditions. Caspase-3 and -7 are the major effector caspases within the cell death machinery and are responsible for the vast majority of proteolysis seen during apoptosis (Walsh *et al.*, 2008). Again we titrated the proteases against known substrates to use protease levels as close as possible to physiological non-saturating levels. The recombinant caspases-1, -3 and -7 were titrated on Jurkat cell-free extract and the proteomes were immunoblotted against RhoGDI-2, co-chaperone p23 and XIAP (Figure 5.2B). To assess the activity of the caspases, the processing of their respective substrates was detected by western blot. Caspases-3 and -7 readily processed both human and murine *in vitro* transcribed and translated IL-33 at a similar efficiency to known caspase-3 and -7 substrates

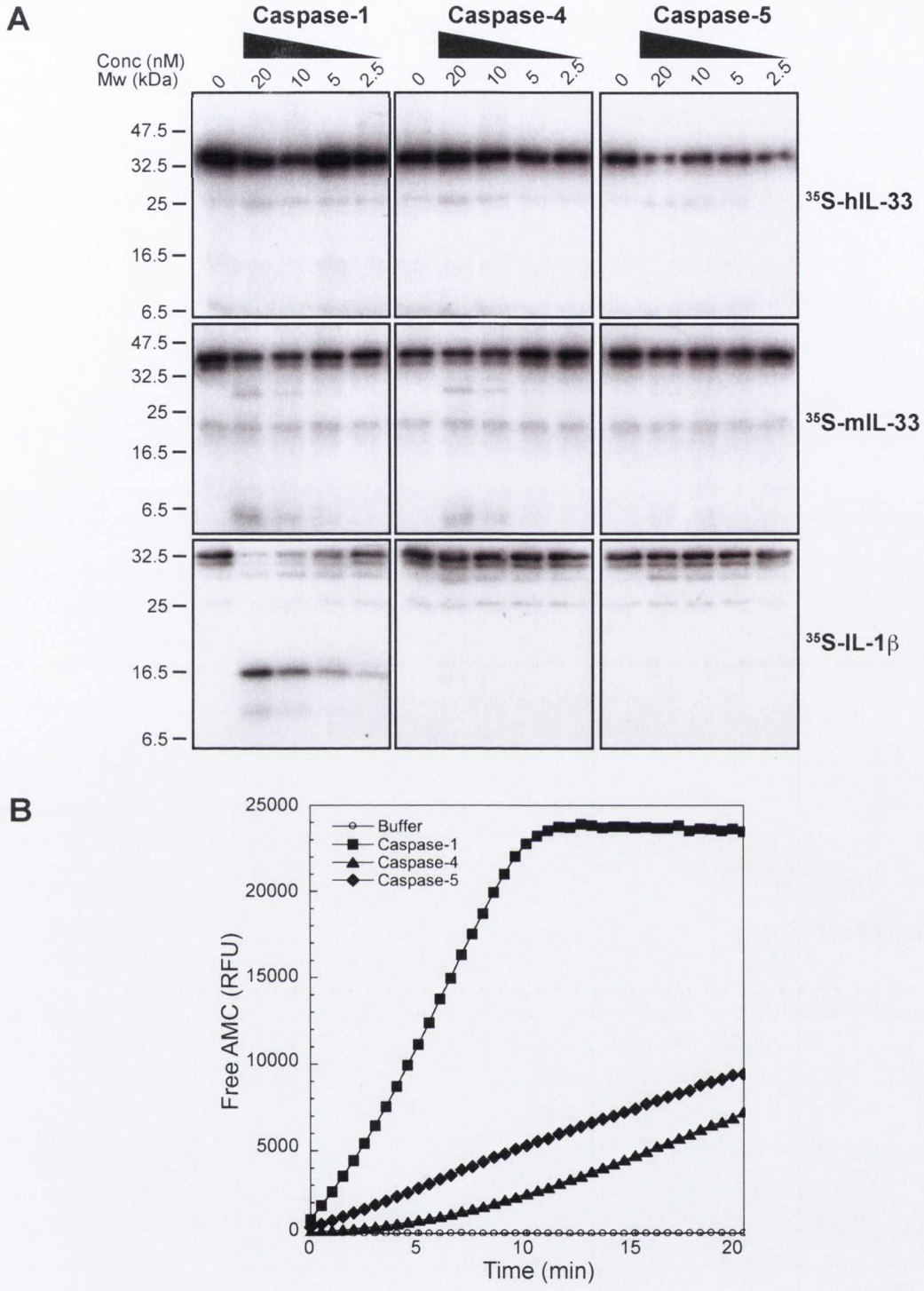

Figure 5.1

Processing of human and murine IL-33 by inflammatory caspases

(A) ^{35}S-labeled hIL-33, mIL-33 and IL-1β were prepared by *in vitro* transcription/translation and were then incubated with the indicated concentrations of recombinant caspase-1, -4 and -5 for 2 h at 37°C followed by analysis by SDS-PAGE and fluorography.

(B) Hydrolysis of the synthetic caspase substrate, WEHD-AMC, by recombinant caspase-1, -4 and –5 (20 nM each). Note that recombinant inflammatory caspases cleave WEHD-AMC with different efficiencies. Active site titrations with zVAD-fmk confirmed that the molar amounts of each caspase were identical (data not shown).

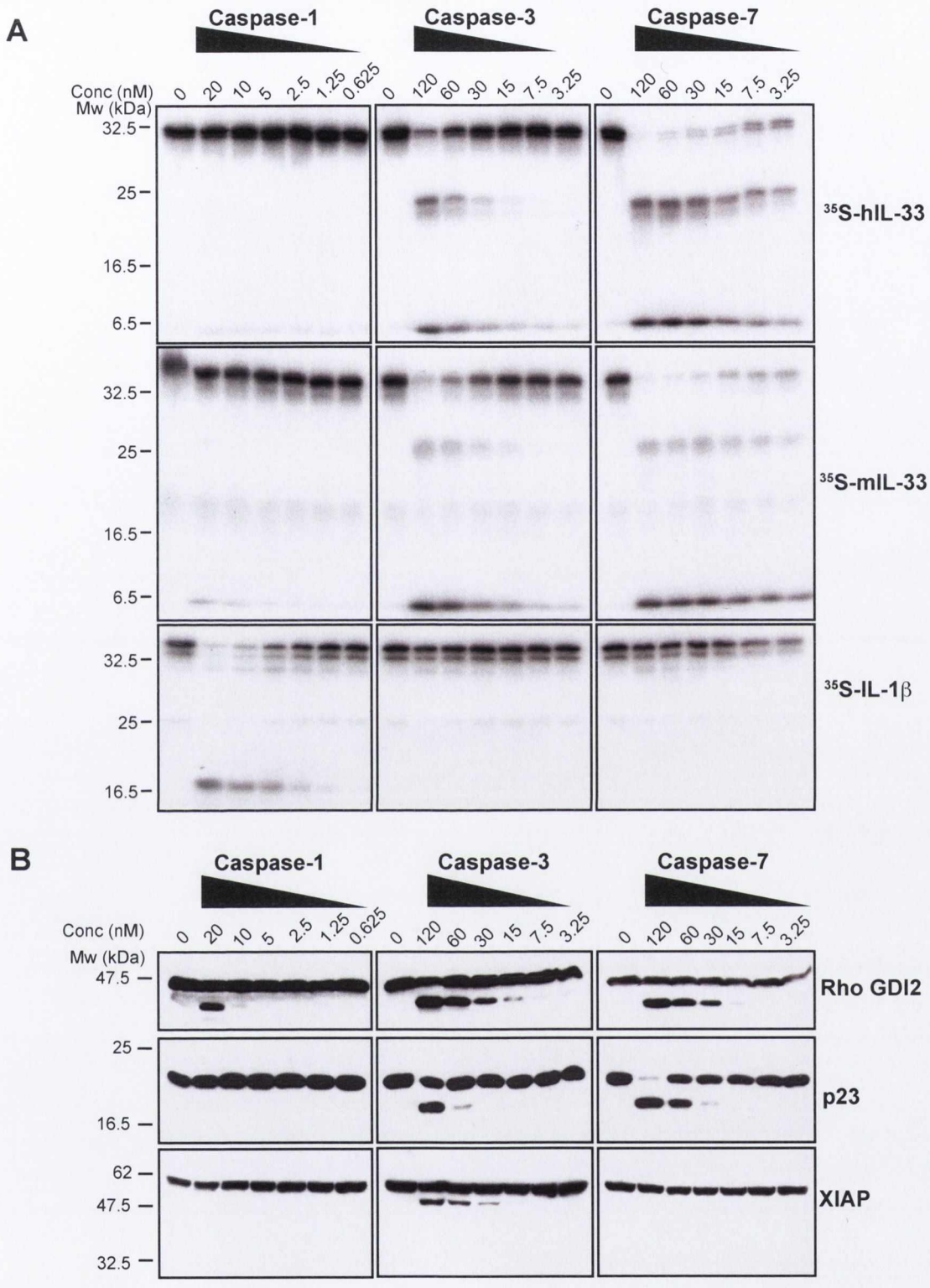

Figure 5.2

Processing of human and murine IL-33 by apoptotic caspases

(A) ^{35}S-labeled hIL-33, mIL-33 and IL-1β, prepared by *in vitro* transcription/translation, were incubated with the indicated concentrations of recombinant caspase-1, -3 and -7 for 2 hours at 37°C followed by analysis by SDS-PAGE / fluorography.

(B) Recombinant caspase –1, -3 and -7 were added to THP-1 cell-free extracts at the indicated concentrations, followed by incubation at 37°C for 2 hours. Extracts were then analysed by SDS-PAGE followed by immunoblotting for the indicated substrate proteins.

(Figure 5.2A). Caspase-7 showed a much more efficient processing of IL-33 than caspase-3. Importantly, neither of the latter caspases cleaved *in vitro* transcribed and translated IL-1β under the same conditions (Figure 5.2A). Caspase-1, on the other hand, failed again to cleave IL-33 even at several higher fold concentrations than when caspase-7 proteolytic activity was detectable. IL-1β was still efficiently processed by caspase-1 where under the same conditions the protease failed to cleave IL-33. This indicates that *in vitro* IL-33 is preferentially cleaved by caspases that are activated during apoptosis.

5.3.2 Processing of IL-33 in THP-1 cell-free extract

To further analyse IL-33 processing by endogenous levels of apoptotic and inflammatory caspases, we used THP-1 cell-free extracts described in the third chapter where we could selectively activate the caspases involved in inflammation or apoptosis. Upon incubation of THP-1 cell-free extracts at 37°C, caspase-1 was processed to its active form and maturation of endogenous IL-1β was readily detected (Figure 5.3A). As previously shown, caspase-3 was not activated under these conditions, indicated by the failure of this protease to undergo proteolytic maturation (Figure 5.3A). As we could not detect endogenous IL-33 in the THP-1 cell-free extract, we added ^{35}S-methionine labelled *in vitro* transcribed and translated proteins instead. In sharp contrast to the robust processing of ^{35}S-IL-1β seen under conditions where the inflammatory caspases were active, processing of human or mouse ^{35}S-IL-33 was barely detectable (Figure 5.3B), again suggesting that IL-33 is a poor substrate for caspase-1 and other inflammatory caspases. In contrast, this protein was processed very efficiently upon activation of apoptotic caspases through addition of cytochrome c and dATP to the extracts (Figure 5.3A and B), again demonstrating that IL-33 is a preferred substrate for apoptotic as opposed to inflammatory caspases.

Next we performed the same experiment with a Jurkat cell-free system, which is essentially devoid of caspase-1 (Chow *et al.*, 1999). As with the THP-1 cell-free extract, addition of cytochrome c and dATP to these Jurkat cytosolic extracts resulted in the rapid assembly of the apoptosome and subsequent activation of the apoptotic caspase cascade and ultimately the proteolytic processing of caspase

substrates XIAP and p23 (Figure 5.3C). Proteolysis of human and murine IL-33 was again readily observed under these conditions (Figure 5.3D). Additionally, mouse embryonic fibroblasts (MEFs) deficient in caspase-1 displayed no impairment of IL-33 proteolysis upon addition of apoptotic stimuli, whereas the processing of IL-33 in MEFs lacking caspase-3 was not detectable (Lüthi *et al.,* 2009).

Taken together with our earlier observations made using recombinant caspases (Figure 5.1 and Figure 5.2), these results strongly suggest that IL-33 is a physiological substrate for caspases activated during apoptosis rather than inflammation. In a recent report, Talabot-Ayer *et al* were also unable to process IL-33 overexpressed in the THP-1 cell line either with recombinant caspase-1 or pro-inflammatory stimuli (Talabot-Ayer *et al.*, 2009) confirming the results seen here.

5.3.3 Identification of the caspase cleavage site in IL-33

In the initial report, Schmitz *et al* proposed that human IL-33 was proteolytically processed *in vitro* by caspase-1 at $ALHD^{110}$. Additionally they assumed, based on the structural homology to IL-18, that the cleaved C-terminal fragment represented the biologically-active form of this cytokine (Schmitz *et al.,* 2005). However, when all the tetrapeptide motifs containing Asp residues at the P1 position that may qualify as caspase cleavage motifs were compared between the human and mouse IL-33 protein sequence, it became apparent that the proposed site at $ALHD^{110}$ was the only one not conserved between the two species (Figure 5.4A). As we saw no difference in the processing pattern between human and mouse IL-33 when they were cleaved *in vitro* (Figure 5.2A and 5.3B and D) it is highly unlikely that IL33 is processed at $ALHD^{110}$.

To identify the caspase-processing site within IL-33, we estimated the approximate molecular weight of the cleavage fragments based upon the cleavage products of IL-33 observed in our experiments (Figure 5.2A and Figure 5.3B and D). A conserved caspase cleavage motif was located at Asp^{178} within human IL-33 ($DGVD^{178}$) and Asp^{175} within murine IL-33 ($DGVD^{175}$) that may represent the site of caspase-mediated proteolysis (Figure 5.4A).

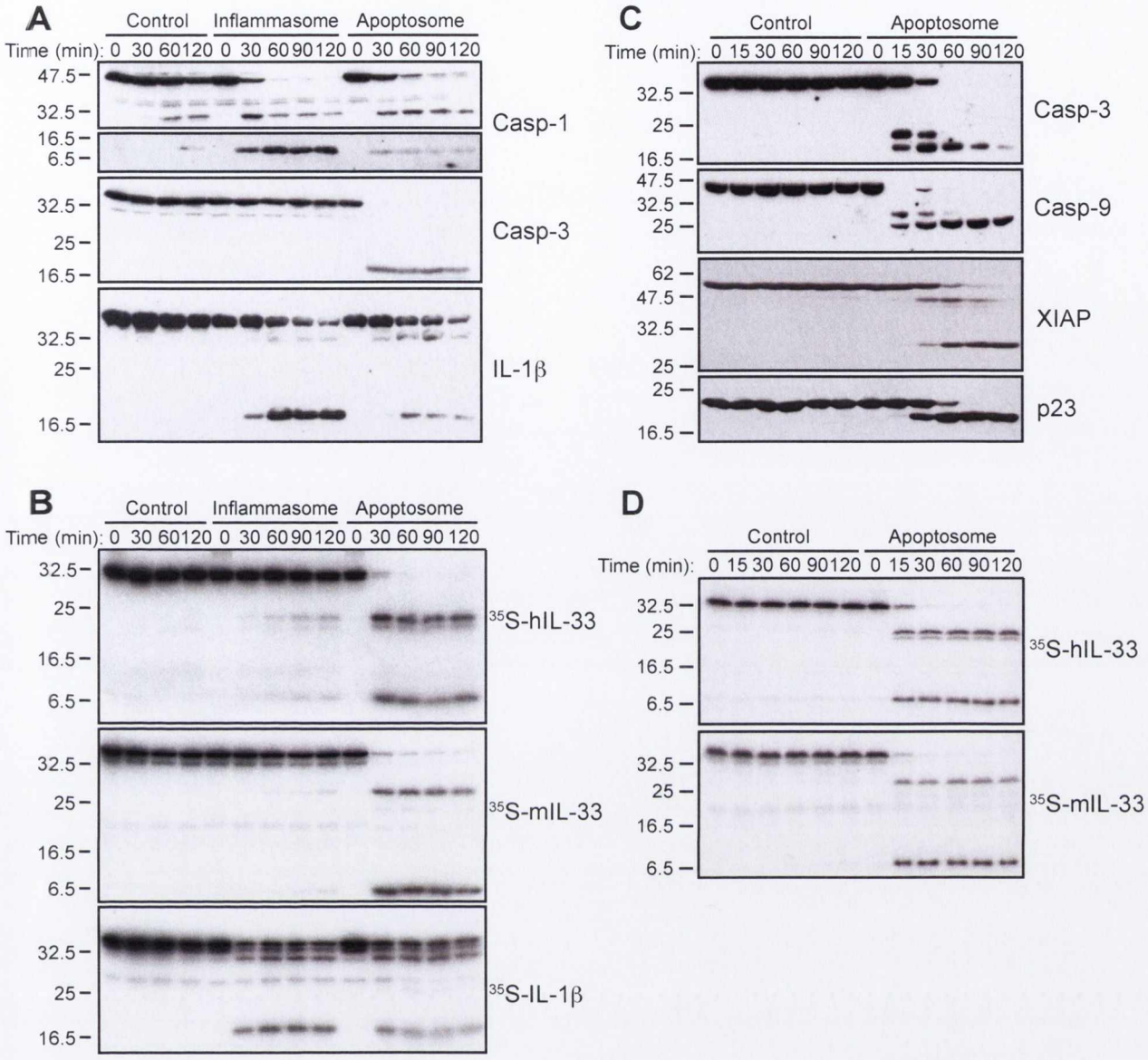

Figure 5.3

Processing of human and murine IL-33 in THP-1 cell-free extract

(A) Cell-free extracts derived from THP-1 cells were incubated at 37°C to permit spontaneous activation of inflammatory caspases ('Inflammasome') or in the presence of 50 µg/ml cytochrome c and 1 mM dATP to promote activation of apoptotic caspases ('Apoptosome'). As a control, caspase activation was suppressed through addition of 5 µM YVAD-CHO. Extracts were then immunoblotted for caspase-1, caspase-3 and IL-1β, as indicated.

(B) ^{35}S-labeled hIL-33, mIL-33 and IL-1β were added to THP-1 cell-free extracts followed by treatment as described in A. Reactions were sampled at the indicated times and were subsequently analysed by SDS-PAGE/fluorography.

(C) Jurkat cell-free extracts were incubated in the presence (Apoptosome) or absence (Control) of 50 µg/ml cytochrome c and 1 mM dATP for the time indicated. Extracts were then immunoblotted for caspase-3, -9, XIAP and co chaperone p23.

(D) ^{35}S-labeled hIL-33 and mIL-33 were added to Jurkat cell-free extracts followed by treatment as described in C. Reactions were sampled at the indicated times and were subsequently analysed by SDS-PAGE/fluorography.

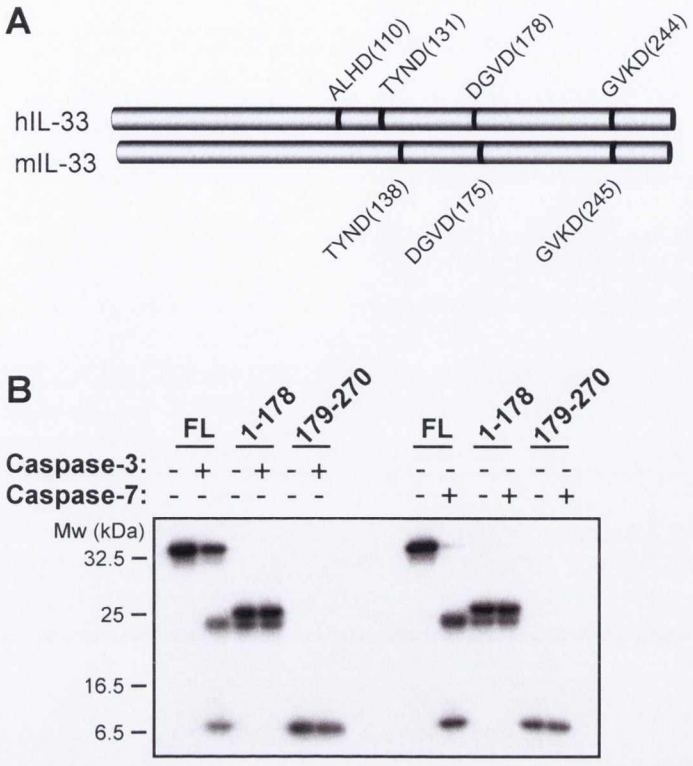

Figure 5.4

Mapping of the caspase cleavage site of human IL-33 to Asp^{178}

(A) Schematic representation of human and murine IL-33 depicting potential caspase cleavage motifs.

(B) ^{35}S-labeled full length (FL) hIL-33 and the indicated IL-33 deletion mutants were incubated in the presence of recombinant caspase-3 (60 nM, left) or caspase-7 (40 nM, right) for 2 h at 37°C followed by analysis by SDS-PAGE/fluorography.

We next amplified the DNA for the putative cleavage fragments corresponding to amino acids 1-178 and 179-270 by PCR and subcloned these fragments into pcDNA3. After *in vitro* transcribing and translating the full-length protein and the two truncations, we incubated each protein with non-saturating amounts of recombinant caspase-3 or -7 and analyzed the proteolytic pattern. The truncated forms showed the exact same SDS-PAGE mobilities as the full-length IL-33 when partially cleaved by either caspase-3 or -7 (Figure 5.4B). In addition, the truncated IL-33 forms failed to be further processed by either of the caspases. Together with the analysis of conserved putative caspase cleavage sites between human and mouse IL-33 this strongly suggests that human IL-33 is processed at $DGVD^{178}$ and not at $ALHD^{110}$ as initially proposed.

5.3.4 Expression of recombinant IL-33

In order to test the processing not only on *in vitro* transcribed and translated protein but also on purified recombinant protein, we decided to use a bacterial expression system to produce larger amounts of recombinant IL-33. Additionally this protein could be further used for any subsequent cell-based and *in vivo* studies. The full-length IL-33 DNA sequence was cloned into the pET45b vector to produce N-terminally His-tagged IL-33. However, initial expression from this plasmid resulted in insoluble protein largely sequestered within bacterial inclusion bodies (Figure 5.5A). Assaying different expression conditions by using a lower induction temperature, shorter or longer expression time or different amount of IPTG induction did not result in any increase in soluble full-length IL-33. Eukaryotic proteins expressed in the prokaryotic *E. coli* expression system are sometimes folded incorrectly and may lack essential post-transcriptional modifications. A second approach to express IL-33 was therefore taken by cloning the full-length DNA sequence into the pPIC6α vector and expressing it in the yeast *P. pastoris*. Unfortunately, the IL-33 protein yield was extremely low and reselection for clones with a higher IL-33 protein expression or a considerable up scaling of the induction culture did not provide satisfactory amounts of the full-length IL-33 protein (Data not shown).

We therefore employed another protein modification that frequently improves the solubility and purification of the proteins. GST tags have been previously shown to improve protein solubility when fused to the expressed protein. Therefore we cloned the full-length human and murine IL-33 into pGEX4TK2 to express IL-33 with an N-terminal GST-tag. With this construct we were able to induce and purify sufficient amounts of GST-IL-33 (Figure 5.5B). The truncated form of IL-33 covering amino acids 112 to 270 was also cloned and expressed with an N-terminal poly-histidine tag in the *E. coli* expression system. The induced protein was mostly soluble and could be captured and purified according to the normal procedure (Figure 5.5C).

5.3.5 Identification of the caspase cleaved fragments by mass spectrometry

The human (Figure 5.6A) and murine (Data not shown) GST-IL-33 were then cleaved with recombinant caspase-7, resolved by SDS-PAGE and coomassie blue stained. The full-length IL-33 and the cleavage fragments were then in-gel trypsin digested and the peptides generated analysed using MALDI-TOF mass spectrometry. Identified peptide coverage of these fragments indicate that the caspase cleavage site is located between amino acids 159 to 187 (Figure 5.6B). $DGVD^{175/178}$ is within this region. Unfortunately, the exact cleavage site could not be identified with this method. Numerous trypsin cleavage sites in the region of the caspase cleavage site result in many small peptides of less than 700 Dalton each that could not be reliably detected by MALDI TOF mass spectrometry.

To definitely determine the cleavage site, we decided to mutate $ASP^{175/178}$ to a ALA rendering the caspases incapable of processing IL-33 at this site. I*n vitro* transcribed and translated mutants were completely resistant to processing by any of the caspases tested whereas wild-type IL-33 or IL-1β were cleaved by caspases-3, -7 or caspase-1 respectively (Figure 5.7A and data not shown). Furthermore, the point mutant was not cleaved by the endogenous caspases in an apoptotic Jurkat cell-free extract whereas wild-type IL-33 and the control proteins caspase-3 and XIAP were processed as seen earlier (Figure 5.7B)

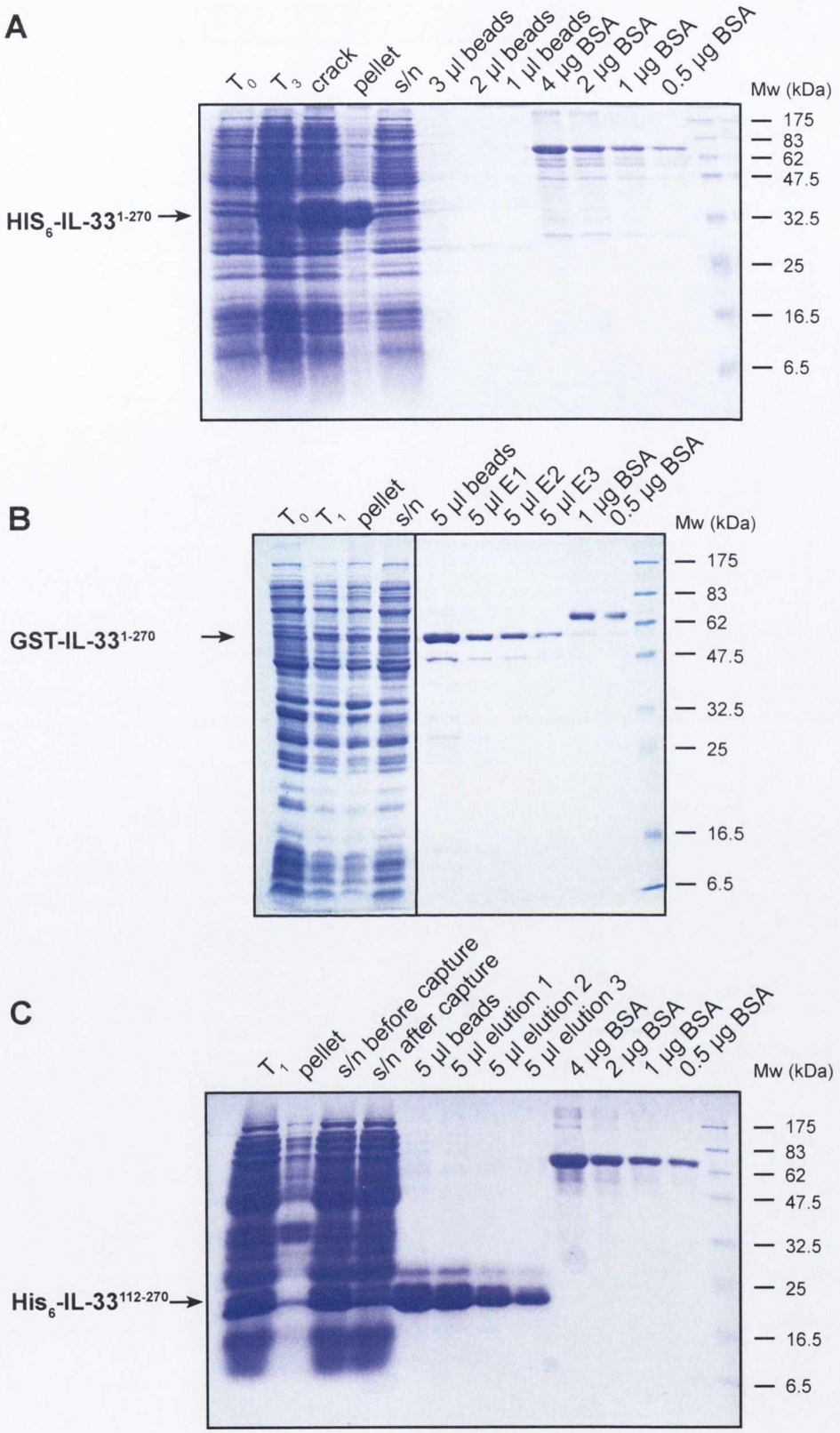

Figure 5.5

Expression and purification of recombinant IL-33

pET45b-hIL33$^{1-270}$ (A), pGEX2-hIL33$^{1-270}$ (B) and pET45b-hIL33$^{112-270}$ (C) plasmids were transformed into *E. coli* DH5α bacteria and expression was induced with IPTG. Cells were lysed by sonication and soluble supernatants incubated with Ni-agarose beads (A, C) or glutathione sepharose (B). Samples of bacteria before (T_0) and after(T_1/T_3) induction, lysis (crack), insoluble (pellet) and soluble (s/n) fractions, beads and elutions of GST-IL-33 and HIS$_6$-IL33$^{112-270}$ along with a BSA standard were run on 12% SDS-PAGE gels and stained with Coomassie blue.

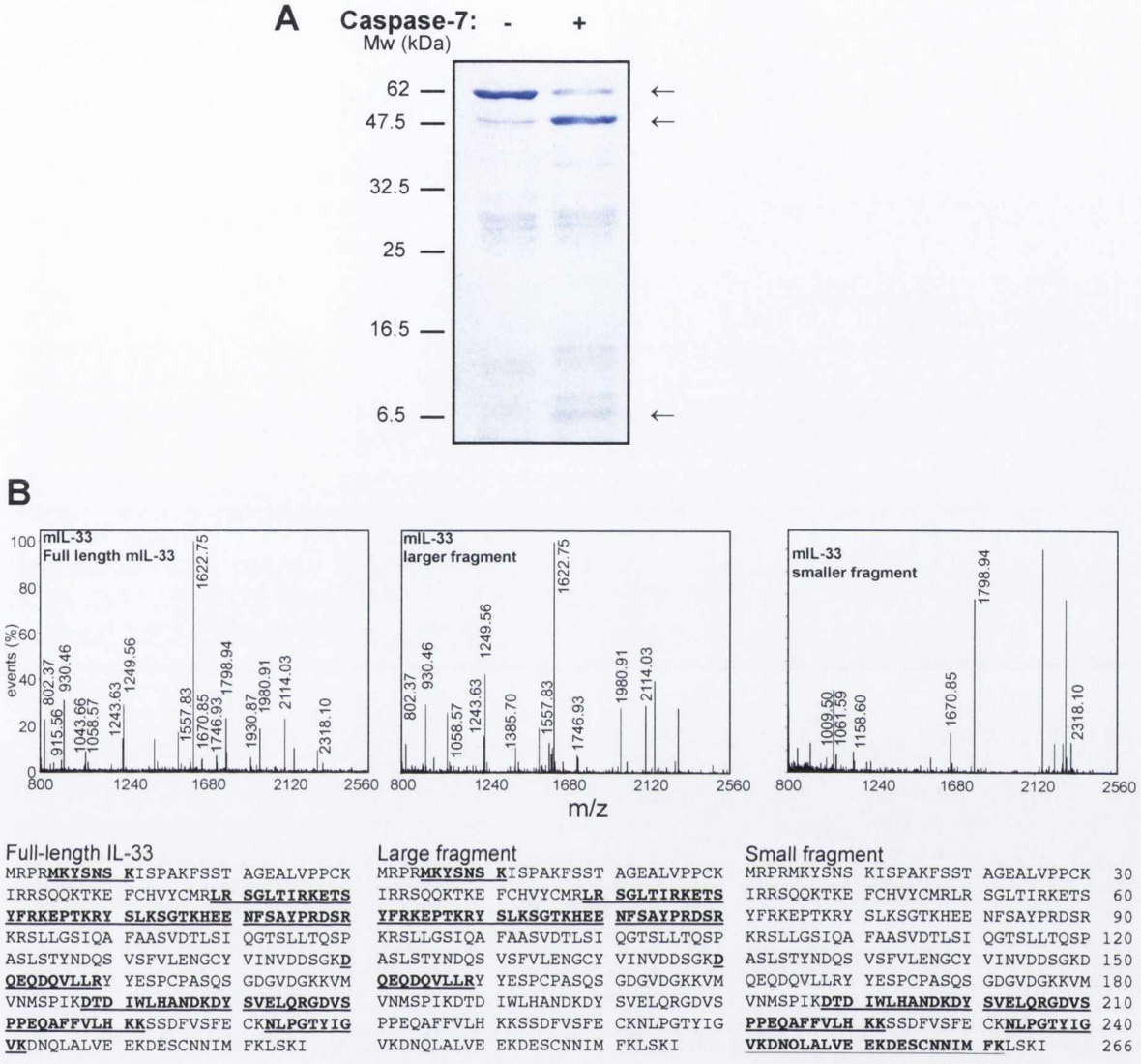

Figure 5.6

Identification of IL-33 cleavage products by mass spectrometry

(A) Recombinant GST-IL-33 was incubated for 2 h at 37°C in the presence or absence of recombinant caspase-7 (600 nM), followed by SDS-PAGE / Coomassie blue staining. Arrows indicate the full-length IL-33 and cleavage fragments thereof.

(B) The protein bands depicted in (A) are analysed by MALDI-TOF mass spectrometry. Mass spectrograms for each IL-33 species (i.e. full length, large and small fragments) are shown (top), along with the corresponding peptide coverage of each (bottom). IL-33 specific peptides identified in the spectra are indicated by the identified m/z ratio and the corresponding peptide sequences are underlined.

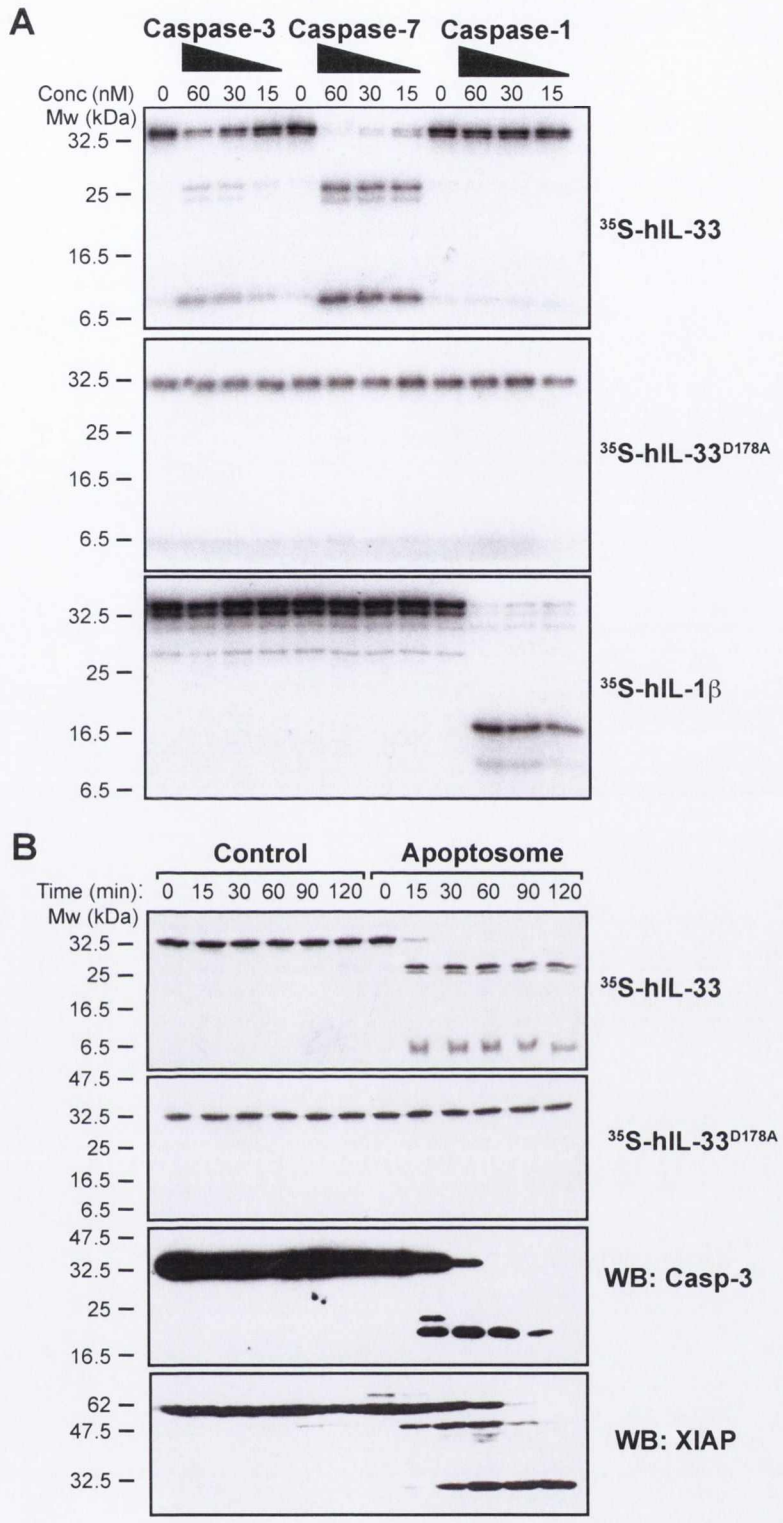

Figure 5.7

IL-33^{D178A} is not processed by recombinant caspases or in apoptotic cell-free extract

(A) ^{35}S-labeled wild-type hIL-33 and IL-33^{D178A} point mutant were incubated for 2 hours at 37°C with recombinant caspase-3, -7 and –1, as shown. Reactions were analysed by SDS-PAGE/fluorography.

(B) ^{35}S-labeled wild-type hIL-33 and IL-33^{D178A} point mutant were added to Jurkat cell-free extracts followed by activation of apoptotic caspases by addition of cytochrome c and dATP. Reactions were sampled at the indicated times and were subsequently analysed by SDS-PAGE/fluorography. Samples of the same reactions were also immunoblotted for caspase-3 and XIAP, as indicated.

5.3.6 Processing of IL-33 in apoptotic cells

Next we confirmed that IL-33 is cleaved by apoptotic caspases in a cell based model. We transiently overexpressed FLAG-tagged wild-type IL-33 or the IL-33^{D178A} point mutant in human HeLa cells and induced apoptosis by exposure of the cells to different, well described pro-apoptotic stimuli, including Daunorubicin, TNFα or Cisplatin. The percentage of cell death was estimated by morphological features (Figure 5.8A) and cell-lysates were probed for IL-33 and the caspase substrates: caspase-3, co-chaperone p23 and XIAP (Figure 5.8B). As expected, IL-33 underwent processing under conditions where apoptosis was initiated, but importantly, the IL-33^{D178A} point mutant was not cleaved under the same conditions (Figure 5.8B).

To further confirm the involvement of caspases in the proteolysis of IL-33, inhibitors were used to specifically block the activation of the caspase cascade or the specific activity of the proteases. Bcl-xL sequesters BH3 domain-only proteins, preventing BAX- and BAK-mediated cytochrome c release with subsequent apoptosome formation and caspase activation (Cheng *et al.*, 2001), whereas the synthetic peptide methyl ester zVAD-fmk acts as a broad range caspase inhibitor, irreversibly binding the active site of the protease (Rodriguez *et al.*, 1996). We co-expressed Bcl-xL or added the cell permeable poly-caspase inhibitor z-VAD-fmk in the medium, which both strongly reduced the percentage of cells displaying an apoptotic phenotype (Figure 5.8C) and blocked apoptosis-associated proteolysis of IL-33 (Figure 5.8D). These results add further proof that IL-33 is cleaved during apoptosis that this proteolysis occurs at the same site ($DGVD^{178}$) as caspase-mediated processing of IL-33 *in vitro*.

5.3.7 Signalling capability of the full length vs. cleaved IL-33

IL-1β and IL-18 are both required to be proteolytically processed to become active cytokines and to be able to bind and activate their respective receptor complex (Mosley *et al.*, 1987a; Mosley *et al.*, 1987b; Thornberry *et al.*, 1992). However, IL-1α, another member of the IL-1 family displays biological activity regardless of its cleavage status (Mosley *et al.*, 1987a; Mosley *et al.*, 1987b).

The orphan ST2 receptor was identified as the IL-33 receptor, which in conjunction with IL1RAcP activates NF-κB (Chackerian *et al.*, 2007; Ali *et al.*, 2007).Based upon the initial observations of Schmitz *et al*, the vast majority of investigations carried out to date with IL-33 have used an artificially truncated form of this cytokine, IL-$33^{112\text{-}270}$, that was proposed to represent the caspase cleaved and active form of this protein. However, our experiments indicate that this form would still contain the actual caspase cleavage site and therefore be susceptible to caspase-mediated proteolysis. It is therefore not clear whether the full length or IL-33 cleaved by caspases at position $DVGD^{175/178}$ represents the active cytokine.

To address this question, we titrated both full-length GST-IL-33 and caspase-7 cleaved GST-IL-33 (see Figure 5.6A) on HEK293 cells stably expressing the membrane bound ST2-receptor and an NF-κB induced secreted alkaline phosphatase (SEAP) reporter plasmid. The alkaline phosphatase activity of the cell supernatant was measured in a colometric assay (Figure 5.9A top graph). We detected robust NF-κB activation in response to the full-length IL-33 protein but dramatically reduced activity of the caspase-cleaved form of this protein. HEK293 cells not expressing either plasmid showed no increase of NF-κB activation upon full-length GST-IL-33 stimulation (Data not shown). We also measured NF-κB activation in the same system using the artificially-truncated form of IL-33 (amino acids 112-270) either uncleaved or processed by caspase-7. The artificially-truncated form retained the ability to activate the ST2-NF-κB pathway, however this activity was also strongly reduced upon caspase-mediated proteolysis of IL-$33^{112\text{-}270}$ (Figure 5.9A lower graph).

To measure the individual activity of the caspase-generated proteolytic fragments we subcloned and expressed the N- and C-terminal cleavage products in *E. coli*. The N-terminal fragment again proved to be insoluble in the bacterial expression system, therefore the artificially truncated version containing amino acids 112-178 was subcloned and expressed in *E. coli* instead (Data not shown).

Both cleavage fragments, the full-length and artificially truncated form of IL-33 (Figure 5.9B) were then titrated onto the cell reporter system and the fold NF-κB

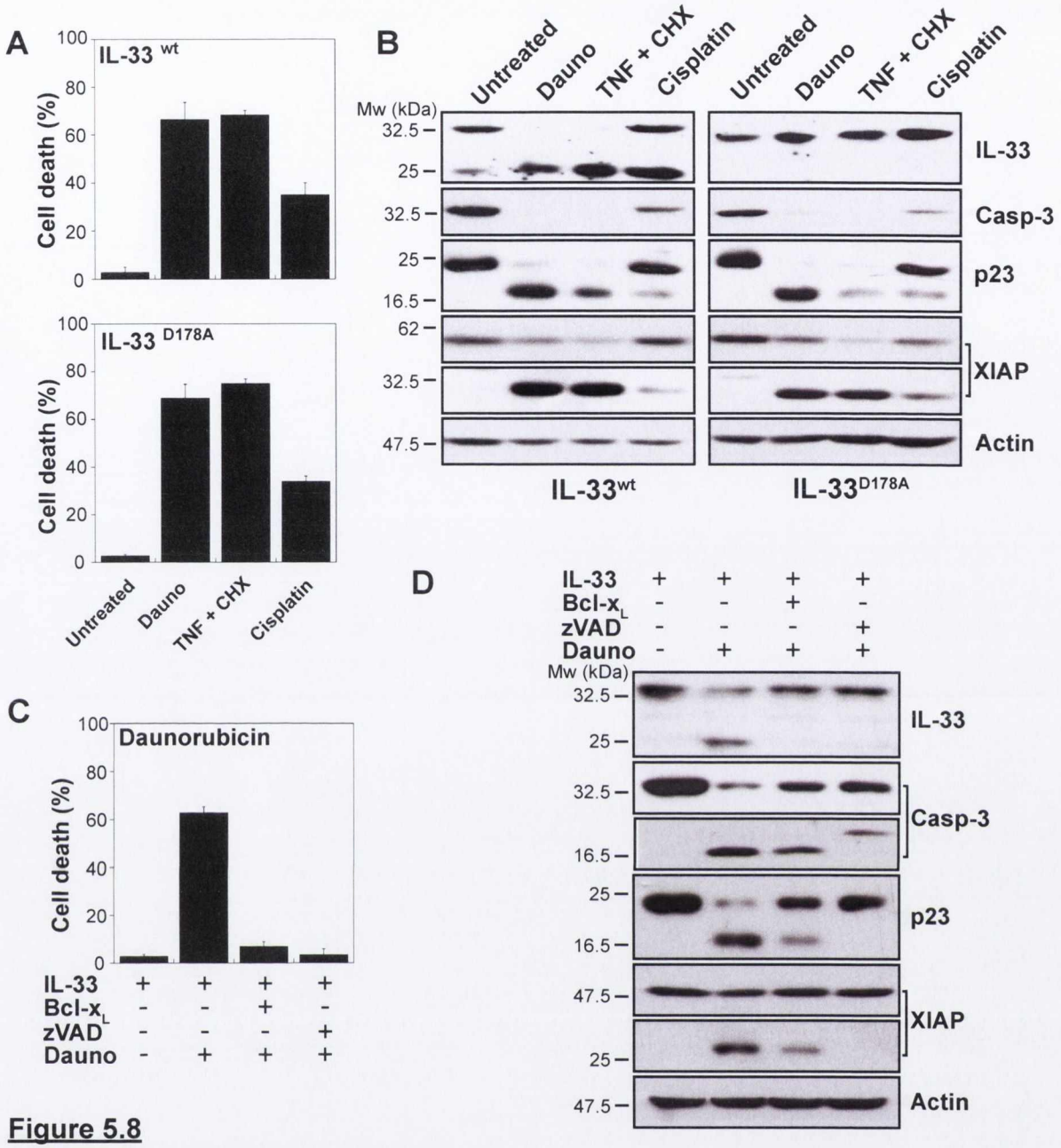

Figure 5.8

IL-33 is cleaved during apoptosis

(A) HeLa cells were transfected with expression plasmids encoding either wild type IL-33 (top panel), or IL-33^{D178A} point mutant (bottom panel). 24 h later, cells were treated with daunorubicin (Dauno; 5 μM), TNF (10 ng/ml), cycloheximide (CHX; 1 μM) and cisplatin (50 μM) and incubated for a further 8 h before assessement of apoptosis.

(B) Western blot analysis of cell lysates derived from HeLa cells transfected either with wild type IL-33 (left panel) or the D178A point mutant (right panel), followed by incubation in the presence or absence of daunorubicin (Dauno), TNF/cycloheximide, or cisplatin at concentrations indicated in (A).

(C) HeLa cells were transfected with an IL-33 expression plasmid for 24 h followed by treatment for 8 h with daunorubicin (5 μM) to induce apoptosis. In parallel, HeLa cells were also treated with the poly-caspase inhibitor zVAD-fmk (50 μM), or were transfected with a Bcl-xL expression plasmid as indicated.

(D) Cell lysates were generated from the cells treated in C and were immunoblotted for the indicated proteins.

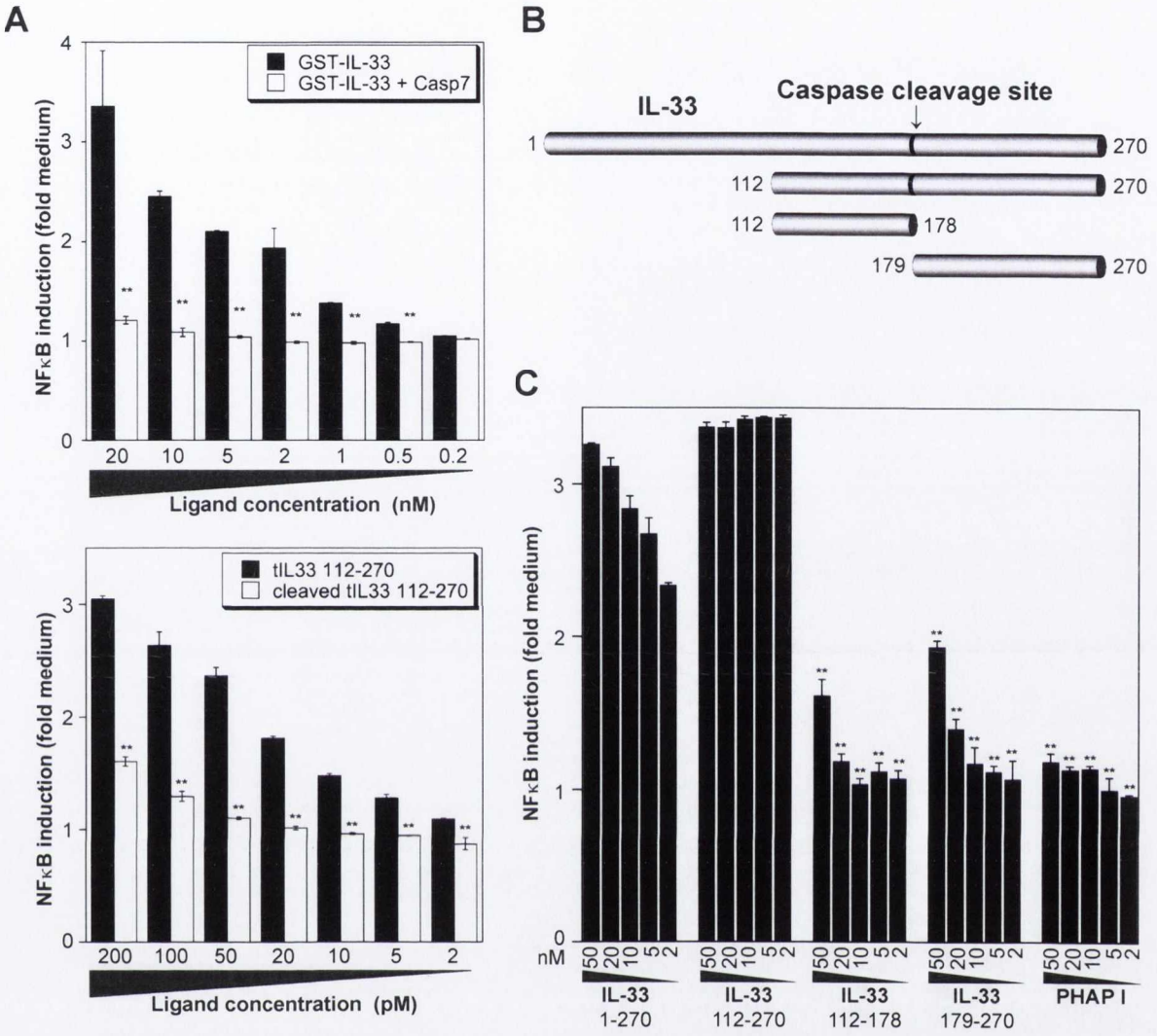

Figure 5.9

Proteolysis of IL-33 attenuates its activity *in vitro*

(A) HEK293 cells stably expressing the ST2L receptor expression plasmid along with an NFκB-SEAP reporter plasmid are incubated with the indicated concentrations of recombinant GST-IL-33 and caspase-7-cleaved GST-IL-33 for 16 hours. Alkaline phosphatase activity of the supernatant was assayed with a chromogenic substrate and normalised against medium only treated cells.

(B) Schematic representation of IL-33 depicting the caspase cleavage site and the various His-tagged IL-33 deletion mutants generated for this study.

(C)The indicated amounts of the IL-33 recombinant proteins or the control protein, PHAP I were added to the cells and the induced NF-κB activity was measured as described in (A). A representative of at least three independent experiments are shown. Error bars represent the mean of triplicates +/- SEM, **:$p<0.01$

induction against medium only treated cells was graphed (Figure 5.9C). Putative human leukocyte antigen-DR-associated protein I (PHAP I) was included as a nonspecific control protein, expressed and purified under the same conditions as the IL-33 constructs. As with the caspase cleaved IL-33 constructs, the individual fragments were not able to induce ST2-dependent NF-κB activation.

Taken together, these results clearly show that full-length IL-33 is biologically active and caspase-mediated proteolysis of IL-33 results in a complete loss or strong decrease in activity. This inactivation of IL-33 through proteolytic processing by caspases is in direct opposition to the initially published observation but has since been recently independently confirmed by other groups (Cayrol *et al.*, 2009; Talabot-Ayer *et al.*, 2009).

5.3.8 IL-33 / ST2 receptor binding assay

In a further step we wanted to verify if the loss of NF-κB activation by the caspase cleaved IL-33 protein was due to a decrease in binding efficiency to the ST2 receptor. We therefore performed *in vitro* pulldown assays where we either incubated sepharose-immobilized full-length GST-IL-33 or caspase-cleaved GST-IL-33 with a soluble Fc-ST2 fusion protein and determined which form of IL-33 bound to the ST2 receptor. Surprisingly, both full-length and caspase cleaved IL-33 bound to the Fc-ST2 fusion protein (Figure 5.10A). To confirm this result we also performed the reciprocal approach and immobilized Fc-ST2 on Protein A/G agarose and incubated it with the full-length or caspase cleaved GST-IL-33. Again both forms were able to bind the ST2 receptor as indicated in Figure 5.10B.

These results demonstrate that upon proteolytic caspase mediated cleavage of IL-33 the cytokine can still bind to the ST2 receptor. It is however also possible that due to the difficulties in achieving 100% proteolysis of the recombinant GST-IL33, the full-length protein could bind the receptor and at the same time interact with cleaved GST-IL-33 fragments. Additionally, although binding to the ST2 receptor might not be interrupted by proteolytic processing of IL-33, the sensing and signalling through IL1RAcP might be impeded by the caspase cleaved cytokine.

5.3.9 Differential degradation of IL-33 by serum proteases

Serum proteases are known to degrade secreted proteins and hence regulate their half-life and bioavailability. The removal of cytokines is essential to dampen down and terminate any inflammatory response once the inflammatory stimulus has been cleared (Kudo *et al.*, 1990; Shechter *et al.*, 2001).

To explore whether caspase-mediated cleavage of IL-33 could enhance susceptibility to protease degradation, we incubated either the full-length or caspase-7 cleaved form of truncated IL-33 with different amounts of α-chymotrypsin, proteinase K, thrombin or trypsin over two hours. Whereas IL-33 was quite resistant to proteolysis by all tested proteases, caspase-7 cleaved IL-33 was much more susceptible to degradation by α-chymotrypsin and proteinase K over a wide range of protease concentrations (Figure 5.11A). When we treated both full-length and caspase-7 cleaved IL-33 with a fixed amount of α-chymotrypsin and proteinase K, a clear time-dependant disappearance of the caspase cleaved cytokine could be observed (Figure 5.11B).

These results indicate that cleavage of IL-33 by caspases at $DGVD^{175/178}$ possibly leads to a structural change, revealing serum protease cleavage sites, which results in an increased degradation rate of the cleaved cytokine. This suggests that caspases may be involved in reducing the half-life and therefore the bioavailability of IL-33 by enhancing its vulnerability to serum-protease degradation.

5.3.10 Effects of full-length and caspase cleaved IL-33 in vivo

Over the past three years, biological effects of IL-33 both *in vitro* and *in vivo* have been explored and research is still ongoing to expand the knowledge of the exact role of this novel cytokine. IL-33 was reported to enhance the production of the Th2 cytokines, IL-5 and IL-13 in *in vitro* polarised Th2 cells (Schmitz *et al.*, 2005). Additionally, i.p. administration of IL-33 induced splenomegaly, blood eosinophilia, epithelial hyperplasia in the digestive tract, hypertrophy of bronchial epithelial cells with increased mucus production and increased serum levels of IL-5, IL-13, IgE and IgA amongst other symptoms (Schmitz *et al.*, 2005).

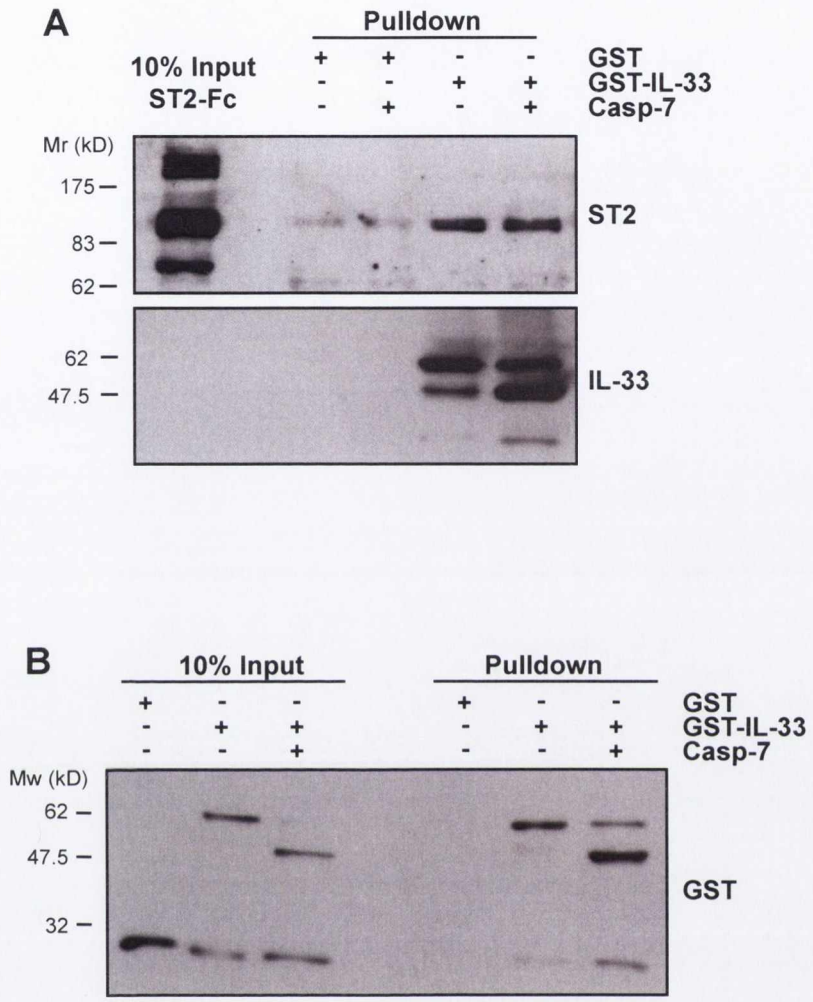

Figure 5.10

Proteolysis of IL-33 has no apparent effect on the ST2 receptor binding

(A) Upper panel, capture of soluble ST2-Fc after incubation with sepharose immobilized GST, GST treated with caspase-7, GST-IL-33, or GST-IL-33 treated with caspase-7, followed by probing for ST2. Lower panel, cleavage status of the IL-33 used for the pulldown assay was revealed by blotting for this protein. Note that ST2-Fc was pulled down with both the full length as well as the cleaved form of IL-33 (upper panel)

(B) Protein A/G immobilized ST2-Fc was used to assess binding of GST, GST-IL-33 full-length or cleaved GST-IL-33. Note that both full length as well as the cleaved forms of IL-33 were captured by ST2 whereas the GST control was not.

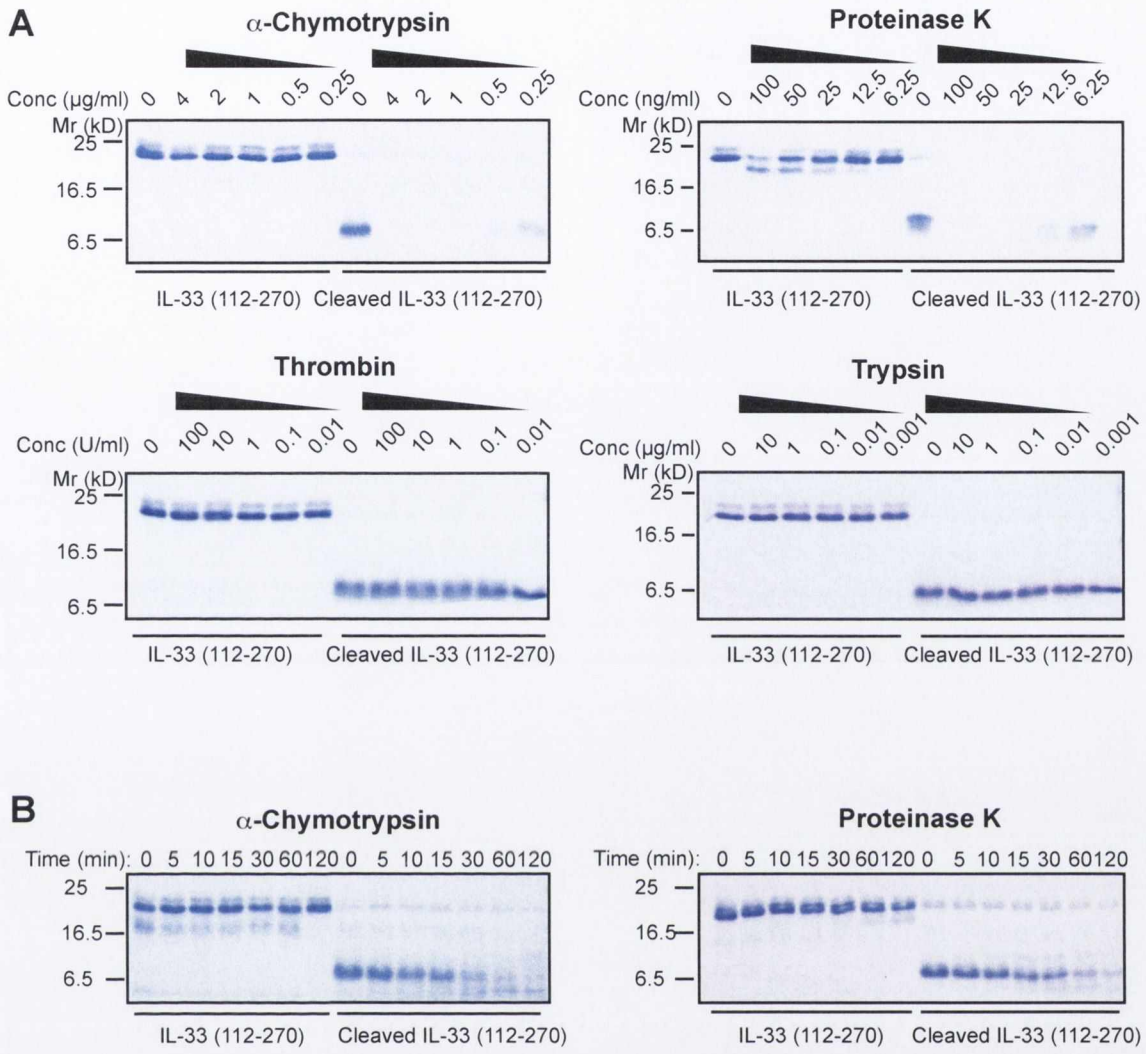

Figure 5.11

Caspase-dependent proteolysis of IL-33 increases its susceptibility to degradation by serum proteases

(A) Purified recombinant IL-33$^{112\text{-}270}$, or caspase-cleaved IL-33$^{112\text{-}270}$, were incubated for 2 h at 37°C in the presence of the indicated concentrations of α-chymotrypsin, proteinase K, thrombin or trypsin, followed by analysis by SDS-PAGE/Coomassie blue staining.

(B) Purified recombinant IL-33$^{112\text{-}270}$, or caspase-cleaved IL-33$^{112\text{-}270}$, were incubated at 37°C with either α-chymotrypsin (1 μg/ml) or proteinase K (25 ng/ml) for the indicated times followed by analysis by SDS-PAGE/Coomassie blue staining.

To evaluate the effect of IL-33 proteolysis by caspases *in vivo* we decided to treat mice with the full-length and caspase cleaved form of IL-33 and compare morphological and physiological effects of both proteins in a mouse model. As we could not produce sufficient amounts of full-length IL-33 with the bacterial expression system, the truncated IL-33 form described by Schmitz *et al.* was used, as this artificially truncated version showed very similar activity to the full-length cytokine in our cell based reporter assay (Figure 5.9A and C). The purified protein was LPS depleted with polymyxin B beads and then incubated with the same amounts of either heat-inactivated or active caspase-7. The former was included as a control for any improbable immunogenic reaction provoked by the protease (Figure 5.12A). In the first experiment, 15 C57BL6 mice were divided into three groups and the groups were each daily i.p injected with PBS, 1 μg IL-33 or 1 μg caspase-7 cleaved IL-33 respectively. After 5 days a tail vein blood sample was taken and the following day the mice were sacrificed and different organs were harvested for analysis. No altered behavioural pattern, weight loss or gain was observed between the different groups during the course of treatment (Data not shown). We next examined in detail different organs of the animal to determine any difference in biological activity between the full-length versus caspase cleaved IL-33. To identify changes in the cellular composition of the blood, spleen and the interperitoneum lavage we generated cytospins and stained the cells with hematoxylin and eosin stain (H&E). The cells were then scored according to their staining pattern, nuclear shape and size into lymphocytes, monocytes, neutrophils and eosinophils. For an additional unbiased scoring method, we also analysed the remainder of these samples by flow cytometry to quantify granulocytes according to their high side scatter. As IL-33 was reported to be an inducer of the Th2 response, we also quantified Th2 associated cytokines in the serum, the intraperitoneal lavage fluid and from homogenized lung tissue.

5.3.11 The caspase-cleaved form of IL-33 shows an attenuated biological activity *in vivo*

As previously described, mice injected with IL-33 showed dramatic splenomegaly. Indeed, mice injected with IL-33 exhibited a striking increase in splenic weight and cellularity (Figure 5.12B). Upon examining and enumerating the splenocytes by

cytospin we could detect a dramatic augmentation of eosinophilic and neutrophil cells (Figure 5.12C). This was also confirmed by the FACS results which showed a doubling of the relative granulocyte numbers (Figure 5.12D). All of these responses were strongly reduced when caspase-cleaved IL-33 was injected into the mice.

Peripheral blood samples showed remarkably similar results. Granulocytes and their subpopulation, eosinophils and to a lesser extent neutrophils showed elevated numbers upon IL-33 treatment. Caspase-cleavage of the cytokine abrogated the effects of IL-33 to near control levels (Figure 5.13A and B).
The same was true for the cells examined in the peritoneal lavage fluid. IL-33 induced a massive infiltration of eosinophils which was reduced when compared to animals injected with cleaved IL-33 (Figure 5.14A). This effect was also confirmed by flow cytometry analysis (Figure 5.14B).

Taken together, these results demonstrate that IL-33 dramatically increased the ratio of granulocytes, particularly eosinophils, in the total cell population. All of these cellular responses were strongly reduced in mice injected with caspase-7 cleaved IL-33.

Upon measuring the cytokine response in the serum, in the homogenized lung and the i.p. lavage samples the resulting patterns were very similar to the previous cell based analyses. Treatment of the animals with IL-33 lead to an increase in IL-5 in the serum, the lavage and the lung and increase in IL-4 in the serum and the lavage (Figure 5.15A to C). Notably, such high concentrations of IL-5 in the lung have so far never been detected by our collaborators in any experiment they performed.

We could only observe a significant induction of IgA but not IgE with IL-33 (Figure 5.15B) as previously reported (Schmitz *et al.*, 2005). All of these effects were reduced in most instances to approaching control levels when the mice were injected with the caspase-cleaved IL-33. The amounts of IFN-γ and IL-6 were not significantly altered in animals injected by IL-33 or cleaved IL-33 compared to PBS control mice (Data not shown).

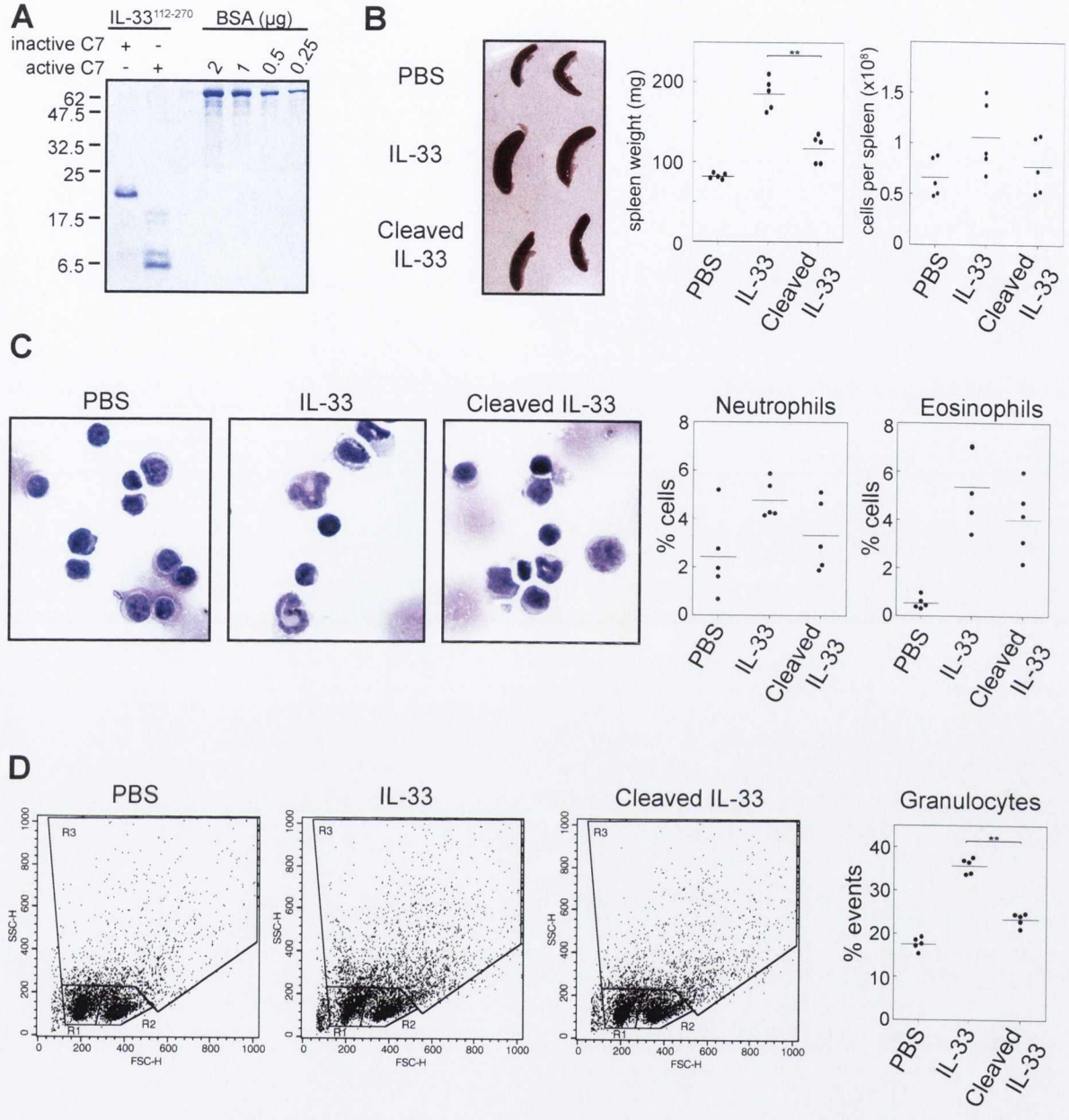

Figure 5.12

The caspase-cleaved form of IL-33 displays diminished biological activity *in vivo*: analysis of the spleen

C57BL/6 mice (5 per treatment group) were injected (i.p.) either with PBS, IL-33$^{112\text{-}270}$ (1 µg per mouse per day), or caspase-cleaved IL-33$^{112\text{-}270}$ (1 µg per mouse per day) for 6 consecutive days.

(A) Coomassie gel of the protein preparatinons used in this experiment (B) Spleen size, weight and cellularity for each group of mice are shown. Photographs show representative spleens for four mice per group. (C) H&E-stained cytospins of Splenocytes were prepared (left) and neutrophil and eosinophil numbers were scored (right). (D) Splenocytes were analysed by flow cytometry (FSC / SSC) and the granulocyte population (R3) were graphed on the right. Error bars represent the mean +/- SEM, *:p<0.05; **: p<0.01

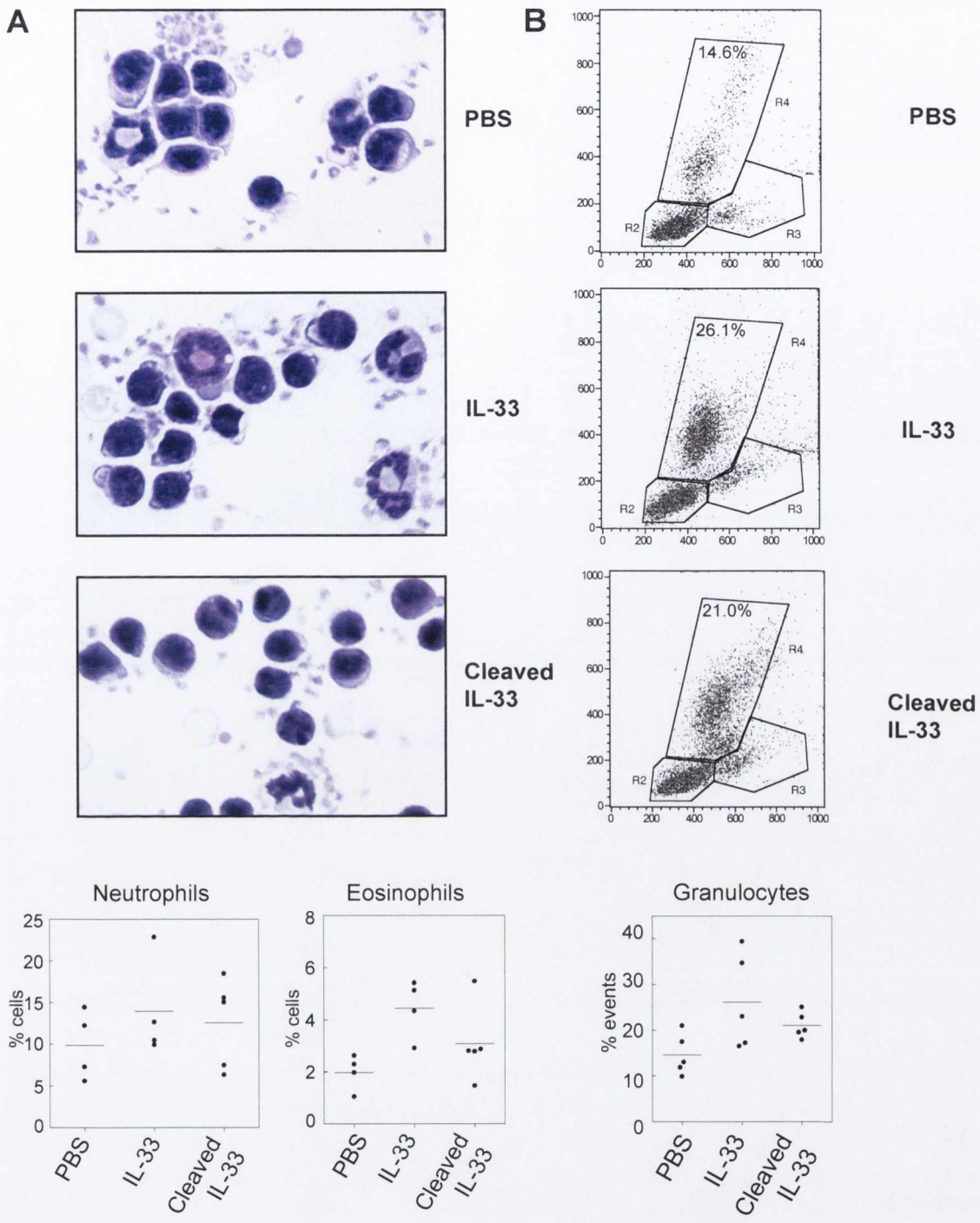

Figure 5.13

The caspase-cleaved form of IL-33 displays diminished biological activity *in vivo*: analysis of the peripheral blood

Mice were treated as described in Figure 5.12.

(A) H&E-stained cytospins of peripheral blood cells were prepared (top), neutrophil and eosinophil numbers were scored and graphed (bottom).

(B) RBCs of peripheral bloods were lysed with FACS lysis solution and the remaining cells were analysed by flow cytometry (FSC/SSC) and gated according to lymphocytes (R2), monocytes (R3) and granulocytes (R4). The granulocyte population was graphed on the bottom

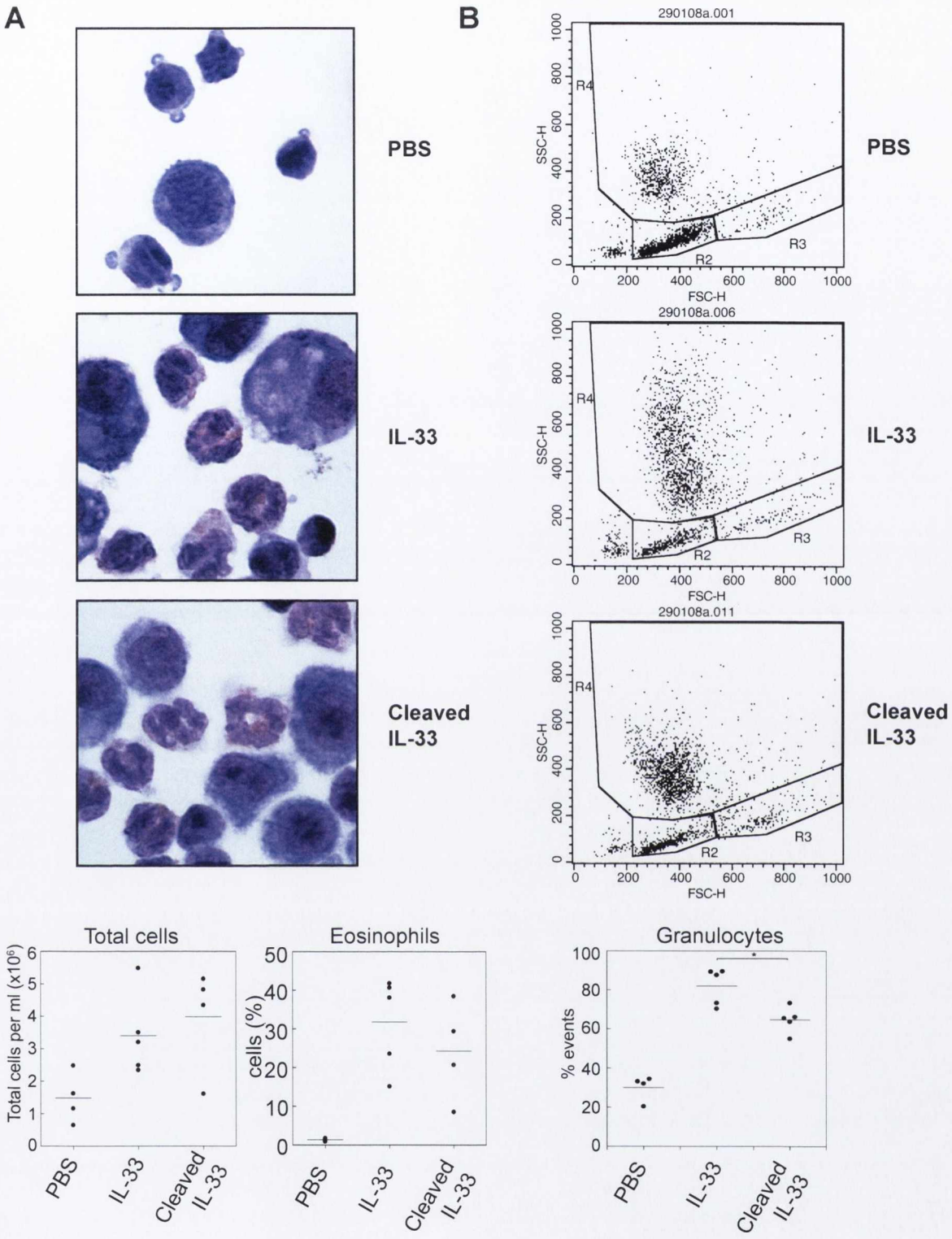

Figure 5.14

The caspase-cleaved form of IL-33 displays diminished biological activity *in vivo*: Analysis of the peritoneal lavage fluid

Mice were treated as described in Figure 5.12.

(A) H&E-stained cytospins of peritoneal lavage cells were prepared (top) and neutrophil and eosinophil numbers were scored (bottom).

(B) Cells were analysed by flow cytometry as described in Figure 5.13B. The granulocyte population (R4) was graphed on the bottom.

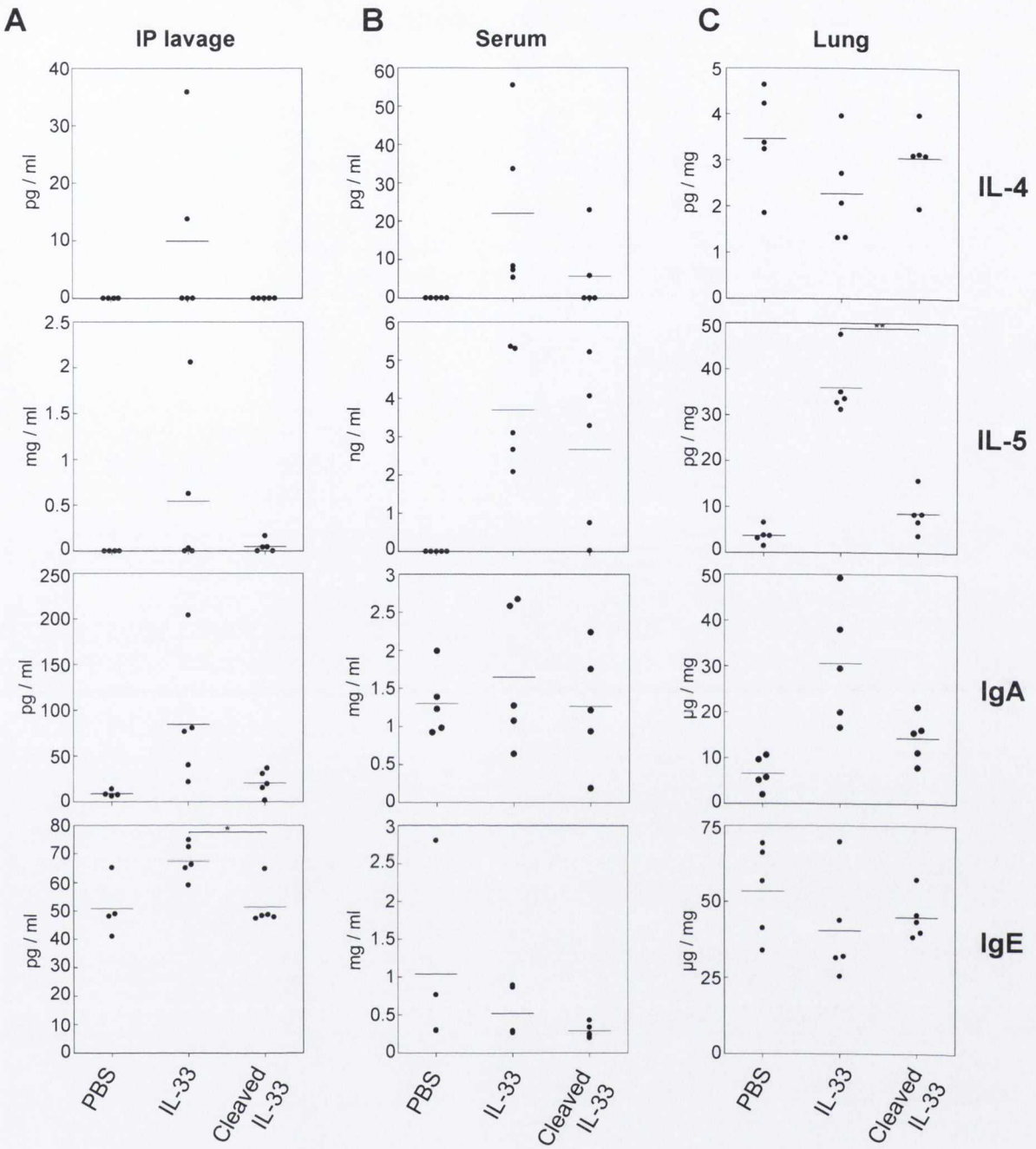

Figure 5.15

The caspase-cleaved form of IL-33 displays diminished biological activity *in vivo* : analysis of cytokines

Mice were treated as described in Figure 5.12

IL-4, IL-5, IgA and IgE levels were determined by ELISA in the IP lavage, plasma samples or lung homogenates. Note that lung data are expressed per mg of total protein. Error bars represent the mean +/- SEM, *:$p<0.05$; **: $p<0.01$

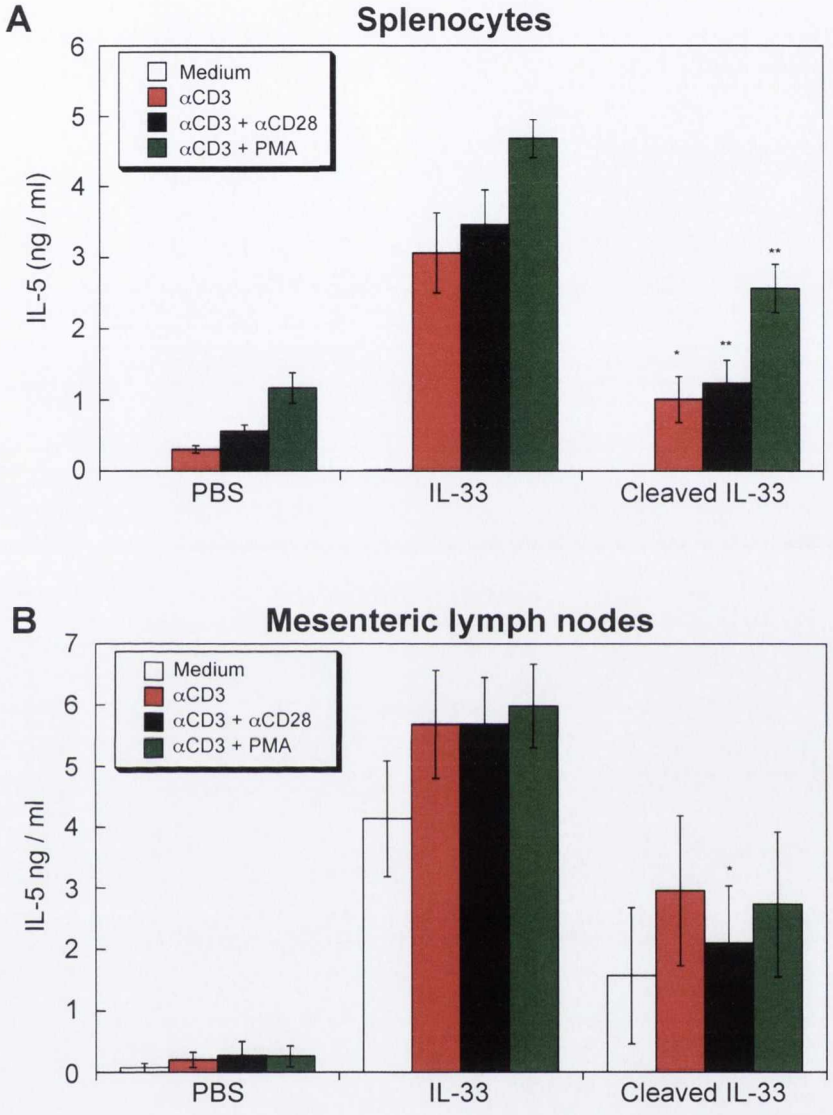

Figure 5.16

The caspase-cleaved form of IL-33 displays diminished biological activity *in vivo*: analysis of re-stimulated lymphocytes

Mice were treated as described in Figure 5.12 and the splenocytes (A) and mesenteric lymph node cells (B) (10^6 cells/ml) were restimulated with medium, 1 µg/ml anti-CD3, 1 µg/ml anti-CD3 and 1 µg/ml anti-CD28, or 1 µg/ml anti-CD3 and 20 ng/ml PMA, as indicated. Supernatants were collected after 3 days and IL-5 concentrations were determined by ELISA. Error bars represent the mean of triplicate assays +/- SEM, *:$p<0.05$; **: $p<0.01$

To determine the status of T cells in lymphoid organs the splenocytes and cells from the mesenteric lymph nodes were *in vitro* restimulated with cross-linking antibodies against CD3 and/or CD28 or with CD3 and PMA respectively. Activated T cells of animals treated with IL-33 showed a strong induction of IL-5 in the splenocytes (Figure 5.16A) and mesenteric lymph nodes (Figure 5.16B), whereas no significant difference in IFNγ, IL-4 or IL-6 amounts were found (Data not shown).

5.3.12 The caspase cleavage site DGVD is essential for IL-33 activity

In the previous experiment the mice were injected with caspase-cleaved IL-33 protein, still containing potentially active caspase-7. Therefore, possible involvement of this protease in the reduction of biological readouts, albeit unlikely, could not be excluded. We therefore repeated the experiment, including a non-cleavable IL-33^{D178A} mutant. $IL33^{wt}$ and $IL33^{D178A}$ were both incubated with either heat inactivated or active caspase-7 as in the previous experiment.

To our surprise the mutant IL-33^{D178A} completely lost its biological activity *in vivo*. Whereas wild-type IL-33 dramatically increased the size and cellularity of the spleens (Figure 5.17A), increased the amount of granulocytes and especially eosinophils in the peripheral blood, spleen and i.p. lavage (Figure 5.17B and data not shown) and enhanced the activation of CTLs of the inguinal and mesenteric lymphnodes (Figure 5.17C), mice treated with the IL-33^{D178A} mutant showed a dramatic reduction in the biological activity of the cytokine (Figure 5.17 A-C). On the other hand, the caspase-7 cleaved IL-33 showed a dramatically reduced biological activity, as was demonstrated before. We also confirmed this finding in our *in vitro* based cell reporter assay where the IL-33^{D178A} mutant showed no ST2 dependent NF-κB activation (Figure 5.17D).

These results strongly suggest that the caspase cleavage site at $DVGD^{178}$ is crucial for the biological activity of IL-33 and a single point mutation in this region destroys any signalling capability of the cytokine.

5.3.13 Caspase-7 activity is not responsible for the loss of IL-33 function by caspase-cleavage

With the previous experiment we could still not rule out any involvement of the caspase-7 activity in the effects seen *in vivo*. Another approach was taken to block any remaining caspase-7 activity after processing of IL-33. The irreversible pan-caspase inhibitor zVAD-fmk was added to all preparations and the proteolytic activity of the caspase was assayed. Caspase-7 still had a high DEVDase proteolytic activity after 4 hours incubation at 37°C, but addition of a 3 fold molar amount of the inhibitor completely blocked any remaining caspase activity (Figure 5.18A).

Once more, the caspase-cleaved IL-33 showed a greatly reduced effect compared to the intact cytokine *in vivo*. The splenomegaly induced by IL-33 (Figure 5.18B), the increase of granulocytes and especially eosinophils in the spleen (Figure 5.18B), peripheral blood (Figure 5.18D) and i.p. lavage (Data not shown) was greatly reduced when the animals were injected with the caspase cleaved IL-33, as was the CTL activation in the mesenteric lymph nodes (Figure 5.18E). Additionally we detected granulocyte differentiation antigen 1 (GR-1, a marker for mature granulocytes) positive cells in the i.p. lavage by flow cytometry. Again, a strong increase in GR-1 positive cells in IL-33 treated animals was detected and albeit a non significant outlier, a substantial decrease was seen in cleaved IL-33 injected mice (Figure 5.18F).

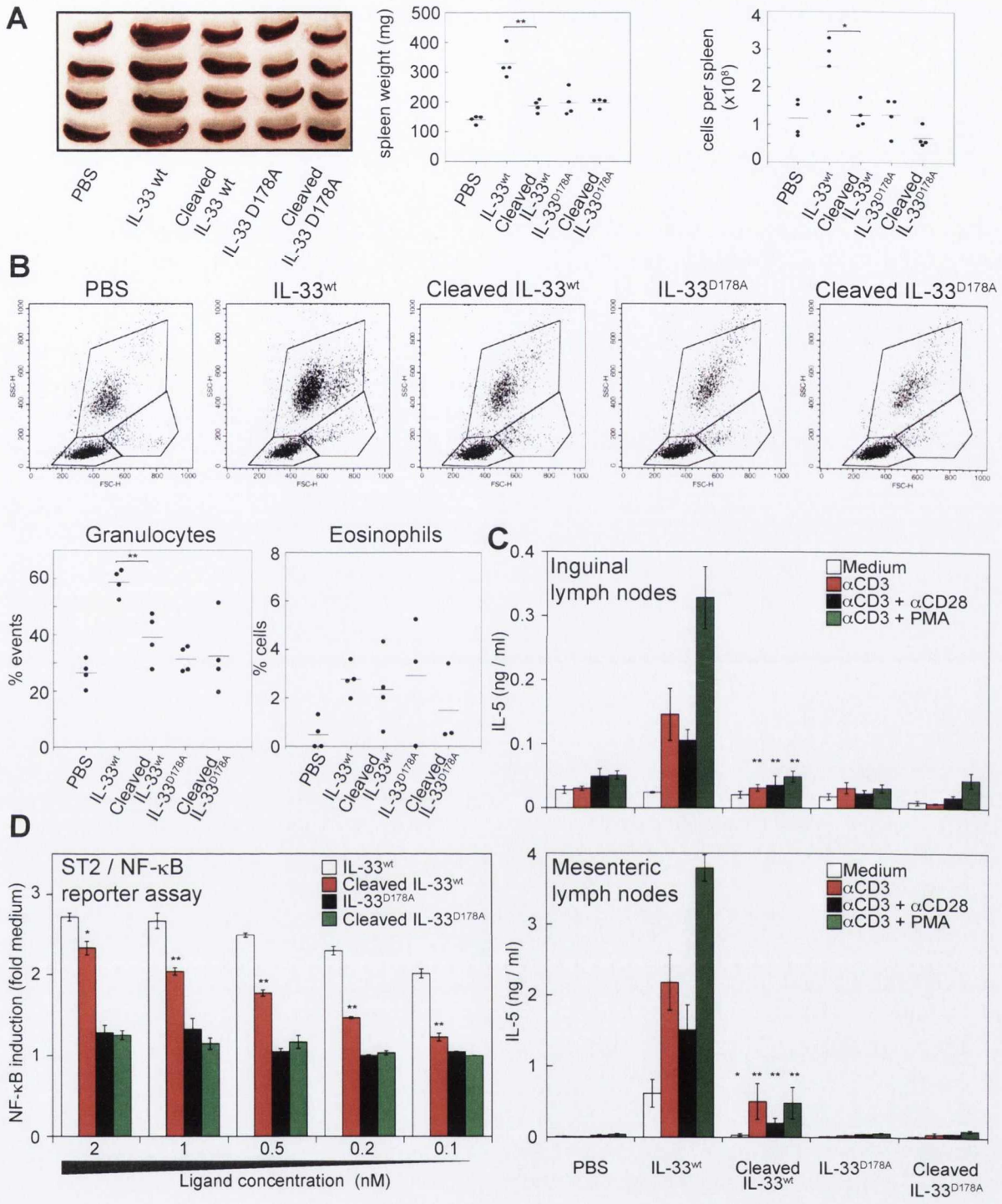

Figure 5.17

The caspase cleavage site is essential for the biological activity of IL-33

(A) BALB/c mice were i.p injected with uncleaved or cleaved IL-33^{wt} or IL-33^{D178A} as described in Figure 5.12 and the spleen morphology and cellularity are shown. (B) Lymphocytes in the peripheral blood were analyzed by flow cytometry (top), the high SSC population and eosinophils determined from H&E stained cytospins are graphed below. (C) Inginual (top) and meseneric (bottom) lymphnodes were restimulated as described in Figure 5.16. Supernatants were collected after 3 days and IL-5 concentrations were determined by ELISA. (D) The indicated amounts of uncleaved or caspase cleaved IL33^{wt} or IL33^{D178A} was added to the HEK293 ST2-NF-κB reporter cell line as described in Figure 5.9. Error bars represent the mean of triplicate assays +/- SEM, *:p<0.05; **: p<0.01

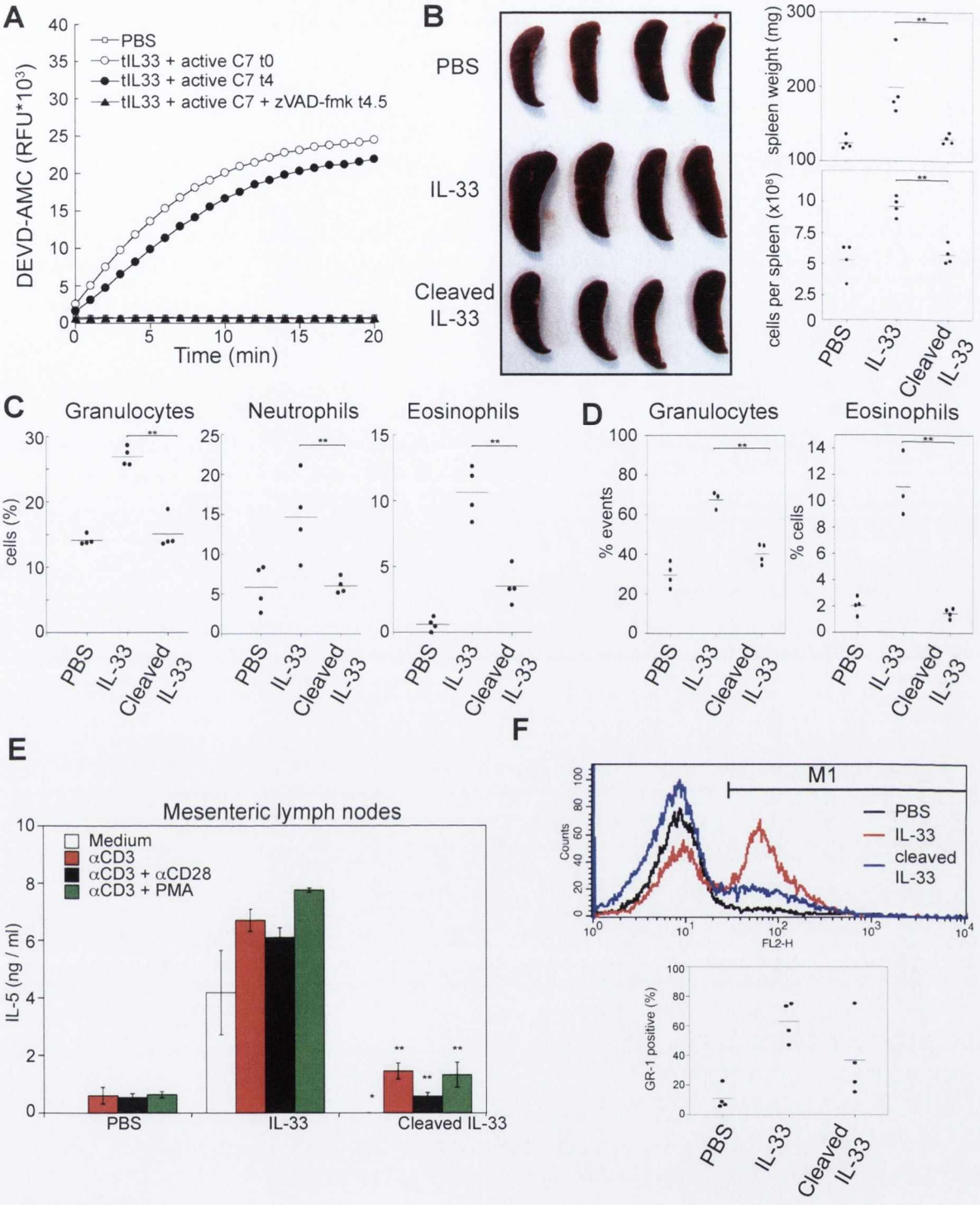

Figure 5.18

The diminished biological activity of caspase cleaved IL-33 *in vivo* is not due to residual caspase-7 activity

(A) The DEVDase activity of caspase-7 before (open circles), after 4 hour incubation (closed circles) and after excess additon of zVAD-fmk (triangles) was measured over time and graphed. (B) Mice were treated as described in Figure 5.12 and the spleen size, weight and cellularity is shown for each animal. Granulocytes from splenocytes (C) or peripheral blood (D) were determined by flow cytometry and neutrophils and/or eosinophils were enumerated from H&E stained cytospins. (E) Mesenteric lymphnodes were restimulated and the IL-5 concentration was determined and graphed as described in Figure 5.16. (F) GR-1$^+$ cells from i.p. lavages were measured by flow cytometry and the percentage of events within M1 are graphed below. Error bars represent the mean +/- SEM, *:$p<0.05$; **: $p<0.01$.

5.4 DISCUSSION

5.4.1 Summary

The aim of this chapter was to validate the novel cytokine IL-33 as a substrate for the inflammatory caspase-1. Our initial experiments with *in vitro* generated human and murine IL-33 clearly showed that IL-33 was not efficiently processed by caspase-1 at levels where the protease readily cleaved the known substrate IL-1β. Instead we show that caspases associated with apoptosis cleave IL-33 at a site different to the initially described $ALHD^{110}$. We subsequently mapped the novel caspase cleavage site to $DGVD^{178}$ in human and $DGVD^{175}$ in mouse. The processing of IL-33 was further confirmed by incubating the *in vitro* transcribed and translated wild-type IL-33 or mutant $IL\text{-}33^{D178A}$ protein in THP-1 or Jurkat cell-free extract where we specifically activated endogenous caspases involved in either inflammation or apoptosis. We expressed different truncations of IL-33 and showed that although the full-length and the caspase cleaved form of IL-33 were both able to bind the ST2 receptor, only intact IL-33 induced ST2 dependant NF-κB activation. We further showed that IL-33 cleaved by caspase-7 was more susceptible to degradation by serum proteases, hence reducing its half-life and bioavailability.

When measuring the activity of full-length IL-33 *in vivo* we detected a massive increase in lymphocyte numbers and cytokine levels as previously reported. However, all these effects were strongly reduced in mice treated with the caspase-7 cleaved IL-33. We could rule out a contribution of the remaining caspase-7 activity in the protein preparation but thereby also uncovered the region of the caspase cleavage site as a functionally essential part of IL-33 signalling. We therefore demonstrate for the first time, that an extremely potent cytokine is inactivated by caspase processing during apoptosis.

5.4.2 IL-33 is cleaved by apoptotic caspases

Interleukin-33 was originally cloned from canine vasospastic arteries (Onda *et al.*, 1999) and later discovered in the nucleus of human high endothelial cells (Baekkevold *et al.*, 2003). These cells can take part in the innate immune response by monitoring for potential pathogenic microbes and further provide the

entry site to the inflamed tissue for activated lymphocytes. Ever since the discovery of IL-33 as a novel interleukin family member, it was widely assumed that this cytokine required proteolytic processing for its activation because it shares a strong structural similarity with cytokines of the IL-1 family (Figure 1.9).

Our data here clearly shows that IL-33 is cleaved by caspases activated during apoptosis and is not processed when caspases associated with inflammation are active. As a further proof, IL-33 was cleaved in apoptotic mouse embryonic fibroblasts deficient of caspase-1, whereas MEFs lacking caspase-3 no longer cleave the cytokine (Lüthi *et al.,* 2009). A recently published report independently identified the genuine caspase cleavage site in IL-33. Unfortunately the authors still used inappropriately high amounts of recombinant caspases and falsely concluded the inflammatory capsase-1 is capable of cleaving IL-33 at the apoptotic caspase site in spite of the typical DXXD cleavage motif (Cayrol and Girard, 2009).

5.4.3 Caspase cleaved IL-33 fails to signal through ST2

Our data clearly demonstrates that IL-33 is cleaved by caspases at the conserved $DGVD^{178}$ motive in the human form of this cytokine ($DGVD^{175}$ in the mouse). This has important implications, as previous studies on IL-33 have exclusively used an artificially truncated form of this protein based on a predicted caspase cleavage site (at Asp^{110}). This caspase cleavage site has failed to be verified by our investigations and is not conserved between human and mouse IL-33. Functionally, this artificially truncated form of IL-33 retains biological activity. Unless technical difficulties involved in the *in vitro* production of the full-length cytokine are resolved, the truncated IL-33 will probably be used for further investigations in the near future.

Proteolytic processing of IL-33 does not seem to impair ST2 receptor binding, as full-length and cleaved IL-33 are able to bind to the receptor *in vitro*. However, as complete processing of full-length IL-33 was not achievable in our experiments, the receptor binding capability of the individual fragments should be assessed. The N-terminal caspase cleavage fragment could still bind to the receptor and

possibly inhibit any further binding of active full-length IL-33, thereby acting as a dominant negative inhibitor.

Cleaving IL-33 strongly diminishes its transactivation capability of NF-κB *in vitro* and rendered it more susceptible to serum proteases. Proteolysis of IL-33 could lead to a destabilisation of the protein and change the tertiary structure rendering it incapable of efficiently stimulating the ST2 receptor complex. The point mutation in the caspase cleavage region of IL-33 renders this cytokine biologically inactive. The Asp to Ala substitution could lead to an additional alteration in the overall conformation of the protein and thereby abolish its cytokine activity both *in vitro* and *in vivo*.

5.4.4 Similarities between IL-33 and IL-1α

Although IL-33 was identified due to its structural homology to IL-18, this cytokine surprisingly shares many functional homologies with IL-1α. The N-terminal part of both IL-1α (Maier *et al.*, 1994) and IL-33 (Moussion *et al.*, 2008) appear to contain an atypical nuclear localisation signal and both proteins were implicated in transcriptional regulation (Carriere *et al.*, 2007). Additionally, like IL-33, IL-1α does not require further processing for activation (Mosley *et al.,* 1987) and both full-length cytokines are able to bind to their respective IL-1 receptors. Furthermore, both cytokines can undergo proteolytic processing by different proteases under certain conditions and as we have shown here, caspase-3 and -7 clearly inactivate the biological functions of IL-33. Unlike IL-1β or IL-18, biologically active IL-1α is generally not detected in the circulation of humans. This is possibly due to its inhibition by soluble IL-1 receptor type II (sIL-1RII), a secreted receptor sequestering any active IL-1 in circulation and preventing its binding and activation of an IL-1 receptor (Colotta *et al.*, 1994). In parallel soluble ST2 (sST2), a spliced isoform of the transmembrane ST2L receptor with an alternative promotor, has been found to dramatically reduce the effects of IL-33 *in vitro* and *in vivo* (Hayakawa *et al.*, 2007) and is generally found to be up-regulated in autoimmune diseases (Kuroiwa *et al.*, 2001), asthma (Oshikawa *et al.*, 2001) and sepsis (Brunner *et al.*, 2004).

It is also proposed that the main release mechanism of IL-1α is predominantly by necrosis, a result which we have also found to be the case with IL-33 and is discussed in the next section.

5.4.5 Cellular release of IL-33

Most secreted proteins in a cell are transported through the Golgi apparatus. This does not seem to be the case for the IL-1 family of cytokines. IL-33 along with IL-1α, IL-1β and IL-18 are all lacking a classical secretory signal sequence and their mode of cellular release is not fully resolved to date. We investigated the localisation and a possible release mechanism of endogenous IL-33 and its caspase cleaved fragments but this was further hindered by the extremely low levels of this cytokine. Multi-tissue and multi-cell line western blots revealed no cross reactive protein with 6 different commercial and self made antibodies against IL-33 at the expected molecular weight. Only stimulated THP-1 cells and densely grown HUVEC cells expressed a detectable amount of endogenous IL-33 ((Lüthi *et al.,* 2009) and data not shown). More sensitive reagents including a high affinity antibody could improve this detection problem in the future.

In a recent publication we have shown that exponentially growing or apoptotic THP-1 cells do not release any substantial amount of IL-33, even upon inflammatory stimuli where IL-1β release was dramatically increased (Lüthi *et al.,* 2009). Additionally the amounts of cell-associated or released endogenous IL-33 in THP-1 cells were almost two log lower than IL-1β. In contrast, full-length IL-33 could only be detected in the cell supernatant after the cell walls were ruptured during necrosis. This mode of release is similar to the one suspected with IL-1α and the non-classical cytokine HMGB1 (Scaffidi *et al.*, 2002). Additionally, as the apoptotic caspases are not active during necrosis (Kroemer *et al.*, 2005), IL-33 would be released as a full-length, active cytokine. Processing and thereby inactivating IL-33 during apoptosis would ensure a silencing of this very potent pro-inflammatory cytokine. This observation would have a similar outcome to HMGB1 as it is inactivated by mitochondrial reactive oxygen species generated by activation of the apoptotic caspase cascade (Kazama *et al.*, 2008). This silencing effect has been observed in cells when the immunogenetic potency of apoptotic

and necrotic cells was compared. Apoptotic cells activate the immune system to a much lower extent compared to necrotic cells and under certain conditions can even inhibit an inflammatory reaction (Voll *et al.*, 1997; Patel *et al.*, 2007). Additionally, apoptotic cells express 'eat me' signals and are subsequently rapidly engulfed and cleared by phagocytes preventing the release their intracellular contents and with it potential signalling molecules.

5.4.6 IL-33, a novel danger signal?

Polly Matzinger initially proposed the Danger Theory as an alternative model completely opposing the well established inflammatory model discriminating between self and non-self (Matzinger et al 1994). She later expanded her theory by defining "danger" with the unprogrammed tissue destruction of necrosis or other molecules associated with a stressed cell. Other investigators incorporated her theory and coined the term 'alarmins' or damage-associated molecular patterns (DAMPs) for such danger signals (Oppenheim *et al.*, 2005; Bianchi, 2007). Many molecules like HMGB1 (Scaffidi *et al.,* 2002), uric acid (Shi *et al.,* 2003) and members of the heat shock protein (HSP) family (reviewed in Schmitt *et al.*, 2007)) have been subsequently characterised as alarmins due to their rapid release from necrotic but not apoptotic cells and potent stimulatory activity on inflammatory cells like macrophages or DCs.

Given its strong pro-inflammatory properties as a full-length protein, its release during necrosis (Lüthi *et al.,* 2009) but not apoptosis (Data not shown) and the fact that it signals via the TLR/IL-1R/MyD88 signalling pathway (Schmitz *et al.,* 2005), IL-33 classifies clearly as a novel member of the 'alarmin' group of molecules. Given that many different cell types of the innate immune system respond to IL-33 - including mast cells (Allakhverdi *et al.*, 2007), eosinophils (Cherry *et al.*, 2008), basophils and NK cells (Smithgall *et al.*, 2008) – IL-33 my be an important alarmin, although further studies are required to clarify this issue.

5.4.7 Possible functions of IL-33

Investigators have identified IL-33 as a multifunctional protein. The nuclear expression and chromatin binding properties suggest a role in transcriptional

repressor (Carriere *et al.,* 2007) although further investigation is required to identify the target genes and verify the function under possible inflammatory conditions. The proteolytic cleavage during apoptosis might disable these putative transcriptional activities, reducing any induction of further possible pro-inflammatory mediators in a 'destined to die' cell. Seeing as IL-33 is a potent danger signal, it might also be retained in the nucleus to prevent it from accidentally triggering the transmembrane ST2 receptor.

IL-33 is generally expressed in cells close to vessel walls and epithelial surfaces exposed to the environment (Kuchler *et al.*, 2008; Moussion *et al.,* 2008). These tissues are more likely to be exposed to pathogens, allergens, other inflammatory triggers or mechanical injury which could result in tissue damage and the release of IL-33 in the extracellular space to rapidly activate the immune cells mentioned above which in turn then further activate and coordinate the immune response.

CHAPTER VI

Final discussion

6.1 INTRODUCTION

The inflammatory process is essential for protection from pathogens and the repair of damaged tissues and has been studied extensively over the past decades. Knowing more about the molecules involved in such a pathway is essential for the design of therapeutic drugs. The proteolytic activity of specific caspases play a crucial part in the signalling pathways that activate and control the inflammatory response. Other members of the caspase family play an essential part in apoptosis by cleaving proteins and thereby activate or inactivate processes that lead to the coordinated dismantling of the cell. Over 700 caspase substrates cleaved during apoptosis have been identified to date (Lüthi and Martin, 2007), whereas to date only 2 have been confirmed for the caspases activated during inflammation.

The overall aim of the work outlined in this thesis was to gain a better understanding of the inflammatory process by identifying and characterising novel molecules cleaved by caspases that modulate the inflammatory process. To identify proteins that are processed by caspases, different approaches have been previously employed. These *in vitro* screens range from a one-dimensional approach, separating control and apoptotic cell lysates by SDS-PAGE and identifying any difference in banding by mass spectrometry (Thiede *et al.*, 2005), diagonal gel analysis with recombinant caspases (Ricci *et al.*, 2004; Shao *et al.*, 2007) and two-dimensional resolution of apoptotic proteomes (Thiede *et al.*, 2001).

6.2 CONCLUSIONS OF CHAPTER III

In order to identify novel inflammatory caspase substrates we adapted a cell-free extract where we could specifically control the protease activity of caspase-1, resolved both proteomes by 2D-SDS-PAGE and compared the different silver-stained gels. Only very few alterations were detectable when the THP-1 cell-free extract proteome, where inflammatory caspases were activated, was compared with the control proteome. This suggests that caspase-1, -4 and -5 are highly specific proteases compared to the executioner caspases involved in apoptosis and is consistent with the lack of inflammatory caspase substrates reported to date.

Additionally these results suggest that endogenous levels of caspase-1, -4 and -5, do not activate apoptotic caspases. This is indicated by the finding that cleavage of apoptotic substrates was not detected when inflammatory caspases were active in a system where activation of apoptotic caspases was possible. These results are in contrast to several reports where caspase-1 was shown to induce apoptosis upon overexpression (Miura *et al.,* 1993; Kondo *et al.*, 1995; Jung *et al.*, 1996; Hawkins *et al.,* 1996; Feng *et al.,* 2004). This result is also in accordance with the data obtained from caspase-1 and -11 deficient mice versus caspase-3, -7 and -9 deficient mice. Overall these results indicate that the inflammatory caspases are unlikely to participate in programmed cell death.

When comparing the control and inflammatory caspase activated proteomes by 2D-SDS-PAGE, we have observed some differences, too faint for reproducible silver staining. Recently, new proteomic methods were developed and improved, including a gel-free method whereby control and apoptotic proteomes were labelled with different radioisotopes. This was followed by fractional diagonal chromatography (COFRADIC) and any differences were identified by LC/MS/MS analysis. This sensitive screen resulted in the identification of 92 processed proteins (Van Damme *et al.,* 2005). Another method, whereby a specific enzyme selectively biotinylated free protein N termini yielded 292 caspase substrates (Mahrus *et al.*, 2008). A combinatory approach of SDS-PAGE and LC-MS/MS visually comparing the size, topography, and abundance of each protein resulting in the identification of 261 apoptotic caspase substrates (Dix *et al.*, 2008). Besides identifying the proteins undergoing a proteolytic event, the first two methods also allowed for the identification of the exact caspase cleavage site in the protein substrate sequence. A screen utilising a more sensitive method like the ones mentioned above could have the potential to reveal additional novel inflammatory caspase substrates in our THP-1 cell-free extract system.

6.3 CONCLUSIONS OF CHAPTER IV

In our next approach to identify novel inflammatory caspase substrates we utilised an *in vitro* expression cloning approach. This required the use of recombinant

caspases but carried with it the complication of determining physiological levels for each protease to be used in the screen. Having established the THP-1 cell-free system in the third chapter, we could subsequently verify any putative inflammatory caspase substrates with endogenous levels of the protease. The verification of the substrate with non-saturating, endogenous levels of the protease can be the most important step in the search for novel caspase substrates. Ideally the processing is tested on endogenous substrate in a cell with a relevant inflammatory stimulus. The majority of the previously published studies unfortunately fail in this aspect of verification.

We conclude that GDAP1L1, MAGE-D1, L-SOX5 and TDP-43 are validated inflammatory caspase substrates, cleaved by endogenous caspase levels of the THP-1 cell-free extract.

6.4 CONCLUSION OF CHAPTER V

Our initial aim was to validate IL-33 as a caspase-1 substrate. We have shown conclusively through this work, that IL-33 is not processed by caspase-1 at levels where the protease efficiently processes its confirmed substrate, IL-1β. Further, this study provides clear evidence that IL-33 is active only as a full-length molecule and does not require proteolytic maturation by caspase-1.

Importantly, we demonstrated that IL-33 is processed by endogenous levels of caspase-3 and -7. We have mapped the apoptotic caspase cleavage site to $DGVD^{178}$, a conserved region between human and mouse within the β-trefoil fold. Processing of the cytokine at this site inactivates or greatly diminishes its biological activity. We have demonstrated this both *in vitro*, using an ST2 NF-κB reporter assay and *in vivo*, by treating animals with full-length and cleaved IL-33. Full-length IL-33 results in dramatic effects throughout the whole body, including a massive increase in granulocytes, splenomegaly, inflammation of the mucosal tissues and an atypical Th2 response. Caspase-7 cleaved IL-33 displayed a marked decrease in the observed phenotype.

Therefore IL-33 is a potent alarmin alerting the immune system to tissue injury and necrosis in order to activate an immune response and repair any damage.
Conversely, in an apoptotic cell, it is essential to neutralise this cytokine by cleavage in order to prevent an irrelevant immune response.

The functions and actions of IL-33 are uncertain and wide ranging Current assay methods are not sensitive enough to detect extracellular IL-33 *in vivo*. A variant of its receptor, the soluble ST2 receptor, has the capability to sequester and neutralise any extracellular IL-33 (Hayakawa *et al.,* 2007) and is more than likely upregulated upon detection of the cytokine. Indeed researchers have found increased release of sST2 upon cellular stress or inflammatory conditions. It has been speculated that IL-33 may play a role in asthma (Oshikawa *et al.,* 2001), rheumatoid arthritis (Leung *et al.*, 2004), atherosclerosis (Miller *et al.*, 2008) septic shock (Brunner *et al.,* 2004) and as a prognostic marker for myocardial infarction (Shimpo *et al.*, 2004). Interestingly, increased IL-33 was also detected in fibroblasts when they were subjected to biomechanical strain. The cytokine induced cardiomyocyte NF-κB levels, resulting in a tolerance to the effects of cardiac pressure overload injury in an *in vivo* model (Sanada *et al.*, 2007). Whether IL-33 is a major or minor component of any of these systems also remains to be determined.

6.5 OVERALL CONCLUSIONS

The specific conclusions this thesis supports are:

(I) The inflammatory caspases are highly specific and are not involved in the apoptotic process

(II) Endogenous MAGE-D1, *in vitro* transcribed and translated GDAP1L1, L-SOX5 and TDP-43 are processed by endogenous inflammatory caspases

(III) The novel cytokine IL-33 is not cleaved by caspase-1 but by caspases activated during apoptosis at DGVD^{178} in humans and DGVD^{175} in mouse

(IV) Proteolysis of IL-33 by caspase-3 and -7 leads to a loss of ST2 receptor activation *in vitro* and diminished cytokine response *in vivo*

(V) The release of IL-33 during necrosis and its potent cytokine activity suggests that this cytokine may represent a novel alarmin

APPENDICES

Table A.1 Constructs used in this study

Plasmid name	Source
pET15b.Casp-1.p30	Alexander Lüthi, Lab of Prof. Seamus Martin
pcDNA3.caspase-1.AU1	Prof. Vishva Dixit
pET21b.caspase-2	Prof. Emad Alnehmri
pcDNA3.caspase-3	Prof. Vishva Dixit
pET23b.caspase-3	Prof. Guy Salvesen
pcDNA3.caspase-4	Dr. Elizabeth Slee, Lab of Prof. Seamus Martin
pGEX-4T-1.caspase-4.p30	Dr. Xiaoyu Lin, Lab of Prof. Alan Porter
pcDNA3.caspase-5	Dr. Elizabeth Slee, Lab of Prof. Seamus Martin
pGEX-4T-1.caspase-5.p30	Dr. Xiaoyu Lin Lab of Prof. Alan Porter
pET23b.caspase-7	Prof. Guy Salvesen
pcDNA3.caspase-9	Helen Egan, Lab of Prof. Seamus Martin
pcDNA3.IL-1β	Dr. Lisa Boucher-Hayes, Lab of Prof. Seamus Martin
pcDNA3.MAGE-D1	Dr. Patrick Duriez, Lab of Prof. Seamus Martin
pCR.T7.MYC.capG.V5.His	Prof. Jan Gettemans
pet23a.co-chaperone p23	Dr. Sean Cullen, Lab of Prof. Seamus Martin
pcDNA3-Bcl-XL	Prof. Doug Green
pcDNA3.hIL-33	Dr. Patrick Duriez, Lab of Prof. Seamus Martin
pcDNA3.mIL-33	Dr. Patrick Duriez, Lab of Prof. Seamus Martin
pET45b.hIL-33	Dr. Patrick Duriez, Lab of Prof. Seamus Martin
pcDNA3.hIL33.FLAG	Dr. Patrick Duriez, Lab of Prof. Seamus Martin
pGEX-4T2.hIL33$^{1-270}$	Dr. Rebecca Taylor, Lab of Prof. Seamus Martin
pET45b.hIL33	Dr. Patrick Duriez, Lab of Prof. Seamus Martin
pET45b.mIL33	Dr. Patrick Duriez, Lab of Prof. Seamus Martin
pET45b.hIL33^{D178A}	Dr. Patrick Duriez, Lab of Prof. Seamus Martin
pET45b.mIL33^{D175A}	Dr. Patrick Duriez, Lab of Prof. Seamus Martin
pET45b.hIL33$^{1-178}$	Dr. Patrick Duriez, Lab of Prof. Seamus Martin
pET45b.hIL33$^{179-270}$	Dr. Patrick Duriez, Lab of Prof. Seamus Martin
pET45b.hIL33$^{112-270}$	Inna Afonina, Lab of Prof. Seamus Martin
pET45b.hIL33$^{112-270\ D178A}$	Inna Afonina, Lab of Prof. Seamus Martin

pET45b.hIL33$^{112\text{-}178}$	Inna Afonina, Lab of Prof. Seamus Martin
pcDNA3.hIL33^{D178A}	Dr. Rebecca Taylor, Lab of Prof. Seamus Martin

REFERENCES

Acampora, D., Merlo, G.R., Paleari, L., Zerega, B., Postiglione, M.P., Mantero, S., Bober, E., Barbieri, O., Simeone, A. and Levi, G. (1999). Craniofacial, vestibular and bone defects in mice lacking the Distal-less-related gene Dlx5. *Development* **126**: 3795-809.

Adrain, C., Creagh, E.M., Cullen, S.P. and Martin, S.J. (2004). Caspase-dependent inactivation of proteasome function during programmed cell death in Drosophila and man. *J Biol Chem* **279**: 36923-30.

Adrain, C. and Martin, S.J. (2001). The mitochondrial apoptosome: a killer unleashed by the cytochrome seas. *Trends Biochem Sci* **26**: 390-7.

Adrain, C., Murphy, B.M. and Martin, S.J. (2005). Molecular ordering of the caspase activation cascade initiated by the cytotoxic T lymphocyte/natural killer (CTL/NK) protease granzyme B. *J Biol Chem* **280**: 4663-73.

Agostini, L., Martinon, F., Burns, K., McDermott, M.F., Hawkins, P.N. and Tschopp, J. (2004). NALP3 forms an IL-1beta-processing inflammasome with increased activity in Muckle-Wells autoinflammatory disorder. *Immunity* **20**: 319-25.

Ali, S., Huber, M., Kollewe, C., Bischoff, S.C., Falk, W. and Martin, M.U. (2007). IL-1 receptor accessory protein is essential for IL-33-induced activation of T lymphocytes and mast cells. *Proc Natl Acad Sci U S A* **104**: 18660-5.

Allakhverdi, Z., Smith, D.E., Comeau, M.R. and Delespesse, G. (2007). Cutting edge: The ST2 ligand IL-33 potently activates and drives maturation of human mast cells. *J Immunol* **179**: 2051-4.

Alnemri, E.S., Fernandes-Alnemri, T. and Litwack, G. (1995). Cloning and expression of four novel isoforms of human interleukin-1 beta converting enzyme with different apoptotic activities. *J Biol Chem* **270**: 4312-7.

Alnemri, E.S., Livingston, D.J., Nicholson, D.W., Salvesen, G., Thornberry, N.A., Wong, W.W. and Yuan, J. (1996). Human ICE/CED-3 protease nomenclature. *Cell* **87**: 171.

Arai, T., Hasegawa, M., Akiyama, H., Ikeda, K., Nonaka, T., Mori, H., Mann, D., Tsuchiya, K., Yoshida, M., Hashizume, Y. and Oda, T. (2006). TDP-43 is a component of ubiquitin-positive tau-negative inclusions in frontotemporal lobar degeneration and amyotrophic lateral sclerosis. *Biochem Biophys Res Commun* **351**: 602-11.

Baekkevold, E.S., Roussigne, M., Yamanaka, T., Johansen, F.E., Jahnsen, F.L., Amalric, F., Brandtzaeg, P., Erard, M., Haraldsen, G. and Girard, J.P. (2003). Molecular characterization of NF-HEV, a nuclear factor preferentially expressed in human high endothelial venules. *Am J Pathol* **163**: 69-79.

Bannerman, D.D., Sathyamoorthy, M. and Goldblum, S.E. (1998). Bacterial lipopolysaccharide disrupts endothelial monolayer integrity and survival signaling events through caspase cleavage of adherens junction proteins. *J Biol Chem* **273**: 35371-80.

Barker, P.A. and Salehi, A. (2002). The MAGE proteins: emerging roles in cell cycle progression, apoptosis, and neurogenetic disease. *J Neurosci Res* **67**: 705-12.

Baxter, R.V., Ben Othmane, K., Rochelle, J.M., Stajich, J.E., Hulette, C., Dew-Knight, S., Hentati, F., Ben Hamida, M., Bel, S., Stenger, J.E., Gilbert, J.R., Pericak-Vance, M.A. and Vance, J.M. (2002). Ganglioside-induced differentiation-associated protein-1 is mutant in Charcot-Marie-Tooth disease type 4A/8q21. *Nat Genet* **30**: 21-2.

Bell, J.K., Mullen, G.E., Leifer, C.A., Mazzoni, A., Davies, D.R. and Segal, D.M. (2003). Leucine-rich repeats and pathogen recognition in Toll-like receptors. *Trends Immunol* **24**: 528-33.

Bertin, J., Nir, W.J., Fischer, C.M., Tayber, O.V., Errada, P.R., Grant, J.R., Keilty, J.J., Gosselin, M.L., Robison, K.E., Wong, G.H., Glucksmann, M.A. and DiStefano, P.S. (1999). Human CARD4 protein is a novel CED-4/Apaf-1 cell death family member that activates NF-kappaB. *J Biol Chem* **274**: 12955-8.

Bertrand, M.J., Kenchappa, R.S., Andrieu, D., Leclercq-Smekens, M., Nguyen, H.N., Carter, B.D., Muscatelli, F., Barker, P.A. and De Backer, O. (2008). NRAGE, a p75NTR adaptor protein, is required for developmental apoptosis in vivo. *Cell Death Differ* **15**: 1921-9.

Bianchi, M.E. (2007). DAMPs, PAMPs and alarmins: all we need to know about danger. *J Leukoc Biol* **81**: 1-5.

Brunner, M., Krenn, C., Roth, G., Moser, B., Dworschak, M., Jensen-Jarolim, E., Spittler, A., Sautner, T., Bonaros, N., Wolner, E., Boltz-Nitulescu, G. and Ankersmit, H.J. (2004). Increased levels of soluble ST2 protein and IgG1 production in patients with sepsis and trauma. *Intensive Care Med* **30**: 1468-73.

Buratti, E., Brindisi, A., Giombi, M., Tisminetzky, S., Ayala, Y.M. and Baralle, F.E. (2005). TDP-43 binds heterogeneous nuclear ribonucleoprotein A/B through its C-terminal tail: an important region for the inhibition of cystic fibrosis transmembrane conductance regulator exon 9 splicing. *J Biol Chem* **280**: 37572-84.

Buratti, E., Dork, T., Zuccato, E., Pagani, F., Romano, M. and Baralle, F.E. (2001). Nuclear factor TDP-43 and SR proteins promote in vitro and in vivo CFTR exon 9 skipping. *Embo J* **20**: 1774-84.

Burckstummer, T., Baumann, C., Bluml, S., Dixit, E., Durnberger, G., Jahn, H., Planyavsky, M., Bilban, M., Colinge, J., Bennett, K.L. and Superti-Furga, G. (2009). An orthogonal proteomic-genomic screen identifies AIM2 as a cytoplasmic DNA sensor for the inflammasome. *Nat Immunol* **10**: 266-72.

Byun, Y., Chen, F., Chang, R., Trivedi, M., Green, K.J. and Cryns, V.L. (2001). Caspase cleavage of vimentin disrupts intermediate filaments and promotes apoptosis. *Cell Death Differ* **8**: 443-50.

Campos, M.A., Almeida, I.C., Takeuchi, O., Akira, S., Valente, E.P., Procopio, D.O., Travassos, L.R., Smith, J.A., Golenbock, D.T. and Gazzinelli, R.T. (2001). Activation of Toll-like receptor-2 by glycosylphosphatidylinositol anchors from a protozoan parasite. *J Immunol* **167**: 416-23.

Carriere, V., Roussel, L., Ortega, N., Lacorre, D.A., Americh, L., Aguilar, L., Bouche, G. and Girard, J.P. (2007). IL-33, the IL-1-like cytokine ligand for ST2 receptor, is a chromatin-associated nuclear factor in vivo. *Proc Natl Acad Sci U S A* **104**: 282-7.

Cassel, S.L., Eisenbarth, S.C., Iyer, S.S., Sadler, J.J., Colegio, O.R., Tephly, L.A., Carter, A.B., Rothman, P.B., Flavell, R.A. and Sutterwala, F.S. (2008). The Nalp3 inflammasome is essential for the development of silicosis. *Proc Natl Acad Sci U S A* **105**: 9035-40.

Cassel, S.L., Joly, S. and Sutterwala, F.S. (2009). The NLRP3 inflammasome: A sensor of immune danger signals. *Semin Immunol.*

Cayrol, C. and Girard, J.P. (2009). The IL-1-like cytokine IL-33 is inactivated after maturation by caspase-1. *Proc Natl Acad Sci U S A* **106**: 9021-6.

Cerretti, D.P., Kozlosky, C.J., Mosley, B., Nelson, N., Van Ness, K., Greenstreet, T.A., March, C.J., Kronheim, S.R., Druck, T. and Cannizzaro, L.A. (1992). Molecular cloning of the interleukin-1 beta converting enzyme. *Science* **256**: 97-100.

Chackerian, A.A., Oldham, E.R., Murphy, E.E., Schmitz, J., Pflanz, S. and Kastelein, R.A. (2007). IL-1 receptor accessory protein and ST2 comprise the IL-33 receptor complex. *J Immunol* **179**: 2551-5.

Cheng, E.H., Wei, M.C., Weiler, S., Flavell, R.A., Mak, T.W., Lindsten, T. and Korsmeyer, S.J. (2001). BCL-2, BCL-X(L) sequester BH3 domain-only molecules preventing BAX- and BAK-mediated mitochondrial apoptosis. *Mol Cell* **8**: 705-11.

Cherry, W.B., Yoon, J., Bartemes, K.R., Iijima, K. and Kita, H. (2008). A novel IL-1 family cytokine, IL-33, potently activates human eosinophils. *J Allergy Clin Immunol* **121**: 1484-90.

Chinnaiyan, A.M., O'Rourke, K., Tewari, M. and Dixit, V.M. (1995). FADD, a novel death domain-containing protein, interacts with the death domain of Fas and initiates apoptosis. *Cell* **81**: 505-12.

Chipuk, J.E., Fisher, J.C., Dillon, C.P., Kriwacki, R.W., Kuwana, T. and Green, D.R. (2008). Mechanism of apoptosis induction by inhibition of the anti-apoptotic BCL-2 proteins. *Proc Natl Acad Sci U S A* **105**: 20327-32.

Chow, S.C., Slee, E.A., MacFarlane, M. and Cohen, G.M. (1999). Caspase-1 is not involved in CD95/Fas-induced apoptosis in Jurkat T cells. *Exp Cell Res* **246**: 491-500.

Chun, H.J., Zheng, L., Ahmad, M., Wang, J., Speirs, C.K., Siegel, R.M., Dale, J.K., Puck, J., Davis, J., Hall, C.G., Skoda-Smith, S., Atkinson, T.P., Straus, S.E. and Lenardo, M.J. (2002). Pleiotropic defects in lymphocyte activation caused by caspase-8 mutations lead to human immunodeficiency. *Nature* **419**: 395-9.

Clements, K.M., Price, J.S., Chambers, M.G., Visco, D.M., Poole, A.R. and Mason, R.M. (2003). Gene deletion of either interleukin-1beta, interleukin-1beta-converting enzyme, inducible nitric oxide synthase, or stromelysin 1 accelerates the development of knee osteoarthritis in mice after surgical transection of the medial collateral ligament and partial medial meniscectomy. *Arthritis Rheum* **48**: 3452-63.

Cohen, G.M. (1997). Caspases: the executioners of apoptosis. *Biochem J* **326**: 1-16.

Colotta, F., Dower, S.K., Sims, J.E. and Mantovani, A. (1994). The type II 'decoy' receptor: a novel regulatory pathway for interleukin 1. *Immunol Today* **15**: 562-6.

Creagh, E.M., Brumatti, G., Sheridan, C., Duriez, P.J., Taylor, R.C., Cullen, S.P., Adrain, C. and Martin, S.J. (2009). Bicaudal is a conserved substrate for Drosophila and mammalian caspases and is essential for cell survival. *PLoS ONE* **4**: e5055.

Cryns, V.L., Byun, Y., Rana, A., Mellor, H., Lustig, K.D., Ghanem, L., Parker, P.J., Kirschner, M.W. and Yuan, J. (1997). Specific proteolysis of the kinase protein kinase C-related kinase 2 by caspase-3 during apoptosis. Identification by a novel, small pool expression cloning strategy. *J Biol Chem* **272**: 29449-53.

Cullen S.P and Martin S.J. (2008). Mechanisms of granule-dependent killing. *Cell Death Differ* **15**: 251-62.

D'Lima, D., Hermida, J., Hashimoto, S., Colwell, C. and Lotz, M. (2006). Caspase inhibitors reduce severity of cartilage lesions in experimental osteoarthritis. *Arthritis Rheum* **54**: 1814-21.

David, G., Bai, X.M., Van der Schueren, B., Cassiman, J.J. and Van den Berghe, H. (1992). Developmental changes in heparan sulfate expression: in situ detection with mAbs. *J Cell Biol* **119**: 961-75.

Deretic, V., and Levine, B. (2009). Autophagy, immunity, and microbial adaptations. *Cell Host Microbe* **5**:527–549

Dinarello, C.A. (2000). Proinflammatory cytokines. *Chest* **118**: 503-8.

Dix, M.M., Simon, G.M. and Cravatt, B.F. (2008). Global mapping of the topography and magnitude of proteolytic events in apoptosis. *Cell* **134**: 679-91.

Dy, P., Han, Y. and Lefebvre, V. (2008). Generation of mice harboring a Sox5 conditional null allele. *Genesis* **46**: 294-9.

Eckhart, L., Declercq, W., Ban, J., Rendl, M., Lengauer, B., Mayer, C., Lippens, S., Vandenabeele, P. and Tschachler, E. (2000). Terminal differentiation of human keratinocytes and stratum corneum formation is associated with caspase-14 activation. *J Invest Dermatol* **115**: 1148-51.

Ellis, H.M. and Horvitz, H.R. (1986). Genetic control of programmed cell death in the nematode C. elegans. *Cell* **44**: 817-29.

Faucheu, C., Diu, A., Chan, A.W., Blanchet, A.M., Miossec, C., Herve, F., Collard-Dutilleul, V., Gu, Y., Aldape, R.A. and Lippke, J.A. (1995). A novel human protease similar to the interleukin-1 beta converting enzyme induces apoptosis in transfected cells. *Embo J* **14**: 1914-22.

Faustin, B., Lartigue, L., Bruey, J.M., Luciano, F., Sergienko, E., Bailly-Maitre, B., Volkmann, N., Hanein, D., Rouiller, I. and Reed, J.C. (2007). Reconstituted NALP1 inflammasome reveals two-step mechanism of caspase-1 activation. *Mol Cell* **25**: 713-24.

Feng, Q., Li, P., Leung, P.C. and Auersperg, N. (2004). Caspase-1zeta, a new splice variant of the caspase-1 gene. *Genomics* **84**: 587-91.

Fernandes-Alnemri, T., Armstrong, R.C., Krebs, J., Srinivasula, S.M., Wang, L., Bullrich, F., Fritz, L.C., Trapani, J.A., Tomaselli, K.J., Litwack, G. and Alnemri, E.S. (1996). In vitro activation of CPP32 and Mch3 by Mch4, a novel human apoptotic cysteine protease containing two FADD-like domains. *Proc Natl Acad Sci U S A* **93**: 7464-9.

Fernandes-Alnemri, T., Wu, J., Yu, J.W., Datta, P., Miller, B., Jankowski, W., Rosenberg, S., Zhang, J. and Alnemri, E.S. (2007). The pyroptosome: a supramolecular assembly of ASC dimers mediating inflammatory cell death via caspase-1 activation. *Cell Death Differ* **14**: 1590-604.

Fernandes-Alnemri, T., Yu, J.W., Datta, P., Wu, J. and Alnemri, E.S. (2009). AIM2 activates the inflammasome and cell death in response to cytoplasmic DNA. *Nature* **458**: 509-13.

Fiorentino, L., Stehlik, C., Oliveira, V., Ariza, M.E., Godzik, A. and Reed, J.C. (2002). A novel PAAD-containing protein that modulates NF-kappa B induction by cytokines tumor necrosis factor-alpha and interleukin-1beta. *J Biol Chem* **277**: 35333-40.

Fischer, H., Koenig, U., Eckhart, L. and Tschachler, E. (2002). Human caspase 12 has acquired deleterious mutations. *Biochem Biophys Res Commun* **293**: 722-6.

Ghayur, T., Banerjee, S., Hugunin, M., Butler, D., Herzog, L., Carter, A., Quintal, L., Sekut, L., Talanian, R., Paskind, M., Wong, W., Kamen, R., Tracey, D. and Allen, H. (1997). Caspase-1 processes IFN-gamma-inducing factor and regulates LPS-induced IFN-gamma production. *Nature* **386**: 619-23.

Girardin, S.E., Travassos, L.H., Herve, M., Blanot, D., Boneca, I.G., Philpott, D.J., Sansonetti, P.J. and Mengin-Lecreulx, D. (2003). Peptidoglycan molecular requirements allowing detection by Nod1 and Nod2. *J Biol Chem* **278**: 41702-8.

Gu, Y., Kuida, K., Tsutsui, H., Ku, G., Hsiao, K., Fleming, M.A., Hayashi, N., Higashino, K., Okamura, H., Nakanishi, K., Kurimoto, M., Tanimoto, T., Flavell, R.A., Sato, V., Harding, M.W., Livingston, D.J. and Su, M.S. (1997). Activation of interferon-gamma inducing factor mediated by interleukin-1beta converting enzyme. *Science* **275**: 206-9.

Guegan, C., Vila, M., Teismann, P., Chen, C., Onteniente, B., Li, M., Friedlander, R.M. and Przedborski, S. (2002). Instrumental activation of bid by caspase-1 in a transgenic mouse model of ALS. *Mol Cell Neurosci* **20**: 553-62.

Hakem, R., Hakem, A., Duncan, G.S., Henderson, J.T., Woo, M., Soengas, M.S., Elia, A., de la Pompa, J.L., Kagi, D., Khoo, W., Potter, J., Yoshida, R., Kaufman,

S.A., Lowe, S.W., Penninger, J.M. and Mak, T.W. (1998). Differential requirement for caspase 9 in apoptotic pathways in vivo. *Cell* **94**: 339-52.

Hall, P.A., Coates, P.J., Ansari, B. and Hopwood, D. (1994). Regulation of cell number in the mammalian gastrointestinal tract: the importance of apoptosis. *J Cell Sci* **107**: 3569-77.

Halle, A., Hornung, V., Petzold, G.C., Stewart, C.R., Monks, B.G., Reinheckel, T., Fitzgerald, K.A., Latz, E., Moore, K.J. and Golenbock, D.T. (2008). The NALP3 inflammasome is involved in the innate immune response to amyloid-beta. *Nat Immunol* **9**: 857-65.

Haushalter, K.A., Todd Stukenberg, M.W., Kirschner, M.W. and Verdine, G.L. (1999). Identification of a new uracil-DNA glycosylase family by expression cloning using synthetic inhibitors. *Curr Biol* **9**: 174-85.

Hawkins, C.J., Uren, A.G., Hacker, G., Medcalf, R.L. and Vaux, D.L. (1996). Inhibition of interleukin 1 beta-converting enzyme-mediated apoptosis of mammalian cells by baculovirus IAP. *Proc Natl Acad Sci U S A* **93**: 13786-90.

Hayakawa, H., Hayakawa, M., Kume, A. and Tominaga, S. (2007). Soluble ST2 blocks interleukin-33 signaling in allergic airway inflammation. *J Biol Chem* **282**: 26369-80.

Heil, F., Hemmi, H., Hochrein, H., Ampenberger, F., Kirschning, C., Akira, S., Lipford, G., Wagner, H. and Bauer, S. (2004). Species-specific recognition of single-stranded RNA via toll-like receptor 7 and 8. *Science* **303**: 1526-9.

Helfer, B., Boswell, B.C., Finlay, D., Cipres, A., Vuori, K., Bong Kang, T., Wallach, D., Dorfleutner, A., Lahti, J.M., Flynn, D.C. and Frisch, S.M. (2006). Caspase-8 promotes cell motility and calpain activity under nonapoptotic conditions. *Cancer Res* **66**: 4273-8.

Ho, L.H., Taylor, R., Dorstyn, L., Cakouros, D., Bouillet, P. and Kumar, S. (2009). A tumor suppressor function for caspase-2. *Proc Natl Acad Sci U S A* **106**: 5336-41.

Hoffman, H.M., Mueller, J.L., Broide, D.H., Wanderer, A.A. and Kolodner, R.D. (2001). Mutation of a new gene encoding a putative pyrin-like protein causes familial cold autoinflammatory syndrome and Muckle-Wells syndrome. *Nat Genet* **29**: 301-5.

Hornung, V., Ablasser, A., Charrel-Dennis, M., Bauernfeind, F., Horvath, G., Caffrey, D.R., Latz, E. and Fitzgerald, K.A. (2009). AIM2 recognizes cytosolic dsDNA and forms a caspase-1-activating inflammasome with ASC. *Nature* **458**: 514-8.

Hornung, V., Bauernfeind, F., Halle, A., Samstad, E.O., Kono, H., Rock, K.L., Fitzgerald, K.A. and Latz, E. (2008). Silica crystals and aluminum salts activate the NALP3 inflammasome through phagosomal destabilization. *Nat Immunol* **9**: 847-56.

Hsieh, S.Y., Hsieh, P.S., Chiu, C.T. and Chen, W.Y. (2004). Dickkopf-3/REIC functions as a suppressor gene of tumor growth. *Oncogene* **23**: 9183-9.

Ichinohe, T., Lee, H.K., Ogura, Y., Flavell, R. and Iwasaki, A. (2009). Inflammasome recognition of influenza virus is essential for adaptive immune responses. *J Exp Med* **206**: 79-87.

Inohara, N., Koseki, T., del Peso, L., Hu, Y., Yee, C., Chen, S., Carrio, R., Merino, J., Liu, D., Ni, J. and Nunez, G. (1999). Nod1, an Apaf-1-like activator of caspase-9 and nuclear factor-kappaB. *J Biol Chem* **274**: 14560-7.

Inoue, S., Browne, G., Melino, G. and Cohen, G.M. (2009). Ordering of caspases in cells undergoing apoptosis by the intrinsic pathway. *Cell Death Differ* **16**: 1053-61.

Janeway, C.A., Jr. and Medzhitov, R. (1998). Introduction: the role of innate immunity in the adaptive immune response. *Semin Immunol* **10**: 349-50.

Jin, Y., Mailloux, C.M., Gowan, K., Riccardi, S.L., LaBerge, G., Bennett, D.C., Fain, P.R. and Spritz, R.A. (2007). NALP1 in vitiligo-associated multiple autoimmune disease. *N Engl J Med* **356**: 1216-25.

Jordan, B.W., Dinev, D., LeMellay, V., Troppmair, J., Gotz, R., Wixler, L., Sendtner, M., Ludwig, S. and Rapp, U.R. (2001). Neurotrophin receptor-interacting mage homologue is an inducible inhibitor of apoptosis protein-interacting protein that augments cell death. *J Biol Chem* **276**: 39985-9.

Jung, Y., Miura, M. and Yuan, J. (1996). Suppression of interleukin-1 beta-converting enzyme-mediated cell death by insulin-like growth factor. *J Biol Chem* **271**: 5112-7.

Kahns, S., Kalai, M., Jakobsen, L.D., Clark, B.F., Vandenabeele, P. and Jensen, P.H. (2003). Caspase-1 and caspase-8 cleave and inactivate cellular parkin. *J Biol Chem* **278**: 23376-80.

Kalai, M., Lamkanfi, M., Denecker, G., Boogmans, M., Lippens, S., Meeus, A., Declercq, W. and Vandenabeele, P. (2003). Regulation of the expression and processing of caspase-12. *J Cell Biol* **162**: 457-67.

Kang, T.B., Ben-Moshe, T., Varfolomeev, E.E., Pewzner-Jung, Y., Yogev, N., Jurewicz, A., Waisman, A., Brenner, O., Haffner, R., Gustafsson, E., Ramakrishnan, P., Lapidot, T. and Wallach, D. (2004). Caspase-8 serves both apoptotic and nonapoptotic roles. *J Immunol* **173**: 2976-84.

Kaplan, D.R. and Miller, F.D. (2000). Neurotrophin signal transduction in the nervous system. *Curr Opin Neurobiol* **10**: 381-91.

Kayalar, C., Ord, T., Testa, M.P., Zhong, L.T. and Bredesen, D.E. (1996). Cleavage of actin by interleukin 1 beta-converting enzyme to reverse DNase I inhibition. *Proc Natl Acad Sci U S A* **93**: 2234-8.

Kazama, H., Ricci, J.E., Herndon, J.M., Hoppe, G., Green, D.R. and Ferguson, T.A. (2008). Induction of immunological tolerance by apoptotic cells requires caspase-dependent oxidation of high-mobility group box-1 protein. *Immunity* **29**: 21-32.

Kerr, J.F., Wyllie, A.H. and Currie, A.R. (1972). Apoptosis: a basic biological phenomenon with wide-ranging implications in tissue kinetics. *Br J Cancer* **26**: 239-57.

Kischkel, F.C., Hellbardt, S., Behrmann, I., Germer, M., Pawlita, M., Krammer, P.H. and Peter, M.E. (1995). Cytotoxicity-dependent APO-1 (Fas/CD95)-associated proteins form a death-inducing signaling complex (DISC) with the receptor. *Embo J* **14**: 5579-88.

Kondo, S., Barna, B.P., Morimura, T., Takeuchi, J., Yuan, J., Akbasak, A. and Barnett, G.H. (1995). Interleukin-1 beta-converting enzyme mediates cisplatin-induced apoptosis in malignant glioma cells. *Cancer Res* **55**: 6166-71.

Kostura, M.J., Tocci, M.J., Limjuco, G., Chin, J., Cameron, P., Hillman, A.G., Chartrain, N.A. and Schmidt, J.A. (1989). Identification of a monocyte specific pre-interleukin 1 beta convertase activity. *Proc Natl Acad Sci U S A* **86**: 5227-31.

Kroemer, G. and Martin, S.J. (2005). Caspase-independent cell death. *Nat Med* **11**: 725-30.

Kuchler, A.M., Pollheimer, J., Balogh, J., Sponheim, J., Manley, L., Sorensen, D.R., De Angelis, P.M., Scott, H. and Haraldsen, G. (2008). Nuclear interleukin-33 is generally expressed in resting endothelium but rapidly lost upon angiogenic or proinflammatory activation. *Am J Pathol* **173**: 1229-42.

Kudo, S., Mizuno, K., Hirai, Y. and Shimizu, T. (1990). Clearance and tissue distribution of recombinant human interleukin 1 beta in rats. *Cancer Res* **50**: 5751-5.

Kuida, K., Haydar, T.F., Kuan, C.Y., Gu, Y., Taya, C., Karasuyama, H., Su, M.S., Rakic, P. and Flavell, R.A. (1998). Reduced apoptosis and cytochrome c-mediated caspase activation in mice lacking caspase 9. *Cell* **94**: 325-37.

Kuida, K., Lippke, J.A., Ku, G., Harding, M.W., Livingston, D.J., Su, M.S. and Flavell, R.A. (1995). Altered cytokine export and apoptosis in mice deficient in interleukin-1 beta converting enzyme. *Science* **267**: 2000-3.

Kuida, K., Zheng, T.S., Na, S., Kuan, C., Yang, D., Karasuyama, H., Rakic, P. and Flavell, R.A. (1996). Decreased apoptosis in the brain and premature lethality in CPP32-deficient mice. *Nature* **384**: 368-72.

Kuroiwa, K., Arai, T., Okazaki, H., Minota, S. and Tominaga, S. (2001). Identification of human ST2 protein in the sera of patients with autoimmune diseases. *Biochem Biophys Res Commun* **284**: 1104-8.

Lakhani S.A., Masud A., Kuida K., Porter G.A. Jr, Booth C.J., Mehal W.Z., Inayat I., Flavell R.A. (2006) Caspases 3 and 7: key mediators of mitochondrial events of apoptosis. *Science* **311**: 847-51.

Lamkanfi, M., Declercq, W., Kalai, M., Saelens, X. and Vandenabeele, P. (2002). Alice in caspase land. A phylogenetic analysis of caspases from worm to man. *Cell Death Differ* **9**: 358-61.

Lamkanfi, M., Kanneganti, T.D., Van Damme, P., Vanden Berghe, T., Vanoverberghe, I., Vandekerckhove, J., Vandenabeele, P., Gevaert, K. and Nunez, G. (2008). Targeted peptidecentric proteomics reveals caspase-7 as a substrate of the caspase-1 inflammasomes. *Mol Cell Proteomics* **7**: 2350-63.

Lamkanfi, M., Moreira, L.O., Makena, P., Spierings, D.C., Boyd, K., Murray, P.J., Green, D.R. and Kanneganti, T.D. (2009). Caspase-7 deficiency protects from endotoxin-induced lymphocyte apoptosis and improves survival. *Blood* **113**: 2742-5.

Lazebnik, Y.A., Kaufmann, S.H., Desnoyers, S., Poirier, G.G. and Earnshaw, W.C. (1994). Cleavage of poly(ADP-ribose) polymerase by a proteinase with properties like ICE. *Nature* **371**: 346-7.

Lefebvre, V., Li, P. and de Crombrugghe, B. (1998). A new long form of Sox5 (L-Sox5), Sox6 and Sox9 are coexpressed in chondrogenesis and cooperatively activate the type II collagen gene. *Embo J* **17**: 5718-33.

Lemaitre, B., Nicolas, E., Michaut, L., Reichhart, J.M. and Hoffmann, J.A. (1996). The dorsoventral regulatory gene cassette spatzle/Toll/cactus controls the potent antifungal response in Drosophila adults. *Cell* **86**: 973-83.

Leonard, J.R., Klocke, B.J., D'Sa, C., Flavell, R.A. and Roth, K.A. (2002). Strain-dependent neurodevelopmental abnormalities in caspase-3-deficient mice. *J Neuropathol Exp Neurol* **61**: 673-7.

Leung, B.P., Xu, D., Culshaw, S., McInnes, I.B. and Liew, F.Y. (2004). A novel therapy of murine collagen-induced arthritis with soluble T1/ST2. *J Immunol* **173**: 145-50.

Li, P., Allen, H., Banerjee, S., Franklin, S., Herzog, L., Johnston, C., McDowell, J., Paskind, M., Rodman, L. and Salfeld, J. (1995). Mice deficient in IL-1 beta-converting enzyme are defective in production of mature IL-1 beta and resistant to endotoxic shock. *Cell* **80**: 401-11.

Lin, X.Y., Choi, M.S. and Porter, A.G. (2000). Expression analysis of the human caspase-1 subfamily reveals specific regulation of the CASP5 gene by lipopolysaccharide and interferon-gamma. *J Biol Chem* **275**: 39920-6.

Liu, X., Kim, C.N., Yang, J., Jemmerson, R. and Wang, X. (1996). Induction of apoptotic program in cell-free extracts: requirement for dATP and cytochrome c. *Cell* **86**: 147-57.

Luo, X., Budihardjo, I., Zou, H., Slaughter, C. and Wang, X. (1998). Bid, a Bcl2 interacting protein, mediates cytochrome c release from mitochondria in response to activation of cell surface death receptors. *Cell* **94**: 481-90.

Lustig, K.D., Stukenberg, P.T., McGarry, T.J., King, R.W., Cryns, V.L., Mead, P.E., Zon, L.I., Yuan, J. and Kirschner, M.W. (1997). Small pool expression screening: identification of genes involved in cell cycle control, apoptosis, and early development. *Methods Enzymol* **283**: 83-99.

Lüthi, A.U., Cullen, S.P., McNeela, E.A., Duriez, P.J., Afonina, I.S., Sheridan, C., Brumatti, G., Taylor, R.C., Kersse, K., Vandenabeele, P., Lavelle, E.C. and Martin, S.J. (2009). Suppression of interleukin-33 bioactivity through proteolysis by apoptotic caspases. *Immunity* **31**: 84-98.

Lüthi, A.U. and Martin, S.J. (2007). The CASBAH: a searchable database of caspase substrates. *Cell Death Differ* **14**: 641-50.

Mahrus, S., Trinidad, J.C., Barkan, D.T., Sali, A., Burlingame, A.L. and Wells, J.A. (2008). Global sequencing of proteolytic cleavage sites in apoptosis by specific labeling of protein N termini. *Cell* **134**: 866-76.

Maier, J.A., Statuto, M. and Ragnotti, G. (1994). Endogenous interleukin 1 alpha must be transported to the nucleus to exert its activity in human endothelial cells. *Mol Cell Biol* **14**: 1845-51.

Malinowski, J.J., Grasberger, B.L., Trakshel, G., Huston, E.E., Helaszek, C.T., Smallwood, A.M., Ator, M.A., Banks, T.M., Brake, P.G., Ciccarelli, R.B. and et al. (1995). Production, purification, and crystallization of human interleukin-1 beta converting enzyme derived from an Escherichia coli expression system. *Protein Sci* **4**: 2149-55.

Marco, A., Cuesta, A., Pedrola, L., Palau, F. and Marin, I. (2004). Evolutionary and structural analyses of GDAP1, involved in Charcot-Marie-Tooth disease, characterize a novel class of glutathione transferase-related genes. *Mol Biol Evol* **21**: 176-87.

Mariathasan, S., Newton, K., Monack, D.M., Vucic, D., French, D.M., Lee, W.P., Roose-Girma, M., Erickson, S. and Dixit, V.M. (2004). Differential activation of the inflammasome by caspase-1 adaptors ASC and Ipaf. *Nature* **430**: 213-8.

Marina-Garcia, N., Franchi, L., Kim, Y.G., Miller, D., McDonald, C., Boons, G.J. and Nunez, G. (2008). Pannexin-1-mediated intracellular delivery of muramyl dipeptide induces caspase-1 activation via cryopyrin/NLRP3 independently of Nod2. *J Immunol* **180**: 4050-7.

Martin, S.J., Amarante-Mendes, G.P., Shi, L., Chuang, T.H., Casiano, C.A., O'Brien, G.A., Fitzgerald, P., Tan, E.M., Bokoch, G.M., Greenberg, A.H. and Green, D.R. (1996). The cytotoxic cell protease granzyme B initiates apoptosis in a cell-free system by proteolytic processing and activation of the ICE/CED-3 family protease, CPP32, via a novel two-step mechanism. *Embo J* **15**: 2407-16.

Martin, S.J., Newmeyer, D.D., Mathias, S., Farschon, D.M., Wang, H.G., Reed, J.C., Kolesnick, R.N. and Green, D.R. (1995). Cell-free reconstitution of Fas-, UV radiation- and ceramide-induced apoptosis. *Embo J* **14**: 5191-200.

Martinon, F., Burns, K. and Tschopp, J. (2002). The inflammasome: a molecular platform triggering activation of inflammatory caspases and processing of proIL-beta. *Mol Cell* **10**: 417-26.

Martinon, F., Gaide, O., Petrilli, V., Mayor, A. and Tschopp, J. (2007). NALP inflammasomes: a central role in innate immunity. *Semin Immunopathol* **29**: 213-29.

Martinon, F., Petrilli, V., Mayor, A., Tardivel, A. and Tschopp, J. (2006). Gout-associated uric acid crystals activate the NALP3 inflammasome. *Nature* **440**: 237-41.

Martinon, F. and Tschopp, J. (2007). Inflammatory caspases and inflammasomes: master switches of inflammation. *Cell Death Differ* **14**: 10-22.

Masu, Y., Nakayama, K., Tamaki, H., Harada, Y., Kuno, M. and Nakanishi, S. (1987). cDNA cloning of bovine substance-K receptor through oocyte expression system. *Nature* **329**: 836-8.

Masuda, Y., Sasaki, A., Shibuya, H., Ueno, N., Ikeda, K. and Watanabe, K. (2001). Dlxin-1, a novel protein that binds Dlx5 and regulates its transcriptional function. *J Biol Chem* **276**: 5331-8.

Matzinger, P. (1994). Immunology. Memories are made of this? *Nature* **369**: 605-6.

McCarthy, J.V., Ni, J. and Dixit, V.M. (1998). RIP2 is a novel NF-kappaB-activating and cell death-inducing kinase. *J Biol Chem* **273**: 16968-75.

McStay, G.P., Salvesen, G.S. and Green, D.R. (2008). Overlapping cleavage motif selectivity of caspases: implications for analysis of apoptotic pathways. *Cell Death Differ* **15**: 322-31.

Medzhitov, R., Preston-Hurlburt, P. and Janeway, C.A., Jr. (1997). A human homologue of the Drosophila Toll protein signals activation of adaptive immunity. *Nature* **388**: 394-7.

Meier, A., Kirschning, C.J., Nikolaus, T., Wagner, H., Heesemann, J. and Ebel, F. (2003). Toll-like receptor (TLR) 2 and TLR4 are essential for Aspergillus-induced activation of murine macrophages. *Cell Microbiol* **5**: 561-70.

Meinl, E., Fickenscher, H., Thome, M., Tschopp, J. and Fleckenstein, B. (1998). Anti-apoptotic strategies of lymphotropic viruses. *Immunol Today* **19**: 474-9.

Miceli-Richard, C., Lesage, S., Rybojad, M., Prieur, A.M., Manouvrier-Hanu, S., Hafner, R., Chamaillard, M., Zouali, H., Thomas, G. and Hugot, J.P. (2001). CARD15 mutations in Blau syndrome. *Nat Genet* **29**: 19-20.

Miller, A.M., Xu, D., Asquith, D.L., Denby, L., Li, Y., Sattar, N., Baker, A.H., McInnes, I.B. and Liew, F.Y. (2008). IL-33 reduces the development of atherosclerosis. *J Exp Med* **205**: 339-46.

Miura, M., Zhu, H., Rotello, R., Hartwieg, E.A. and Yuan, J. (1993). Induction of apoptosis in fibroblasts by IL-1 beta-converting enzyme, a mammalian homolog of the C. elegans cell death gene ced-3. *Cell* **75**: 653-60.

Mosley, B., Dower, S.K., Gillis, S. and Cosman, D. (1987). Determination of the minimum polypeptide lengths of the functionally active sites of human interleukins 1 alpha and 1 beta. *Proc Natl Acad Sci U S A* **84**: 4572-6.

Mosley, B., Urdal, D.L., Prickett, K.S., Larsen, A., Cosman, D., Conlon, P.J., Gillis, S. and Dower, S.K. (1987). The interleukin-1 receptor binds the human interleukin-1 alpha precursor but not the interleukin-1 beta precursor. *J Biol Chem* **262**: 2941-4.

Moussion, C., Ortega, N. and Girard, J.P. (2008). The IL-1-like cytokine IL-33 is constitutively expressed in the nucleus of endothelial cells and epithelial cells in vivo: a novel 'alarmin'? *PLoS ONE* **3**: e3331.

Murphy, B.M., O'Neill, A.J., Adrain, C., Watson, R.W. and Martin, S.J. (2003). The apoptosome pathway to caspase activation in primary human neutrophils exhibits dramatically reduced requirements for cytochrome C. *J Exp Med* **197**: 625-32.

Nagata, S. (1997). Apoptosis by death factor. *Cell* **88**: 355-65.

Nagata, S. (1999). Fas ligand-induced apoptosis. *Annu Rev Genet* **33**: 29-55.

Nakagawa, T., Zhu, H., Morishima, N., Li, E., Xu, J., Yankner, B.A. and Yuan, J. (2000). Caspase-12 mediates endoplasmic-reticulum-specific apoptosis and cytotoxicity by amyloid-beta. *Nature* **403**: 98-103.

Neumann, M., Sampathu, D.M., Kwong, L.K., Truax, A.C., Micsenyi, M.C., Chou, T.T., Bruce, J., Schuck, T., Grossman, M., Clark, C.M., McCluskey, L.F., Miller, B.L., Masliah, E., Mackenzie, I.R., Feldman, H., Feiden, W., Kretzschmar, H.A., Trojanowski, J.Q. and Lee, V.M. (2006). Ubiquitinated TDP-43 in frontotemporal lobar degeneration and amyotrophic lateral sclerosis. *Science* **314**: 130-3.

Newmeyer, D.D., Farschon, D.M. and Reed, J.C. (1994). Cell-free apoptosis in Xenopus egg extracts: inhibition by Bcl-2 and requirement for an organelle fraction enriched in mitochondria. *Cell* **79**: 353-64.

Nicholson, D.W. (1999). Caspase structure, proteolytic substrates, and function during apoptotic cell death. *Cell Death Differ* **6**: 1028-42.

Nikolaev A., McLaughlin T., O'Leary D., Tessier-Lavigne M. (2009) N-APP binds DR6 to cause axon pruning and neuronal death via distinct caspases. *Nature* **457**: 981-9

Niemann, A., Ruegg, M., La Padula, V., Schenone, A. and Suter, U. (2005). Ganglioside-induced differentiation associated protein 1 is a regulator of the mitochondrial network: new implications for Charcot-Marie-Tooth disease. *J Cell Biol* **170**: 1067-78.

Ogura, Y., Inohara, N., Benito, A., Chen, F.F., Yamaoka, S. and Nunez, G. (2001). Nod2, a Nod1/Apaf-1 family member that is restricted to monocytes and activates NF-kappaB. *J Biol Chem* **276**: 4812-8.

Onda, H., Kasuya, H., Takakura, K., Hori, T., Imaizumi, T., Takeuchi, T., Inoue, I. and Takeda, J. (1999). Identification of genes differentially expressed in canine

vasospastic cerebral arteries after subarachnoid hemorrhage. *J Cereb Blood Flow Metab* **19**: 1279-88.

Oppenheim, J.J. and Yang, D. (2005). Alarmins: chemotactic activators of immune responses. *Curr Opin Immunol* **17**: 359-65.

Oprica, M., Eriksson, C. and Schultzberg, M. (2003). Inflammatory mechanisms associated with brain damage induced by kainic acid with special reference to the interleukin-1 system. *J Cell Mol Med* **7**: 127-40.

Oshikawa, K., Kuroiwa, K., Tago, K., Iwahana, H., Yanagisawa, K., Ohno, S., Tominaga, S.I. and Sugiyama, Y. (2001). Elevated soluble ST2 protein levels in sera of patients with asthma with an acute exacerbation. *Am J Respir Crit Care Med* **164**: 277-81.

Ou, S.H., Wu, F., Harrich, D., Garcia-Martinez, L.F. and Gaynor, R.B. (1995). Cloning and characterization of a novel cellular protein, TDP-43, that binds to human immunodeficiency virus type 1 TAR DNA sequence motifs. *J Virol* **69**: 3584-96.

Parikh, S.S., Litherland, S.A., Clare-Salzler, M.J., Li, W., Gulig, P.A. and Southwick, F.S. (2003). CapG(-/-) mice have specific host defense defects that render them more susceptible than CapG(+/+) mice to Listeria monocytogenes infection but not to Salmonella enterica serovar Typhimurium infection. *Infect Immun* **71**: 6582-90.

Park, B.S., Song, D.H., Kim, H.M., Choi, B.S., Lee, H. and Lee, J.O. (2009). The structural basis of lipopolysaccharide recognition by the TLR4-MD-2 complex. *Nature* **458**: 1191-5.

Park, H.H., Logette, E., Raunser, S., Cuenin, S., Walz, T., Tschopp, J. and Wu, H. (2007). Death domain assembly mechanism revealed by crystal structure of the oligomeric PIDDosome core complex. *Cell* **128**: 533-46.

Patel, V.A., Longacre-Antoni, A., Cvetanovic, M., Lee, D.J., Feng, L., Fan, H., Rauch, J., Ucker, D.S. and Levine, J.S. (2007). The affirmative response of the innate immune system to apoptotic cells. *Autoimmunity* **40**: 274-80.

Petrilli, V., Papin, S., Dostert, C., Mayor, A., Martinon, F. and Tschopp, J. (2007). Activation of the NALP3 inflammasome is triggered by low intracellular potassium concentration. *Cell Death Differ* **14**: 1583-9.

Poltorak, A., He, X., Smirnova, I., Liu, M.Y., Van Huffel, C., Du, X., Birdwell, D., Alejos, E., Silva, M., Galanos, C., Freudenberg, M., Ricciardi-Castagnoli, P., Layton, B. and Beutler, B. (1998). Defective LPS signaling in C3H/HeJ and C57BL/10ScCr mice: mutations in Tlr4 gene. *Science* **282**: 2085-8.

Poyet, J.L., Srinivasula, S.M., Tnani, M., Razmara, M., Fernandes-Alnemri, T. and Alnemri, E.S. (2001). Identification of Ipaf, a human caspase-1-activating protein related to Apaf-1. *J Biol Chem* **276**: 28309-13.

Pridgeon, J.W., Geetha, T. and Wooten, M.W. (2003). A Method to Identify p62's UBA Domain Interacting Proteins. *Biol Proced Online* **5**: 228-237.

Ramage, P., Cheneval, D., Chvei, M., Graff, P., Hemmig, R., Heng, R., Kocher, H.P., Mackenzie, A., Memmert, K., Revesz, L. and et al. (1995). Expression, refolding, and autocatalytic proteolytic processing of the interleukin-1 beta-converting enzyme precursor. *J Biol Chem* **270**: 9378-83.

Randow, F., Syrbe, U., Meisel, C., Krausch, D., Zuckermann, H., Platzer, C. and Volk, H.D. (1995). Mechanism of endotoxin desensitization: involvement of interleukin 10 and transforming growth factor beta. *J Exp Med* **181**: 1887-92.

Rao, L., Perez, D. and White, E. (1996). Lamin proteolysis facilitates nuclear events during apoptosis. *J Cell Biol* **135**: 1441-55.

Rao, R.V., Peel, A., Logvinova, A., del Rio, G., Hermel, E., Yokota, T., Goldsmith, P.C., Ellerby, L.M., Ellerby, H.M. and Bredesen, D.E. (2002). Coupling

endoplasmic reticulum stress to the cell death program: role of the ER chaperone GRP78. *FEBS Lett* **514**: 122-8.

Rao, V.R., Corradetti, M.N., Chen, J., Peng, J., Yuan, J., Prestwich, G.D. and Brugge, J.S. (1999). Expression cloning of protein targets for 3-phosphorylated phosphoinositides. *J Biol Chem* **274**: 37893-900.

Read, S.H., Baliga, B.C., Ekert, P.G., Vaux, D.L. and Kumar, S. (2002). A novel Apaf-1-independent putative caspase-2 activation complex. *J Cell Biol* **159**: 739-45.

Rebe, C., Cathelin, S., Launay, S., Filomenko, R., Prevotat, L., L'Ollivier, C., Gyan, E., Micheau, O., Grant, S., Dubart-Kupperschmitt, A., Fontenay, M. and Solary, E. (2007). Caspase-8 prevents sustained activation of NF-kappaB in monocytes undergoing macrophagic differentiation. *Blood* **109**: 1442-50.

Ricci, J.E., Munoz-Pinedo, C., Fitzgerald, P., Bailly-Maitre, B., Perkins, G.A., Yadava, N., Scheffler, I.E., Ellisman, M.H. and Green, D.R. (2004). Disruption of mitochondrial function during apoptosis is mediated by caspase cleavage of the p75 subunit of complex I of the electron transport chain. *Cell* **117**: 773-86.

Rocha, C.S., Santos, A.A., Machado, J.P. and Fontes, E.P. (2008). The ribosomal protein L10/QM-like protein is a component of the NIK-mediated antiviral signaling. *Virology* **380**: 165-9.

Rodriguez, I., Matsuura, K., Ody, C., Nagata, S. and Vassalli, P. (1996). Systemic injection of a tripeptide inhibits the intracellular activation of CPP32-like proteases in vivo and fully protects mice against Fas-mediated fulminant liver destruction and death. *J Exp Med* **184**: 2067-72.

Ruchaud, S., Korfali, N., Villa, P., Kottke, T.J., Dingwall, C., Kaufmann, S.H. and Earnshaw, W.C. (2002). Caspase-6 gene disruption reveals a requirement for lamin A cleavage in apoptotic chromatin condensation. *Embo J* **21**: 1967-77.

Rudel, T. and Bokoch, G.M. (1997). Membrane and morphological changes in apoptotic cells regulated by caspase-mediated activation of PAK2. *Science* **276**: 1571-4.

Saitoh, S., Akashi, S., Yamada, T., Tanimura, N., Matsumoto, F., Fukase, K., Kusumoto, S., Kosugi, A. and Miyake, K. (2004). Ligand-dependent Toll-like receptor 4 (TLR4)-oligomerization is directly linked with TLR4-signaling. *J Endotoxin Res* **10**: 257-60.

Saleh, M., Mathison, J.C., Wolinski, M.K., Bensinger, S.J., Fitzgerald, P., Droin, N., Ulevitch, R.J., Green, D.R. and Nicholson, D.W. (2006). Enhanced bacterial clearance and sepsis resistance in caspase-12-deficient mice. *Nature* **440**: 1064-8.

Saleh, M., Vaillancourt, J.P., Graham, R.K., Huyck, M., Srinivasula, S.M., Alnemri, E.S., Steinberg, M.H., Nolan, V., Baldwin, C.T., Hotchkiss, R.S., Buchman, T.G., Zehnbauer, B.A., Hayden, M.R., Farrer, L.A., Roy, S. and Nicholson, D.W. (2004). Differential modulation of endotoxin responsiveness by human caspase-12 polymorphisms. *Nature* **429**: 75-9.

Salehi, A.H., Roux, P.P., Kubu, C.J., Zeindler, C., Bhakar, A., Tannis, L.L., Verdi, J.M. and Barker, P.A. (2000). NRAGE, a novel MAGE protein, interacts with the p75 neurotrophin receptor and facilitates nerve growth factor-dependent apoptosis. *Neuron* **27**: 279-88.

Salehi, A.H., Xanthoudakis, S. and Barker, P.A. (2002). NRAGE, a p75 neurotrophin receptor-interacting protein, induces caspase activation and cell death through a JNK-dependent mitochondrial pathway. *J Biol Chem* **277**: 48043-50.

Salvesen, G.S. and Dixit, V.M. (1999). Caspase activation: the induced-proximity model. *Proc Natl Acad Sci U S A* **96**: 10964-7.

Sanada, S., Hakuno, D., Higgins, L.J., Schreiter, E.R., McKenzie, A.N. and Lee, R.T. (2007). IL-33 and ST2 comprise a critical biomechanically induced and cardioprotective signaling system. *J Clin Invest* **117**: 1538-49.

Scaffidi, P., Misteli, T. and Bianchi, M.E. (2002). Release of chromatin protein HMGB1 by necrotic cells triggers inflammation. *Nature* **418**: 191-5.

Schmitt, E., Gehrmann, M., Brunet, M., Multhoff, G. and Garrido, C. (2007). Intracellular and extracellular functions of heat shock proteins: repercussions in cancer therapy. *J Leukoc Biol* **81**: 15-27.

Schmitz, J., Owyang, A., Oldham, E., Song, Y., Murphy, E., McClanahan, T.K., Zurawski, G., Moshrefi, M., Qin, J., Li, X., Gorman, D.M., Bazan, J.F. and Kastelein, R.A. (2005). IL-33, an interleukin-1-like cytokine that signals via the IL-1 receptor-related protein ST2 and induces T helper type 2-associated cytokines. *Immunity* **23**: 479-90.

Shao, W., Yeretssian, G., Doiron, K., Hussain, S.N. and Saleh, M. (2007). The caspase-1 digestome identifies the glycolysis pathway as a target during infection and septic shock. *J Biol Chem* **282**: 36321-9.

Shechter, Y., Preciado-Patt, L., Schreiber, G. and Fridkin, M. (2001). Prolonging the half-life of human interferon-alpha 2 in circulation: Design, preparation, and analysis of (2-sulfo-9-fluorenylmethoxycarbonyl)7- interferon-alpha 2. *Proc Natl Acad Sci U S A* **98**: 1212-7.

Shi, M., Vivian, C.J., Lee, K.J., Ge, C., Morotomi-Yano, K., Manzl, C., Bock, F., Sato, S., Tomomori-Sato, C., Zhu, R., Haug, J.S., Swanson, S.K., Washburn, M.P., Chen, D.J., Chen, B.P., Villunger, A., Florens, L. and Du, C. (2009). DNA-PKcs-PIDDosome: a nuclear caspase-2-activating complex with role in G2/M checkpoint maintenance. *Cell* **136**: 508-20.

Shi, Y., Evans, J.E. and Rock, K.L. (2003). Molecular identification of a danger signal that alerts the immune system to dying cells. *Nature* **425**: 516-21.

Shield, A.J., Murray, T.P. and Board, P.G. (2006). Functional characterisation of ganglioside-induced differentiation-associated protein 1 as a glutathione transferase. *Biochem Biophys Res Commun* **347**: 859-66.

Shimpo, M., Morrow, D.A., Weinberg, E.O., Sabatine, M.S., Murphy, S.A., Antman, E.M. and Lee, R.T. (2004). Serum levels of the interleukin-1 receptor family member ST2 predict mortality and clinical outcome in acute myocardial infarction. *Circulation* **109**: 2186-90.

Slee, E.A., Adrain, C. and Martin, S.J. (1999). Serial killers: ordering caspase activation events in apoptosis. *Cell Death Differ* **6**: 1067-74.

Slee, E.A., Adrain, C. and Martin, S.J. (2001). Executioner caspase-3, -6, and -7 perform distinct, non-redundant roles during the demolition phase of apoptosis. *J Biol Chem* **276**: 7320-6.

Slee, E.A., Harte, M.T., Kluck, R.M., Wolf, B.B., Casiano, C.A., Newmeyer, D.D., Wang, H.G., Reed, J.C., Nicholson, D.W., Alnemri, E.S., Green, D.R. and Martin, S.J. (1999). Ordering the cytochrome c-initiated caspase cascade: hierarchical activation of caspases-2, -3, -6, -7, -8, and -10 in a caspase-9-dependent manner. *J Cell Biol* **144**: 281-92.

Smithgall, M.D., Comeau, M.R., Yoon, B.R., Kaufman, D., Armitage, R. and Smith, D.E. (2008). IL-33 amplifies both Th1- and Th2-type responses through its activity on human basophils, allergen-reactive Th2 cells, iNKT and NK cells. *Int Immunol* **20**: 1019-30.

Smits, P., Li, P., Mandel, J., Zhang, Z., Deng, J.M., Behringer, R.R., de Crombrugghe, B. and Lefebvre, V. (2001). The transcription factors L-Sox5 and Sox6 are essential for cartilage formation. *Dev Cell* **1**: 277-90.

Southwick, F.S. and DiNubile, M.J. (1986). Rabbit alveolar macrophages contain a Ca2+-sensitive, 41,000-dalton protein which reversibly blocks the "barbed" ends of actin filaments but does not sever them. *J Biol Chem* **261**: 14191-5.

Sprick, M.R., Rieser, E., Stahl, H., Grosse-Wilde, A., Weigand, M.A., Walczak, H. (2002). Caspase-10 is recruited to and activated at the native TRAIL and CD95 death-inducing signalling complexes in a FADD-dependent manner but can not functionally substitute caspase-8. *EMBO J.* **21** :4520-30.

Sreedharan, J., Blair, I.P., Tripathi, V.B., Hu, X., Vance, C., Rogelj, B., Ackerley, S., Durnall, J.C., Williams, K.L., Buratti, E., Baralle, F., de Belleroche, J., Mitchell, J.D., Leigh, P.N., Al-Chalabi, A., Miller, C.C., Nicholson, G. and Shaw, C.E. (2008). TDP-43 mutations in familial and sporadic amyotrophic lateral sclerosis. *Science* **319**: 1668-72.

Srinivasula, S.M., Ahmad, M., Fernandes-Alnemri, T., Litwack, G. and Alnemri, E.S. (1996). Molecular ordering of the Fas-apoptotic pathway: the Fas/APO-1 protease Mch5 is a CrmA-inhibitable protease that activates multiple Ced-3/ICE-like cysteine proteases. *Proc Natl Acad Sci U S A* **93**: 14486-91.

Stennicke, H.R. and Salvesen, G.S. (1997). Biochemical characteristics of caspases-3, -6, -7, and -8. *J Biol Chem* **272**: 25719-23.

Takeda, K. and Akira, S. (2005). Toll-like receptors in innate immunity. *Int Immunol* **17**: 1-14.

Takeuchi, O., Hoshino, K., Kawai, T., Sanjo, H., Takada, H., Ogawa, T., Takeda, K. and Akira, S. (1999). Differential roles of TLR2 and TLR4 in recognition of gram-negative and gram-positive bacterial cell wall components. *Immunity* **11**: 443-51.

Talabot-Ayer, D., Lamacchia, C., Gabay, C. and Palmer, G. (2009). Interleukin-33 is biologically active independently of caspase-1 cleavage. *J Biol Chem.*

Talanian, R.V., Quinlan, C., Trautz, S., Hackett, M.C., Mankovich, J.A., Banach, D., Ghayur, T., Brady, K.D. and Wong, W.W. (1997). Substrate specificities of caspase family proteases. *J Biol Chem* **272**: 9677-82.

Taylor, R.C., Brumatti, G., Ito, S., Hengartner, M.O., Derry, W.B. and Martin, S.J. (2007). Establishing a blueprint for CED-3-dependent killing through identification of multiple substrates for this protease. *J Biol Chem* **282**: 15011-21.

Taylor, R.C., Cullen, S.P. and Martin, S.J. (2008). Apoptosis: controlled demolition at the cellular level. *Nat Rev Mol Cell Biol* **9**: 231-41.

Thiede, B., Dimmler, C., Siejak, F. and Rudel, T. (2001). Predominant identification of RNA-binding proteins in Fas-induced apoptosis by proteome analysis. *J Biol Chem* **276**: 26044-50.

Thiede, B., Treumann, A., Kretschmer, A., Sohlke, J. and Rudel, T. (2005). Shotgun proteome analysis of protein cleavage in apoptotic cells. *Proteomics* **5**: 2123-30.

Thornberry, N.A., Bull, H.G., Calaycay, J.R., Chapman, K.T., Howard, A.D., Kostura, M.J., Miller, D.K., Molineaux, S.M., Weidner, J.R. and Aunins, J. (1992). A novel heterodimeric cysteine protease is required for interleukin-1 beta processing in monocytes. *Nature* **356**: 768-74.

Thornberry, N.A., Rano, T.A., Peterson, E.P., Rasper, D.M., Timkey, T., Garcia-Calvo, M., Houtzager, V.M., Nordstrom, P.A., Roy, S., Vaillancourt, J.P., Chapman, K.T. and Nicholson, D.W. (1997). A combinatorial approach defines specificities of members of the caspase family and granzyme B. Functional relationships established for key mediators of apoptosis. *J Biol Chem* **272**: 17907-11.

Tinel, A. and Tschopp, J. (2004). The PIDDosome, a protein complex implicated in activation of caspase-2 in response to genotoxic stress. *Science* **304**: 843-6.

Ting, J.P. and Davis, B.K. (2005). CATERPILLER: a novel gene family important in immunity, cell death, and diseases. *Annu Rev Immunol* **23**: 387-414.

Ting, J.P., Kastner, D.L. and Hoffman, H.M. (2006). CATERPILLERs, pyrin and hereditary immunological disorders. *Nat Rev Immunol* **6**: 183-95.

Ting, J.P., Lovering, R.C., Alnemri, E.S., Bertin, J., Boss, J.M., Davis, B.K., Flavell, R.A., Girardin, S.E., Godzik, A., Harton, J.A., Hoffman, H.M., Hugot, J.P., Inohara, N., Mackenzie, A., Maltais, L.J., Nunez, G., Ogura, Y., Otten, L.A., Philpott, D., Reed, J.C., Reith, W., Schreiber, S., Steimle, V. and Ward, P.A. (2008). The NLR gene family: a standard nomenclature. *Immunity* **28**: 285-7.

Tsuchiya, S., Yamabe, M., Yamaguchi, Y., Kobayashi, Y., Konno, T. and Tada, K. (1980). Establishment and characterization of a human acute monocytic leukemia cell line (THP-1). *Int J Cancer* **26**: 171-6.

Tsujimoto, Y. and Shimizu, S. (2005). Another way to die: autophagic programmed cell death. *Cell Death Differ* **12**: 1528-34.

Van Damme, P., Martens, L., Van Damme, J., Hugelier, K., Staes, A., Vandekerckhove, J. and Gevaert, K. (2005). Caspase-specific and nonspecific in vivo protein processing during Fas-induced apoptosis. *Nat Methods* **2**: 771-7.

Voll, R.E., Herrmann, M., Roth, E.A., Stach, C., Kalden, J.R. and Girkontaite, I. (1997). Immunosuppressive effects of apoptotic cells. *Nature* **390**: 350-1.

Wagner, K.M., Ruegg, M., Niemann, A. and Suter, U. (2009). Targeting and function of the mitochondrial fission factor GDAP1 are dependent on its tail-anchor. *PLoS ONE* **4**: e5160.

Walker, N.P., Talanian, R.V., Brady, K.D., Dang, L.C., Bump, N.J., Ferenz, C.R., Franklin, S., Ghayur, T., Hackett, M.C. and Hammill, L.D. (1994). Crystal structure of the cysteine protease interleukin-1 beta-converting enzyme: a (p20/p10)2 homodimer. *Cell* **78**: 343-52.

Walsh, J.G., Cullen, S.P., Sheridan, C., Lüthi, A.U., Gerner, C. and Martin, S.J. (2008). Executioner caspase-3 and caspase-7 are functionally distinct proteases. *Proc Natl Acad Sci U S A* **105**: 12815-9.

Wang, C.Y., Mayo, M.W., Korneluk, R.G., Goeddel, D.V. and Baldwin, A.S., Jr. (1998). NF-kappaB antiapoptosis: induction of TRAF1 and TRAF2 and c-IAP1 and c-IAP2 to suppress caspase-8 activation. *Science* **281**: 1680-3.

Wang, K., Yin, X.M., Chao, D.T., Milliman, C.L. and Korsmeyer, S.J. (1996). BID: a novel BH3 domain-only death agonist. *Genes Dev* **10**: 2859-69.

Wang, S., Miura, M., Jung, Y.K., Zhu, H., Li, E. and Yuan, J. (1998). Murine caspase-11, an ICE-interacting protease, is essential for the activation of ICE. *Cell* **92**: 501-9.

Watanabe, M., Kashiwakura, Y., Huang, P., Ochiai, K., Futami, J., Li, S.A., Takaoka, M., Nasu, Y., Sakaguchi, M., Huh, N.H. and Kumon, H. (2009). Immunological aspects of REIC/Dkk-3 in monocyte differentiation and tumor regression. *Int J Oncol* **34**: 657-63.

Wehrman, T., He, X., Raab, B., Dukipatti, A., Blau, H. and Garcia, K.C. (2007). Structural and mechanistic insights into nerve growth factor interactions with the TrkA and p75 receptors. *Neuron* **53**: 25-38.

Wilson, K.P., Black, J.A., Thomson, J.A., Kim, E.E., Griffith, J.P., Navia, M.A., Murcko, M.A., Chambers, S.P., Aldape, R.A. and Raybuck, S.A. (1994). Structure and mechanism of interleukin-1 beta converting enzyme. *Nature* **370**: 270-5.

Witke, W., Li, W., Kwiatkowski, D.J. and Southwick, F.S. (2001). Comparisons of CapG and gelsolin-null macrophages: demonstration of a unique role for CapG in receptor-mediated ruffling, phagocytosis, and vesicle rocketing. *J Cell Biol* **154**: 775-84.

Wyllie, A.H., Kerr, J.F. and Currie, A.R. (1980). Cell death: the significance of apoptosis. *Int Rev Cytol* **68**: 251-306.

Xu, Y., Tao, X., Shen, B., Horng, T., Medzhitov, R., Manley, J.L. and Tong, L. (2000). Structural basis for signal transduction by the Toll/interleukin-1 receptor domains. *Nature* **408**: 111-5.

Yamin, T.T., Ayala, J.M. and Miller, D.K. (1996). Activation of the native 45-kDa precursor form of interleukin-1-converting enzyme. *J Biol Chem* **271**: 13273-82.

Yeretssian, G., Doiron, K., Shao, W., Leavitt, B.R., Hayden, M.R., Nicholson, D.W. and Saleh, M. (2009). Gender differences in expression of the human caspase-12 long variant determines susceptibility to Listeria monocytogenes infection. *Proc Natl Acad Sci U S A.*

Yokouchi, Y., Sakiyama, J., Kameda, T., Iba, H., Suzuki, A., Ueno, N. and Kuroiwa, A. (1996). BMP-2/-4 mediate programmed cell death in chicken limb buds. *Development* **122**: 3725-34.

Yoon, S.O., Casaccia-Bonnefil, P., Carter, B., Chao, M.V. (1998). Competitive signaling between TrkA and p75 nerve growth factor receptors determines cell survival. *J Neurosci.* **18**: 3273-81.

Yoshimoto, T., Takeda, K., Tanaka, T., Ohkusu, K., Kashiwamura, S., Okamura, H., Akira, S. and Nakanishi, K. (1998). IL-12 up-regulates IL-18 receptor expression on T cells, Th1 cells, and B cells: synergism with IL-18 for IFN-gamma production. *J Immunol* **161**: 3400-7.

Youle, R.J. and Strasser, A. (2008). The BCL-2 protein family: opposing activities that mediate cell death. *Nat Rev Mol Cell Biol* **9**: 47-59.

Yuan, J., Shaham, S., Ledoux, S., Ellis, H.M. and Horvitz, H.R. (1993). The C. elegans cell death gene ced-3 encodes a protein similar to mammalian interleukin-1 beta-converting enzyme. *Cell* **75**: 641-52.

Zhang, Y.J., Xu, Y.F., Cook, C., Gendron, T.F., Roettges, P., Link, C.D., Lin, W.L., Tong, J., Castanedes-Casey, M., Ash, P., Gass, J., Rangachari, V., Buratti, E., Baralle, F., Golde, T.E., Dickson, D.W. and Petrucelli, L. (2009). Aberrant cleavage of TDP-43 enhances aggregation and cellular toxicity. *Proc Natl Acad Sci U S A* **106**: 7607-12.

Zhang, Y.J., Xu, Y.F., Dickey, C.A., Buratti, E., Baralle, F., Bailey, R., Pickering-Brown, S., Dickson, D. and Petrucelli, L. (2007). Progranulin mediates caspase-dependent cleavage of TAR DNA binding protein-43. *J Neurosci* **27**: 10530-4.

Zou, H., Henzel, W.J., Liu, X., Lutschg, A. and Wang, X. (1997). Apaf-1, a human protein homologous to C. elegans CED-4, participates in cytochrome c-dependent activation of caspase-3. *Cell* **90**: 405-13.